Tectonic Geomorphology of the Acambay graben, Central Mexican Volcanic Belt

María Teresa Ramírez-Herrera

Doctor of Philosophy
University of Edinburgh
1994

rompidos átomos aúllan
enfurecidos reniegan del ansia de las piedras
destripan las pertenencias del tiempo
[...] terrible el rencor de la tierra

J L Campos

Declaration

I hereby declare that this thesis has been composed by myself and the work within it is my own, except where otherwhise referenced.

María Teresa Ramírez-Herrera

Abstract

Tectonics and volcanism in the Mexican Volcanic Belt are related to the subduction of the Cocos plate beneath southern Mexico. The Acambay graben, a major structure in the central part of the Mexican Volcanic Belt, is characterised by Quaternary, generally east-west trending, seismically-active faults reflected in the topography as high scarps, which furnish reliable data on the landforms and their tectonic development. Hence, the characteristics of the Acambay graben and its surface expression make it an ideal place for the geomorphic evaluation of active tectonics and seismicity of the region. Three main aims of this thesis are as follows: 1) to determine the tectonic regime and evaluate the degree of active tectonism of the region, 2) to ascertain the relationship between the tectonic landforms of the Acambay graben and the regional geodynamic setting, and 3) to determine the areal distribution of seismic hazard in the study area. A range of geomorphological evidence indicative of neotectonic activity in the Acambay graben is derived from detailed field mapping in conjunction with morphometric analysis. Remote sensing analysis, large-scale aerial photos and digitally enhanced Landsat imagery is also used in order to identify fault-trends and associated landforms.

Fault systems associated with the graben are categorised on the basis of the morphological features associated with them. Five systems are identified: 1) the Acambay-Tixmadeje faults, 2) the Tepuxtepec faults on the northern flank of the graben, 3) the Pastores fault, 4) the Venta de Bravo faults on the southern flank of the graben, and 5) the Temascalcingo faults located in the centre of the graben. A suite of geomorphic indicators viewed as whole is consistent with recent and active faulting along the Acambay graben. Variations in the relative rates of tectonic activity and relative fault chronologies are derived from the morphometric analysis of landforms along the faulted mountain fronts and a range of morphological evidence. The en echelon arrangement of the faults, the shape of their trace in planform and the surface expression of fault-associated landforms provide evidence of strike-slip displacement.

Except for limited historical evidence, there is as yet no absolute dating available for the most recent fault displacements and consequently estimates are here based on the degree of fault scarp degradation. Prominent fault scarps and triangular facets demonstrate normal faulting, while a suite of evidence such as offset drainage, sag ponds and pull-apart basins, together with linear and compression ridges, confirm an important left-lateral component to fault displacement, a motion which is accordant with regional left-lateral shear along the Mexican Volcanic Belt. The geomorphological evidence and the historical occurrence of seismicity reveal areas of seismic hazard. Morphotectonic characteristics and the location of earthquakes suggest that the Venta de Bravo fault is one of the areas of highest seismic hazard in the Acambay graben. Further analysis of neotectonic activity in the region is required in order to document more precisely both spatial and temporal variations in seismicity. This could be accomplished by the establishment of a precise chronology of fault displacement, the undertaking of trenching for stratigraphic control on times of faulting and the geodetic monitoring of fault movement and deformation in the region.

Acknowledgements

This research has been sponsored by the Universidad Nacional Autónoma de México (UNAM) and travel founds were granted by the Instituto de Geografía, UNAM, for which I am grateful.

I am indebted to my supervisors, Mike Summerfield, for his thorough review and advice which greatly improved the original manuscript, and Mario Arturo Ortiz for many hours of discussion, encouragement and enthusiasm provided during the field work.

I would like to thank Federico Mooser for contributing useful ideas to my research, Max Suter for providing valuable references and field trip, Gabriel Legorreta and Miko Punkari for technical support, and Carmen Valverde for logistic support.

Thank you also to Juan Luis for love, and to all those friends who have made my time in Edinburgh so enjoyable. Finally, my gratitude goes to my family for their moral support.

Table of Contents

Table of Figures

Chapter 4

Chapter 5

Chapter 6

Chapter 8

List of Tables

Chapter 3

Chapter 5

Chapter One: Introduction

1.1 Aims.

The aims of this thesis are the identification of geomorphological evidence indicative of neotectonic activity in the Acambay graben, a major structure in the central part of the Mexican Volcanic Belt, and an assessment of its relationship to regional scale geodynamics. This is accomplished using morphotectonic and neotectonic analyses which endeavour to interpret the recent deformation of the Earth's crust through the study of the landforms. There are three specific objectives:

1) To determine the tectonic regime and evaluate the degrees of active tectonism of the region.

2) To ascertain how far the tectonic landforms of the Acambay graben are accordant with the current regional-tectonic models of southern Mexico.

3) To use tectonic landforms indicative of neotectonic activity in the assessment of the spatial occurrence of seismicity - in other words, to determine the areal distribution of the seismic hazard.

Despite a number of case studies of the large-scale tectonics of central and southern Mexico, morphotectonic approaches have been little used to date and their full potential has yet to be realised. Although there have been local studies of the morphostructures along the Mexican Volcanic Belt (López, 1984; Pasquaré *et al.*, 1987a, b; Ortiz and Bocco, 1989; Ramírez, 1990) and meso-scale features, such as lineaments, have been detected on satellite imagery (Johnson, 1987; Johnson and Harrison, 1989, 1990; Pasquaré *et al.*, 1987a; Martínez-Reyes and Nieto-Samaniego, 1990), an integrated meso- and micro-scale morphotectonic approach has yet to be applied to the investigation of the neotectonic regime in southern Mexico.

In this work, relevant geomorphological data have been derived from detailed field mapping in conjunction with morphometric analysis and remote sensing analysis

employing large-scale aerial photography and digitally-enhanced Landsat imagery. The Acambay graben, as well as the Mexican Volcanic Belt as a whole, have been the subject of a number of geological and geophysical studies in recent years as a consequence of their potential mineral and geothermal resources and the volcanic and seismic hazard threat to several major centres of population and industry in the region (Urbina and Camacho, 1913; Astiz, 1980, 1986; Ferriz, 1985; Lugo-Hubp *et al.*, 1985; Medina, 1985; Venegas *et al.*, 1985; Verma, 1985; Urrutia-Fucugauchi and Böhnel, 1988; Martínez-Reyes and Nieto-Samaniego, 1990). There has, however, been little application of geomorphological techniques to the problem of the nature of recent seismic activity, and to the relationship between the genesis of micro- to meso-scale tectonic landforms and their regional geodynamic setting. This thesis addresses these so far neglected problems.

1.2 Background.

Tectonic geomorphology (regarded as synonymous with the term 'morphotectonics') is concerned with the analysis of the relationship between tectonics and landforms irrespective of scale. Tectonic geomorphology is not only concerned with the macro-scale features of the Earth's surface and long geological time-spans, but also with the more detailed effects of tectonic processes in recent geological time or even at the present day (Embleton, 1987). Recent deformation is often described as neotectonic, although there is no general agreement as to the time scale to which this term refers. In this study the term neotectonics will be used to refer to tectonic activity during the Neogene and Quaternary.

Tectonic geomorphology has involved the application of different approaches to solve the problem of the relationship between neotectonics and landforms at different scales. Examples of the study of neotectonics employing geomorphological evidence at

micro- and meso-scales have been summarised by various workers (Morisawa and Hack 1985; Doornkamp, 1986; Vita-Finzi, 1986; Embleton, 1987; Summerfield, 1987; Sanderson and Gutmains, 1991, Mörner *et al.*, 1992; Stewart *et al.*, 1993). The use of satellite and radar imagery has been of great value in assessing the tectonic regime of large areas experiencing neotectonic activity (e.g. Sanderson and Gutmains, 1991). Meso-scale morphologic evidence such as lineaments, scarps, triangular facets, straight stream segments and offset drainage are well defined on high-resolution satellite imagery (Armijo *et al.*, 1986; Johnson, 1987, 1989; Brias *et al.*, 1990; Ghosh and Viswanathan, 1991; Tapponnier 1991). Since tectonic landform trends provide evidence of the characteristics of the tectonic regime of a region, landforms indicative of neotectonic activity can be used in assessments of the spatial and temporal occurrence of seismicity (Doornkamp and Han, 1985; Han, 1985; Ota, 1985; Weldon and Sieh, 1985; Vita-Finzi, 1991). However, little of this research has been focused on earthquake risk, most previous work being concerned with the post-seismic effects of earthquakes (Cosgrove and Jones, 1992).

Any evaluation of the earthquake hazard implies the recognition of surface *active faults* using geological or geomorphological analysis. The term *active fault* has been widely used with different connotations by different workers. However, it is important in this study to clarify the meaning of this concept given its importance in the use of landform analysis in the tectonic evaluation of faults.

1.2.1 Definition of active faults.

Most of definitions of *active faults* include the notion of past displacements on the fault during the present seismotectonic regime and the probability of future displacements (Slemmons and McKinney, 1977; Haller *et al.*, 1993). It is common to find the time of last displacement or rate of displacement being specified as "Recent", "Holocene" or "Quaternary" , or reference may be made to the occurrence of more than one displacement during a given period of time. Some definitions also specify various criteria of activity, such as "seismically active", "geodetically active" or "geologically active".

A detailed compilation of most definitions of *active faults* is given in the study by Slemmons and McKinney (1977). From this work it is clear that the term *active fault* has not changed substantially since the definitions postulated by Wood (1916) and Willis (1923): "An active fault is one on which a slip is likely to occur", ".... all faults on which there has been a movement within historic time", and also "all faults upon which physiographic evidence of recent surface dislocation --'trace phenomena'-- could be obtained....".

Currently there is no universally accepted definition of an active fault. The wide range of definitions varies from those based on a very low rate of activity or long recurrence interval to definitions restricting the term "active" to faults with an historic offset (Slemmons and McKinney, 1977). The four essential elements constantly used and included in the definition of *active faults* since Wood's (1916) and Willis's (1923) definition are:

(1) Active faults have been offset during the present seismotectonic regime.

(2) Active faults have the probability or potential for future offsets.

(3) Active faults have evidence of recent activity as may be shown by geomorphological evidence.

(4) Active faults may have associated earthquake activity.

"An active fault is a fault that has slipped during the present seismotectonic regime and is therefore likely to have renewed displacement in the future" (Slemmons and McKinney, 1977). Different evidence may indicate fault activity like historic, geological, seismological, geodetic, geomorphological or other geophysical evidence of activity. Active faults can have rates of activity which vary from very low, with long recurrence intervals, to very high, with short recurrence intervals. The most recent offset along a fault with a long recurrence interval may be either recent or ancient (Slemmons and McKinney, 1977).

Most of the definitions of an active fault include geomorphological evidence, such as facets, escarpments, offset streams and incised alluvial fans, longitudinal depressions or sag ponds, and shutter ridges, as an meaningful indictor of recent fault activity (Wood, 1916; Willis, 1923; Louderback, 1937, 1950; Schultz and Cleaves, 1955; Allen *et al.*, 1965; U.S. Atomic Energy Commission, 1973; Nichols and Buchanan Banks, 1974; Wesson *et al.*, 1975; cited in Slemmons and McKinney, 1977). Some of the definitions consider geomorphological evidence as a main indicator of the degree of activity and even use it as essential property for the classification of active faults (International Atomic Energy Agency, 1972; Grading Codes Board, 1973; cited in Slemmons and McKinney, 1977).

It can be concluded, therefore, that geomorphological evidence plays an important role in the classification of fault activity, both in relation to the degree of activity and to the relative rates of movement along, and age of, active faults. Geomorphological studies provide an invaluable tool in the assessment of active faulting and, consequently, in seismic risk evaluation. Recent studies have shown that the activity of faults is non-

uniform and that differences in the rate of activity are reflected in the relief of a segmented fault.

1.2.2 Fault segmentation.

The increasing recognition that earthquakes do not produce ruptures along the entire length of many faults but, instead, surface breaks are restricted to segments bounded by rheological and structural heterogeneities within fault zones, has considerable significance in seismic hazard assessment (Schwartz and Coppersmith, 1984; Crone and Haller, 1991). The fault segmentation concept has most commonly been applied to strike-slip faults (Schwartz and Coppersmith 1984, 1986), but investigations of normal faults (Schwartz and Coppersmith, 1984; Bruhn *et al.*, 1987; Machete *et al.*, 1987; Menges, 1987; Wheeler, 1987; Wheeler and Krystinik, 1987) reveal that these display comparable attributes to those of strike-slip systems. The most commonly recognised features are along-strike variations in the surface orientation and dip of faults (geometric discontinuities - dePolo *et al.* (1989)) and intersections between faults and other major geological structures (structural discontinuities - dePolo *et al.* (1989)).

An essential feature of fault segmentation studies is the ability to identify long-lived or persistent structural features which define earthquake segments - that is, the parts of a fault which rupture as a unit during an earthquake (dePolo *et al.*, 1989). Recent studies of range fronts have highlighted the role of non-uniform fault activity in influencing relief (e.g. Menges, 1987a; Wheeler, 1987). It is becoming increasingly apparent, therefore, that the morphological characteristics of uplifted footwalls may reflect the distribution of major structural hetereogeneties along normal fault zones (Stewart and Hancock, 1991). It is usually suggested that a segmented fault should be defined on the basis of paleoseismology (through trenching and dating) with supporting

geomorphological and geological data (such as scarp morphology, stratigraphic control on times of faulting, geological structures that may control physical segmentation). But where the evidence for independent segments is not compelling (for instance where identification is solely on the basis of morphological data), the fault should be described as having sections (Machette *et al.*, 1993). However, in this study, it has been decided to keep the term 'segment' instead of 'sections' because the segments proposed for each fault coincide with the boundaries of morphostructural blocks along the Acambay graben.

1.2.3 Morphostructural zoning .

Morphostructural analysis is based on the concept that tectonic movements have caused deformation of Earth's surface. It forms part of the Earth sciences that deals with relations between landforms and recent tectonic movements. It is a component of structural geomorphology, the purpose of which is to analyse the relationship between geological structures and landforms (Rantsman, 1979). The concept of "morphostructure" was first introduced into geomorphology during the 1940s by I.P. Gerasimov (1946) and it has been subsequently developed by a number of workers (Gerasimov, 1954; Gerasimov and Mesheriakov, 1967; Gerasimov and Rantsman, 1973; Mesheriakov, 1965, 1972; Kostenko *et al.*, 1972; Simonov, 1972; Ufimtzev and Xudiakov, 1976; Rantsman, 1979). Morphostructural analysis is supported by the plate tectonic model that proposes that the Earth's surface is composed of several lithospheric plates which move over the underlying, more mobile asthenosphere. A mosaic configuration of the Earth's surface is also observed in plate interiors (Orlova, 1980) in the form of territorial units, or 'blocks'. However, in plate interiors horizontal displacements appear overall to be less important than vertical movements of the crust in the generation of landforms (Summerfield, 1991). Large elements of the surface in

mountainous terrain represent in some way or other tectonic movements reflected as block-structures.

Morphostructural zoning is based on the idea of the block structure of the Earth's crust. Morphostructural zoning involves the division of the landsurface into a system of hierarchically-ordered areas, each characterised by a definitive degree of morphostructural uniformity (Rantsman, 1979; Bathia *et al.*, 1992).

Morphostructural analysis aids the identification of tectonic structures and the interpretation of their recent development (Rantsman, 1979). The identification of earthquake-prone areas using recent topographic data is based on the concept that large elements of relief in the mountainous terrain reflect tectonic movements at depths similar to those of shallow earthquake generation.

1.3 Methods.

This thesis involved a combination of approaches, employed in previous morphotectonic studies, to elucidate the characteristics of the tectonic regime of the Acambay graben and to evaluate active tectonism in the region (Fig. 1.1).

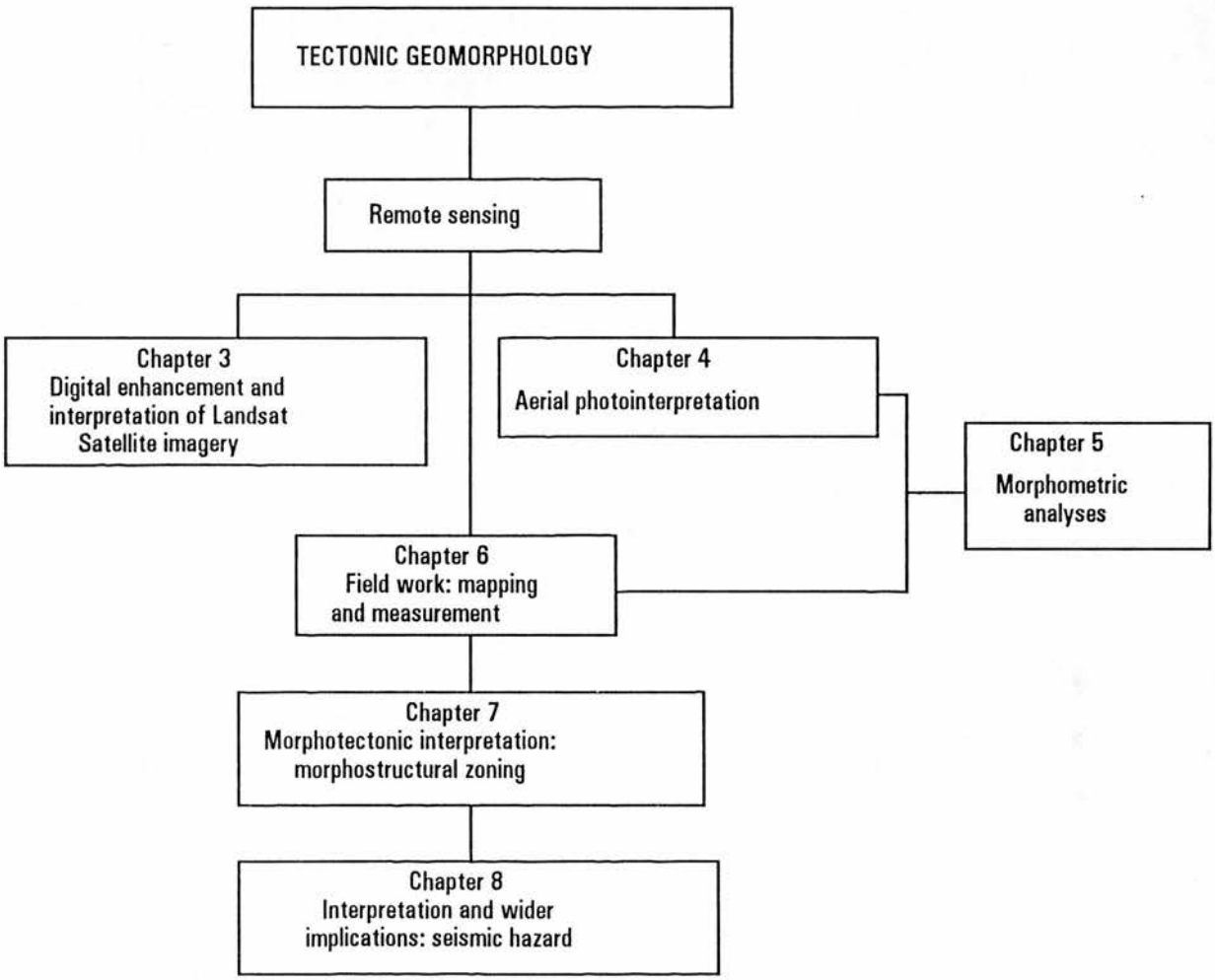

Fig. 1.1 Thesis strategy.

The patterns of surface faulting in the study area were identified in a number of stages. The first procedure involved the analysis of digitally-enhanced imagery. The interpretation of satellite imagery allowed lineaments to be identified and an assessment to be made of their possible neotectonic significance. Statistical analysis of the lineaments identified provided information about the dominant fault trends in the region.

The second approach consisted of interpretation of aerial photography. The geometry of the surface trace of the fault zone along the Acambay graben was identified, based primarily on detailed photointerpretative mapping of fault scarps and the basal topographic junction of the range front on black and white aerial photographs (nominal scales of 1: 50000, 1: 25000 and 1 : 28000). Aerial photo-interpretation included detection, delimitation, determination and selection of geomorphological evidence of tectonic activity. Structures deforming Quaternary sediments, or exhibiting youthful morphology in the field and on aerial photographs, were mapped at a scale of 1:50000.

The third approach involved detailed field surveys aimed at verifying neotectonic structures and identifying the precise geometrical, geological and geomorphological characteristics of any existing faults. The field studies comprised: 1) mapping of landforms indicative of neotectonic deformation; 2) mapping of structures deforming Quaternary sediments or exhibiting youthful morphology; and 3) identification and measurement of small-scale features reflecting tectonic strains (such as slickensides, striations).

The fourth approach involved morphometric analysis and consisted of the systematic analysis of tectonic landforms in order to define regional patterns of tectonic activity along the Acambay graben. The approach used involved regional morphometric analyses of selected landforms in the mountain fronts of the graben in order to define the relative rates of tectonic activity of known, or inferred faults, associated with escarpments

or mountain fronts. Morphometric variables, such as mountain front sinuosity, valley heights and widths, fault scarp profiles, degree of fault escarpment dissection and longitudinal stream profiles, were measured on topographic maps (scale 1:50000). These morphometric variables were then used to determine the relative amounts of Quaternary uplift occurring along mountain-front structures.

The final approach used was morphostructural zoning in order to identify tectonic structures and earthquake prone areas. Three types of morphostructures are normally identified in morphostructural zoning: terrain units (blocks); linear zones separating blocks (morphostructural lineaments); and the intersections of lineaments (morphostructural knots). Blocks, lineaments and knots - in that order - are characterised by increasing tectonic activity (Rantsman, 1979). Morphostructural zoning is hierarchically ordered and blocks are assigned ranks. Mountainous terrains - considered as blocks of first rank - are divided into blocks of second rank called megablocks. Megablocks are further subdivided into blocks. In this study a further subdivision of blocks was required. The rank of lineaments is also designated as first, second, third and fourth depending on their relation to the mountainous terrains, megablocks, blocks and minor blocks, respectively.

Morphostructural lineaments are zones of varying width, ranging up to a few tens of kilometres depending on their ranks and position against large relief elements. Morphostructural knots may include areas greater than the width of lineament zones that form the knot (Rantsman, 1979; Bathia *et al.*, 1992). Morphostructural knots are the key structures for identification in this study because of the fact that a number of known epicentres of strong earthquakes in the study area have occurred in the vicinity of such knots. It is clearly highly probable that the epicentres of future major earthquakes will

also be associated with these morphostructures (Rantsman, 1979; Gvishiani and Soloviev, 1981; Gvishiani *et al.*, 1986; Bathia *et al.*, 1992).

The final procedure for seismic hazard evaluation consists of the comparison of the morphostructural zoning map with the seismicity data in order to identify the morphostructural knots associated with earthquakes. A correlation of morphostructural zoning map and the earthquake data (data provided by the Servicio Sismológico Mexicano and the US Geological Survey, National Earthquake Information Centre) of the study area is analysed to indicate the epicentres of all earthquakes with M> 5.0 known here (after 1900) that occurred within morphostructural knots. The morphostructural knots identified on the basis of morphostructutal zoning can therefore be viewed as potential sites of earthquakes with M> 5.0, so subsequently they could be included as recognition objects in predictions of potential sites of earthquakes of this magnitude in the study area.

1.4 Thesis structure.

This chapter has defined the aims and scope of the thesis and outlined the methodology underpinning the use of morphotectonic studies in the evaluation of active tectonics and seismic hazards. This has involved considering the concepts which support the use of landforms to explain the recent tectonic development of a region and their implications in determining earthquake vulnerability. The approaches and procedures of the morphotectonic study applied to the Acambay graben are reviewed.

In Chapter 2 the tectonic setting of the study region in a plate tectonic context is outlined. The various models that have been proposed for the tectonic development of the Mexican Volcanic Belt are reviewed, the Acambay graben is analysed within the

structural and tectonic framework of the Mexican Volcanic Belt, and an overview of the geology, structure, seismicity and tectonics of the Acambay graben is presented.

The data obtained from the interpretation of satellite imagery is examined in Chapter 3. The different procedures of digital enhancement of satellite imagery and the results obtained from remote sensing analysis are examined, and the main lineament trends of the study area and their correlation to the regional tectonics are identified.

Chapter 4 details the meso-scale geomorphology of the Acambay graben as interpreted from aerial photographs. The results and neotectonic implications of this analysis are discussed, and an assessment is made of which landforms provide the main evidence of neotectonic activity and thus indicate the characteristics of the tectonic regime in the area.

The explanation of the procedures applied in the morphometric analysis and the results obtained are discussed in Chapter 5. The strengths and limitations of the different morphometric variables in indicating neotectonic activity are assessed and the results of the morphometric analysis are presented. It is argued that the interpretation of morphometric variables reveals the degree of active faulting and segmentation of the faults and along the Acambay graben.

Chapter 6 details landform characteristics indicative of neotectonic activity as interpreted from field observation. This chapter also describes those landforms that indicate recent deformation and includes an appraisal of the tectonic style inferred from landform evolution.

The results and implications of the tectonic geomorphology of the Acambay graben are summarised in Chapter 7. It is argued that tectonic landforms provide evidence of relative degrees of tectonic activity along faults. The morphological characteristic of landforms along the fault escarpments indicate fault segmentation, and it

is shown how these fault segments can be correlated with the morphostructural zoning of the area.

Two major themes are covered in Chapter 8. One is a review of the implications of the tectonic geomorphology of the Acambay graben and its relationship to regional tectonics. This includes an assessment of a regional-scale tectonic model involving left-lateral shear for central Mexico, on the basis of morphotectonic evidence. The second theme comprises an interpretation of the morphostructural knots and their implications for seismic hazard evaluation. A history of damage during major historical earthquakes is also presented.

Chapter 9 presents a summary of the thesis and assesses the wider implications of the research.

Chapter Two: Tectonic Setting

The Acambay graben is located in the central part of the Mexican Volcanic Belt, between the 19° 45'- 20° 00' N and 99° 45'- 100° 25' W (Fig. 2.1). It is an east-west trending structure about 80 km long. The Acambay graben is a part of the regional tectonic and structural framework of the Mexican Volcanic Belt . Therefore, the tectonics and seismicity of the Acambay graben need to be analysed in the regional context of the Mexican Volcanic Belt. This chapter provides an overview of the tectonic setting of the Mexican Volcanic Belt in a plate tectonic context and focuses in the analysis of the tectonic, seismic and structural framework in the central part of the belt.

2.1 The Mexican Volcanic Belt in a Plate Tectonics context.

The Mexican Volcanic Belt is located in the southern part of the North American Plate in central Mexico. The Mexican Volcanic Belt is a 20-150 km broad, 1000 km long structure which extends roughly east-west from the coast on the Gulf of Mexico to the Pacific Ocean (Fig. 2.1). The Mexican Volcanic Belt is an active, mostly calc-alkaline volcanic chain ranging from late Miocene to Quaternary in age (Verma, 1987) and although it belongs to the Circum-Pacific volcanic chain, it is not parallel to the associated subduction zone represented by Middle American Trench but is aligned to it at an angle of about 15-20 degrees (Molnar and Sykes, 1969). Volcanism related to subduction is expected to be oriented parallel to the zone of subduction. The oblique orientation of the Mexican Volcanic Belt with respect to the subduction zone makes the origin of this belt distinctive, and most workers have related the east-west orientation of Mexican Volcanic Belt volcanism to north-east subduction of the oceanic lithosphere of the Cocos plate, beneath southern Mexico. In the context of plate tectonics, therefore, the Mexican Volcanic Belt is a highly complex continental-margin arc.

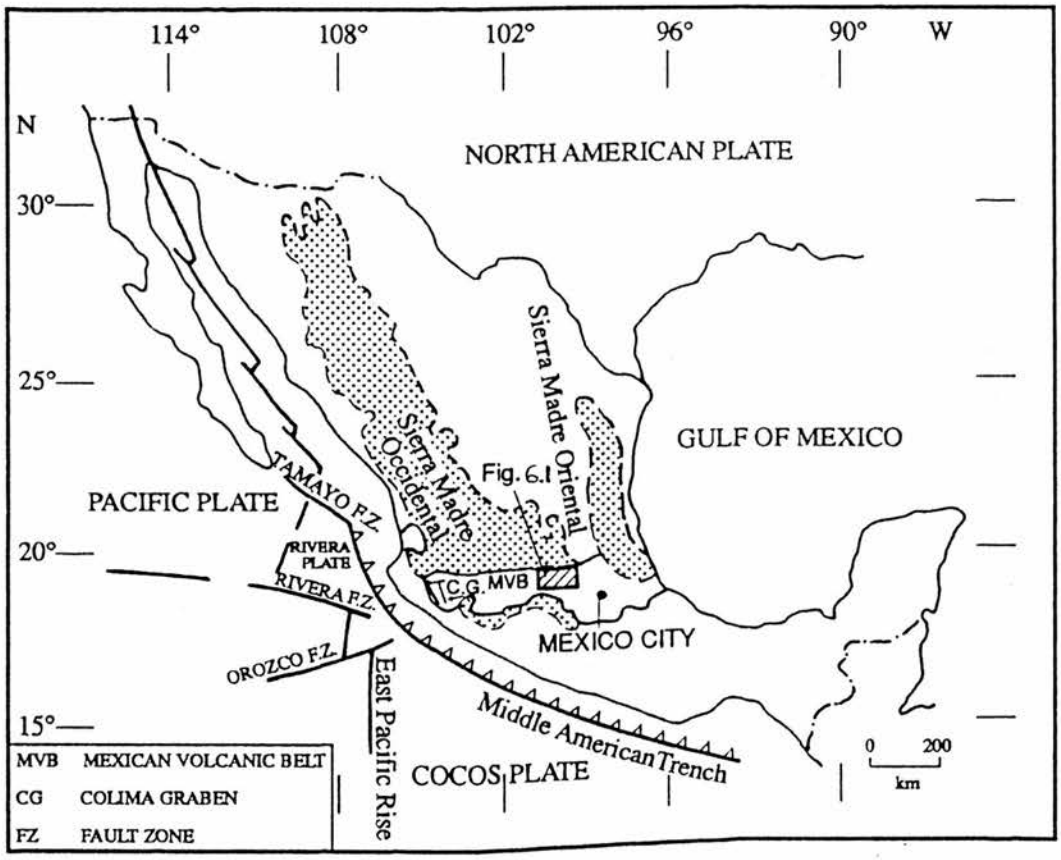

Fig. 2.1. Tectonic setting of the Mexican Volcanic Belt. The obliquely-shaded area shows the location of the Acambay graben.

2.1.1 Plate motions.

At present the Cocos plate is moving to the northeast beneath Central America at a mean rate of 50 mm a^{-1}, while the North American plate is moving to the southwest at a rate of 27 mm a^{-1}. Their convergence rate has been estimated as 60 to 70 mm a^{-1} (Minster and Jordan, 1978; Nixon, 1982) with a north-east vector. This oblique convergence has produced a left-lateral shear of the Mexican Volcanic Belt's upper brittle crust (Mooser and Ramírez, 1989). This left-lateral shear has increased since the Pleistocene due to active 'rifting' in the western part of the Mexican Volcanic Belt (Luhr *et al.*, 1984). The western portion of the Mexican Volcanic Belt has also been influenced by the waning, aseismic subduction of the Rivera plate. Prior to about 2 Ma ago, this small remnant of the Farallon plate was being actively subducted along the Middle American Trench (Larson, 1972). Since that time the Rivera plate has been accreting gradually to North America; convergence is now estimated at 20 mm a^{-1} (Nixon, 1982).

However, the influence of late Cenozoic plate motions on arc volcanism in central Mexico is not well understood. Nixon *et al.* (1987) suggested that the east-west orientation of arc volcanism may have been initiated by major plate reorganisations recorded in east Pacific ocean lithosphere in the Late Miocene at 12.5 - 11 Ma or at 6.5 Ma. The migration of arc volcanism towards the Middle American Trench, which was completed by the early Quaternary, may have been induced by plate readjustments 3.5 Ma ago or earlier. However, the gradual focusing of andesitic volcanism towards the volcanic front in the Quaternary cannot be related to documented plate reorganisations, and occurred much too rapidly to represent a direct response to a significant change in dip of the subducted slab.

2.1.2 Theories of the origin of volcanism in the Mexican Volcanic Belt.

The Mexican Volcanic Belt has been the subject of a large number of studies since the time of Alexander von Humboldt. He provided the first scientific explanation for the alignment of volcanoes in this province by proposing the existence of a crustal fracture dissecting the continent along the 19th parallel from the Atlantic to the Pacific Ocean (Humboldt, 1808). This hypothesis has been modified since by subsequent interpretations (Mooser and Maldonado, 1961; Mooser, 1969; Gastil and Jensky, 1973). There are two primary groups of models that deal with the origin of volcanism in the Mexican Volcanic Belt: i) those that relate the Mexican Volcanic Belt's volcanism to subduction and, ii) those that consider volcanism to be independent of subduction.

i) Tectonic models of volcanism in the Mexican Volcanic Belt dependent on subduction.

With the development of plate tectonics theory , the Mexican Volcanic Belt was initially interpreted as a possible extension of the East Pacific Rise (Mooser ,1969). This hypothesis was further developed by Auboin *et al.* (1982), who suggested that the Gulf of California, the Mexican Volcanic Belt and the Middle American Trench form, as a whole, a coherent neotectonic complex involving interactions between the plates in this area of the Pacific. The Tamayo fault, which bounds on the north-western side of the Cocos plate, is a transform fault linking the East Pacific Rise to the Middle American Trench; it has therefore been suggested that since the Pliocene the Mexican Volcanic Belt has represented the landward continuation of the Tamayo fault with a similarly extensional transcurrent motion and associated volcanism (Auboin, *et al.*, 1982).

Mooser (1972) inferred that the Mexican Volcanic Belt, a zone of weakness, has been reopened since the Tertiary and that volcanism is caused by subduction of the Cocos plate along the Middle American Trench. The hypothesis of the existence of a crustal

fracture under the Mexican Volcanic Belt has again been put forward by Anderson and Schmidt (1983) who interpreted it as a sinistral mega-shear, active mainly during the Jurassic. Recently obtained seismic data (Gomberg, 1986) show that the Mexican Volcanic Belt may be related to processes deep within the lithosphere and is characterised by very low shear velocities at a depth of 20-80 km which may be correlated with partial melting of the lower lithosphere. A direct causal link between the Mexican Volcanic Belt and subduction has also been proposed by several other authors (Molnar and Sykes, 1969; Demant and Robin, 1975; Demant, 1978).

ii) Theory of volcanism independent of subduction.

The theory of reactivation of ancient zones of crustal weakness and possible volcanism independent of subduction has been suggested by Cebull and Shubert (1987), who have presented a modified intraplate transform version of their earlier micro plate model. Although admitting that their interpretation is speculative, they base their discussion on four tectonic events. The oldest (Mesozoic and/or early Cenozoic) is taken to be responsible for the development of a zone of weakness along the trace of the present Mexican Volcanic Belt, while the next event (post-Mesozoic) involves subduction along the west coast of North America. The third event is the beginning of sea-floor spreading in the Cayman trough about 36 Ma ago, and the fourth, and important event to the north of the Mexican Volcanic Belt, is the opening of the Gulf of California and the development of basin-and-range faulting. Thus the lack of parallelism of the Mexican Volcanic Belt and the Middle American Trench is explained in terms of the volcanic and tectonic activity associated with the zone of weakness resulting from the above mentioned events. They also argue that the fracture zone may help propagate volcanism that is independent of subduction processes.

Nevertheless, in spite of models to the contrary, most workers have related the origin of the Mexican Volcanic Belt to the active subduction of the Cocos plate in southern Mexico, and this, together with regional faulting, seem to be the main factors controlling volcanism along the Mexican Volcanic Belt.

2.1.3 Neotectonics in the evaluation of the origin and evolution of the Mexican Volcanic Belt.

Different interpretations of the neotectonic pattern along the Mexican Volcanic Belt have been proposed as an explanation of its origin and evolution. Some authors have suggested that lateral crustal movements along major shear zones occurred during the Mesozoic and Tertiary tectonic development of Mexico (Gastil and Jensky, 1973; Cebull and Shubert, 1987) and that neotectonic activity along the Mexican Volcanic Belt might represent the reactivated offspring of a zone of weakness (Mooser, 1972) as well as the development of an incipient plate boundary (Luhr *et al.*, 1984; Cebull and Shubert, 1987; Johnson, 1987; Johnson and Harrison, 1990).

According to recent studies, neotectonic deformation in central Mexico is controlled by faulting associated with rifting, transtension and shear, mainly with a left-lateral component (Johnson and Harrison, 1990). Johnson and Harrison (1990) state that the crust south of the Mexican Volcanic Belt is divided into three blocks - the Jalisco, Michoacán and Guerrero blocks (Fig. 2.2). Relative motion between them and the North American plate has caused the formation of major zones of neotectonic deformation within, and south of, the Mexican Volcanic Belt. Johnson and Harrison (1990) state that the direction of the maximum extension for the Tepic-Chapala Rift is oriented at approximately N40^{o}E. This means that, on average, the Jalisco block is moving away from the Mexican mainland (North America) along this direction. Johnson and Harrison

(1990) have suggested that the present right-lateral motion between the North America and Rivera plates does not have to extend into western Mexico. Johnson and Harrison (1990) estimated the rate of motion of the aseismically subducting Rivera plate at 12 mm a^{-1} , in a north-northwest direction beneath the Jalisco block (Fig. 2.2). This interpretation implies that the convergence rate perpendicular to the trench between the Rivera plate and the Jalisco block decreases westward. If subduction beneath the Jalisco block were to stop, which appears to be slowly happening, or if rifting in the Colima Rift were to accelerate, then the Jalisco block would eventually follow Baja California to the northwest (Johnson and Harrison, 1990).

Johnson and Harrison (1990) have also reported the probable location of two zones of Mesozoic/Cenozoic deformation in central Mexico that have been reactivated in the Pliocene-Quaternary. These follow the major linear zones of neotectonic deformation proposed by these authors: 1) the Chapala-Oaxaca fault zone, which extends almost parallel to the west coast of Mexico, and 2) the Chapala-Tula fault zone, which stretches eastward from a triple junction (the Colima rift) to an area north of Mexico city (Fig. 2.2). The second linear zone of deformation is considered to be evidence of a zone of weakness in the crust. Therefore, the distribution and character of volcanism in the Mexican Volcanic Belt is thought to be closely linked in space and time to deformation of the crust of central Mexico (Johnson and Harrison, 1990). They point to the role of the Quaternary development of the Chapala-Tula fault zone, which is colinear with the volcanic front of the Mexican Volcanic Belt. This fault zone could act as a conduit to the surface for rising magma. This interpretation implies that deformation in the overriding plate may control the location of volcanism, both locally and regionally. Therefore, the oblique orientation of the Mexican Volcanic Belt relative to its associated trench may not be exclusively due to along-trench variations in subduction geometry and velocity, and

consequently these variations may not be as important as previously suggested (Johnson and Harrison, 1990). Johnson and Harrison's (1990) interpretation also implies that the Pliocene-Quaternary volcanism and tectonism within the Mexican Volcanic Belt is the latest phase in a long and complex history of tectonic events in the area.

DeMets and Stein (1990) have analysed the oblique subduction along the Middle America Trench and its implications for deformation in Mexico. They suggest that opening along the Colima rift is a response to south-eastward translation of the Michoacán block that is, in turn, being induced by oblique subduction of the Cocos plate (Johnson and Harrison, 1990). Geological data along two fault systems in western Mexico are consistent with south-eastward motion of parts of south-western Mexico relative to North America in the past few million years: the Chapala-Oaxaca fault zone has accommodated several kilometres of sinistral motion and sinistral transtension has occurred along the Mexican Volcanic Belt (Johnson and Harrison, 1989, 1990). Either, or both, of these fault zones could accommodate any south-eastward motion of coastal blocks that might result from oblique subduction. Moreover, the observation that earthquake slip vectors from the northern Middle American trench trend systematically counter clockwise from the predicted Cocos-North America convergence direction is also consistent with south-eastward motion. Consequently, if oblique subduction is driving south-eastward transport of a coastal sliver, the Colima rift is a passive, pull-apart zone at the north-western end of this sliver rather than an incipient spreading ridge that will replace the Pacific-Rivera rise (DeMets and Stein, 1990).

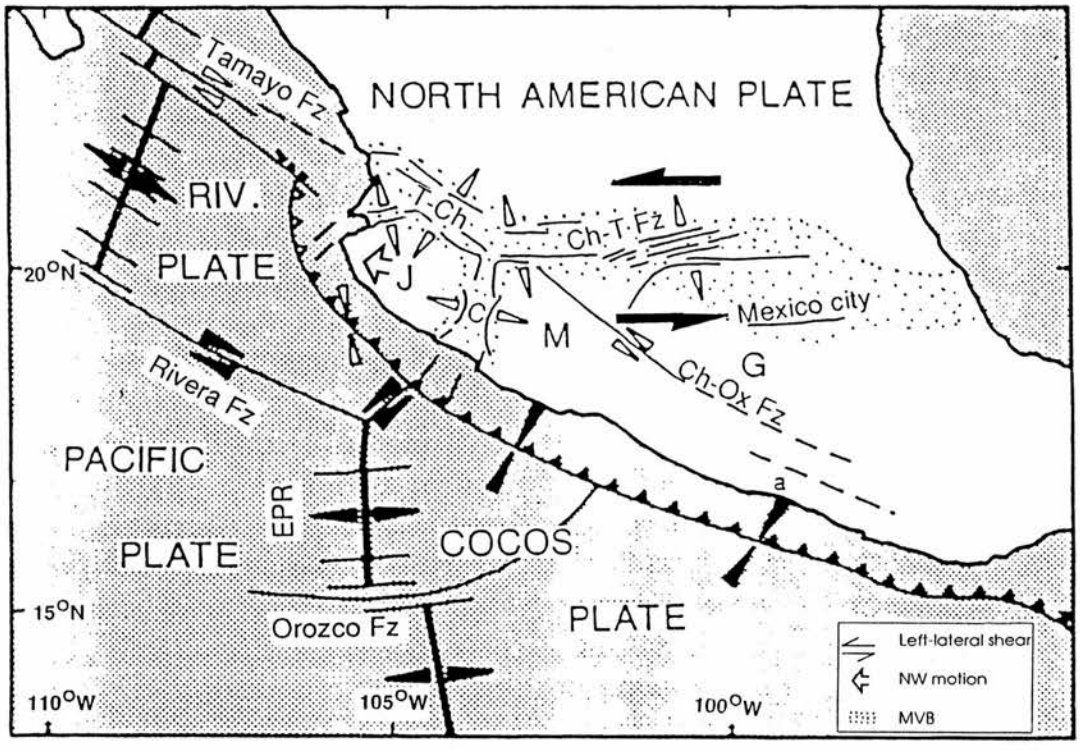

Fig. 2.2. Sketch map showing the regional neotectonics of central Mexico (modified from Johnson and Harrison, 1990). Symbols: EPR, East Pacific Rise; Fz, fault zone; Ch-T Fz, Chapala-Tula fault zone; Ch-Ox Fz, Chapala-Oaxaca fault zone; Tepic-Chapala graben; C, Colima graben; J, Jalisco block; M, Michoacán block; G, Guerrero block; open arrows - motions of blocks south of Mexican Volcanic Belt; black arrows - plate motions in the eastern Pacific; large open arrow - NW motion of the Jalisco block (Luhr, *et al.*, 1985).

2.1.4 Age of the Mexican Volcanic Belt.

K-Ar and geological data presented by Nixon *et al.*, (1987) provide evidence of the spatial and temporal evolution of calc-alkaline volcanism in Central Mexico since the Pliocene. The modern volcanic arc is characterised by an east-west chain of large central volcanoes and monogenetic volcano fields composed predominantly of andesite and dacite. According to K-Ar data major andesitic centres in the western part of the Mexican Volcanic Belt appear to be significantly younger than comparable volcanoes further east; volcanoes in the western part of the Mexican Volcanic Belt date from 0.6 and 0.2 Ma ago, whereas the central part of the belt was formed about 1.7 Ma ago. The difference in age between major andesitic volcanoes in the western part of the Mexican Volcanic Belt and those further east appears to be directly related to the contrasting subduction regimes of the Rivera and Cocos plates which are juxtaposed beneath the Colima graben (Nixon, 1982). However, the available geological and K-Ar data do not allow a precise estimate of the inception of calc-alkaline volcanism with an east - west trend in Central Mexico. It is suggested that "... a southward migration of calc-alkaline volcanism occurred in the central and eastern part of the arc between the Late Miocene or early Pliocene and Early Quaternary" (Nixon *et al.*, 1987).

2.2 The Acambay graben within the Mexican Volcanic Belt structural framework.

The characteristics of the structural framework of the Mexican Volcanic Belt, and particularly its central part, are closely linked to the development of the Acambay graben. Several studies have presented different proposals on the structure of the Mexican Volcanic Belt. Initially the Mexican Volcanic Belt was divided in two parts: 1) the eastern part - from the Gulf of Mexico to the Colima graben, and 2) the western part - from the

Colima graben to the Pacific Ocean (Mooser, 1969). The eastern part, which has the form of a large volcanic arc, has been termed the Tarasco Arc by Mooser (1969). In subsequent studies several structural elements have been recognised along the Mexican Volcanic Belt, including volcanic arcs, en echelon graben, fracture and fault zones, and circular elements (Mooser and Ramírez, 1989). The recognised arcs are: a) the Guadalajara-Tepic and Chapala arcs, in the west; b) the Tarasco-Oaxaca arc in the central part of the Mexican Volcanic Belt; and c) the Tuxtlas arc in the east. The en echelon graben are orientated ENE-WSW (for instance, the Acambay graben) and seem to be associated with left-lateral shear in the upper brittle crust. This left-lateral shear is generated by the subduction in the Middle American Trench and the motion produced by the newly spreading Colima rift (Fig. 2.2) (Luhr, *et al.*, 1984; Mooser and Ramírez, 1989). The existence of these graben structures is also supported by a number of other studies in the region (Johnson, 1987; Pasquaré *et al.*, 1987a; Campos-Enríquez *et al.*, 1990; Johnson and Harrison, 1990; Martínez-Reyes and Nieto-Samaniego, 1990; Suter *et al.*, 1991, 1992). Series of fractures and fault zones are also recognised along the Mexican Volcanic Belt. One is a NE-SW fault system, while another is a NNW-SSE system (termed Taxco-San Miguel de Allende line (Demant, 1978)) which intersects several E-W trending graben, among them the Acambay graben. The general orientation of this system of faults suggests a genetic relationship with the faulting produced by antecedent volcanism associated with subduction of the now disappeared Farallon plate during the Cenozoic. These fractures seem to have been reactivated by the modern volcanism of the Cocos plate. A final group of features are circular-morphostructural elements which have been related to calderas and collapses associated with volcano-tectonic forces (Mooser and Ramírez, 1989).

A somewhat different view of the structural arrangement and tectonics of the Mexican Volcanic Belt has been proposed by Pasquaré *et al.* (1987). They suggest a division of the Mexican Volcanic Belt into a western, central and eastern regions. The western area which was activated during Pliocene time has a NW-SE trending graben system associated with the opening of the Gulf of California. The most important structural elements of this region, which appears to be dominated by faults indicative of extension, are the Colima-Tepic and Chapala graben. The central area consists of block-faulted and tilted ENE-WSW trending graben systems (for instance, the Acambay graben) surrounding a central depression. The eastern area is characterised by N-S fault systems which affect the rigid basement of the Sierra Madre Oriental and control the largest strato-volcanoes of the Mexican Volcanic Belt. It has also been suggested that the Mexican Volcanic Belt intersects older N-S and NNE-SSW oriented block-faulted structures belonging to the Basin and Range province. Reactivated tensional lineaments belonging to the same province have been recognised inside the western and central sectors, and probably in the eastern one too. These structures are considered as reactivated faults which relate to Basin and Range features (Pasquaré *et al.*, 1987).

It has been also suggested that much of the deformation in the eastern and central parts of the Mexican Volcanic Belt can be related to two major linear fault zones; the Chapala-Oaxaca fault zone, a major structure of trench-parallel faults and fractures, and the Chapala-Tula fault zone which is aligned with north-dipping normal faults that cut the Pliocene-Quaternary volcanic deposits of the Mexican Volcanic Belt (Johnson, 1987; Johnson and Harrison, 1990). Many of the faults are arranged in a right-stepping en echelon pattern indicating transtension with a sinistral component across the Chapala-Tula fault zone. Some of the largest fault scarps belonging to this fault zone are located in this area, including the seismically active Acambay graben faults. Fault zones that

traverse nearly the entire region have the same location and orientation as the volcanic belt. This implies that deformation within the crust plays a significant role in determining the unusual orientation of the Mexican Volcanic Belt (Johnson, 1987; Johnson and Harrison, 1990). Thus, in the Mexican Volcanic Belt there is a clear relationship between volcanism and neotectonic activity that applies across all scales ranging from local to regional.

2.2.1 Central and eastern parts of the Mexican Volcanic Belt.

A morphostructural approach to the study of the central and eastern parts of the Mexican Volcanic Belt suggests the existence of three groups of linear morphostructures (E-W trending lineaments, NNW-SSE lineaments and NE-SW lineaments) together with circular features as the main structural features (Mooser and Ramírez, 1989). These structural features are considered to be the result of tectonic and volcano-tectonic forces and they provide evidence of left-lateral shear along the belt. The E-W trending lineaments have a direct relationship with the subduction of the Cocos plate, and specifically with the lateral shear which produces en echelon graben. The Acambay graben is one of these graben structures and it is considered the most active during the Pleistocene and Holocene. NNW-SSE lineaments (for instance, the Querétaro fault system) form NW trending graben produced during the Cenozoic. NE-SW trending lineaments have been produced by left-lateral shear which represents the response of the rigid upper crust to the oblique push of the Cocos plate subduction. Circular features along the belt are considered to be the result of volcano-tectonic forces.

Johnson and Harrison (1990) also recognise a series of NNW-SSE trending fractures. According to Johnson and Harrison (1990), the more eroded nature of the Querétaro fracture zone marks it as older than other neotectonic features in the region,

perhaps as old as Pliocene-Pleistocene. The fact that the faults cut volcanic rocks of Pliocene age indicated that the most recent deformation along the zone cannot be older than Pliocene (Johnson and Harrison, 1990). However, Pasquaré *et al.* (1987) suggest a different chronology for the main volcanic events. They argue that an early tensional tectonic phase was associated with the volcanic activity that formed the pre-Miocene deposits of the Sierra Madre Occidental. A NNW-SSE trending system was dominant during the late Miocene and is related to the Basin and Range province of western USA. NW-SE faulting during the Pliocene along California is thought to be responsible for the initial volcanic activity of the Mexican Volcanic Belt. Late Pliocene trends are WSW-ENE, and the most recent tensional phase produced N-S and NNE-SSW graben as possible reactivation features of Basin and Range structures (Pasquaré, 1987). Pasquaré *et al.* (1987) support the idea of faulting characterised by sinistral normal-slip movements, and they have concluded that the deformations in the central part of the Mexican Volcanic Belt (between Maravatío and Pátzcuaro) are the result of compression, extension and shear tectonic regimes, both pure and oblique. They also argue for an overall tectonic control over volcanism in the central area of the Mexican Volcanic Belt (Pasquaré *et al.*, 1988).

According to a recent study, the central part of Mexican Volcanic Belt can be divided according to observed structural trends into eastern, central and western sectors. In the eastern sector faulting shows E-W, NE-SW and NW-SE trends; the central sector exhibits NE-SW and infrequent N-S trends, and the western sector is characterised by an E-W trend with a less prominent WNW-ESE component (Martínez-Reyes and Nieto-Samaniego, 1990). These authors include the E-W faults of the Acambay graben within the eastern sector. The structural characteristics of faulting in the region reveal an

extensional regime during recent geological time and existing faults in the region can be classified as active faults or potentially active faults.

According to Suter *et al.* (1992) the central part of the Mexican Volcanic Belt is characterised by pronounced, generally E-W striking fault scarps that define a 25 to 55 km wide zone of distributed N-S extension. Additionally, a NNW-SSE striking normal fault system (Demant, 1978) exits south east of Querétaro (Fig. 2.3). This seems to be older than the E-W striking system (Mooser & Ramírez, 1989; Johnson and Harrison, 1990; Suter *et al.*, 1992). A neotectonic division of the central part of the Mexican Volcanic Belt into three segments is proposed by Suter *et al.* (1991) on the basis of major along-strike structural discontinuities in the system of E-W striking normal faults. The western segment (the area between Morelia and Los Azufres) is characterised by E-W striking normal faults (Fig. 2.3). A second, central segment extends between Maravatío in the west and Altamirano in the east (Fig. 2.3), its most prominent structure being the Venta de Bravo fault. The lateral extent of this segment is defined by the limits of the Venta de Bravo fault. The western end of the segment also coincides with the eastern end of the Cuitzeo graben (Fig. 2.3). The third, eastern segment is made up of the 30 km long Acambay graben. The boundary between the eastern and central segments is defined by a transfer zone between the Pastores and Venta de Bravo faults, a 180^{o} change in dip azimuth of the normal fault that cuts off Amealco caldera (Suter *et al.*, 1991), and a discontinuous change of approximately 10 km in the location of the axis of the tectonic depressions formed by the active, E-W striking normal faults. These three features line up at the projected location of the older, NNW-SSE striking Querétaro normal fault system (Fig. 2.3).

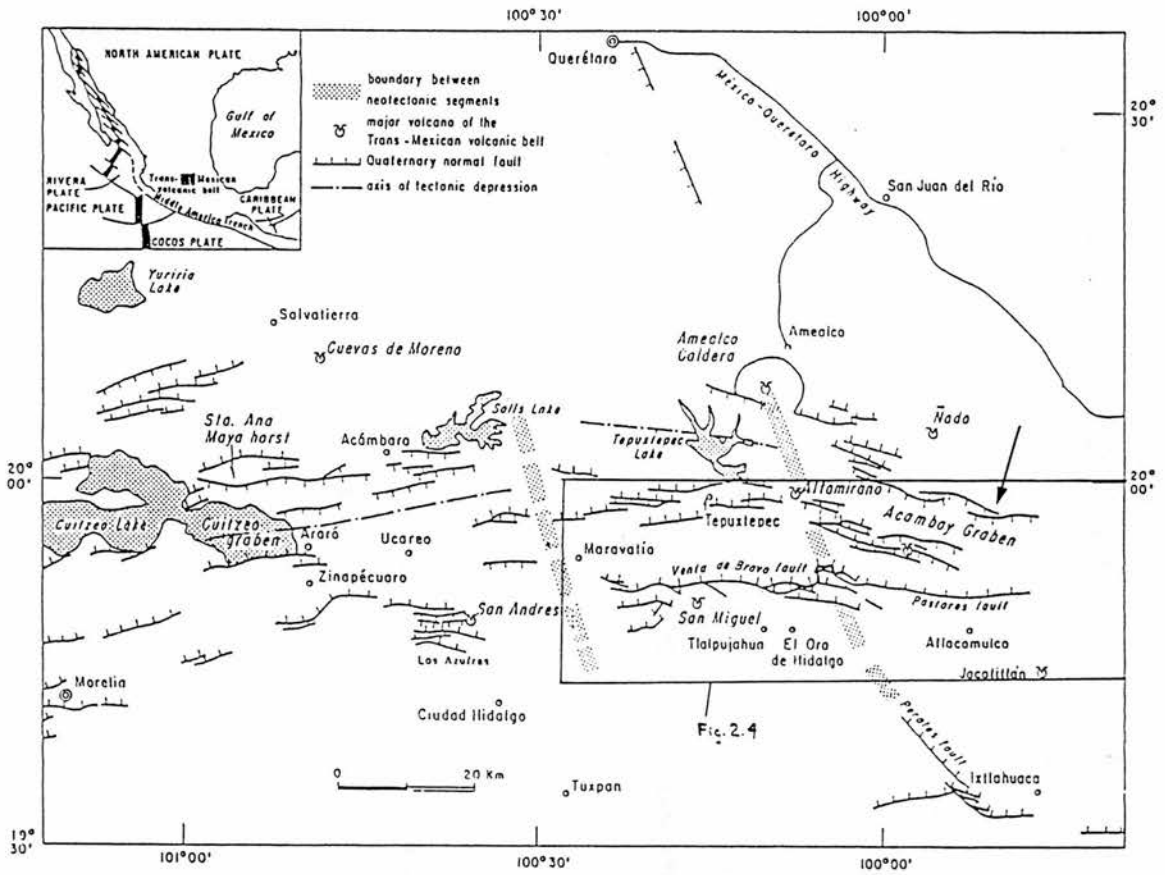

Fig. 2.3. Overview map of late Cenozoic faults in the central part of the Mexican Volcanic Belt (Suter *et al.*, 1992). The Acambay graben is arrowed.

2.3 Tectonics, seismicity and structure of the Acambay graben.

2.3.1 Tectonics and structure.

The east-west trending Acambay graben is considered to be one of the most tectonic active structures of the Mexican Volcanic Belt, and it has been particularly active during the Quaternary (Mooser and Ramírez, 1989). This level of activity is also paralleled by the intensity of volcanism in the area, with several studies (Silva-Mora, 1979; Sánchez-Rubio, 1984; Fries *et al.*, 1977) indicating that volcanic activity in the Acambay graben, which contains several volcanic cones and domes, has been more intense during the Quaternary.

Little research on the structure of the Acambay graben has appeared in the last decade; those studies that have been undertaken (Suter *et al.*, 1991, 1992) show that it is formed by several main faults, namely the Acambay-Tixmadeje, Pastores, Venta de Bravo and Temascalcingo-Altamirano faults. However, there is a lack of agreement regarding the extent of the graben.

Johnson and Harrison (1989) in their regional neotectonic study of the central Mexican Volcanic Belt suggest that the Acambay and Pastores faults together form an east-west trending graben that is aligned along the Chapala-Tula fault zone. They do not consider a further extension to the west of the Acambay graben. Their study shows that the main scarp of the Pastores fault is located about 40 km southeast of the Amealco caldera and that the Lerma River, that crosses this fault, has changed its course several times. This is demonstrated by several abandoned valleys that cut across the upthrown block and intersects its crest. The upper surface of the block south of the fault is now tilted slightly to the south so the flow direction in these blind valleys has reversed since

the formation of the fault. These disturbances of the local fluvial system, combined with an eroded break in slope at the base of the scarp, indicate that faulting was active as recently as the late Pleistocene, and possibly the Holocene. The Acambay-Tixmadeje fault is a major south facing normal fault which is currently active; its eroded morphology indicate that it has been reactivated only recently. The erosion of its scarp indicates that most of the vertical offset on the fault probably occurred in the early Pleistocene or earlier.

Another view of the extent of the Acambay graben is that the Pastores fault can be traced for more than 100 km, from the Maravatío region in the west, to the Santa María Ilucan zone to the northeast. According to Martínez-Reyes and Nieto-Samaniego (1990) the continuity of this lineament to the west is not clear; there are, however, some alignments of volcanoes and cinder cones which may indicate a westward extension. These workers recognise the Pastores, Acambay-Tixmadeje and Temascalcingo-Tepuxtepec-Acámbaro faults. The Pastores fault is considered a normal fault with a 65° north-facing plane that trends E-W, although to the east it is oriented to the NE-SW. The Acambay-Tixmadeje fault is a normal fault 40 km in length, with an ESE-WNW trend and 70° south-facing plane. The Temascalcingo-Tepuxtepec-Acámbaro system of normal faults show a N60°W trend but turn E-W in the area between Tepuxtepec and the volcano of Altamirano. The faults of this system have fault planes with an inclination of up to 80° to the N and S, and they form small graben like the Temascalcingo-San Pedro El Alto graben (Martínez-Reyes and Nieto-Samaniego, 1990).

Perhaps the most detailed work on the structure and tectonics of the Acambay graben was that produced after the 1912 Acambay earthquake, with that by Urbina and Camacho (1913) presenting a detailed field description of the area. Recently, Suter *et al.* (1991, 1992) have suggested that the most prominent structure between Maravatío in the

west and Altamirano volcano in the east is the 45 km long Venta de Bravo fault which has a throw of approximately 600 m. The February 22, 1979, m_b = 5.3 earthquake occurred on this fault (Astiz, 1980) and the late Quaternary vertical slip rate along the easternmost part of the fault is estimated at 2 mm a^{-1}. (Suter *et al.*, 1992). The Venta de Bravo fault is separated in the east by an extensional stopover from the 30 km long Pastores fault. The most recent rupture of the Acambay graben occurred November 19, 1912, in the Ms = 6.9 Acambay event which caused vertical displacements of approximately 50 cm along the faults flanking the graben (Urbina and Camacho, 1913). A minor, but consistent, left-lateral strike slip component along these faults is indicated on various length scales such as palaeomagnetic evidence (Soler, 1990), pull-apart structures, fault surface striations (Suter *et al.*, 1992), and the focal mechanism of the 1979 earthquake (Astiz, 1980).

2.3.2 Seismicity.

Although most of the seismic activity in the Mexican region is concentrated along the adjacent subduction zone, there are some seismic zones within Mexico itself. The Benioff zone of the Cocos plate is associated with earthquakes of up to magnitude 8.5 along the Middle American Trench and under the coast of Mexico. At greater depths (~100 km), where the Cocos plate undergoes tensional stresses due to a change of the angle of subduction earthquakes of M = 7.8 may occur. However, along the Mexican Volcanic Belt only shallow and tensional earthquakes occur with foci between 0-15 km and a maximum M= 6.5-7.0 (Suárez and Ponce, 1986).

A belt of shallow-focus earthquakes in continental Mexico extends several hundred kilometres inland from the Middle American Trench. West of 96° W along the Mexican Volcanic Belt, ongoing work by Suárez, Ponce and Assumpcao (cited in Dewey

and Suárez, 1991) shows normal faulting and reverse faulting mechanisms for shallow intraplate shocks that are quite close to each other. The proximity of the two different modes of faulting may imply that horizontal compressive stresses transmitted from the Middle American thrust interface are approximately balanced by stresses arising from the action of gravity on the high topography of the Mexican Volcanic Belt. The stress relief necessary to maintain the balance is accomplished through the different types of faulting (Dewey and Suárez, 1991). Because of their shallow focal depths, shocks within the overriding North American plate, such as the 1912 and 1920 earthquakes in Central Mexico, have been extremely destructive (e.g. Urbina and Camacho, 1913).

In central Mexico intraplate earthquakes are concentrated on the Mexican Volcanic Belt and along the south-west margin of the Gulf of Mexico. In the Mexican Volcanic Belt, shallow destructive earthquakes have repeatedly affected the cities of Guadalajara, Jalapa and Acambay, and historical reports strongly suggest the city of Mexico has been damage by local earthquakes. The largest earthquake recorded on the Mexican Volcanic Belt Ms= 6.9 was the event near Acambay on November 19, 1912 (Suárez and Ponce, 1986). This earthquake, which affected the towns of Acambay and Tixmadeje also had catastrophic effects in Mexico City where it was classified as a VIII degree event on the Mercalli scale (Yamamoto and Mota, 1991). This level of seismic activity suggests that the Acambay graben is one of the most active seismic zones of inland Mexico.

Local earthquakes are also known from near Araró (May 15, 1845 [Suter *et al.*, 1992]), and in the Ucareo-Zinapécuaro-Acámbaro region (October 1872 to November 1874 [Urquiza, 1872; Ramírez and Reyes, 1873; Orozco and Berra, 1887] cited in Suter *et al.*, 1992). On February 22, 1979, a m_b = 5.3 earthquake occurred 5 km to the north of the town of Venta de Bravo (Astiz 1980) which produced a series of 89 aftershocks,

the largest occurring on 28th February (magnitude m_b = 5.1). The focal mechanisms of three recent events (October 4, 1976; February 22, 1979 [Astiz, 1980]; March 31, 1985) show normal faulting on nodal planes oriented approximately east-west. T axes are nearly horizontal and indicate tensional stress in a north-south direction. This agrees with the orientation of faults and graben mapped throughout the Mexican Volcanic Belt (Suárez and Ponce, 1986).

Detailed monitoring carried out on the western and eastern parts of the Acambay graben during a 3 week period recorded 11 events which were registered and accurately localised. Analysis of the series of earthquakes initiated on the 22nd February 1979 shows a direct relationship between the location of the seismic focus and the trace of the fault zone, while the eleven events monitored appear in groups which may indicate possible N-S lineaments (Yamamoto and Mota, 1991).

A second period of seismic monitoring (two weeks in 1980) revealed a series of twenty one small earthquakes with magnitudes M_L = 2.2 to 3.5 which occurred in the south of the Acambay graben - Toluca valley (19° 12' N - 99° 30' W). The depth of the earthquake foci ranged from 5 to 23 km. Two different groups, separated by an E-W plane show that to the north of this plane the events are deeper (18 - 23 km) than to the south (5 to 14 km deep). The distribution of seismic foci as a function of their depth suggests a block-stepping arrangement descending from the south to the north, and the analysis of fault plane solutions indicates a preferential normal faulting (Yamamoto and Mota, 1991).

2.4 Geology.

The Mexican Volcanic Belt is formed by calc-alkaline volcanic rocks of Pliocene-Quaternary age and is bordered by Oligocene-Miocene ignimbrites and associated rocks of the Sierra Madre Occidental (Fig. 2.4) which form the basement of the region (Auboin *et al.*, 1982). The geology of the Acambay region has been described by Fries *et al.* (1977), Silva-Mora (1979), Sánchez-Rubio (1984) and Suter *et al.* (1991). The oldest outcropping rocks truncated by the Venta de Bravo fault system are folded and slightly metamorphosed Mesozoic sediments (Flores, 1920) which, in the El Oro region (Fries *et al.*, 1977) and at the volcano of San Miguel (Silva-Mora, 1979), are overlain by andesitic-dacitic volcanic rocks (Silva-Mora 1979). Higher in the sequence lake deposits occur south of Canchesdá, and ignimbrite deposits (Las Americas Formation) cover the mainly flat surfaces forming mesas. The ignimbrites, which have a mean thickness of about 50 m, are found north of Tlalpujahua (Fries *et al.*, 1977; Aguirre-Díaz, 1990). The hanging wall of the Venta de Bravo master fault is composed of the lake deposits of the Ixtapantongo Formation (Sánchez-Rubio, 1984), scoria cones with associated basalt flows (Silva-Mora, 1979), and alluvial fan deposits. Although the scoria cones occurring within the study area have not been dated, intercalated palaeosols in cones exhibiting a comparable state of degradation in the nearby Toluca valley have yielded carbon-14 ages of between 8440±70 a and 38950±3210 a (Bloomfield, 1975). This suggests that the east-west trending normal faults of the study area have been active in the late Quaternary (Suter *et al.*, 1992). Further age constraints on seismic activity are provided by the lake deposits of the Ixtapantongo Formation which have a minimum thickness of 5 m and ^{14}C ages of <23 ka (Sánchez-Rubio, 1974). They are displaced by the Pastores fault and are truncated by the Venta de Bravo fault south of Canchesdá (Fig. 2.4). On the basis of an estimated displacement of 50 m and an age of 23 ka for the base of the lake deposits at

Canchesdá, Suter *et al.* (1992) proposed a mean rate of late Quaternary displacement of 2 mm a^{-1} along the eastern section of the Venta de Bravo fault.

At the eastern end of the Pastores fault, near the town of Yondejé, rocks of the Yondejé andesite formation, which consists of massive porphyritic lavas with a K-Ar age of 13 Ma have been displaced by faulting (Sánchez-Rubio, 1984). Although the trace of the fault in these rocks is not continuous, there are some lineaments which appear to follow the general east-west trend of the Pastores fault. The Yondejé andesite formation is one of the most extensive lithological units in the Acambay graben. It outcrops from the town of Acambay southwards to the south of Yondejé, creating a north-south ridge which encloses the eastern end of the valley formed by the Acambay graben.

The Atlacomulco lithological unit (Early Miocene) is also truncated by the Pastores fault. These volcanic rocks appear to be mineralogically comparable to the Yondejé andesites except that they are aphyric (Sánchez-Rubio, 1984). The two formations also have a different polarity, which indicates that they are not contemporaneous (Soler, 1990).

The Pleistocene Atlacomulco andesites form a lava field which appears partially to cover the Pastores fault as well as the lacustrine tuff beds in the area of Atlacomulco.

The scarp of the Pastores fault is formed in grey aphyric basaltic andesites (the Pastores volcanics (Upper Miocene?)). These rocks appear to be partly mantled by andesitic conglomerates and pumice-rich tuffs. At the western end of the Acambay-Tixmadeje fault the La Loma andesite (Pliocene) has been brought into contact with pumice fall-out deposits (K-Ar age < 5 Ma) (Sánchez-Rubio, 1984), although the fault does not continue into the alluvium of the Lerma River to the west.

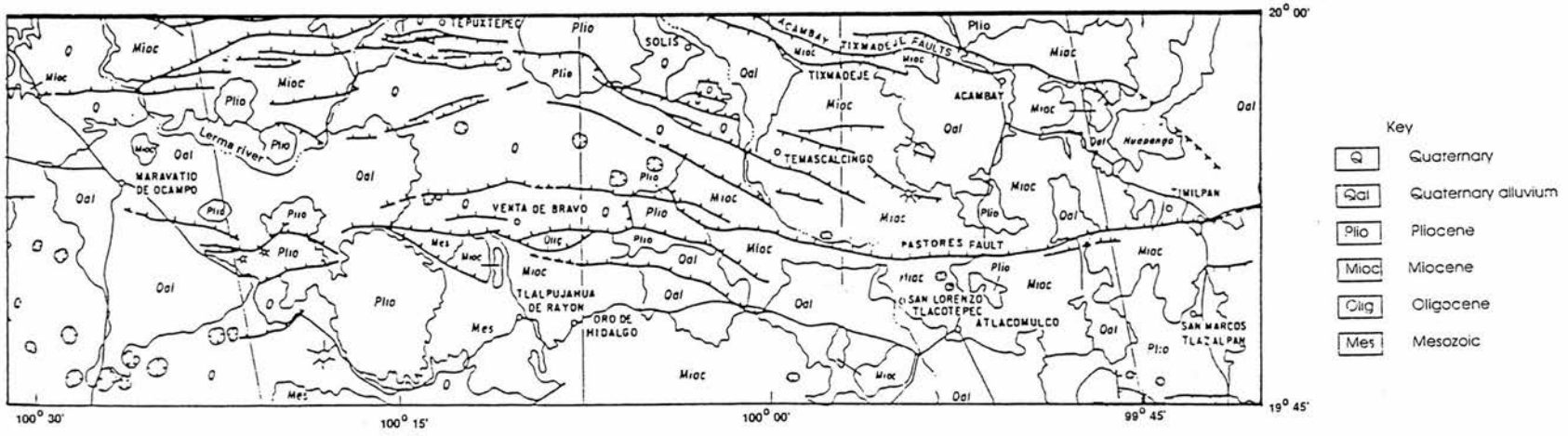

Fig. 2.4. Geological map of the Acambay graben (from Martínez-Reyes and Nieto-Samaniego, 1990).

The volcano of Temascalcingo is a complex structure formed by massive andesitic lavas as well as by a thick agglomerate of andesitic composition. The northern flank of Temascalcingo is mainly composed of a thick agglomerate, which appears to lie on massive aphyric andesites underlain by dacitic lavas. By contrast the southern part of the volcano is almost wholly composed of massive aphyric andesite. A dome-like body of dacitic composition (K-Ar age 8.5 Ma (Sánchez-Rubio, 1984)) occurs inside the graben by the eastern foot of the volcano, where it is partly mantled by tuffs and alluvium.

In the central part of the Acambay graben there are Quaternary rhyolitic lavas truncated by ESE-WNW trending faults and forming lava domes with a K-Ar age of 1.57 ± 0.15 Ma according to Demant and Robin (1975). Several areas in the Acambay region are also covered by the Amealco ignimbrite which has a K-Ar age of <5 Ma (Sánchez-Rubio, 1984). This is a product of the Amealco caldera, an andesitic-trachydacitic Pliocene volcanic centre located 15 km north-west of the western end of the Acambay- Tixmadeje master fault. The southern extremity of the caldera is cut by ESE-WNW normal faults and is covered by alluvium of the Lerma River (Suter *et al.*, 1991).

Chapter Three: Large-Scale Tectonic Geomorphology from Satellite Imagery

3.1 Introduction

The availability of remotely sensed satellite data since the early 1970s has significantly assisted the study of many aspects of the Earth's surface. Both reconnaissance and more detailed geological and geomorphological mapping programmes have benefited from the ready availability, the low cost, extensive coverage and multispectral nature of the data, most notably those collected by the Landsat satellites. As well as recording information in selected wavelength ranges of the visible area of the electromagnetic spectrum, satellite imagery is sensed in infrared wavelengths whose data analysis has yielded invaluable, new sources of information for structural mapping. In addition to being available in analogue form, that is, as in the case of aerial photography, satellite data are provided in digital form that enables their spectral and radiometric resolution to be exploited even more fully and extraction of their information content to be maximised by computer analysis using digital image processing methods.

Analysis of remotely sensed satellite data provides economically synoptic statistical information on geomorphological-geological features known as lineaments. The word lineament is used here to denote those features that represent segments, straight or arcuate, that might include faults, fractures, joints, any of which can produce lithological discontinuities. Lineaments observed in the Acambay graben are not only straight lines but also arcuate features. Image interpretation follows several steps from data acquisition to data analysis and these stages are summarised schematically in Figure 3.1.

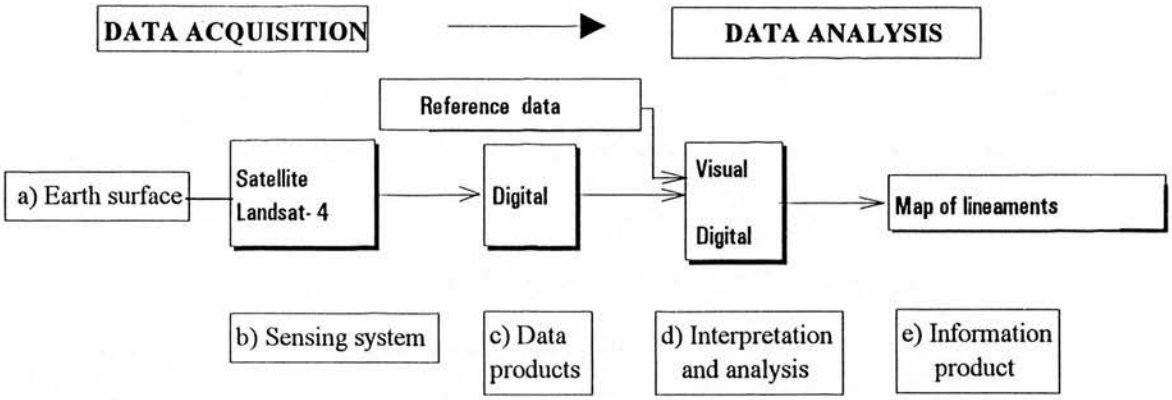

Fig. 3.1 Remote sensing of tectonic features (modified from Lillesand and Kiefer, 1987).

Several workers have demonstrated the utility of satellite imagery in neotectonic studies. Ford *et al.* (1990) detected previously undocumented faults in the east and central Mojave Desert region of California using Landsat TM images enhanced by a four-component processing technique. Ghosh and Viswanathan (1991) studied the tectonically active Mendha River basin, India, applying Landsat TM images for the extraction of neotectonic features through the digital analysis of the principal component and directional filtered images. Oakes (1988) has described a system to explore the feasibility of automatically performing low-level, routine recognition of lineaments.

Satellite imagery has previously been used for geologic and structural purposes in the study of the Mexican Volcanic Belt. For instance, Mooser and Ramírez (1989) and Ramírez (1990) have detected lineaments in the central and eastern parts of the Mexican Volcanic Belt and discovered previously unmapped regional linear features and major circular features using Landsat TM images. In another study Johnson (1987) has applied computer enhancement techniques to detect and determine neotectonic features in Central Mexico. The objectives of this chapter are to extract and map neotectonic features from digitally enhanced Landsat TM images along the Acambay graben, and to determine the main fault trend in this area.

3.2 Data and methodology

3.2.1 Data acquisition

Satellite images, lineaments and tectonic features in the Acambay graben were extracted from a LANDSAT- 5 Thematic Map per image, which was acquired on 14th March 1986. Landsat - TM data have been sensed in 7 spectral bands obtained from the Instituto de Geografía, Universidad Nacional Autónoma de México, Mexico city.

3.2.2 Data processing system

The digital analysis of the remotely sensed data was carried out using ERDAS version 7.4 software which was mounted on a PC workstation and a UNIX workstation. More detailed information on ERDAS and its applications is available in the ERDAS Manual and Field guide.

3.2.3 Image processing

Image enhancement is the process of making an image more interpretable for a particular application. Image enhancement procedures were applied to image data in order to assist subsequent visual interpretation. However, there are no simple rules for producing the single "best" image for lineament extraction. Several enhancements were necessary from the same "raw" image to interpret neotectonic features.

The computer processing involved a series of techniques that have proved to be useful in lineament detection (Gillespie, 1980; Lo, 1986; Johnson, 1987; Ford *et al.*, 1990; Ghosh and Viswanathan, 1991). These techniques include:

i) Colour enhancement

-false colour compositing

ii) Contrast enhancement

iii) Edge enhancement

-spatial filtering

iv) Multi-image enhancement

- IHS- intensity-hue-saturation transformation
- principal component analysis
- band ratioing

i) Colour enhancement

The use of colour images can dramatically increase the amount of information that can be displayed. Normal and false colour composites are used to display three images of a scene (Lillesand and Kiefer, 1987). A false colour composite image is generated by using any three spectral components (the TM has seven) combined using appropriate colour filters (with a primary colour red, green and blue R, G, B) (Fig. 3.2). The variations in the spectral response of objects in these three bands result in colour differences which aid in the object's identification (Curran, 1985).

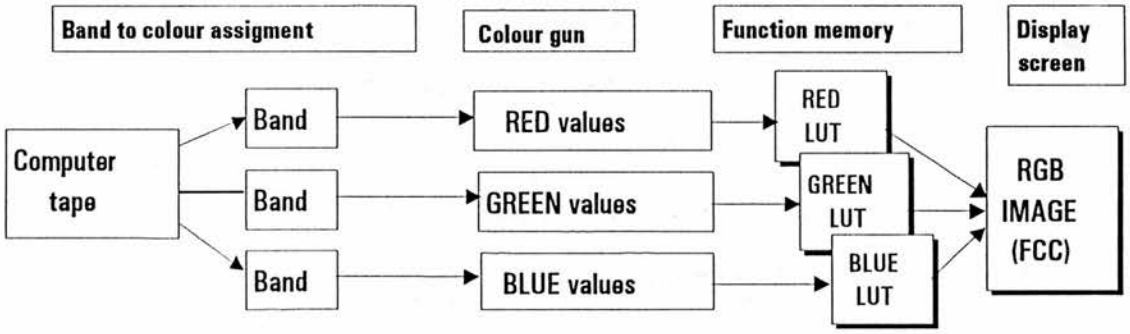

Fig. 3.2 Colour display process.

ii) Contrast enhancement

Image displays and recording devices typically operate over a range of 256 grey levels (the maximum number represented in 8-bit computer encoding). The purpose of contrast stretching is to expand the narrow range of brightness values typically present in an input image over a wider range of grey values by using the display capabilities of the computer hardware. Through careful adjustment, the result is an output image that is designed to accentuate the contrast between features of interest in the image interpretation (Lillesand and Kiefer, 1987).

iii) Edge enhancement

Edge enhanced images attempt to preserve both local and low frequency brightness information. They are produced by adding back all, or a portion, of the grey-values in an original image to a high-frequency component image of the same scene in accordance with a specific set of rules.

iv) Multi-image enhancement

a) Intensity-hue-saturation (IHS) colour space transformation

As explained earlier, digital images are typically displayed as additive colour composites using the three primary colours: red, green and blue (RGB) (Lillesand, 1987). An alternative to describing colours by their RGB components is the use of the intensity-hue-saturation (IHS) system. Intensity refers to the total brightness of a colour. Hue refers to the dominant average wave length of light contributing to a colour. Saturation specifies the purity of a colour relative to grey. Transforming RGB components into IHS components before processing provides more control over colour enhancements (Lillesand and Kiefer, 1987). Such transformation was useful as an intermediate step in image enhancement.

b) Principal component analysis

The problem of optimising the information context of the multiple spectral bands of a scene can be eased if the information that is particular to each image is

combined into a new image by means of a statistical transformation. The most popular procedure for the transformation of multispectral images is the statistical techniques of principal component analysis (PCA) (Curran, 1985). This technique aims to replace the original spectral bands that describe the data with a mathematically calculated set of new data that is based in the original data and better describe the particular scene under study (Curran, 1985; Drury, 1987).

c) band ratioing

Ratio images are enhancements resulting from the division of digital number (DN) values in one spectral band by the corresponding values in another band. A ratio-image of the scene effectively compensates for the brightness variation caused by the varying topography and emphasises the colour content of the data. Ratio-images are often useful for discriminating subtle spectral variations in a scene that are masked by the brightness variations in images from individual spectral bands or in standard colour composites (Lillesand and Kiefer, 1987).

Ratio-images can be combined in RGB components to generate false-colour ratio images. Ratioing has been successfully employed for geological applications (Gillespie, 1980; Drury, 1987; Johnson, 1987; Crippen, 1989; Ford *et al.*, 1989, 1990). Despite the problems presented during the process of ratioing (Drury, 1987; Johnson, 1987) this method has proved to be one of the most useful because it enhances subtle tonal variations and allows the discrimination and mapping of many types of surface materials that do not display strong visible colour contrasts (Ford *et al.*, 1990).

Ratio enhanced images have allowed the recognition of faults which are visible in images by abrupt linear colour or textural discontinuities (Crippen, 1989; Ford *et al.*, 1990). Thus, ratioing could be extremely useful when the appropriate band-ratio selection is performed.

3.3 Data analysis and interpretation

3.3.1 Analysis

The analysis was carried out in two parts. The first involved digital processing of the TM data formed by 1088 rows and 2224 columns in six spectral bands (1 to 5 and 7) covering the study area (19° 45'-20° 00' N and 99° 40'-100° 15' W), and the adjacent area to the south. Different image interpretation techniques were applied to extract neotectonic features. The analysis was conducted on full resolution 512 x 512 pixel sub-scenes. The second part of the analysis involved relating some of the previously identified tectonic features to those derived from digital analysis or interpretation.

i) Colour enhancement

In this study, many band combinations where tried prior to the selection of those that seemed to yield the best contrast in topography and separation of rock units. All spectral band combinations are assigned in the order red, green and blue order (R G B). Each scene was depicted in different combinations (Table 3.1).

FCC (before digital processing) in RGB order	Results
4,3,2 *	Identification of some features with grey shadows is reasonably clear. Some lineaments are visible. Geology is not clear. Identification of topography is possible.
4,3,7	Identification of some features is reasonably clear. Lineaments still visible. Vegetation coverage is less evident than in the previous colour combination. Geology is not clear. Topography is less evident. Clarity of features seems to be diminished.
7,4,2 *	Close to the natural. Vegetation very clearly depicted. Topography is clear. Identification of great lineaments is possible. Geology is not clear.
4,5,2 *	Identification of features with dark shadows is clear. Topography is clear. Great lineaments are partially visible. Vegetation is discernible. Good for geomorphology.
7,4,1	Close to the natural. Vegetation clearly depicted in green colour. Clarity of features. Geology is clear. Slopes depicted with shadows. Colourful. Easy to interpret. Good for geomorphology.
4,5,7	Not good definition. Vegetation is less clear. Geology is lost.
7,5,4	Good definition. Difficult to interpret. Topography is less clear.

Table 3.1 False colour composites - combinations. (*) Best RGB combinations.

The 4,3,2 standard combination (R G B) allowed the identification of topographic features with grey shadows and slopes were partially discernible. Some lineaments were visible. Vegetation was depicted in red and water elements were also visible. This combination proved to be useful for the identification of topographic features after improving the contrast stretch of each band.

The 4,3,7 combination was found to be inferior to the alternative standard combination, with the clarity of features being inferior. The 7,4,2 combination was found to be close to natural colours after contrast stretching. Topography was clearly depicted, vegetation was visible and appeared as in red, and the lithology was easily identified. Another combination that was often found to be useful was that of bands 4,5,2. This combination allowed the identification of features with dark shadows. Topography was very clear, scarps were well defined and lineaments could be identified. Vegetation was also clearly depicted. This image seemed to be one of the most useful for the interpretation of geomorphology because of the good definition of topography. The results of false colour composites-combinations are summarised in table 3.1. FCC were used together with further procedures of image enhancement (Fig. 3.3).

ii) Contrast enhancement

For each image the characteristics of the grey-scale histogram are unique, and they also vary considerably between the different spectral bands of an image. The standard deviations of the histograms varied from a minimum of 11.48 grey levels (for band 2) to a maximum of 49.62 (for the band 7). Table 3.2 shows the characteristics of the grey-scale histogram of each band.

band	minimum data value	maximum data value	mean value	standard deviation	media	mode
1	43	208	86.65799	17.7662	88	89
2	8	98	41.07705	11.48975	42	43
3	13	139	59.95504	20.41628	63	69
4	5	151	64.01306	13.77257	64	66
5	0	214	117.0775	38.7519	124	127
7	0	194	124.9917	49.62705	150	160

Table 3.2. Characteristics of the grey-scale histograms from bands 1 - 5 and 7.

A larger standard deviation means a broader grey-scale histogram, which directly translates into a greater contrast in the image. Band 7 exhibited the highest contrast in all the digital images, with band 2 generally showing the least contrast. These characteristics are important in terms of band-selection for colour composite images.

Contrast stretching was performed for each band. This procedure improved the image contrast and aided interpretation. Contrast stretching was use in each case before and after the edge enhancement process that is discussed below.

iii) Edge enhancement (spatial filtering)

Lineaments of geological significance, such as faults, topographic crests and valleys, and structural contacts can be sharpened using edge enhancement. Edge enhancement was achieved in three basic steps:

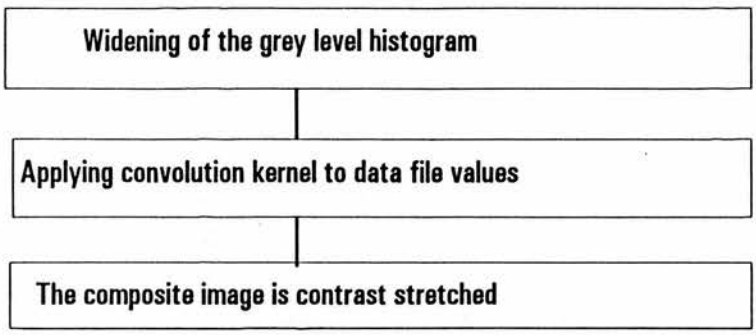

1) The raw data were moved to the mid-range of the grey scale prior to the edge convolution, to solve the problem related to the generally low average radiance of the TM scenes (Fig. 3.4).

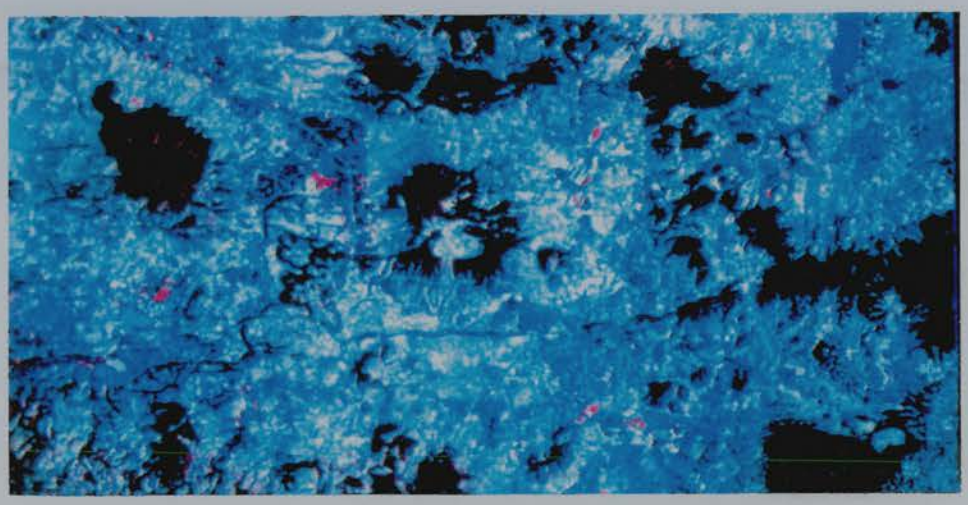

Fig. 3.3 False-colour composite combination using bands 4,5,2 in red-green-blue order. Central and eastern parts of the Acambay graben.

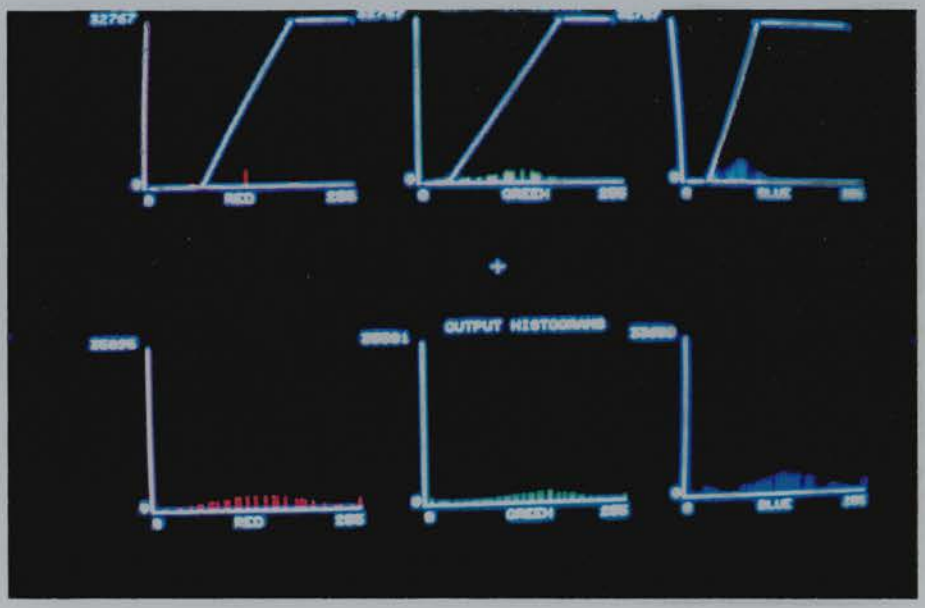

Fig. 3.4 Histograms before and after edge enhancement. Upper histograms in red-green-blue order - before contrast stretching, and lower histograms - after contrast stretching.

2) The image was then convoluted using carefully selected convolution kernels (Table 3.3).

3) The composite image was contrast stretched.

NAME	KERNEL	PROCESS	RESULT
Edge	-1 -1 -1 1 -2 1 1 1 1	FCC Contrast stretching Filtering	Enhance edges. Easy to identify linear features and linear pattern.
Laplacian	-1 -1 -1 -1 8 -1 -1 -1 -1	FCC Filtering	Difficult to understand. Too many lines.
3 x 3 minhi	-1 -1 -1 -1 16 -1 -1 -1 -1	FCC Filtering	Smooth the image. Loss of topography.
3 x 3 medhi	-1 -1 -1 -1 12 -1 -1 -1 -1	FCC Contrast stretching Filtering	Edges are clear and sharp. Easy to interpret. Very useful for edge detection.
High pass	0 -5 0 -5 3 -5 0 -5 0	FCC Rationing Filtering	Smooths the topography but brings out edges.

Directional	0 -1 -2 1 0 -1 2 1 0	FCC Contrast stretching	Brings out edges
Noise	1 1 1 1 2 1 1 1 1	FCC Filtering	Smooths the image. Good when applied after edge enhancement.
Edge enhancement	-1 -1 -1 -1 17 -1 -1 -1 -1	FCC	Brings out edges but smooths topography.

Table 3.3. Convolution kernels.

Filtering was performed applying a kernel to an image on the screen and the file. As a result of the filtering process described above, the enhanced images displayed much greater detail and sharpness than the unenhanced images (Fig. 3.5). The filtering process was applied after other enhancement procedures such as band ratioing, principal component analysis and intensity-hue-saturation (IHS) colour space transformation. One of the most useful filters was the "Edge" filter which enhanced edges and here linear patterns were easily identified. When this filter was applied to one source channel the topography was still visible. When applied to all source channels it smoothed the topography but brought out edges. The results of this process are described below.

iv) Multi-image enhancement

a) IHS- intensity-hue-saturation transformation

IHS transformation was performed using mathematical functions in ERDAS. The IHS transformation was developed in several steps (Fig. 3.6).

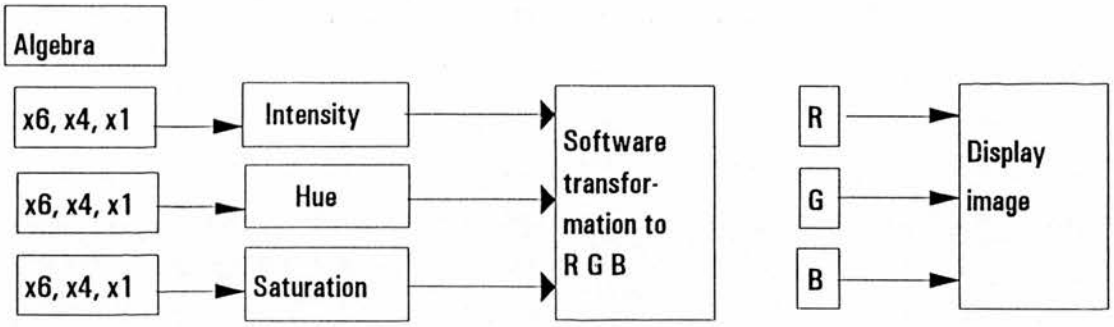

Fig. 3.6 Intensity-Hue-Saturation process.

The most useful combination for IHS transformation was x7,x4,x1 then applying an edge enhancement filter (Fig. 3.7). This composite image shows lineaments depicted in blue. These lineaments were in many cases fault-scarps. Although the topography is suppressed, elevated areas were depicted in green. The geology, however, was not very clear. It was also found useful to display the image in 3,2,1 (RGB) order, the IHS image then being contrast stretched.

Fig. 3.5 Filtered image. This is a convoluted image applying an edge enhancement kernel.

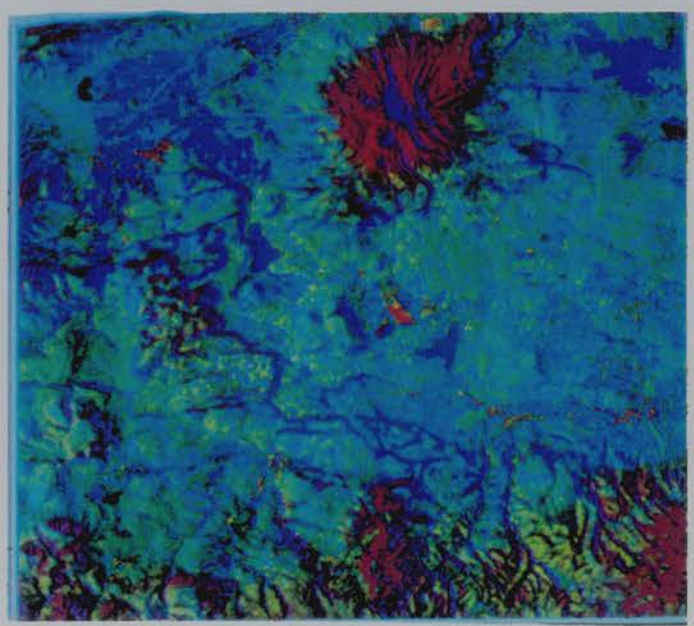

Fig. 3.7 IHS image using an x7,x4,x1 algebraic combination and an edge enhancement filter.

b) Principal component analysis

Principal component analysis was performed on several bands and the covariance matrix for each band was also calculated (Table 3.4). Principal components may be displayed in any RGB combination to produce a false-color image.

BANDS	1	2	3
1	727.54	641.70	351.78
2	641.70	1405.36	790.38
3	351.78	790.38	457.44

Bands	Eigenvalues	Var. %	Total %	Angle	Scale
1	2213.36	85.45	85.45	17.67	1
2	367.41	14.18	99.63	72.92	1
3	9.56	0.37	100.00	85.64	1

Eigenvectors:

1	2	3
0.44	0.90	0.02
0.78	- 0.37	- 0.50
0.44	- 0.24	0.87

Table 3.4. Principal components. Covariance Matrix for the Landsat TM image (bands 4,3,2).Table 3.4. Principal components. Covariance Matrix for the Landsat TM image (bands 4,3,2)

The generation of a principal component image (PC) was performed by loading the TM data of bands 4, 3 and 2 at three different planes. The 4,3,2 standard combination (R G B), was also useful for principal component analysis (PC). PC1 and PC2 extracted a high proportion of information whereas the lower-order components contributed very little. The percentage of variance in PC1 was 85.45 per cent whereas in PC2 it was 14.18 per cent and in PC3 0.37 per cent. The image for principal component was displayed and all images (PC1, PC2 and PC3) were loaded in different planes to produce and enhance the colour composite. This composite principal component image highlighted the characteristic differences between rocks, drainage, vegetation and topography. Different combinations were tried to select the best image for lineament interpretation (Table 3.5). The results show that the best combination was PC1, PC2, PC3 in the RGB channels respectively (Fig. 3.8).

Principal component combinations	Results
PC1, PC2, PC3	Topography is fairly clear. Identification of features is reliable.
PC3, PC2, PC1	Identification of features is difficult. Difficult to interpret.

Table 3.5. PCC combinations.

Fig. 3.8 Principal component image.

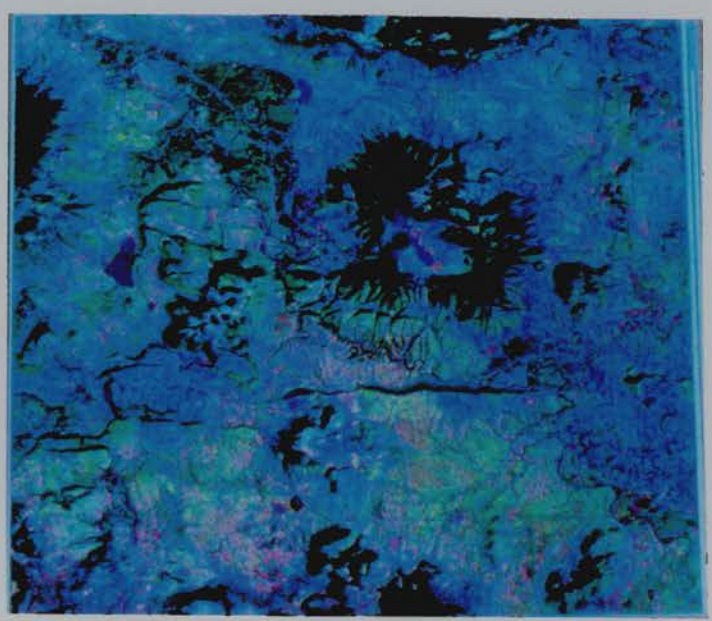

Fig. 3.9 Ratio-band image using band ratios 5/7, 5/4, 3/1 combined in red-green-blue colour respectively.

c) Band ratioing

The band-ratioing process involved the following steps:

1) each of three band ratio channels was modulated by the band-average reflectivity

2) ratioing was performed by dividing the values in one band/colour gun from another.

A combination of simple box-filters was used to suppress scan-line noise in Landsat TM images. Removal of these problems resulted in image products that were more readily interpretable.

The selection of spectral bands for the different ratio images began with information found in the literature on the most useful band ratios. Band ratios 5/7, 3/2, 4/5 and 2/5 were determined to be useful for discrimination and mapping of iron oxidation, vegetation communities, and for relating image spectra to mineralogy (Johnson, 1987). The equivalent differences (5-7, 3-2, 4-5, and 2-5) were tried for the east-central part of the Mexican Volcanic Belt (Taxco) by Johnson (1987) but a fourth difference, 7-3, seemed well suited for discrimination of vegetation types, which in turn were thought to be useful for lithological mapping using geobotanical characteristics (Johnson, 1987). According to Crippen (1989) band ratios 3/1, 5/4, 5/7 are preferable for lithological discrimination. Ford *et al.* (1990) used band ratios (5/7, 5/4, and 3/1) which emphasised compositional differences of the rocks . The capability of ratioing for tracing lithology and delineating areas of alteration might point to mineralization and/or faulting. After the most likely candidates were tested, additional expressions were tried experimentally, based on visual estimations of brightness contrast between bands.

The most useful ratios are the equivalent of bands 5/7, 5/4, 3/1 combined in a colour RGB respectively (Fig. 3.9). This image clearly shows lineaments by deep green colour and shadows, and water elements are depicted in blue. This band-ratio

image also preserves and primarily enhances topographic features. New lineaments not observed before seem to be enhanced in this image. When adjusting the scaling, this step enhanced small features and showed small linear features. However, the clarity of regional lineaments was less evident. Lithology was clear with metamorphic rocks being depicted in red-purple while volcanic rocks appeared grey-blue. Drainage patterns were also well depicted. The visual identification of features on the band-ratio images were further enhanced by contrast stretching.

Diverse filters were applied to the ratio image for edge enhancement and noise removal. 'High pass' filters smoothed small features and brought out large lineaments. 'Edge' filters were found to be useful for the identification of large lineaments since they enhanced edges but smoothed the topography. 'Edge enhancement' filters brought out the edges and preserved the topography. This process resulted in an image that was easy to interpret. The 'edge enhancement' filter was found to be the most useful for the band-ratio image. It was also found to be the most useful for further band-ratio enhancement of images.

The application of the techniques previously described for edge enhancement demonstrated that there is not a simple 'rule' for using one procedure in edge enhancement. Only through experimentation involving several techniques can the most useful image for the identification of neotectonic features be identified.

3.3.2 Interpretation

The use of satellite-imagery provided a regional view of the study area and enabled regional lineaments to be identified. Features of geological significance on Landsat images, such as faults, topographic crests, and valleys, as well as lithological and structural contacts, were sharpened using the edge enhancement procedures described above. The interpretation of these lineaments was supported by field work observations.

The primarily purpose of this study was to detect and map active or recently active faults from the interpretation of TM images (that is faults that could clearly be shown to cut, or offset, deposits of Pliocene-Quaternary age). Various criteria were used in this study to distinguish young faults from numerous other forms of linear features that are invariably present on satellite images. Features indicative of recent or renewed faulting (fault scarps) include:

1. Relative displacement of Quaternary deposits. The Acambay graben is a region with a youthful volcanic cover. The generally smooth surfaces of these deposits (or predictably rough surfaces such as the cones of volcanoes) clearly display any disruption caused by faulting. As a subset of these features, offsets of young erosional or depositional surfaces (alluvial surfaces), were also included.
2. The presence of scarps in unconsolidated deposits; such scarps are relatively rapidly degraded by erosion.
3. Frequent earthquakes are clear evidence for continued deformation, and shallow earthquakes may be related to recent or active faults exposed at the surface.
4. Two additional features strongly indicate recent faulting where no significant variations exist in the erosional resistance of rocks on either side of a fault. The first is an increasing stream gradient as the fault line approaches (a "wine-glass" or "hour-glass" valley), which results from rejuvenation of the stream near the fault when renewed fault movement occurs. If the movement is rapid enough to exceed the rate of stream erosion, the stream bed is actually separated in a "hanging valley", the second indicative feature (Johnson and Harrison, 1989).

During the interpretation of the TM images the undiscriminating tracing of alignments of various unrelated geomorphological features and/ or tonal contrast (image "lineaments") was avoided. These types of feature are of questionable value, primarily because of their non-unique causes and the consequent difficulty in explaining their origin or relationship to specific geological or tectonic events.

Lineaments enhanced with digital remote sensing techniques were selected based on the criteria listed above and manually transferred to the topographic maps (scale 1: 50000) of the study area. During this process discriminant analysis was utilised; only those lineaments that were expressed in the topography were considered to have structural associations and included in the map for further analysis (Fig. 3.10). The topographic maps were used to help determine the approximate offset on faults with near vertical displacement, and the direction of throw on faults where this was not easy to determine on the images. Mapping of the satellite-enhanced lineaments showed that the majority are expressed on the surface as scarps, fault-controlled river valleys, alignments of positive forms (e.g. cinder and lava cones), linear and rectangular drainage patterns, and changes in relief (Thornbury,1969).

Subsequent field reconnaissance at several locations both throughout the Acambay graben and to the north and south generally confirmed the image interpretations, and no significant modification was necessary. In order to corroborate image interpretation, field reconnaissance was performed during a field season in 1991. More than forty sites were visited in the field . Observations of features indicative of Quaternary faulting were collected at 45 sites along the southern flank of the graben, in several sites along the Pastores and Venta de Bravo fault system, in the inner graben, along the Temascalcingo faults and in the alluvial basins of the Valle de los Espejos, Toxi, and Lerma rivers, around lakes Tepuxtepec and Maravatío, and in the northern flank of the graben, along the Acambay-Tixmadeje and Tepuxtepec faults.

The length and the orientation of each lineament were measured and computed. In order to provide an accurate analysis of the trend of the lineaments, faults forming the northern and southern flanks of the Acambay graben were measured in small sectors according to their sometimes subtle changes in orientation.

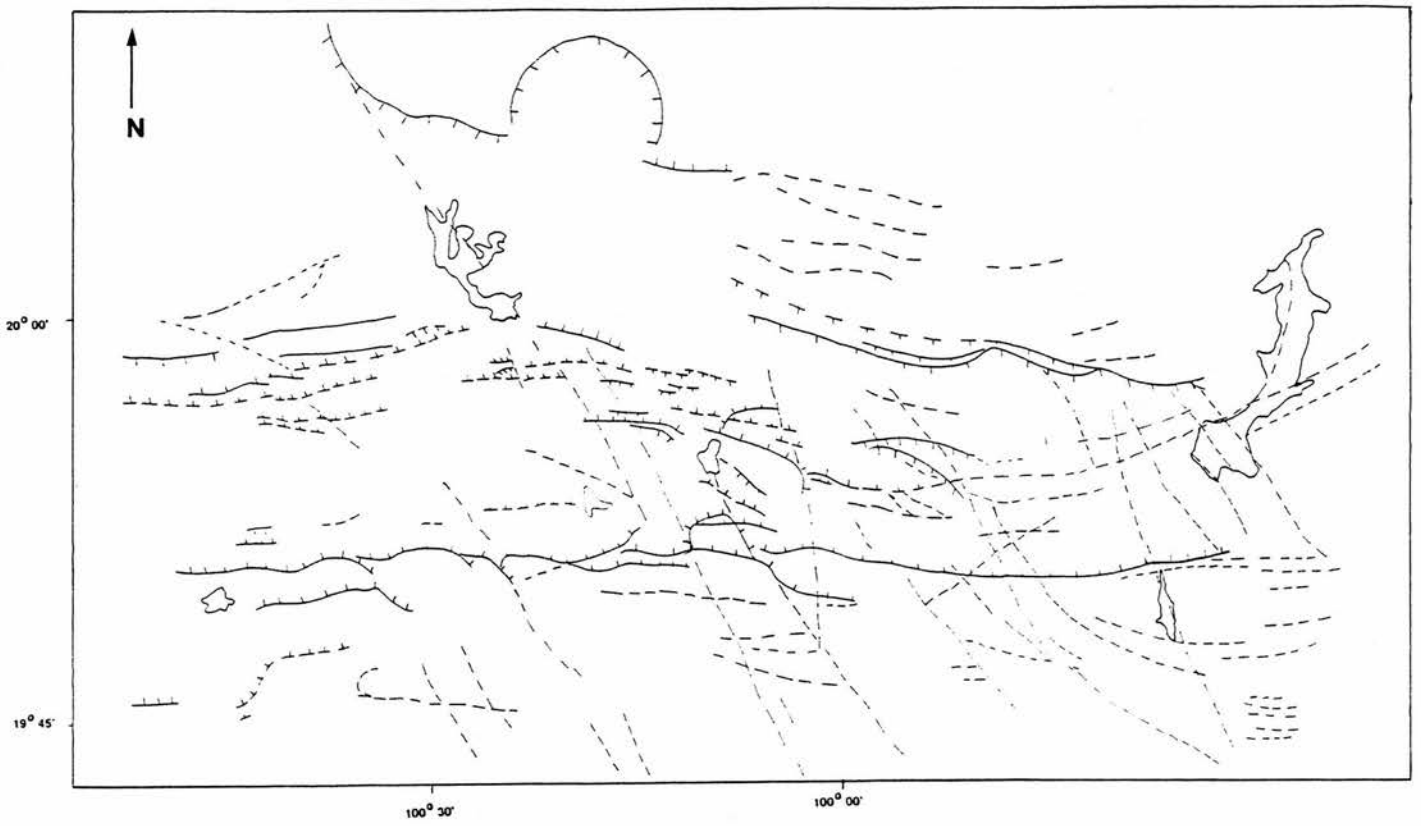

Fig. 3.10 Map of lineaments. Lineaments detected from digitally enhanced Lansat TM image applying a combination of filtering techniques, PCC, IHS, and band-ratioing.

Different trends were clearly recognised in the map of lineaments (Fig. 3.10), as illustrated in Figures 3.11 to 3.14. The interpretation of the main trends was based on the statistical analysis of the lineaments (Berhe and Rothery, 1986; Vergeley and Zadeh-Kabir, 1988; Rabie and Ammar, 1990; Alexander and Formichi, 1993) involving correlation with data on tectonic trends for the Mexican Volcanic Belt (Mooser, 1969, 1986; Mooser and Ramírez, 1989, Johnson, 1987; Johnson and Harrison, 1990, Pasquaré *et al.*, 1987; Martínez-Reyes and Nieto-Samaniego, 1990; Ramírez, 1990; Suter *et al.*, 1991, 1992).

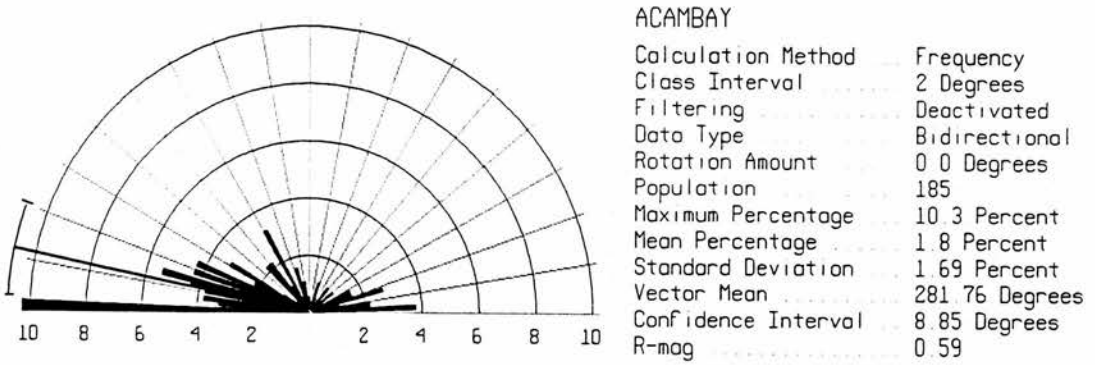

Fig. 3.11 Rose diagram, produced from lineament interpretation of the enhanced images of the TM scenes, showing the preferential orientation of the whole lineament network. "T" vector shows the mean and preferential rank.

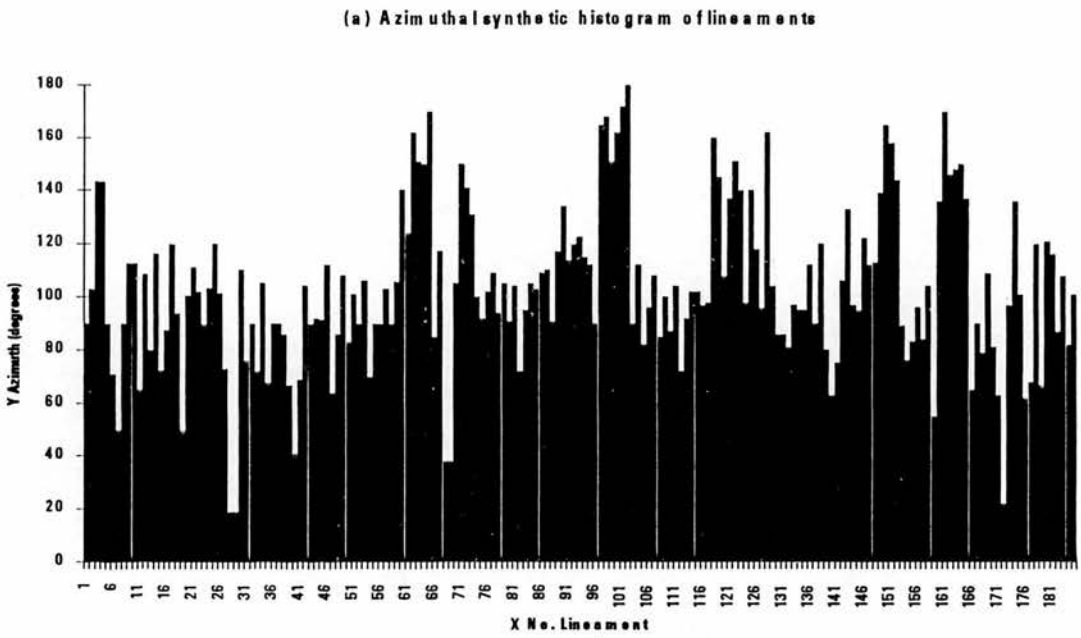

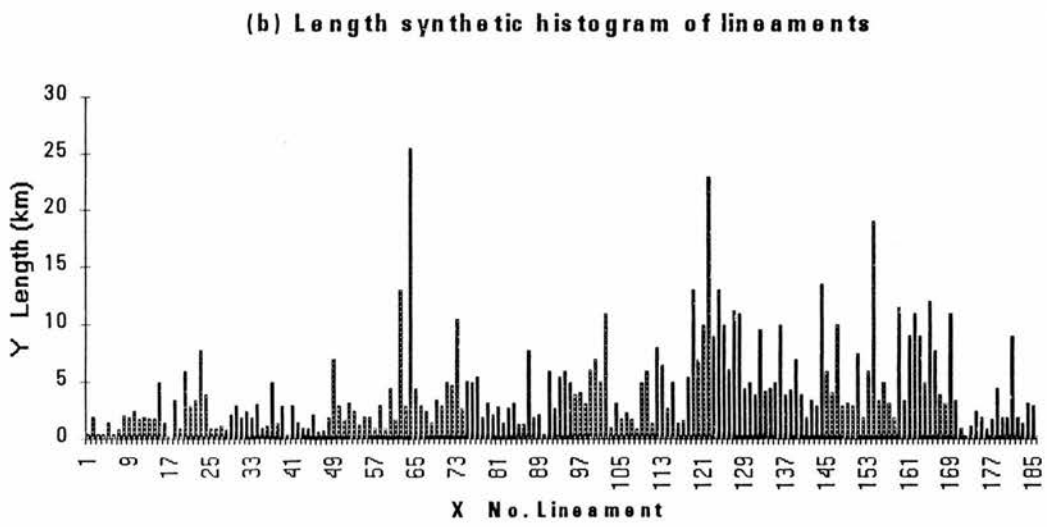

Fig. 3.12 a- Azimuthal synthetic histogram of lineaments as inferred from the interpretation of enhanced satellite images; b- Length synthetic histogram of lineaments.

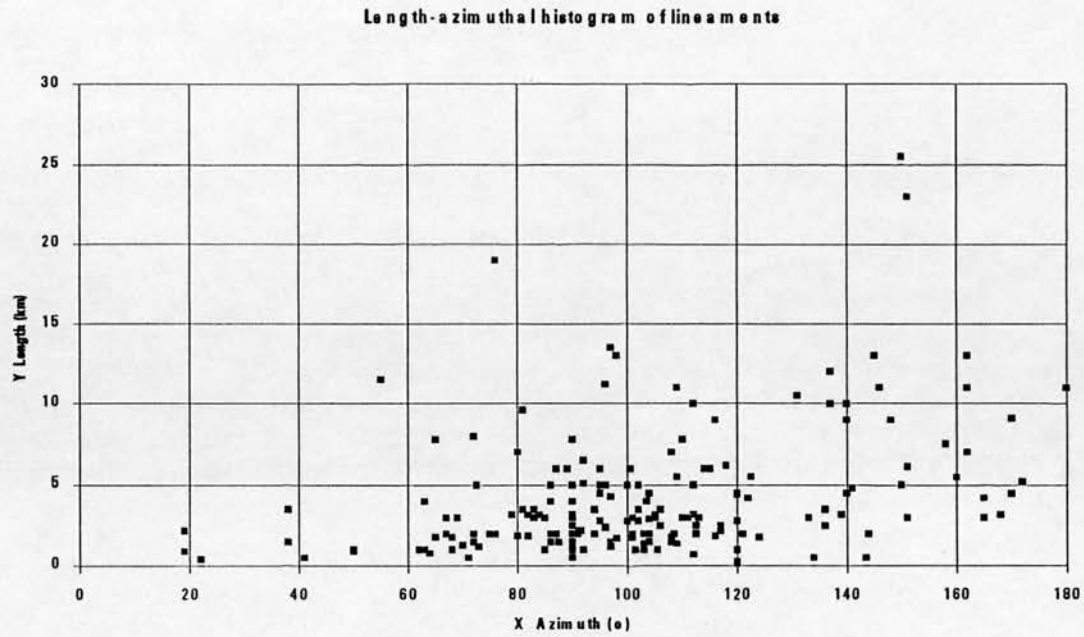

Fig. 3.13 Length-azimuthal histogram of lineaments.

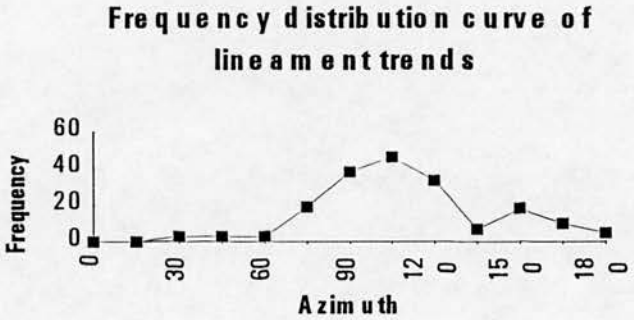

3.14 Frequency distribution curve of the main lineament trends in the Acambay graben.

Statistical analysis of the measured rectilinear segments (a total of 185 lineaments) shows an azimuthal average of 103.16° and a mean length of 4.28 km. The maximum and minimum azimuthal values are 180° and 19° respectively, and the mean azimuthal value (indicating the central tendency of the lineament orientation in

the Acambay graben) is 101.76°. The standard deviation is 1.69% and the lengths of the individual lineaments show that the maximum length is 25.5 km and the minimum is 0.25 km.

The rose diagram and histograms of the lineaments in the Acambay graben shows the prevalence of the ESE -WNW domain (lineaments related to preferential orientations) (Fig. 3.11). The majority of lineament lie between the 90° and 120° (Fig. 3.11 and 3.12 a, 3.14), but some of the largest lineaments seem to be preferentially oriented E-W (Fig. 3.11). Although not very numerous there are long individual lineaments orientated ENE-WSW, ESE-WNW and NNW-SSE (Fig. 3.13). The vector mean clearly indicates a 101.76° central tendency (Fig. 3.11). More minor domains, E-W and NNW-SSE (N 30° W), are also identifiable in the distribution. Beside these domains small secondary peaks are also present whose significance will become apparent in the regional analysis.

The results of the analysis allowed indicate six main trends for lineament domains in the Acambay graben area, namely:

1) E-W
2) ESE-WNW
3) NNW-SSE
4) ENE-WSW
5) NNE-SSW
6) Semicircular lineaments

1) E-W trend. Although the east-west trend is perhaps not primarily important in terms of the quantity of lineaments, it is important because the master faults flanking the Acambay graben show a general east-west trend and these are the longest lineaments in the study area. The east-west trending lineaments are in most cases concordant with prominent scarps easily recognised in the satellite imagery. Some of

these lineaments may be associated with the northern and southern-facing normal faults of the Acambay graben that were created during the Quaternary. Among the east-west trending faults some are considered to be seismically active and are apparently associated with several historic seismic events (November 1912 and February 1979 earthquakes). The spatial arrangement of these lineaments reveals their relationship with the subduction of the Cocos plate that is associated with left-lateral shear of the Mexican Volcanic Belt's upper brittle crust.

2) ESE-WNW trend. The majority of lineaments in the Acambay graben are apparently ESE-WNW trending. However, most of these lineaments are shorter than 10 km in length, and most are around 3 km long. Some of them are reflected as scarps that are concordant with the system of normal faults along the graben. These lineaments might also be the result of left-lateral shear in central Mexico produced by the subduction of the Cocos plate. Like the E-W trending lineaments, those orientated ESE-WNW may be seismically active at present. Both groups follow the general trend of the en echelon regional lineaments of the Mexican Volcanic Belt.

3) NNW-SSE trend. The NNW-SSE trending lineaments include some of the longest straight segments (up to 20 km) along the Acambay graben. However, these lineaments are not the most common, only a few of them being visible in the satellite images, a feature reflected in the length-azimuth histogram (Fig. 3.13). NNW-SSE trending lineaments are generally reflected in the topography, but sometimes their potential expression in landforms is partially obscured by Quaternary sediments. The NNW-SSE lineaments seem to mark a gap in the Acambay graben that reflects a half-graben structure to the west of the location of these lineaments. The general orientation of these lineaments is precisely correlated with the well known Querétaro lineaments suggesting that the NNW-SSE lineaments might have originated during a previous (older) subduction episode- possibly that of the Farallon plate, which is

associated with NW-trending graben during the early Tertiary (Mooser and Ramírez, 1989).

4) ENE-WSW trend. The ENE-WSW trending lineaments are common. However, most of these lineaments are shorter than 5 km in length. The ENE-WSW trending lineaments are associated to the master faults of the Acambay graben and might also be related with the left-lateral shear in central Mexico produced by the subduction of the Cocos plate.

5) NNE-SSW trend. The NNE-SSW trending lineaments are rather uncommon, consisting mainly of short straight segments which are sparingly distributed along the Acambay graben. These lineaments might be associated with the NE trending lineaments that cross the Mexican Volcanic Belt in several locations. The origin of the NE-SW lineaments and structures of the Mexican Volcanic Belt has been recently associated with an older alternating right-lateral shear across central Mexico that has produced lineaments with an elongated Z-shape. This process might have produced the volcanic ridges of the Sierra de las Cruces (Pliocene-Pleistocene) west of Mexico City, and also probably the Sierra Nevada located east of Mexico City (Mooser *et al.*, 1992).

6) Semicircular lineaments. These lineaments show arch and semicircular shapes in planform. They are of considerable length but few in number. Some of these features may be components of bigger regional lineaments in the Mexican Volcanic Belt. The longest of these lineaments has been previously identified and named the Huapango-Nado lineament by Mooser and Ramírez (1989). It crosses Huapango dam to the centre of the graben, and it also seems to cut the volcano, Temascalcingo. These arc-and-semicircular shaped lineaments may be the result of volcano-tectonic forces that produced vertical deformations of the surface due to magmatic bodies and/or the collapse of volcanic structures.

To summarise, the most significant lineaments of the Acambay graben in the regional neotectonic context are the E-W and ESE-WNW trending lineaments that are tectonically associated with large-scale left-lateral shear through central Mexico arising from the subduction of the Cocos plate beneath southern Mexico. The NNW-SSE trending lineaments also seem to be significant in the regional tectonic framework and mark an apparent segmentation of the graben, that displays a half-graben structure to the west of the NNW-SSE regional lineament.

Chapter Four:
Meso-Scale Geomorphic Analysis. Interpretation from Aerial Photographs

4.1 Introduction

Geomorphological mapping of neotectonic structures along the Acambay graben has been carried out using aerial photography. Photographic images are the cheapest and most readily available remote-sensing data for geomorphological and geological interpretation (Drury, 1987). The images used here are vertical black-and-white stereopair photographs which were used in conjunction with a single hard copy from the Landsat TM system and a false color hard copy photograph from Landsat MSS (Fig. 4.1)

Available operational sensor - cloud-free, high-resolution, black-and-white aerial photographs at a range of scales (1: 50000, 1: 25000 and 1: 28000) were used. A qualitative approach to photo interpretation was used employing three basic steps:

1) primary reconnaissance, including all available corroborative data;

2) regional analysis;

3) detailed local analysis

Landforms were delimited on the basis of topography expressed as drainage texture, drainage and topographic patterns, tone, and characteristics of gullies and vegetation. Air-photographs at large scales ($\geq$ 1:50000) are a reliable tool in the identification of linear features and supply detailed information on the morphology of an area. As is well known, the photo-interpretation of faults is often more reliable than their detection in the field. The vertical exaggeration associated with stereoscopic viewing accentuates even the most subdued topographic features, and clearly reveals vertical displacements associated with faulting.

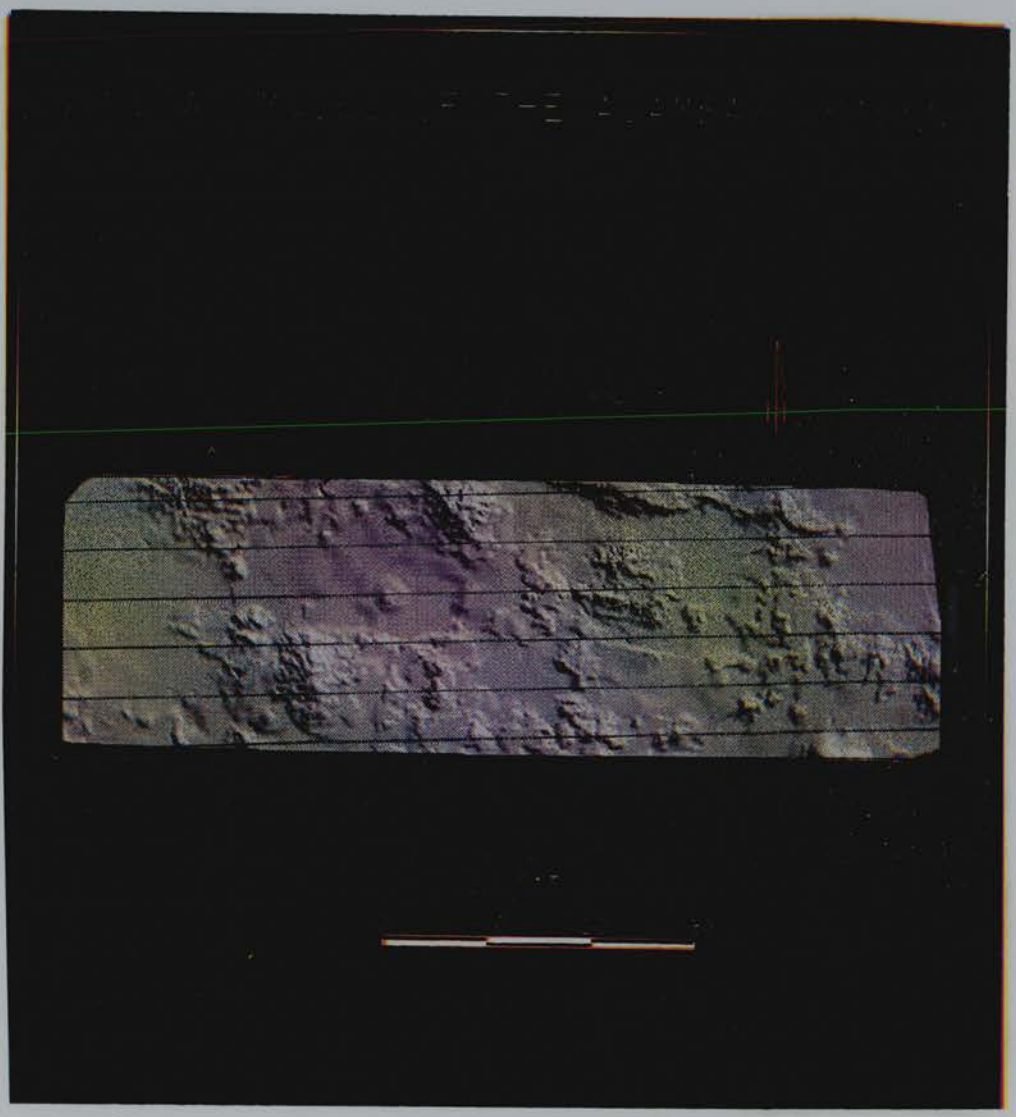

Fig. 4.1 Sketch-map showing the area covered by the aerial-photographs.

Reconnaissance work to identify areas where active tectonics is particularly significant involved the use of geomorphic indices (see Chapter 5) and the recognition of assemblages of landforms produced or modified by active-tectonic processes (this chapter and Chapter 6). Active tectonics often modify or produce characteristic landform assemblages along fault zones. A tacit assumption in the evaluation of landform assemblages produced by active tectonics is that the more dominant the tectonic control on a landform is, the younger the tectonics is assumed to be (Keller, 1986). The assumptions underlying the concepts mentioned above are discussed below.

An alluvial fan is a depositional landform that forms a segment of a cone radiating downslope from the point where the stream leaves the source area. Alluvial-fan morphology is an indicator of active tectonics because the fan form reflects varying rates of tectonic processes such as uplift of the source mountain along a bounding fault. Thus, tilting of the fan surface can illustrate differential movement. When the rate of uplift of the mountain front is high relative to both the rate of stream-channel downcutting in the mountain and to fan deposition, deposition tends to occur at the fanhead, the youngest fan segment being near the apex of the fan. Some of the rift valleys of the world provide ideal tectonics settings for rapid accumulation of alluvial-fan deposits. This process is illustrated on the alluvial fans along the eastern margin of the Sinai Peninsula. Here, Bull (1977) found that alluvial fans are steep and consist of water-laid gravel that has an undissected surficial morphology and only minimal soil-profile development, indicative of rapid accumulation. The typical alluvial fan along this mountain front is unentrenched and fan deposition occurs at the fanhead. A similar pattern was found for the alluvial fans on the piedmont of the escarpment of the Garlock fault in the Mojave Desert where thick alluvial fans are actively accumulating (Bull and McFadden, 1977). If the rate of uplift of the mountain front is less than or equal to the rate of downcutting of the

stream in the mountain, then fanhead trenching occurs and deposition is shifted downfan. Younger fan segments will then be found well away from the mountain front (Bull, 1977). Change in sediment or water yield may also cause fanhead trenching, but this tends to be temporary if mountain front uplift persists (Keller, 1986).

The above model of segmented alluvial fans relative to active tectonics has been successfully tested for alluvial fans in Death Valley, California. Hooke (1972) found that eastward tilting and normal faulting produced segmented alluvial fans. On the east side of the valley alluvial fans are relatively small and steep, and active normal faulting produces a straight mountain front with young fan segments being deposited on the fanhead areas. On the west side of the valley alluvial fans are larger, not so steep, and not so influenced by mountain-front uplift. Lesser uplift and eastward tilting of the fans has shifted the locus of fan deposition downfan; fanhead trenching occurs, and the younger fan segments are located well away from the fan apex. A similar tendency was noticed by Rockwell *et al.* (1985) for alluvial fans in the Ventura, California, area that are being tilted basinward by active tectonics.

Tectonically-active fronts display prominent, high, steep and undissected facets that are generated and/or maintained by recurrent faulting along the base of the escarpments (Bull, 1984). Less tectonically-active fronts contain fewer, smaller, and/or more internally dissected facets, due to the combined effects of the establishment of more channels across the front, the internal dissection of existing facets, and the lateral migration of larger streams crossing the front. The more tectonically-active mountain front escarpments tend to be less dissected, ranging from laterally continuous undissected escarpment to a nearly continuous front with only a few large and undissected facets. This tendency has been demonstrated by Wells *et al.* (1988) on the fronts of the Pacific coastal region of Costa Rica, which showed less dissected mountain front escarpments in areas of increasing uplift. Similarly, Menges

(1990) demonstrated the dependence of facet morphology on tectonics in the range-bounding fault zone, Sangre de Cristo Mountains, New Mexico.

Details of the scarp morphology produced by faulting is an additional indicator of active tectonics. The slope morphology of scarps shows several elements associated with a fault scarp and because slopes are dynamic changing landforms, the dominance of one element relative to others changes with time (Wallace, 1977). In due course the angle of a scarp degrades to a lower-slope angle. Several surface processes, controlled by climatic and geologic factors, contribute to the morphologic evolution of the scarps. In the cohesionless materials that make up most of the surface deposits in which such evolution has been studied by Wallace (1977) in north-central Nevada, scarp degradation starts with a gravity-driven phase of slope decline leading to the destruction of the free face and to the formation of a debris wedge at the angle of repose of the alluvium or soil. Following this phase usually of short duration (10 to 100 years), slower erosional processes, such as wash slope, rain splash, or solifluxion, become dominant. Such processes round off the angularities at the base and crest of the scarp. Wallace (1977) suggested that either the maximum scarp slope or the curvature of the crest are age-dependent geometric characteristics and may be used as quantitative age indicators. A chronology for faults on the Great Basin area in Nevada was developed based on the study of fault scarps that truncate ^{14}C-dated shorelines of Pleistocene Lake Lahontan, are associated with volcanic ash of known age, were produced by known earthquakes, or can be dated by tree rings (dendrochronology) (Wallace, 1977). Bucknam and Anderson (1979) developed relations between scarp height and scarp slope for fault scarps in Utah with estimated ages ranging from 1000 to 100,000 yr. Their studies confirm Wallace's (1977) conclusion that with time the angle of a scarp degrades to a lower-slope angle. Change in fault-scarp morphology with time has also been treated quantitatively by Nash (1986) and Avouac (1993). Therefore, estimated ages can be assigned on fault scarps of known height and slope

angle. However, differences in lithology and temporal and spatial variations in climate may produce a variable fault-scarp morphology (Keller, 1986).

Finally, there are a group of landforms which are formed directly as a result of active tectonics. Active-strike slip faulting produces a characteristic assemblage of landforms including linear valleys parallel to/and on the foot of the fault, offset or deflected streams crossing a fault, shutter ridges, sag ponds on the foot of the fault, pressure ridges, benches, scarps, and small horsts and graben known as microtopography (Keller, 1986). Therefore, active-strike slip faults can be recognised by distinctive geomorphic features (Sylvester, 1988). However, recognition of strike-slip faults by geomorphic features is limited by the durability of small easily eroded landforms such as sag ponds and deflected streams, whose preservation depends mainly on climate. Moreover, many of the geomorphic features associated with active strike-slip faulting (i.e. sag ponds, pressure ridges, and fault scarps) can be explained by simple shear that produces contraction and extension (Keller, 1986). Others are better explained by extension or contraction associated with releasing or constraining bends or steps on fault traces (Crowell, 1974).

The great length and the linearity of "rift" topography with an array of distinctive geomorphic features are the most distinctive characteristics of active or recently active strike-slip faults as described by Noble (1927) with reference to the San Andreas fault. When the opposing blocks of the fault move in strike-slip, elongate blocks and slivers subside between parallel or en echelon fault strands, or they warp, sag, or tilt to form closed depressions (rhomb graben or pull-apart basins (Aydin and Nur, 1982)) in the "rift" zone, and they do so from the smallest to the to the largest scale (Sylvester, 1988). These basins are morphologically expressed as elongated lakes and sag ponds, which often contain young sedimentary deposits. Other blocks may rise, tilt, or slide obliquely to produce uplifted terranes (rhomb horsts or pressure ridges (Aydin and Nur, 1982)). Many rhomb graben and rhomb horsts have been

recognised along major strike-slip faults throughout the world (Aydin and Nur, 1982). Notched ridges, fault-parallel trenches, or troughs along the fault may reflect increased erosion of the crushed and broken rocks in the fault zone (Wallace 1976).

Deflected streams must be used with caution to determine the direction of lateral displacement. The offsets must be in an uphill direction, or else they may be explained by stream piracy or differential erosion (Wallace, 1976). Offset stream channels have yielded slip rates for active faults. Sieh (1984) and Sieh and Jahns (1984) estimated that the slip rate during the latest Pleistocene and Holocene was about 30 to 40 mm/yr, judging from offset stream channels of Wallace Creek along the south-central part of the San Andreas fault.

Fault scarps can be formed by rising, tilting or oblique displacement of blocks. On a small scale, shutter ridges are formed by lateral or oblique displacement on faults transecting a ridge and canyon topography. A displaced part of a ridge shuts off a canyon, hence the term "shutter" (Sylvester, 1988). On a larger scale, an entire mountain front may be exposed by lateral displacement of its toes or its other half, as Noble (1932) postulated for the south face of the San Bernardino Mountains in southern California.

Fault-related landforms have been used to demonstrate strike-slip displacement and rates of slip on the San Andreas fault in the Indio Hills of southern California (Keller *et al.*, 1982), where small streams at the upper part of an alluvial fan are offset several meters and the fan as well is offset about 700 m. Keller *et al.* (1982), making an assumption concerning the age of the fan from soils, determined a 1-3 cm/yr slip rate for this part of the San Andreas fault. More studies have provided evidence of landform association with strike-slip faulting in different areas of the world, as in the Karliova continental triple junction, east Turkey (Tutkun and Hancock, 1990) where tectonic landforms (small flat-floored pull-apart basin, offset stream courses and pressure ridges) reflect short fault segments with lateral and

normal combined displacements. Armijo et al. (1986) found rhomb-shaped sags and displaced stream channels to be consistent with left-lateral slip along more linear piedmont faults in the Karakorum-Jiali fault zone, north Tibet.

In this research, firstly, faults have been identified using a range of morphological evidence: a) scarps and triangular facets (which are consistent with vertical displacement); b) offset stream channels, pull-apart basins, sag ponds, shutter and pressure ridges. When found together, this assemblage of landforms is consistent with a lateral component to fault displacement. Secondly, an attempt to evaluate the relative tectonic activity and chronology of the faults is based in the analysis of morphological evidence, notably alluvial fans, V-shaped valleys, the gradient of scarps, the degree of denudation of fault scarps, and valley downcutting. Therefore, the evaluation of the tectonics is based on a suite of morphological evidence as whole, and not on single features. In some places individual landforms and assemblage agree, in others it is the assemblage of landforms that is consistent with lateral shear. Moreover, a suite of landforms may also be consistent with vertical displacement as mentioned above. Thus, it is the analysis of landform assemblages and its components that provides evidence of the tectonics of the region.

This chapter presents the results of qualitative photo-interpretation of geological-geomorphological features in the Acambay graben, placing emphasis on their relation to tectonics. For the purposes of analysis the graben is divided into three areas: the southern flank (eastern and western areas), the northern flank (eastern and western areas) and the central area.

4.2 Meso-scale geomorphic features along the southern flank of the Acambay graben

4.2.1 Southern flank of the graben - eastern area: Pastores fault

The southern flank of the Acambay graben shows a disturbance that seems to break the continuity of the flank. This disturbance is produced by a NNW-SSE trending lineament that disrupts the graben from east to west. This produces an overlap of two great lineaments, namely the Pastores and Venta de Bravo faults. The analysis of the southern flank is based on this natural division into the eastern (Pastores fault) and western (Venta de Bravo fault) areas of the southern flank.

Eastern termination of the Pastores fault. Drainage here has a rectangular pattern that is interpreted as resulting from the structural control exerted on these streams. A discontinuous lineament was detected in air-photographs that showed straight segments along some stream channels following an E-W direction. These straight sectors that continue the east-west trend of the master fault of the southern flank of the graben might represent the eastern end of the Acambay graben. Despite this fact, it still not clear where this lineament ends to the east. To the south of this area, and adjacent to the trace of the fault, several lava cones are clearly identified by their differences in relief and a semi-circular shape. These cones exhibit a dense radial drainage pattern (Fig. 4.2-a, see envelope with maps attached to the back cover). Rippled texture and "tongue" forms makes it possible to identify the surface that is occupied by lava flows south of the fault. The stream density is high and has a radial and semi-dendritic pattern. To the south, several small, semicircular forms elevated above a plain indicate the presence of a lava and cinder cone field which extends over a wide area. This smooth surface, that surrounds the Trinidad Fabela dam, has a centripetal drainage pattern.

North of the eastern termination of the Pastores fault, the air-photographs reveal a high relief area. This is interpreted as a volcanic mountain area formed by lava domes strongly dissected by stream and gully erosion. The relief, slope and texture in the air-photographs indicate the presence of lava domes which have a massive appearance. The drainage pattern here is apparently radial and does not show evidence of faulting.

Dam Trinidad Fabela - Atlacomulco (Acambay highway) Sector. West of the Trinidad Fabela dam the air-photographs clearly show a scarp that indicates the trace of a fault. This scarp shows differences in the vegetation coverage: more dense coverage to the north contrasting with scant vegetation on the southern slope. The scarp faces north and follows an E-W alignment of lava domes and cones. The straightness of this lineament (about 8 km long in the sector described) suggests the existence of a fault structure. The face of the scarp shows several gullies arranged perpendicular to the trace of the fault and with a parallel drainage pattern. Some gullies are deeply developed, and the development of gully erosion seems to be dependent not only on weather and soil conditions in this area but also on the tectonic activity. There is a high density of gully erosion on the fault scarps. The gullies sometimes extend beyond the edges of the scarps as a result of headward erosion. Active incision and valley down-cutting might be intensify by active tectonics in this area.

The flat, and smooth texture and clear grey tone observed in the air-photographs help to identify a small elongated depression (300 m length), occupied by an ephemeral lake, and observed along the foot of a scarp. This is a sag pond that may indicate small scale tilting associated with fault movements (Fig. 4.3). The air photographs also show several lava domes, lava cones and lava flows that are well preserved and are located to the northern part of this area. Although gully erosion has developed on the domes, lava flows seem to be less dissected by gullies in the same

area. Gullies and streams have a radial pattern but in some parts they have a rectangular pattern that is apparently controlled by the presence of fractures and perhaps to some degree, by a prominent lineament observed in the Landsat image.

The lava domes, lava cones and lava flows form a high volcanic mountain area in the inner graben that encloses the eastern end of the graben, separating the lacustrine basin of Valle de los Espejos from the lacustrine basin of the Huapango dam (Fig. 4.2, a). The air photographs reveal several lava cones and domes south of the E-W trending lineament. These landforms are apparently aligned and cut by the major Pastores fault. South of the fault, near Atlacomulco, there are cones, lava flows and lava surfaces covered by pyroclastic material. The alignment of some of these cones detected in the air photographs show that these landforms are apparently controlled by faults. The drainage pattern here is predominantly radial.

The southernmost part of this sector exhibits the slopes of the apparently active volcano of Jocotlitlan and several conical hills, or hummocks, located to the north of the volcano (Siebe, *et al.*, 1988). A large depression can also be observed consisting of an almost flat surface that contains the meandering channel of the Lerma River. This river has developed entrenched meanders that may have been produced by uplift in the area, an interpretation supported by the presence of elevated conglomerates near the Perales fault (Ortiz and Bocco, 1989) (Fig. 4.2, a).

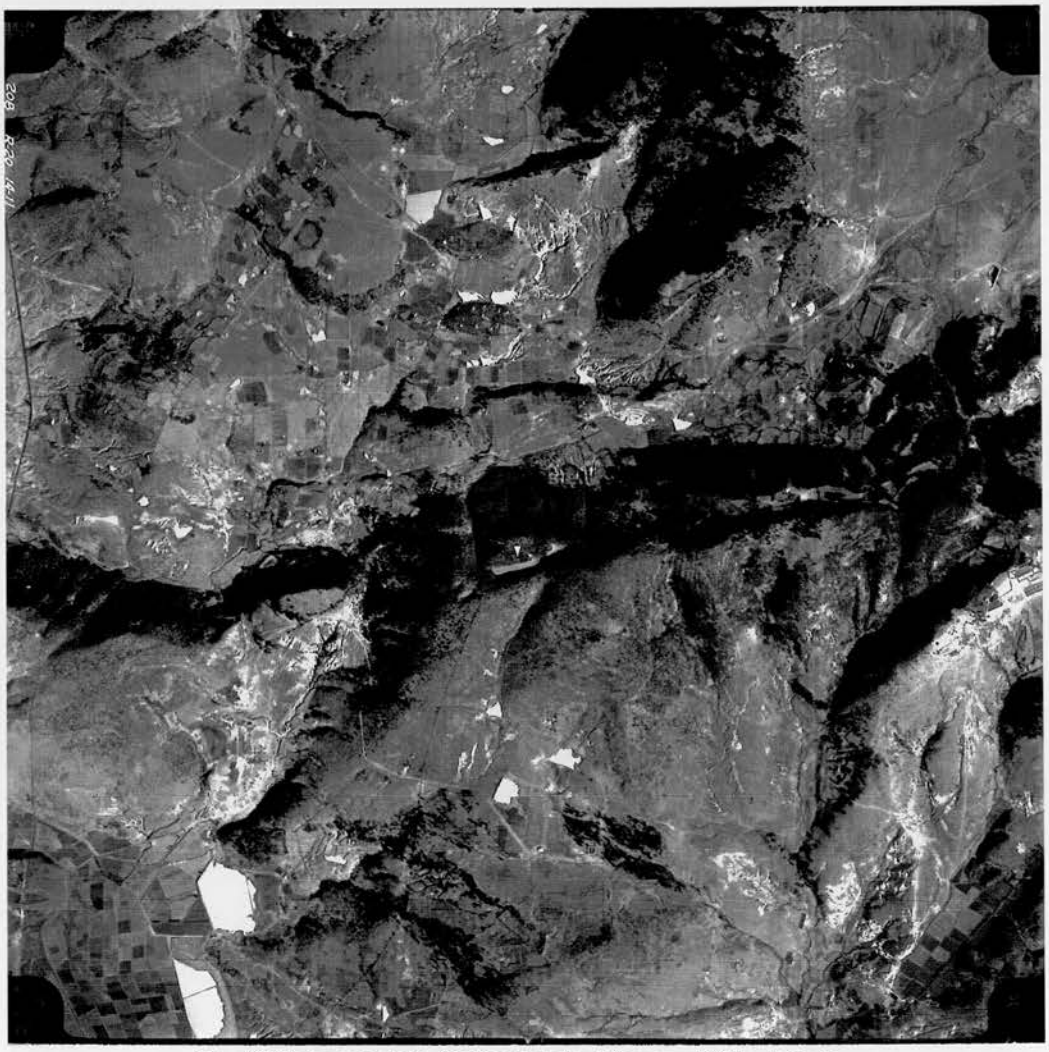

Fig. 4.3 Sag pond along the Pastores fault (arrowed).The dashed line indicates the location of the Pastores fault. (Scale 1: 50 000).

Atlacomulco-Acambay Sector. The surface expression of the southern flank faults, as well as differences in elevation, are less evident in this sector of the Pastores fault where it is partially buried by Quaternary lava flows. The trace of the fault is apparent here from the alignment of lava cones, and of low scarps in a lava flow. Although it is difficult to follow the trace of the fault in this area, lava flows here are apparently cut off by the fault that produced low gradient scarps facing to the north. The trace of the fault is more visible near to the Lerma River, where the differences in elevation denote the presence of the scarp. The scarp seems very well preserved in this area and does not show evidence of gully erosion.

South of this area, the surface is covered by lava flows distinguished in the aerial photographs by differences in relief and a rippled texture. There are also several aligned lava cones representing fault control. To the south, the surface is almost flat and is occupied the Lerma River and a lacustrine basin with several small lakes.

North from the fault lava flows are evident and exhibit scarps produced by lava fronts. Small depressions between them appear to be filled with tuff deposits. To the north, a SW-NE oriented valley seems to be controlled by a lineament with the same orientation. Several gullies dissect this valley and expose almost white lake deposits. In the north-eastern part of this valley there are lava domes and flows which seem to bound the lacustrine basin "Valle de los Espejos" to the north and the Toxi basin to the south (Fig. 4.2, a).

Lerma River - western termination of the Pastores fault. The trace of the fault is quite remarkable along this sector. A long and straight fault scarp is evident, the elevation of the scarp contrasting with the adjacent lower surface. The cover of vegetation is also denser on the face of the scarp due to its exposure to sun. The high gradient of the slope of the scarp contrasts with the smoothness and low gradient of the slope facing to the south. An elongated E-W oriented ridge indicates the presence

of the fault and this is emphasised by the presence of small elongated hills along the Pastores fault which are rather similar to linear ridges. The aerial photographs also show parallel gullies along the face of the scarp and the drainage divide along the scarps is sinuous in planform. At the foot of the scarp there is a much lower gradient surface interpreted as a piedmont composed of colluvial material (Fig. 4.4).

To the north, the Lerma River flows sub-parallel to the Pastores fault, but in places it meanders and deviates from this sector direction. The river flows across a wide and almost flat surface interpreted as fluvial-lacustrine basin (Toxi plain) and a terrace is alternately on either side of the river channel. To the north of the Pastores fault, the surface is occupied by a large volcanic cone, Temascalcingo (Fig. 4.2, a).

South of the fault, the land surface is smooth and only partially dissected by gullies. This flat surface has a semi-dendritic drainage pattern, and is interpreted as a lava surface covered by pyroclastic material. To the south, the aerial photographs show differences in elevation and texture that indicate the presence of lava domes and flows in this area. The Lerma River flows from south to north and crosses the fault, in the same direction, in the place occupied by lava flows. The river shows straight segments that are apparently fault-controlled. Here, the form of the valley changes to V-shaped. There are two terraces on both sides of the river in the place where the river crosses the fault. These terraces could be related to the uplift of the southern block south of the fault (Fig. 4.2, a).

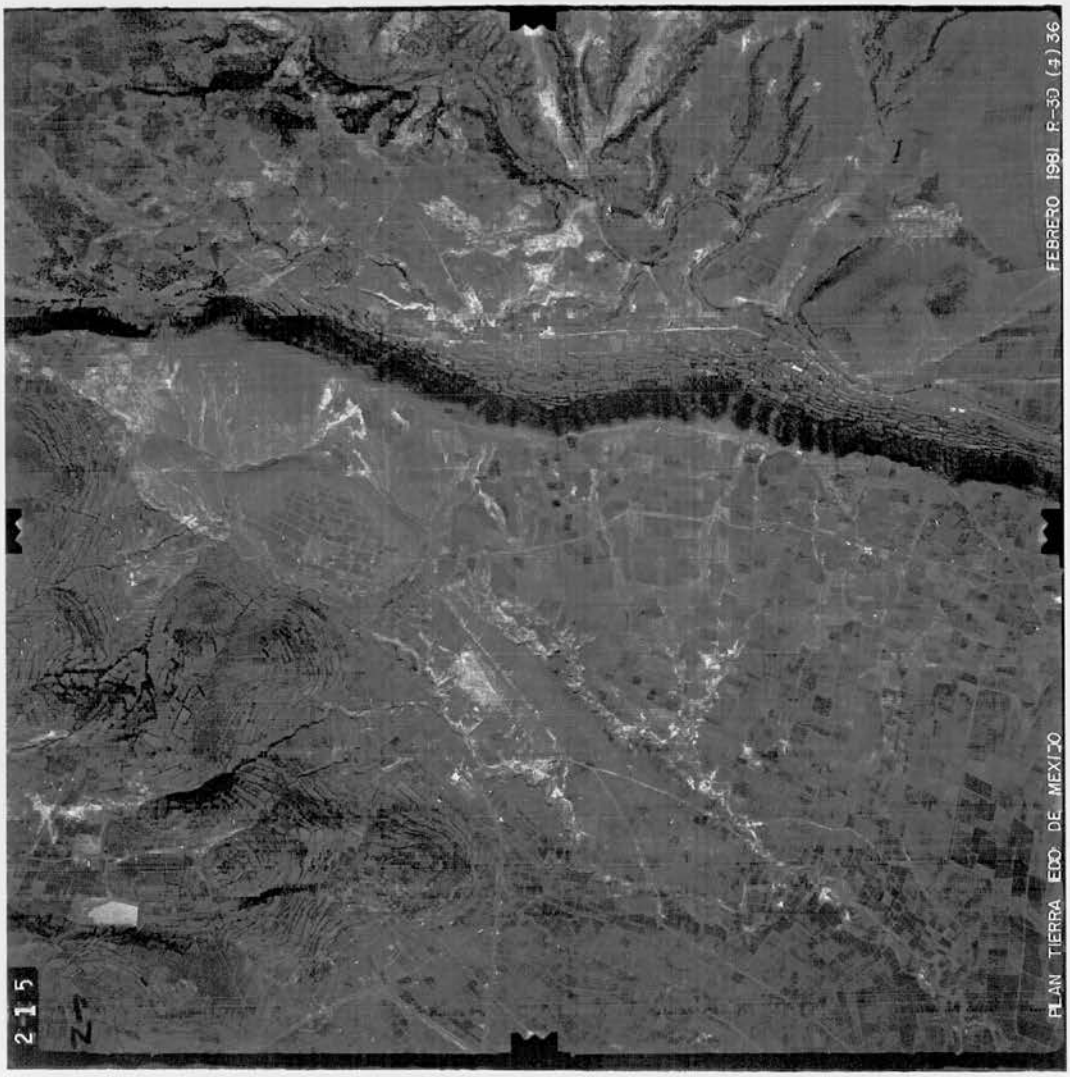

Fig. 4.4 Fault scarp of the Pastores fault.

Western termination of the Pastores fault and eastern termination of the Venta de Bravo fault. The western termination of the Pastores fault and the eastern termination of the Venta de Bravo fault exhibit a large overlap. These faults have en echelon arrangement, the aerial photographs revealing two parallel lineaments: the southern lineament is an extension of the Venta de Bravo fault, whereas the northern one corresponds to the Pastores fault. The northern lineament, the Pastores fault, is straight and clearly shows a fresh scarp that is almost undissected. The lineament is also evident from the presence of linear ridges with asymmetric slopes formed by lava domes that are cut by the fault.

This lineament becomes gradually less marked to the west, with the relief diminishing to produce a less prominent scarp. Drainage shows a parallel pattern and the streams and gullies are perpendicular to the scarp (Fig. 4.2, b; Fig. 4.5). The aerial photographs show apparent offsets of the streams in this area which indicate a left-lateral displacement of about 37.5 m.

To the south of this lineament, the landsurface consists of lava domes. These are partially tree covered by tree vegetation and have a radial drainage pattern. Further south, lava domes seem to be aligned and some of them have a linear ridge form that may be a result of being cut by a fault. This lineament is the easternmost extension of the great Venta de Bravo fault, and the associated fault scarp is clearly apparent with triangular facets visible along the scarp, which have been produced by the incision of V-shaped valleys into the scarp face. The terrain between these faults consists of a rhomboid-shaped shallow basin incorporating ephemeral lakes and swampy depressions and filled with alluvium. The southernmost part of this area consists of an elevated volcanic region comprising lava cones and massive lava domes (Fig. 4.2, b). North of the fault-overlap sector, air- photographs offer a clear view of a succession of almost E-W trending lineaments north of Santa María Canchesdá. The interpretation of these lineaments is discussed below.

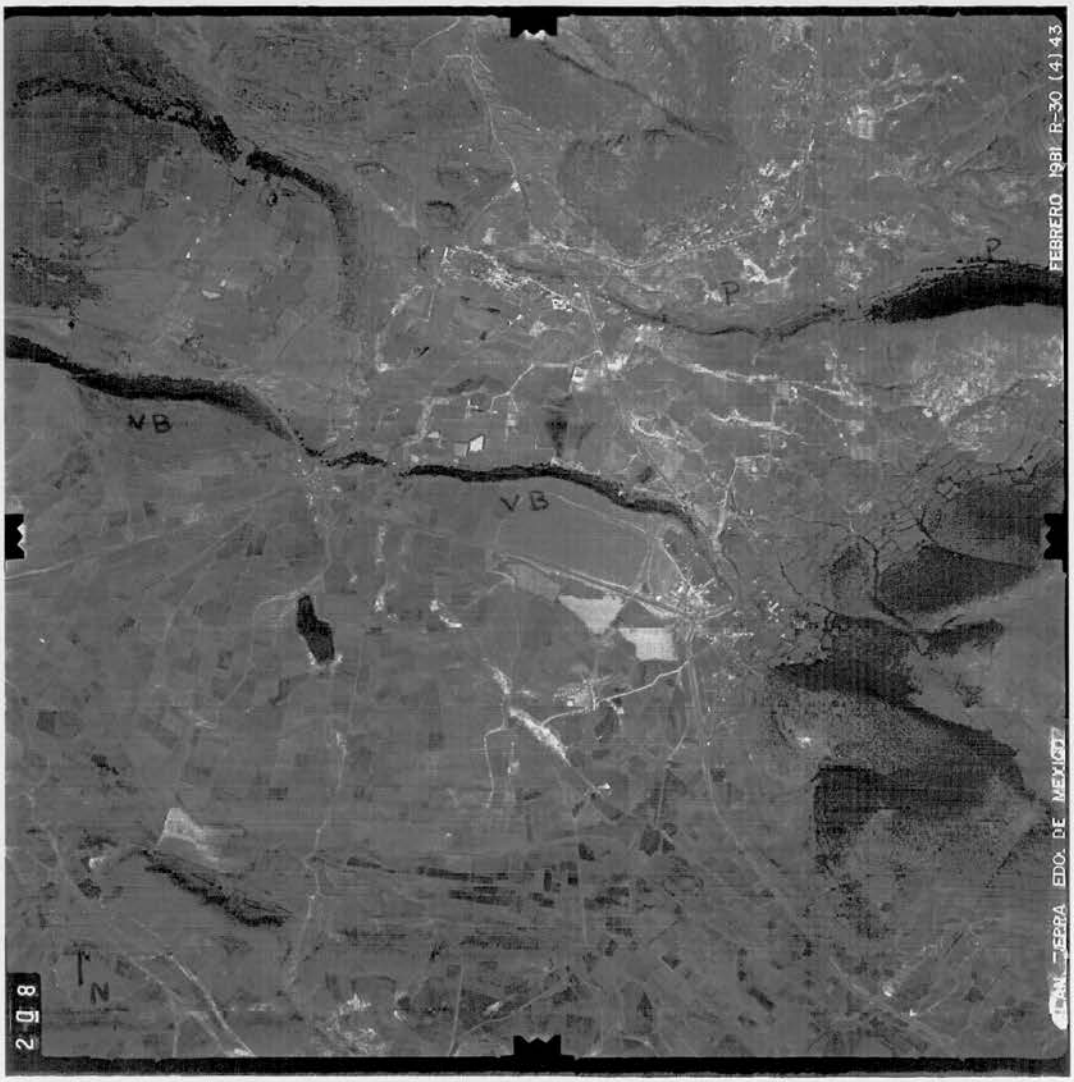

Fig. 4.5 Fault overlap of the Pastores and Venta de Bravo faults.
(P- Pastores fault; VB - Venta de Bravo fault).

4.2.2 Southern flank of the graben - western area: Venta de Bravo fault

Santa María Canchesdá - El Mogote sector. The lineament observed in this sector is remarkable for its straightness and the clear relief that demarcates a fault scarp. This feature appears to be a cuesta or a homoclinal ridge. Small valleys divide this long structure into segments consisting of linear ridges with asymmetrical slopes. The form of these linear ridges suggests lava domes cut by the fault (Fig. 4.2, b).

North of this sector two swampy depressions and sag ponds, along the fault scarp, indicate fault activity. These features are very clearly distinguishable, because they show a clear-grey tone and a flat, smooth texture in the aerial photographs. To the north this depression is closed by the lava front of a volcanic mesa that forms an escarpment parallel to the fault. To the south of the fault there is a flat, smooth land surface aligned to the foot of the fault scarp and incorporating a series of water-filled swampy depressions. The aerial photographs also show another straight lineament to the south with a north-facing scarp. The relief in this case is not as great as along the master fault, but the scarp slope still has a significant gradient. To the south, there is a volcanic area characterised by a high elevation and radial drainage pattern (Fig. 4.2, b).

El Mogote - Venta de Bravo Sector . The Venta de Bravo fault does not always define a straight line and it shows several slight changes in direction along its length. This geometry produces a sinuous appearance in planform on small-scale aerial photographs. There are several features on this sector indicative of the fault and its recent activity. One of the clearest of these are three parallel fault scarps. The northern one seems to be a continuation of the main master fault. Its characteristics change in an east-west direction with more vegetation cover (trees and bushes), a high scarp and a well-developed piedmont slope in the east. To the west the fault scarp has less vegetation cover but its relief is still evident. This sector of the scarp is dissected

by streams perpendicular to the fault and consequently has flat triangular facets (Fig 4.3).

At the foot of the scarp the slope is more gentle and dissected by gullies. The streams on the scarp seem slightly offset in the aerial photographs. Clear evidence of these offsets is observed on the southern faults, parallel to the master fault. Two offsets of 125 and 150 m indicating left-lateral displacement of the river (Fig. 4.6) were measured from the aerial photographs along the El Encinal River.

The surface between the master fault and a second fault to the south is almost flat and is dissected by parallel streams with evidence of slight gully erosion. This flat land surface is bounded to the south by a fault that has a semicircular or arcuate planform. This fault could be confused in the aerial photographs with the edges of lava flows. However, the offset of the river provides confirmatory evidence of its existence and recent activity. Other features further support the identification of active tectonism. These are small swampy depressions located along the faults which may indicate sag ponds. They have clear tone, a flat smooth texture and elongated shape on the aerial photographs. These depressions are typically around 250 m in length and 125 m in width. Offset drainage, sag ponds, fault scarps and triangular facets all provide evidence of fault activity (Fig. 4.6). A notable landform in this morphotectonic complex is a smooth rounded ridge approximately 340 m in diameter. This feature is associated with two faults that join at their western ends and may be a compression ridge (Fig. 4.2, b).

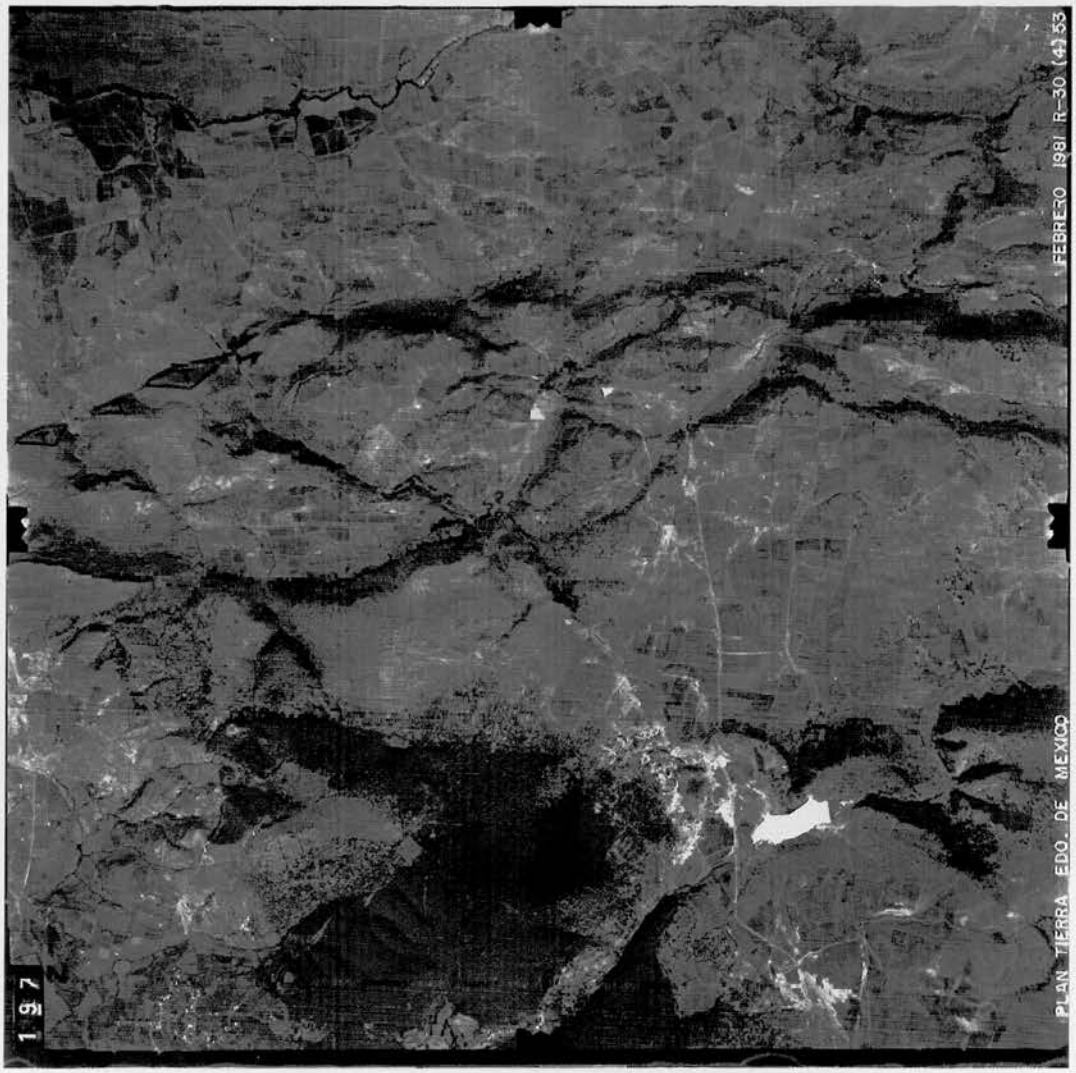

Fig. 4.6 Venta de Bravo master fault and parallel faults exposing triangular facets (T), offset drainage (dots) and sag ponds(sp).

To the south there is a third fault scarp about 11.5 km in length. It is less prominent than those located to the north but can still be differentiated on the basis of its relief, linear segments and a dense coverage of vegetation which highlights the face of the scarp. Southernmost of this fault scarp the surface is formed by lava domes, lava flows and a mountainous area with a dendritic drainage pattern and gully erosion. This high relief area has a rough texture on the aerial photographs that indicates a change in lithology from volcanic to metamorphic rocks.

To the north of the master fault there is an essentially flat and sometimes rippled surface with a gentle gradient. This surface has a parallel drainage pattern and may be interpreted as an initial piedmont formed at the foot of the scarp by colluvial material. Further north, the surface is flatter and shows less stream erosion. The centre of this plain is occupied by a large ephemeral lake. This surface is interpreted as a lacustrine basin filled with alluvial and tuff deposits.

Venta de Bravo - El Moral Sector. In this sector linear features are not evident and the differences in relief have been smoothed by erosion, although there are several gullies in this area. Despite the smoothness of the relief, the vegetation and drainage indicate the position of lineaments. For instance, an offset stream indicates lateral displacement by a fault. The surface north of this lineament has a gentle slope. It is dissected by several streams and gullies which form a parallel drainage pattern. Along the lineament and adjacent to it the surface appear rippled because of the accumulation of tuff and conglomerates forming the piedmont (Fig 4.2, d).

El Moral - La Laja - El Cementerio Sector. The fault scarp here is high and densely cover by vegetation and has an adjacent piedmont. The scarp is deeply dissected by streams perpendicular to the fault producing a series of V-shaped valleys. This lineament is traceable along 1.3 km. The height and the gradient of the scarp are lower than in the Pastores fault and the eastern part of the Venta de Bravo fault. To

the west, a succession of isolated ridges provides the continuing trace of the lineament.

West of La Laja, several straight lineaments with an ENE-WSW orientation can be observed in the aerial photographs but the presence of a major fault is less evident. The height of the scarp is not great, although a subtle change in the elevation indicates the location of a fault. Vegetation contrasts, however, provide a clear evidence of the trace of the fault, and its position is also indicated by the location of stream channels.

To the west along the foot of the scarp between El Moral and El Cementerio the surface of the piedmont is strongly dissected by gully erosion. There is also a high elongated ridge opposite the scarp which seems to be a lava front emerging from the piedmont. Further north, the La Venta River has straight channel segments with an E-W orientation, which parallel the trace of the major Venta de Bravo fault. These straight channel segments may be a response to structural control. Moreover, there are also some isolated aligned lava cones that show the direction of an almost E-W fault parallel to the Venta de Bravo fault (Fig. 4.2,b).

North of the Venta the Bravo fault and in the inner graben a wide depression extends for several kilometres. This is indicated on aerial photography by an almost flat, sometimes rippled surface that forms a lacustrine basin, filled with lake and tuff deposits. Isolated lava and scoria cones rise from the basin. South of the sector between Venta de Bravo and El Cementerio the surface has a rough texture and displays clear differences in height. The drainage pattern is generally parallel, but locally dendritic. The surface of this mountainous area is characteristically marked by well-developed gullies caused by erosion (Fig. 4.2, b).

El Cementerio-Santa Ana-La Huerta Sector. The Venta de Bravo fault is oriented ESE-WNW in this sector. This lineament is straight for a length of 2.8 km, and is marked by a clear change in elevation which also coincides with changes in vegetation, with more vegetation on the face of the scarp contrasting with less in the piedmont. The scarp is characterised by streams draining perpendicular to the trace of the fault, and forming V-shaped valleys. The scarp is constantly interrupted by these V-shaped valleys which give rise to triangular facets along its face. The aerial photographs also indicate stream offsets across the scarp of 56-84 m.

La Huerta - Presa Quebrada Sector. Here the trace of the fault is similarly indicated by elevation and vegetation differences, and the scarp also has V-shaped valleys and triangular facets. The fault scarp is straight for 3.6 km before it changes direction slightly to a WSW alignment. Differences in lithology are marked by changes in the drainage pattern and variations in the intensity of dissection. The lineament of the Venta de Bravo fault seems to be multi-segmented and in this sector there is a clear overlap of two parallel fault segments.

Western termination of the Venta de Bravo fault. The western termination of the Venta de Bravo fault is indicated by a clear scarp detected in the aerial photographs because of its height and the alignment of elongated ridges corresponding to lava domes. The scarp has high gradient and dense vegetation cover and there are highly dissected lava domes with a radial drainage pattern. The southern flank of these lava domes has a slightly prominent scarp which may indicate the presence of a second fault parallel to the master fault. The surface between the master fault and this lineament consists of a small river depression (Fig. 4.6).

The aerial photointerpretation of features differentiated by their form and texture indicates the location of two parallel lineaments. The alignment of scoria and lava cones and the differences in relief clearly show fault scarps south of the master fault. These lineaments are straight for approximately 10 km. The western termination

of the master fault is indicated by a gradual decrease in height and the smoothness of the surface. The northern lineament (master fault) terminates in the Maravatío basin - a flat surface - where the features that indicate the presence of faults are buried by lacustrine sediments. However, the southern lineaments parallel to the master fault can still be detected to the west being evident for several kilometres from the alignment of scoria and lava cones. Differences in elevation are evident and escarpments are present along these faults. The straightness of these lineaments is also indicative of the existence of faults.

North of the master fault there is a massive lava dome that has straight lineaments at its centre that coincide with the direction of the master fault. These lineaments are marked by relatively low scarps. To the west, the surface is formed by the flat and wide lacustrine basin of Maravatío which occupies the inner graben where the trace of the fault is buried by lacustrine deposits (Fig. 4.2,b; c).

4.3 Meso-scale geomorphic features along the northern flank of the Acambay graben

4.3.1 Northern flank of the Acambay graben - eastern area: Acambay-Tixmadeje faults.

The eastern area of the northern flank of the Acambay graben is clearly reflected by the relief, from Acambay to the Lerma River flood-plain, and is bordered to the west by a fluvial-lacustrine basin. It consists of a series of E-W lineaments extending for around 30 km and associated with the Acambay-Tixmadeje master fault.

Eastern termination of the Acambay-Tixmadeje faults. The eastern termination of the Acambay graben is marked by an easily detected E-W lineament which is arcuate in planform. It is differentiated by a prominent scarp and elongated ridges. The scarp has a piedmont at its foot. The alignment of linear ridges and the disruption of lava cones also show the trace of the fault. The scarp surface has a

rippled appearance and is dissected by gullies. The drainage pattern on the ridges is predominantly sub-radial, but locally sub-parallel.

North of the lineament the surface in the aerial photographs appears rough, highly dissected and locally rippled. These features indicate the presence of lava flows. South of the fault, and in the inner graben, the surface has a predominantly radial but locally dendritic, drainage pattern, and which is characterised by deep gullies. This surface represents a volcanic relief consisting of massive lava domes. Fan-shaped and ripple-textured surfaces show the location of alluvial fans at the foot of this volcanic area. The fans are entrenched and orientated towards an extensive lacustrine basin (El Valle de los Espejos). This broad basin contains several small ephemeral and permanent lakes (Fig. 4.2, a).

Lineaments west of Acambay to Tixmadeje. Two great parallel lineaments are observed to the west of Acambay. The northern one shows a sinuous shape in planform, but the southern one has a arcuate-shape at the regional scale. The northern lineament has higher relief and is demarcated by a remarkable scarp formed in lava. Near the town of Acambay a large alluvial fan is entrenched at the foot of the scarp. Further west there is another smaller entrenched alluvial fan. The northern lineament is also marked by elongated ridges indicating the fault trace. The fault terminates in the west near the town of Tixmadeje. Here, a lava dome disrupts the fault and the fault trace disappears. A parallel lineament can be observed to the south which is visible from the presence of a scarp. The surface between these two lineaments is occupied by a small depression. The scarp of this lineament is an evidence of the existence of a fault (Fig. 4.2, a).

The southern lineament extends for several kilometres and is the longest feature in the area. At the regional scale this feature has an arcuate-shape in planform. A scarp marks this lineament although it has a lower gradient than that associated with the northern lineament. Again, there is a piedmont slope at the foot of the scarp.

To the west of a linear ridge named El Colmilludo, the straightness of the northern lineament indicates the trace of the fault. However, here the gradient of the scarp has been reduced by denudation. From the El Colmilludo ridge, a new, parallel lineament shows the location of the fault. The southern lineament is straight and marked by a high, steep scarp. It is less dissected, the face of the scarp being smoother, and its top-edge is clearly differentiated on the aerial photographs from the rough surface to the north which consists of lava domes.

Western termination of the Acambay-Tixmadeje faults. The southern scarp shows several gullies and has V-shaped valleys and triangular facets. A small elongated ridge interpreted as a shutter ridge seems to interrupt and offset streams along this slope. The northern lineament still has a remarkable scarp and seems to slightly turn to WNW direction. The western termination of these lineaments is interrupted by a flat surface formed by the Lerma River and a previously existing lake that erases all the elevation differences (Fig. 4.2, a; b).

4.3.2 Northern flank of the Acambay graben - western area: Tepuxtepec faults.

Lineaments in the western part of the northern flank of the graben are not continuous. They seem to be an extension of lineaments from the centre and northern flank of the graben.

Lineaments of the Altamirano volcano. Lineaments with an ESE-WNW direction show the position of faults on the eastern flank of the volcanic pick of Altamirano. Height differences as well as a dense coverage of vegetation show the presence of south-facing fault scarps. These faults become less straight near to the centre of the volcano where the trace of the fault disappears. Evidence of the trace of these faults reappears on the western flank of the volcano, but here they have north- rather than south-facing fault scarps (Fig. 4.2, b).

Lineaments between Altamirano volcano and Tepuxtepec. Western termination of the Tepuxtepec faults. Faults from the central part of the graben identified from relief and differences in vegetation seem to extend to the west of Altamirano. Scarps here face both to the north and the south. To the west, the northern flank of the graben consists of a series of segmented lineaments, arranged parallel to each other and distributed across a wide area from south to north. The straightness of these lineaments is clear although they are short compared with the faults of the northern-eastern flank and those of the southern flank. Straight channel segments and aligned positive landforms, such as scoria cones, indicate the direction and alignment of the Tepuxtepec faults. Elevation differences here are not significant enough to produce a prominent scarp, but the straight channels provide evidence of the existence of the faults. To the west, the trace of the faults disappears beneath the sediments of the Maravatío lacustrine basin (Fig. 4.2, b, c).

4.4 Central faults - inner graben

Lineaments in the Temascalcingo area. The central part of the inner graben, which contains the volcano of Temascalcingo shows a remarkable series of E-W lineaments which can be easily detected in aerial photographs. These are straight and parallel to each other for several kilometres (up to 12 km). Various morphological features indicate the presence of north-and-south-facing faults in this area including changes in the direction and sinuosity of streams, triangular facets on the scarps, and sag ponds. These sag ponds may also be evidence that the faults are active.

There are two lineaments on the northern flank of the volcano with scarps facing to the south, and two parallel lineaments with north-facing scarps on the southern flank of the volcano. This arrangement produces a depression in its centre. The arrangement of these faults may be interpreted as providing a small graben within

the volcano. The drainage pattern is radial but some streams are straight and this indicates fault control (Fig. 4.2, a).

The southern flank of the volcano shows fan shapes in the aerial photographs that are interpreted as entrenched alluvial fans. These fans exhibit strong dissection produced by gullies. To the south, the Lerma River flows along the southern flank of Mount Temascalcingo. The river in this area has a meandering channel which is partly entrenched. The Lerma River exhibits a V-shaped valley on the southwestern flank of Mount Temascalcingo. These features may suggest vertical movements, perhaps even a general uplift in the area (Fig. 4.2, a). The northern flank of Mount Temascalcingo also shows several fan-shaped features which are interpreted as alluvial fans. These fans are also entrenched and their apex lie high up on the slopes of the volcano. Some of these fans seem to overlap each other (Fig. 4.2, a).

Lineaments of the lava field in the inner graben (Santa María Canchesdá-Solís). North of Santa María Canchesdá the surface consists of a series of essentially flat surfaces bounded by scarps and series of lava cones and lava flows. This area shows several ESE-WNW trending lineaments that are clearly visible in the aerial photographs. They are distinguished by changes in elevation along scarps which are also characterised by the vegetation cover. The smoothness of the surfaces bounded by the scarps indicates minimal amounts of erosion with little stream dissection. The alignment of positive topographic features also helps to distinguish fault traces in this area. There is a sequence of cinder and lava cones which follow the trace of the faults in ESE-WNW direction, which continues as prominent scarps to the east which are visible in the aerial photographs because of their vegetation coverage and relief. The parallel and en echelon arrangement of these faults produces several, almost flat, intervening surfaces. These flat surfaces contain small swampy depressions parallel to the lineaments, sometimes filled with water, and these may represent sag ponds.

Lineaments between the Canchesdá lava field and Mt Temascalcingo. The area between Temascalcingo and the volcanic field of Canchesdá consists of a surface deeply dissected by the Lerma River, which flows from south-east to north-west, in a deep canyon. The Temascalcingo lineaments seem to continue the east-west general trend, only apparently being disrupted by the Lerma River (Fig. 4.2, b). Scarps here have a dense vegetation coverage and high gradient facing to the north. These lineaments are straight for several kilometres and some of them are divided by streams and V-shaped valleys.

Lineaments between Mount Temascalcingo and Mount Altamirano. Between the north-western part of the volcanoes of Temascalcingo and Altamirano there is a flat surface representing a fluvial-lacustrine basin formed by the Lerma River. To the west of this basin and near to the foot of the Mount Altamirano, differences in elevation and in vegetation coverage reveal the trace of E-W straight lineaments. Here the scarps are dissected by small V-shaped valleys producing triangular faceted spurs. The continuation of one of these lineaments to the west is demonstrated by the shape of a cinder cone the nothern part of which has apparently been laterally displaced to the left (Fig. 4.2, a; b).

Lineaments south of Mount Altamirano. Lineaments are clearly distinguishable in this part of the graben. Along scarp ridges there are flat surfaces with scarce vegetation compared to dense vegetation on scarp faces. These lineaments are parallel to each other and the intervening surfaces sometimes correspond to depressions dissected by streams. The scarps seem well preserved and only a few streams and gullies dissect them (Fig. 4.2, b). The southern slopes of Mount Altamirano are dissected by ESE-WNW lineaments that show scarps visible through vegetation and relief contrasts.

4.5 Summary

In summary, a detailed interpretation of the aerial photographs has revealed several faults within the Acambay graben. These faults have been identified using morphological indicators such as scarps, triangular facets, linear ridges, and parallel and rectangular drainage. The activity and youth of the faults has also been interpreted using morphological features, including offset drainage, V-shaped valleys, high-gradient scarps, low-levels of denudation of some scarps, active incision and valley-down cutting and sag ponds. Aerial photo-interpretation has proved to be a useful tool in the morphotectonic and neotectonic analysis of the Acambay graben and could also be effective in other areas.

Chapter Five: Morphometric Analysis: Use of Geomorphic Indices in the Assessment of Active Tectonism

Geomorphic indices are useful tools in evaluating active tectonics because they quickly provide insights concerning specific areas or sites in a region that is adjusting to relatively rapid, and even slow, rates of active tectonics (Keller, 1986). The Acambay graben provides an opportunity to study systematically landforms produced or modified by active tectonic processes and to deduce spatial variations of Quaternary deformation and active tectonics in the region. Some workers have already documented Quaternary tectonism, active surface faulting and historical seismicity in this part of central Mexico (Urbina and Camacho, 1913; Suter *et al.*, 1991, 1992; Astiz, 1980). However, none of these studies has used a systematic analysis of landforms to define patterns of tectonic activity in the region.

This chapter includes an approach to this problem that involves a morphometric analysis of selected landforms including the mountain fronts, fault scarps, and adjacent piedmonts of the Acambay graben to define the relative rates of tectonic activity on known faults that have generated escarpments or mountain fronts.

Morphometric analysis in tectonic geomorphology involves the measurement on topographic maps of landform variables such as mountain front sinuosity, valley morphology, longitudinal stream profile form, fault scarp heights and percentage of faceting. Morphometric variables have been defined so as to relate the adjustments of the fluvial and hillslope systems to the relative amounts of Quaternary uplift localised along mountain-front structures (Wells, *et al.*, 1988). Most of the morphometric variables used in this study were developed by Kostenko (1958, 1976, 1980), Hack (1973), Orlova (1975), Bull and McFadden (1977), Wallace (1977), Rantsman (1979), Mayer (1986), Nash (1986), Schumm (1986), and Wells *et al.* (1988) (Table 5.1).

Morphometric variable	Mathematical derivation *	Source
S_{mf} - Mountain front sinuosity	$S_{mf} = L_{mf} / L_s$	Bull and McFadden, 1977
Percent faceting along mountain fronts	L_f / L_s	Wells *et al.*, 1988
F_d - Percent dissected mountain fronts	L_{mfd} / L_s	Wells *et al.*, 1988
E_u - Percent undissected escarpments	L_{ce} / L_s	this study
Fault-scarp profiles	none	Wallace, 1977 and others
Stream long-profiles	none	Hack, 1973
V_f - Valley floor - Valley height ratio	$V_f = 2V_{fw} / [(E_{ld} - E_{sc}) + (E_{rd}-E_{sc})]$	Bull and McFadden, 1977
B_s - Drainage basin shape ratio	$B_s = B_l / B_w$	this study, after Cannon (1976)
S_r - River sinuosity	$S_r = L_s / L$	

* symbols are explained in the text.

Table 5.1 Summary of the morphometric variables used in tectonic landform analysis of individual mountain fronts of the Acambay graben.

The theoretical basis for the morphometric analysis presented here involves relative adjustments between local base level processes (tectonic uplift, stream downcutting, basin sedimentation and erosion) and the fluvial systems which cross structurally controlled topographic mountain fronts (Bull and McFadden, 1977). This type of morphometric analysis has not previously been applied to the fault-controlled mountain fronts of the Acambay graben .

Five major study areas associated with the systems of faults composing the graben were selected for morphometric analysis. Mountain fronts were selected for this study on the basis of topographic, lithological, geomorphological, and structural continuity. The selection of locations for morphometric measurements attempted to encompass as far as possible the most representative cases in the area of study. However, due to the large size of the area of study (2400 km^2) it was necessary to

apply sampling for some of the morphometric indices used. Sample selection was determined according to particular geomorphological criteria that provided high reliability and confidence in the representativeness of the morphometric data produced. Criteria for selection of the sites of slope profiling, stream profiling and river cross-sections are explained in detail in the following sections.

5.1 Tectonic geomorphic indices

5.1.1 Mountain fronts

i) Mountain front sinuosity.

Mountain front sinuosity is an index of the degree of irregularity or sinuosity along the base of an escarpment (Wells *et al.*, 1988). Because the plan view of most faults is straight or only gently curved, the degree of erosional modification of tectonic structures can be measured by a mountain front sinuosity index (Bull and McFadden, 1977). This is defined as

$$S_{mf} = L_{mf} / L_{s},$$

where L_{mf} is the length of mountain front along the mountain-piedmont junction and L_s is the straight-line length of the front. The S_{mf} index reflects a balance between the tendency of stream and slope processes to produce irregular (sinuous) mountain front and vertical active tectonics that tends to produce a prominent straight front (Keller, 1986). Values of S_{mf} approach 1.0 on the most tectonically active fronts, whereas S_{mf} increases if the rate of uplift is reduced or ceases, and erosional processes begin to form a sinuous front which becomes more irregular with time.

In this study mountain fronts were defined as major fault-bounded escarpments with measurable relief exceeding two contour intervals (20 m). For the

analysis, long escarpments were subdivided along strike into discrete segments with similar geological and morphological characteristics. The following criteria suggested by Wells *et al.* (1988) were applied: (a) intersection with cross-cutting drainages large in scale, relative to the front, (b) abrupt changes in lithology, (c) abrupt changes in the major morphological characteristics of the mountain front relative to adjoining front segments, and (d) changes in mountain front orientation.

Mountain front sinuosity was measured on large scale topographic maps (1: 50000). The sinuosities for the mountain fronts in the study area, which range from 1.0 to 1.38, are summarised in Table 5.2. Mean mountain front sinuosities are 1.1 and 1.32 for the northern flank of the graben, and 1.20 and 1.06 for the southern flank. Differences between the northern and southern flanks are almost insignificant. The mountain front is considered to coincide with fault-bounding structures in all these cases.

ii) Facets

A facet is a triangular-to polyhedral-shaped hillslope that lies between two adjacent drainages within a given mountain front escarpment. Tectonically active fronts display prominent, large facets that are generated and/or maintained by recurrent faulting along the base of the escarpments (Bull 1978, 1984). Less tectonically active mountain fronts contain fewer, smaller, and/or more internally dissected facets. Nevertheless, both small and large facets occur in tectonically active areas (Wells *et al.*, 1988).

More tectonically active mountain fronts tend to be less dissected, giving a range from laterally continuous undissected escarpments to a nearly continuous front with only a few large and distinct facets with minimal internal dissection (Wells *et al.*, 1988).

Three indices related to facet development were used in this study: (1) the proportion of faceting along mountain fronts, (2) the proportion of dissected mountain fronts, and (3) the proportion of undissected escarpments (Table 5.1).

(1) Percent faceting along mountain fronts. The purpose of this morphometric parameter is to define the proportion of a mountain front that has well-defined triangular facets, using the ratio of the cumulative lengths of facets to overall mountain front length (L_f / L_s, Wells *et al.* 1988).

(2) Proportion of dissected mountain front. This morphometric variable was used to define the proportion of a mountain front that has been dissected into distinct facets. This index is defined as the length of dissected mountain front to total mountain front length: $F_d = L_{mfd} / L_s$; where L_{mfd} - is the length of dissected mountain front.

(3) Proportion of undissected escarpments. This morphometric variable was developed in this study as a complement of the one mentioned above. Here mountain fronts that showed laterally continuous undissected escarpments were distinguished from individual facets in order to avoid confusion in the systematic definition of facets. This morphometric index was developed in order to define the proportion of a mountain front that has not been dissected. This index is defined as

$$E_u = L_{ce} / L_s ;$$

where L_{ce} - is the cumulative length of all laterally continuous undissected escarpments along a given mountain front. Tectonically active fronts have a high proportion of continuous undissected escarpments.

The dissection of overall escarpments was semi-quantitatively assessed to indicate relative levels of tectonic activity along the mountain fronts. In this study the proportion of faceting was calculated for each of the mountain fronts along the graben and the segments defined for each front.

iii) Fault scarp morphology

The morphology of scarps produced by faulting provides a successful geomorphic indicator of active tectonics (Keller, 1986). Slopes are dynamic forms, with the dominance of one element of slope morphology relative to others changing over time (Wallace, 1977). The preservation of morphological elements characteristic of young scarps suggests active tectonism and recurrent displacement along the same fault line produces a composite fault scarp (Wallace, 1977). Multiple displacements on a compound fault scarp can be recognised from various features. These include sharp breaks in slope on scarp benches or terraces associated with small channels that have eroded through the fault scarp, knickpoints in channels that cross the scarp, scarp heights that exceed those likely to have been produced by a single event, and progressive displacement (older sediments being displaced more than younger) (Keller, 1986).

Thus, the geomorphic characteristics of young scarps can be used as a key to dating fault displacements. Scarps with steep slopes are younger (Wallace, 1977) since the principal slope of scarps declines with the age. Several workers have established relationships between fault scarp morphology and age (Wallace, 1977, Bucknam and Anderson, 1979; Mayer, 1984, 1986; Horst, 1985; Hanks and Wallace, 1985; Nash, 1986; Menges, 1990; Avouac, 1993; Avouac *et al.*, 1993).

Quantitative and qualitative morphological characteristics of fault scarps were determined in this study for the escarpments bordering the Acambay graben and the fault scarps on the flanks of Mount Temascalcingo. Profiles of the fault scarps (total of 27) were traced from 10 metre contour maps (scale 1:50000) along the main faults of the Acambay graben. The detailed 10 m contour maps, produced from photogrametric and topographic levelling techniques provided reliable detail for the tracing of fault scarp profiles. The sites for profiling where selected according to at

least one of the following criteria: 1) slopes that represented the main morphological features on each section of fault scarp, 2) slopes that exhibited particular morphotectonic features, and 3) a minimum of two randomly selected slopes for each fault scarp. The analysis of fault scarp profiles included consideration of slope materials and climate as factors controlling the rate of scarp degradation and affecting scarp morphology.

The purpose of analysing fault-scarp profiles within the context of the present study is to quantify, as far as possible, characteristics of scarp morphology and to relate the change in morphology to active tectonics and to ageing and/or degradational processes.

5.1.2 Fluvial systems

The morphology of small- to medium-sized channels and valleys (5-20 km length, and exceptionally the more than 50 km long Lerma River) that cross mountain fronts may reflect the impact of local base-level changes due to relative uplift along active structures associated with the frontal escarpments (Wells *et al.*, 1988). This study uses detailed longitudinal profiles, cross-river sections, cross-valley relief ratios, channel-sinuosity ratios and basin-shape ratios measured on 10 m contour maps to isolate anomalous patterns in channel or valley forms attributable to tectonic activity.

i) Longitudinal profiles

Longitudinal stream profiles were plotted at 10 times vertical exaggeration in order to highlight any irregularities in channel slope. This study uses semi-log plots of some streams in order to counteract the exponential flattening of an equilibrium fluvial long profile (Bishop and Bousquet, 1989). The semi-log plot of an equilibrium long profile is a straight line on the axes if the river is flowing across uniform bedrock (Hack, 1973a, 1973b). Oversteepened reaches that cannot be explained by resistant

lithology in the stream bed reflect disequilibrium conditions, and a common cause of such disequilibrium is tectonic disruption of the bed (Bishop and Bousquet, 1989). Several workers have demonstrated such stream over-steepening in association with uplift along active faults (Keller and Rockwell, 1984; Bull and Knuepfer, 1987; Bishop and Bousquet, 1989).

A small number of streams cross transversally the fault-bounding mountain fronts in the Acambay graben. Long profiles were plotted for those streams that reached the drainage divide and transversely cross main fault systems along the graben. River-long profiles were plotted from topographic maps at a scale of 1: 50000 with a 10 m contour interval. The bedrock on the channel bed was also considered for the long profile analysis.

ii) River cross-sections and cross-valley relief ratios

Transverse valley profiles were defined using a valley floor-valley height ratio variable. Comparison of the width of the floor of a valley with its mean height, provides an index that indicates whether the stream is actively downcutting (being dominated by the influence of a base level fall at some point downstream) or is primarily eroding laterally into the adjacent hillslopes. This index can be expressed by

$$V_f = 2V_{fw} / [(E_{ld} - E_{sc}) + (E_{rd} - E_{sc})],$$

where V_{fw} is the width of valley floor, E_{ld} and E_{rd} are the respective elevations of the left and right valley divides and E_{sc} is the elevation of the valley floor (Bull and McFadden, 1977). The index reflects differences between broad-floored canyons with relatively high values of V_f, and V-shaped canyons with relatively low values.
The location of the cross-valley transects within a drainage basin affects the values of V_f. Thus, in this study transverse valley profiles were located 0.5 km upstream from

the mountain front in smaller drainage basins, and in large drainage basins transverse valley profiles were located 0.5 and 1 km upstream from the mountain front. The reason for working with different ranges for the location of the cross-valley transects is that valley floors tend to become progressively narrower upstream from the mountain front in larger drainage basins for a given mountain range. These data were combined with the analysis of valley morphology.

iii) Drainage basin shape

The typical basin of a tectonically active mountain range is elongate and basin shapes become progressively more circular with time after cessation of mountain uplift (Bull and McFadden, 1977). Thus, the planimetric shape of a basin may be described by an elongation ratio B_S that can be expressed as

$$B_S = B_l / B_W$$

where B_l is the length of the basin, measured from its mouth to the most distant drainage divide, and B_W is the width of the basin measured across the short axis (Fig. 5.1). The index reflects differences between elongated basins with high values of B_S and more circular basins with low values. Drainage basin widths are much narrower near the mountain front in tectonically active areas where the streams energy has been directed primarily to downcutting; by contrast, a lack of continuing rapid uplift permits widening of the basins upstream from the mountain front.

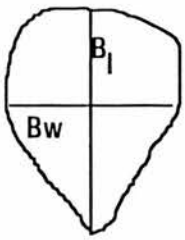

Fig. 5.1 Diagram showing drainage basin shape variables: B_l - length and B_w - width of the basin.

The B_s index, developed in this study after Cannon (1976), can be computed from large- to medium-scale topographic maps and also from elevation data stored in computer systems. Therefore it can be quickly and easily calculated. In this study the B_s index was calculated for the 27 drainage basins of streams that cross the main faults of the Acambay graben .

iv) River sinuosity

Stream patterns are sensitive indicators of valley slope change. In order to maintain a constant gradient a river that is being steepened by a downstream tilt will increase its sinuosity, whereas a reduction of valley slope will lead to a reduction of sinuosity (Ouchi, 1985; Schumm, 1986). The sinuosity of a river can be described as

$$S_r = L_s / L,$$

where S_r is the length of a sinuous river in a given sector and L is the straight-line length in a given sector. An anomalous increase in S_r index can be interpreted as response to active tectonics. Care, however, has to be taken in evaluating such changes in channel pattern because of the potential effects of changes in other variables. In this study an S_r index was calculated only for the Lerma River because it is the only stream that exhibits a clear change in channel pattern.

5.2 Results of the morphometric analysis.

Variations in the morphology of the fault systems that form the Acambay graben described in chapters 3 and 4 provided the basis for the morphometric analysis. The areas considered are: 1) Acambay-Tixmadeje, 2) Tepuxtepec, 3) Pastores, 4) Venta de Bravo and 5) Temascalcingo.

5.2.1 Acambay-Tixmadeje.

i) Mountain front.

Sinuosity and facet-dissection characteristics (Proportion of faceting, proportion of dissected mountain fronts, proportion of undissected escarpments, morphology of facets, and fault scarp morphology) were analysed for the Acambay-Tixmadeje mountain front (Fig. 5.2). Mountain front sinuosity is low (mean = 1.1) for the whole mountain front (Table 5.2). This relatively low sinuosity value (the highest mean value for the all Acambay graben mountain fronts being 1.32) reflects a fairly straight front that coincides with an active tectonic structure along which erosional retreat by streams from the range bounding faults has been very limited.

The degree of facet development present along individual sub-areas (morphostructural blocks) ranges from 3 % to 29 % (Table 5.2). The proportion of faceting for sub-areas I and III is considerably higher (15 % and 29 % respectively) than that for sub-area II. The mean proportion of faceting for the Acambay-Tixmadeje mountain front is 15.6 %. The undissected escarpment index (E_u) ranges from 5.9 % to 26.5 %, with a mean value of 13.7 %. The highest value for the undissected escarpment index occurs in sub-area I (26.5 %).

The degree of mountain front dissection ranges from 12.5 % to 37.5 %, the maximum value occurring in sub-area III. The mean value for the Acambay-Tixmadeje area is 27.7 %, which is relatively low. Sub-area I shows a relatively high degree of undissected escarpments (26.5 %) whereas the proportion of faceting is

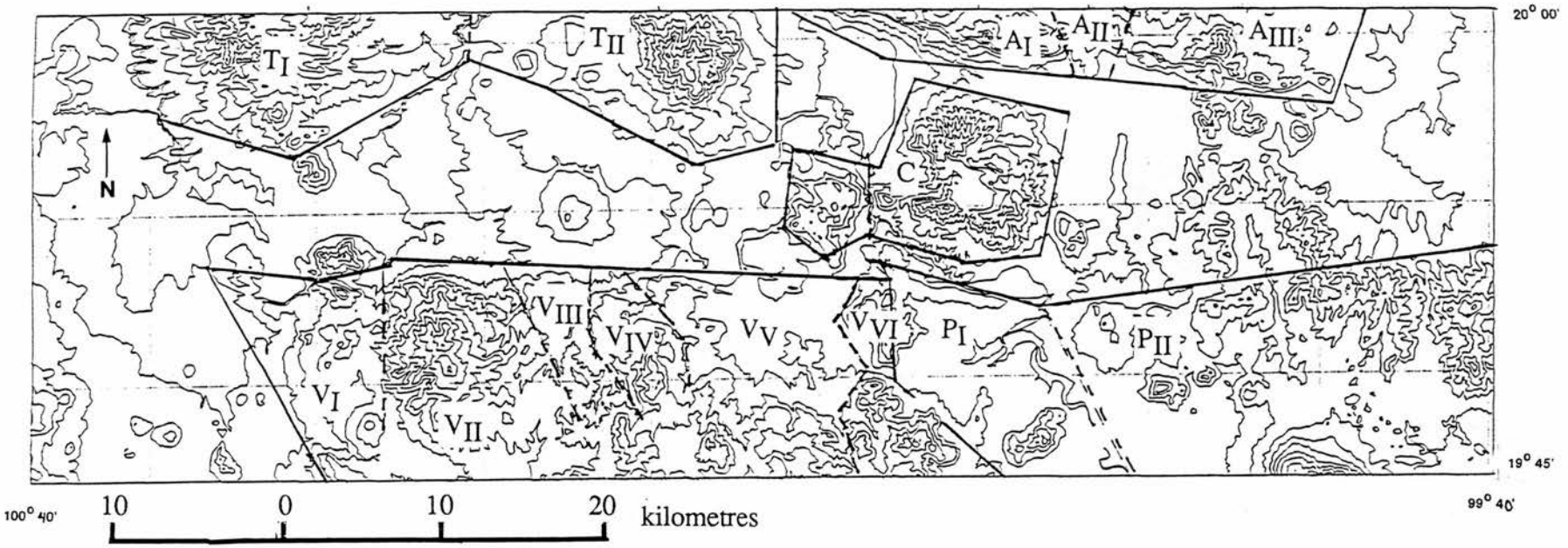

Fig. 5.2 Generalised topographic map of Acambay graben including the study areas for morphometric analysis. Thick lines indicate the approximate boundaries of the five sub-areas studied, labelled by area (letters) and sub-area (Roman numerals): A - Acambay-Tixmadeje, T - Tepuxtepec, P - Pastores, V - Venta de Bravo, C - Temascalcingo. Source maps for this digital compilation are from the Instituto Nacional de Estadística, Geografía e Informática (Scale 1: 50000).

moderate (15 %). The proportion of dissected mountain front here is the lowest (12.5 %) for the whole sub-area, whereas the proportion of faceting of sub-area III is the highest of all sub-areas. Sub-area III also has the highest proportion of dissected mountain front (37.5 %), and a moderate value for undissected escarpments (8.8 %). This peculiarity may be explained in terms of the height of the scarp (350 m) which is subject to more intensive dissection. Here, facets exhibit elongated triangular shapes and few of them are internally dissected. The morphology of facets here displays differences among the three sub-areas. Sub-area I has facets with an elongated triangular-shape while sub-area II displays almost equilateral triangular facets. Along sub-area III facet development is restricted to near to the base of the scarp, while the upper part of the scarp looks like a continuous scarp. These morphometric variables indicate more dissection along the escarpment of sub-area III, but in some parts the scarp is laterally continuous and undissected. Thus, it appears that this sub-area may be relatively the less tectonically active compared with sub-areas I and II.

The analysis of the morphometric data suggests moderate to high levels of tectonic activity along mountain fronts throughout the Acambay-Tixmadeje area. Differences in faceting and dissection are inferred to represent variations in tectonic activity among the three sub-areas. The relatively high values of faceting and the low dissection of mountain fronts in sub-area I imply particularly active faulting in this area. These variations of tectonic activity for the three sub-areas may be related to differences in uplift between a series of adjacent fault-blocks.

Mountain front and sub-areas	S - Mountain front sinuosity	% Facet L_f / L_s	E_u - Undissected escarpments	% Facet + % E_u	% F_d - dissected mountain fronts
1. Acambay-Tixmadeje	1.1	15.6	13.7	16.4	27.7
I		15	26.5	33.5	12.5
II		3	5.9	6.5	33
III		29	8.8	9.1	37.5
2. Tepuxtepec	1.32		25.8	25.8	-
I	1.38	-	28.6	28.6	-
II	1.26	-	23	23	-
3. Pastores	1.20	8.5	39.3	47.8	11
I	1.06	0	78.6	78.6	22
II	1.33	17	0	17	0
4. Venta de Bravo	1.06	16.6	37.3	53.8	28.6
I	1.0	0	80	80	1.2
II	1.0	31	0	31	16.2
III	1.15	28	16.7	44.7	4.6
IV	1.15	40	0	40	4.2
V	1.05	0.7	77	77	1.2
VI	1.0.5	0	50	50	1.2
5. Temascal-cingo	-	18.2	34.7	53	28.5
I	-	6	48.8	54.8	23
II	-	3	40	43	25
III	-	31	50	81	33
IV	-	33	0	33	33

Table 5.2 Morphometric variables for the mountain fronts of the Acambay graben.

ii) Fault scarps.

Fault-scarp characteristics for six profiles were derived from detailed 10 m contour maps of the Acambay-Tixmadeje area (Fig. 5.3). Most of the scarps discussed are in extrusive igneous rocks (andesite, basalt and tuff). All of them are steep and the majority of them exhibit one or two breaks in slope with an straight segment (Fig. 5.4). Profile 1, from the eastern part of the scarp, is 700 m high and has a mean slope of 27°. It shows a break along slope (gradients are 16° at the base of the slope and 30° in the upper part) that indicate the presence of two faults. The base of the scarp is composed of colluvium and tuff deposits. The geomorphological characteristics of this scarp, according to Wallace's (1977) study of faults scarps, suggest a mainly fault-controlled scarp, with an initial stage of development of gravity and debris control over the scarp form.

Profile 2 is 610 m high and has a 20° mean slope. The geomorphological characteristics of this profile are similar to those of profile 1. However, here the debris slope is smaller than in profile 1. This profile also shows one break in slope, the lower part averaging 31° and the upper 33°, that similarly indicate the presence of two faults. Profile 3 is 450 m high with gradient 15° at the base of the slope. There are two apparent breaks of slope (gradients 27° in the middle part and 30° in the upper). The debris slope is wider and is composed of tuff and conglomeratic deposits. The free face has been slightly smoothed, but the scarp is still fault-controlled. Profile 4 has a mean slope of about 20° and 37° on the top. Two breaks along the slope indicate the presence of two faults. The continuity of the base of the slope which has an angle of about 10° is interrupted by a probable dome. Between the upper surface and the first break in slope the gradient is very steep, while the second segment, down-slope, has a lower gradient due to debris deposition.

Profile 5 is 650 m high and has a mean slope of 20° that increases in the upper part of the slope up to 40°. This scarp is the highest in the whole Acambay graben. The

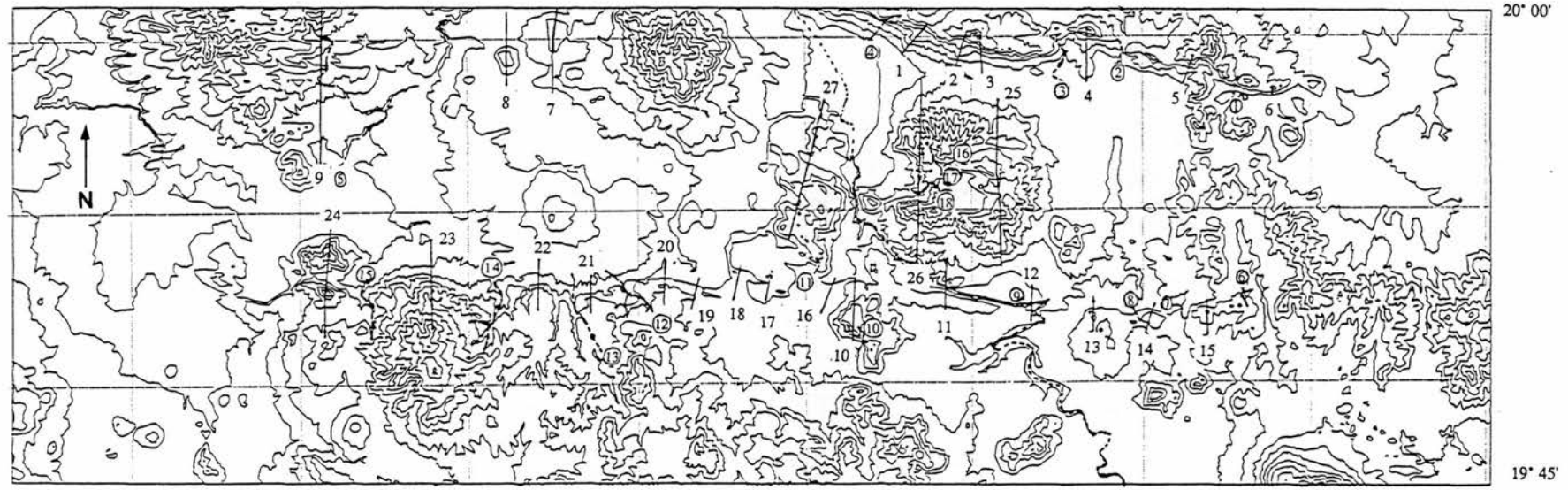

Fig. 5.3 Map showing the location of the profiles for fault-scarps and streams selected for morphometric analysis. Continuous lines indicate the trace of profiles for fault-scarps. Numbers 1 to 6 - profiles of the Acambay-Tixmadeje area, 7 to 9 - profiles of the Tepuxtepec area, 10 to 15 - profiles of the Pastores area, 16 - 21 - profiles of the Venta de Bravo area, and 25 to 27 - profiles of the Temascalcingo area. The dotted lines indicate river courses. Encircled numbers indicate: 1-4 streams of Acambay-Tixmadeje area, 5 stream in the Tepuxtepec area, 6-9 streams of the Pastores area, 10-15 streams of the Venta de Bravo area, and 16-18 streams of Temascalcingo area.

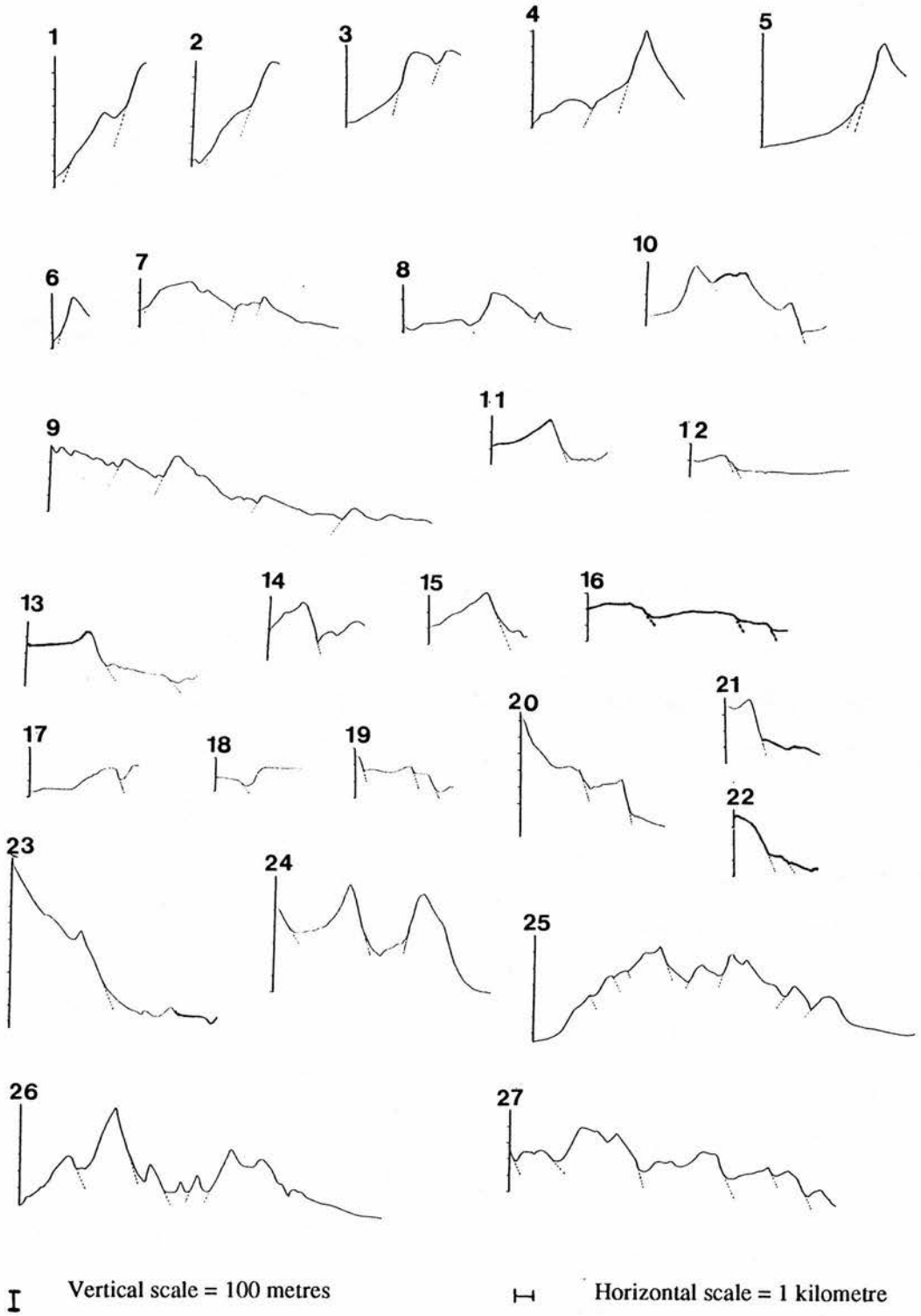

Fig. 5.4 Fault-scarp profiles showing fault positions. Vertical exaggeration is 10x. Dotted lines indicate the location of faults. See Fig. 5.3 for location of profiles.

profile has two breaks of slope and a moderately wide wash-slope on the base with a gradient of 10°. The geomorphological characteristics of this profile suggest a generally fault-controlled scarp.

Profile 6 is the lowest in this area, being only 280 m high, although it has a high mean gradient of 33°. The profile shows only a subtle break in slope and this reflects the position of the master fault. The low height of this scarp is presumably a response to its location on the eastern termination of the mountain front. The morphology of this profile reflects a clear fault-control.

The geomorphological characteristics of the six transverse profiles traced along the Acambay-Tixmadeje mountain front display fault-controlled slopes. Most of these profiles have steep slopes and one or two breaks of slope that indicate the position of faults. It appears that here the rocks composing these fault-scarps are mainly resistant to erosion and that climate is moderate-sub-humid. These factors and the recent tectonic activity have helped to preserve fault morphology more effectively. Thus, it can be assumed that these scarps are tectonically active and relative young.

iii) Fluvial systems

The longitudinal profiles of the four streams studied in Acambay-Tixmadeje area exhibit mainly convex and semi-concave profiles (Fig. 5.3 and 5.5). All the profiles have some convex reaches, and steeper gradient reaches are located at, or a small distance upstream, from where the channels cross the line of topographic escarpments (Fig. 5.5).

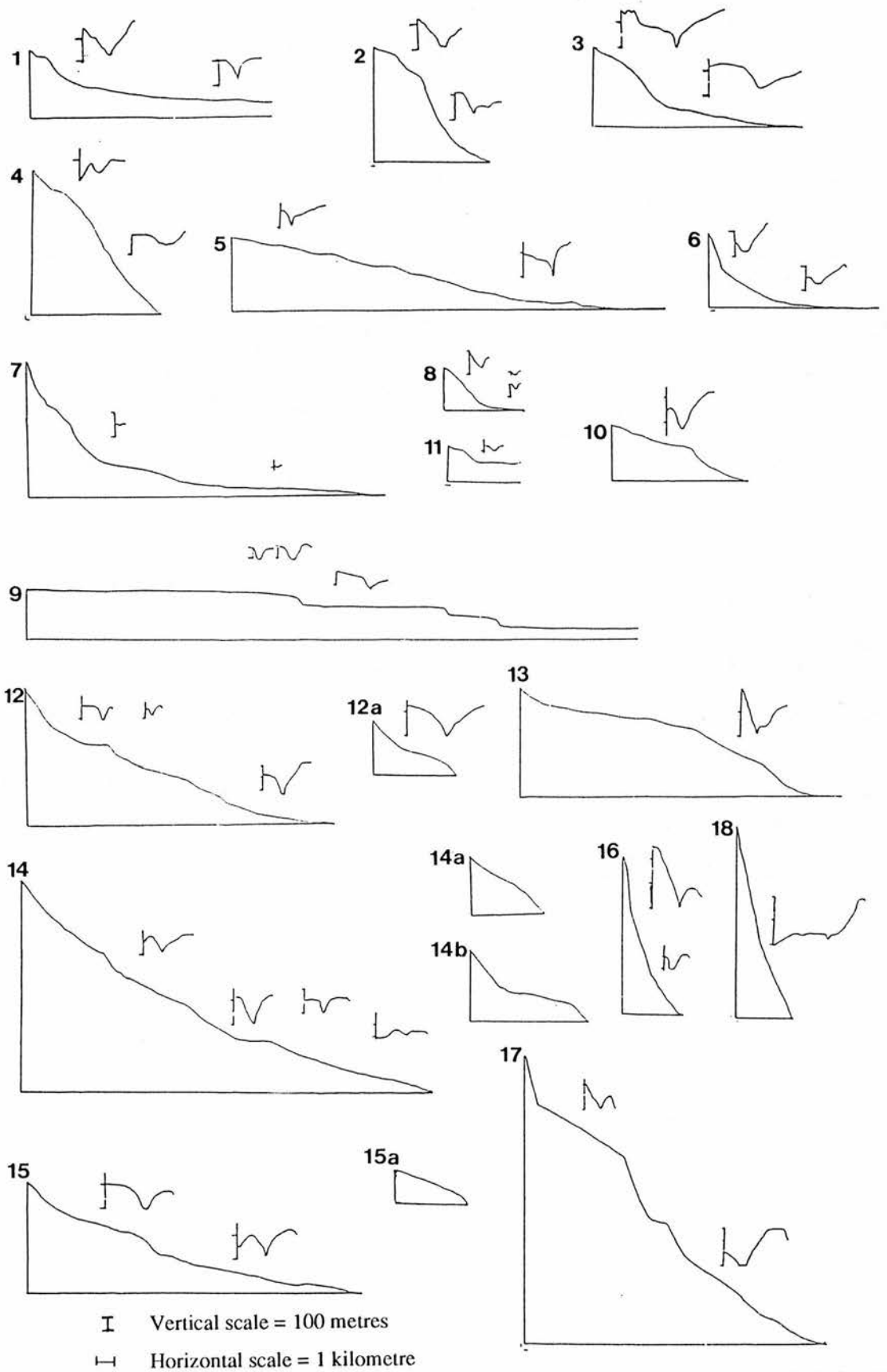

Fig. 5.5 Longitudinal profiles of streams transverse to mountain fronts in the Acambay area. Numbers: 1-4, Acambay-Tixmadeje area; 5 - Tepuxtepec area; 6-9, Pastores area; 10-5, Venta de Bravo area; and 16-18, Temascalcingo area. Inserts show valley cross-profiles. Vertical exaggeration is 10x. See Fig. 5.3 for location of profiles.

V_f values along these four streams range from 0.07 to 1.5 (Table 5.3). Typical V_f values are 0.1 to 0.9, although individual V_f ratios fluctuate slightly along individual streams. A general pattern of variations of V_f ratios for the streams can be established; for instance, the Tepozán (3) and Boshi Grande (1) V_f ratios remain somewhat low (<1.2) in headwater regions , probably reflecting persistent channel downcutting in these reaches, but further downstream the general ranges of V_f ratios increase, presumably in responses to a relative increase in the amount of lateral stream migration and valley floor widening. In the profiles for Cañada Honda (4) and Río San Miguel (2) V_f ratios fluctuate along these streams. Cañada Honda (4) has the largest V_f value, and valley cross-profile, the latter also being the case for the downstream sector of Tepozán (Fig. 5.4). Drainage basin shape (B_s) or l/w ratio values along the four streams range from 1.1 to 6 (Table 5.3). The mean B_s values range from 1.1 to 1.8, values greater than 1 indicate elongated basins.

Table 5.3 Fluvial system indices for the streams crossing mountain fronts through the Acambay graben. Symbols: a- upstream, b-downstream.

Mountain front / stream	V_f -mean valley morphology	B_s -drainage basin shape
Acambay-Tixmadeje		
1. Boshi Grande		1.83
a	0.07	
b	0.12	
2. San Miguel		1.1
a	0.53	
b	0.4	
3. Tepozán		1.17
a	0.33	
b	0.82	
4. Canada Honda		6
a	1.2	
b	1.5	

Tepuxtepec		
Las Palomas		-
a	0.2	
b	0.35	
Pastores		
1. El Cielito		2.4
a	0.7	
b	0.3	
2.B. Fresno		1.29
a	0.45	
b	1.7	
3. El Fresno	10	3.2
4. El Caracol		1.5
a	0.2	
b	0.43	
5. Lerma		-
a	0.54	
a*	0.90	
b	0.75	
Venta de Bravo		
1. Santa Ana	0.43	1.59
2. La Chiquita	2.5	6
3. Encinal	1	3.14
4. El Encinal		2.73
a	0.95	
b	0.35	
5. América	0.18	2.28
6. San Miguel		2.23
a	0.17	
b	0.54	
7.	1.5	2.12
8.	0.46	2.07
9. Río Grande		0.9
a	0.58	
b	0.10	
Temascalcingo		
1. A. Bajomi		1.56
a	0.13	
b	1.8	
2. Bajomi (branch)		3.2
a	0.66	

b	0.4	
3. Campanario	0.5	1.14

The combined V_f ratios, longitudinal profiles, valleys cross-sections and B_s ratios of the four analysed streams in the Acambay-Tixmadeje area suggest that their profiles exhibit an abrupt steepening of gradient at, or immediately upstream of, fault-escarpments. These observations accord with the general pattern of channel gradient variations in an active tectonic region of the Pacific coast of Costa Rica studied by Wells *et al.* (1988). These gradient changes appear to represent knickpoints generated by local tectonic uplift along faults. The steepened reaches generally coincide with decreases in V_f ratios indicative of downcutting within narrow, V-shaped, canyons; this is interpreted as a stream response to local base level changes caused by relative local uplift across mountain front. Regardless of differences in lithology, gradient and V_f values are similar for most of the small sized streams that cross the mountain front of the Acambay-Tixmadeje area.

5.2.2 Tepuxtepec.

i) Mountain front.

The Tepuxtepec area does not display a continuous mountain front because it is disrupted by the basin of the Lerma River and Lake Tepuxtepec (Fig. 5.2). However, some of the morphometric indices were applied to the fault-bounding fronts of this area. The values of sinuosity of mountain fronts for sub-areas I and II are 1.38 and 1.26 respectively (Table 5.2), mean value of mountain front sinuosity being 1.32. This value is relatively low and may represent the relative straightness of mountain fronts in the area.

In this region emphasis was given to the analysis of long continuous escarpments, proportion of dissection and fault-scarp analyses. The degree of facet

development is considered to be equal to 0 % because there are no proper triangular facets present. However, it is possible to observe and evaluate laterally continuous escarpments along these fault-bounding fronts. The degree of continuous escarpments present in sub-areas I and II are 28.6 % and 23% respectively (Table 5.2). The mean value is 25.8 %. The lack of facets and these low values are indicative of a relatively low tectonic activity in the Tepuxtepec area in comparison with higher mean values of faceting and predominance of undissected escarpments in the Acambay area as a whole. These morphometric characteristics and the relatively short length of fault-scarps in the Tepuxtepec area suggest a relatively low level of tectonic activity.

ii) Fault scarps

The fault scarp characteristics of 3 profiles in the Tepuxtepec area were analysed (Fig. 5.3, profiles 7,6 and 9). These profiles show moderate to gentle gradients (13^{o} to 24^{o}). The height of these scarps is generally low (Fig. 5.4), ranging from 30 to 120 m. Only one break in slope indicates the presence of a fault. These profiles, in this case traced across the mountain front, show evidence of several en-echelon faults. The low gradients and morphology of these slopes suggest that debris accumulation exerts an important control. This implies lower levels of tectonic activity in this area and/or more extensive dissection related to the time since exposure of the fault scarps.

iii) Fluvial systems

The analysis of fluvial systems in the Tepuxtepec area was limited to the single stream that crosses this mountain front and that is of significant length (more than 2 km)(Fig. 5.3). The longitudinal profile of the Las Palmas, a tributary of the Lerma River, exhibits several alternate convex and concave reaches similar to the profiles described for streams in the Acambay-Tixmadeje area (Fig. 5.5). Differences in

gradient in the Tepuxtepec area likewise occur upstream from points where the stream crosses mapped or inferred faults. These convex segments are similarly interpreted as reflecting localised uplift along this fault-bounding front at a rate that exceeds the stream's capacity to remove the imposed channel slope discontinuity. However, some of the changes evident in channel gradient may be controlled by variations in lithology. Nevertheless, these gradient changes along the river profile might still reflect the location of faults on the Tepuxtepec fault-bounding fronts.

V_f ratios in the Las Palmas River, in the Tepuxtepec area are low both upstream (0.2) and downstream (0.35) (Table 5.3), but the V_f value is relatively higher downstream and reflects a broader valley and an increase in lateral stream migration downstream. However, the valley profile is almost V-shaped, probably as result of channel downcutting in response to active tectonism (uplift) along these faults (Fig 5.5).

5.2.3 Pastores.

i) Mountain front.

Mountain front sinuosities in the Pastores area range from 1.06 to 1.33 (Fig. 5.2, Table 5.2), the mean S_{mf} value for this area being 1.2. These values suggest relatively active tectonism in the area. According to Bull's classification (Bull and McFadden, 1977) these values coincide with the first class of active tectonism (the most active). The degree of facet development present in sub-area I (Table 5.2) is 0 % which means that no identified facet segment exists, and 17% in sub-area II (Table 5.2). The mean value of proportion of faceting is 8.5 %, which is relatively low. However, the laterally continuous undissected escarpment value is 78.6 % for sub-area I and 0 % for sub-area II (Table 5.2). The mean value is 39.3 %. Faceted scarps in sub-area II have developed facets at the scarp base. Differences in the proportion of faceting and values of proportion of undissected escarpment between the two sub-

areas do not seem to indicate differences in the tectonic regime. Values of the proportion of dissected mountain fronts are significantly different for sub-area I (22 %) and II (0 %)(Table 5.2). The mean value is 11 %.

These morphometric data suggest high levels of tectonic activity for the Pastores fault and particularly for sub-area I. Difference in faceting, undissected mountain fronts and dissected mountain front values might suggest variations in tectonic activity between the two sub-areas and this may indicate the presence of different structural blocks.

ii) Fault scarps

The fault-scarp characteristics of the Pastores mountain front were analysed in six transverse profiles (Fig. 5.3). Most of the scarps have high to moderate mean gradients (21° to 26°). All of them are composed of andesite and basalt. At the western end of the Pastores area, profile 10 (Fig. 5.4) displays two breaks in slope indicating faults facing to the north, the mean slope here being 34°. The first break in slope from north to south marks the location of a fault. These sharp changes in gradient and the steepnes of the scarp suggest fault-control. In the south, the same profile displays another fault-scarp with a lower gradient slope (22°) associated with a north-facing fault. The base of the scarp has a gentler slope (15°), but it might still be essentially fault-controlled. To the east, profile 11 has a steep to moderate slope of 24° and is 240 m high. This profile shows only one break of slope near to the base of the scarp where there is a partially debris-controlled slope.

Profile 12 is located close to the Lerma River. This scarp is relatively low (80 m), but there are two breaks of slope that indicate the presence of two faults. Profile 13 is 240 m high and has a steep gradient of nearly 21° in its upper part, but with a lower gradient basal section (less than 10°). The base of the scarp is covered with

debris material. The profile displays one break in slope along the scarp that might indicate the continuity of the Pastores fault to the east.

Profile 14 has a steep gradient (46°) and is 210 m high. Profile 15 is less steep (23°) in the upper part of the scarp and has a moderate gradient (10°) near to its base. The scarp here is 270 m in height . The profile shows a break in slope related to a north-facing fault. The morphology of the slope resembles a fault-controlled scarp.

The fault-scarps of the Pastores fault are generally steep and most of them show an incipient debris segment near to the base of the slope. A main fault is clearly reflected in the morphology of the slopes. The geomorphological characteristics of these profiles suggest fault control over the scarp along Pastores mountain front and a probable relatively young age for these escarpments.

iii) Fluvial system

Few streams cross the fault-bounded mountain front in the Pastores area. The longitudinal profiles of five streams were analysed, including the Lerma River, the longest in the whole Acambay graben (Fig. 5.3). The long profiles exhibit a few alternate convex and concave reaches (Fig 5.5). The oversteepened reaches occur upstream from points where channels cross faults in the mountain front. The convex segments along the profile can be interpreted as a reflection of local uplift in the mountain front, as described for streams in the Acambay-Tixmadeje area. Most of the long profiles here have a nearly concave form. However, the Lerma River long profile has a convex form reflecting active tectonism in the area. Small streams may be less susceptible to such effects.

V_f ratios, in the studied streams in the Pastores area range from 0.2 to 10 (Table 5.3), with typical V_f values being between 0.2 and 0.9. Low V_f ratios are, however, predominant in these streams and they suggest that channel downcutting is the predominant process. V_f values upstream tend to be lower than downstream. The

exception to this generalisation is the Lerma River which has a higher V_f value (0.75) immediately upstream from the top of the scarp, but a decrease downstream near its base. The general pattern of V_f values along most of the streams suggest that channel downcutting reflects the high level of tectonic activity in the area. Cross-valley profiles for these streams (Fig. 5.5), along the Pastores fault-bounding mountain front are V-shaped and indicative of active tectonics (Bull and McFadden, 1977). The analysis of drainage basin shape gave B_s values ranging from 1.5 to 3.2 (Table 5.3). These relatively high values suggest elongated basins for all streams in the Pastores mountain front, and similarly reflect active tectonics in the area.

The sinuosity index (S_r) along the Lerma River shows an increase in the area surrounding the point where the river crosses the Pastores fault (Fig. 5.6). The meandering channel pattern changes as a result of faulting between downthrown and upthrown blocks. Upstream (south of the point where the river crosses the fault) the sinuosity value is relatively high (1.91), the meanders of the Lerma River having a high amplitude and wavelength. The sinuosity value is still high immediately downstream from the point where the river crosses the fault, but on the downthrown block the size of the meanders decreases, although the meander sinuosity value increases. The area near to the faults, on both the upthrown and downthrown blocks, shows an increase in sinuosity ($S_r = 2$) but decrease in meander dimension. In addition there are knickpoints in the long profile, degradation in the area of faulting and local narrowing of the channel of the River Lerma. Thus, the sinuosity values increase as the fault is approached or crossed. These observations indicate that degradation has occurred at, and upstream of, the fault.

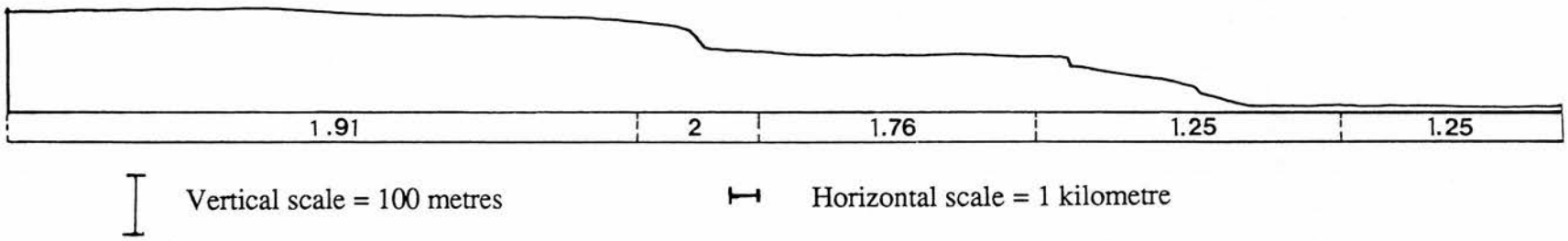

Fig. 5.6 Lerma River sinuosity index in the Acambay graben area.

5.2.4 Venta de Bravo

i) Mountain front

Mountain front sinuosities in the Venta de Bravo area range from 1.0 to 1.15 (Table 5.2). For all the sub-areas in Venta de Bravo area (Fig. 5.2) the S_{mf} values are quite similar (Table 5.2). The mean value of sinuosity for the whole area is 1.06, the low S_{mf} values reflecting the tendency for mountain fronts to be straighter at the termination of the fronts that in the interior sub-areas.

The proportion of faceting along the Venta de Bravo mountain front ranges from 0 % to 40 % (Table 5.2), with a mean value 16.6 %. These data indicate that the low values for sub-areas I, V, and VI contribute to the relatively low value of the proportion of faceting in this area. The lowest values for the proportion of faceting correspond to the terminal sub-areas of the Venta de Bravo mountain front (sub-areas I, V, and VI); whereas the central part of the mountain front displays relatively high values of the proportion of faceting (40, 28 and 31 % for sub-areas IV, III and II respectively). The amounts of undissected laterally continuous escarpments show values ranging from 0 to 80 % (Table 5.2), and the mean value is relatively high at 37.3 %. The terminal sub-areas of the Venta de Bravo mountain front have the highest values for the proportion of undissected escarpments (80 %, 77 % and 50 % for respectively, sub-areas I, V and VI). The mean value of undissected escarpments is 45.3 % for the whole Venta de Bravo mountain front. This reduced mean value for undissected escarpments is produced by the contribution of sub-areas II and IV, both of which have no undissected escarpments.

Considering the proportion of faceting together with the undissected escarpment variable it can be seen that sub-area I exhibits the most continuous undissected escarpment development, while sub-areas V and VI also show high values (77 % and 50 % respectively). By contrast the central part of the Venta de Bravo mountain front displays moderate values for these morphometric variables.

The morphology of triangular facets is especially notable in sub-area III, where the scarp shows triangular shaped facets in its upper part and is almost continuous towards the base. This particular morphology may suggest variations in the tectonic regime and/or two distinct tectonic events.

The proportion of dissected mountain fronts are relatively low, with the exception of sub-area II (16.2 %). Values range from 1.2 to 16.2 % (Table 5.2). The mean value is 4.8 %. These morphometric data suggest generally high levels of tectonic activity along the mountain front through out the Venta de Bravo area. The low values of the proportion of faceting for sub-areas I, V, and III are compensated for by high values of undissected escarpments. These sub-areas also show low levels of dissection. The central part of the mountain front (sub-areas II, III and IV) shows relatively high values of facet development and relatively low to moderate values for dissected escarpments. Sub-area II shows rather anomalously high values of dissection. These may be related to variations in lithology, with corresponding changes in susceptibility to fluvial erosion. However differences in these morphometric values along the Venta de Bravo mountain front may also indicate variations in tectonic activity between the six sub-areas.

ii) Fault scarps

Profiles of fault-scarps were traced at nine sites across the Venta de Bravo mountain front (Fig. 5.3), most of them showing steep slopes (Fig. 5.4). In the eastern termination of the Venta de Bravo front three parallel faults are indicated by the profiles. The northernmost scarp is 60 m high and has a steep gradient (43^{o}). The base of the profile has a gentler gradient (10^{o}) representing a debris and wash slope (Profile 16, Fig. 5.4). To the south, this profile displays a second, 40 m high, scarp with a steep gradient (45^{o}) that has a break in slope near its base. This break in slope

indicates the position of the Venta de Bravo fault. The southernmost scarp has a gradient of 14° and has a wash-slope.

Profile 17 (Fig. 5.4) has a 70 m high scarp with a steep gradient (31°) and a wash-slope. Profile 18 (Fig. 5.4) exhibits a short scarp only 30 m high and with a moderate slope (18°) and a very narrow debris slope. Profile 19 (Fig. 5.4) has two steep rectilinear slopes with a gradient of 29° to 43°. The height of these scarps ranges from 140 m for the frontal scarp, to only 40 m for the southern scarp. A third 90 m high scarp can be identified in the southermost part of this profile. The morphology of these all scarps clearly indicates fault control.

Profile 20 (Fig. 5.4) has two scarps. The first has a steep slope (30°) and is 210 m high. It is a predominantly straight slope with a gentler gradient at the base suggesting slope wash activity. This scarp reflects important fault control by the Venta de Bravo master fault in this area. The second scarp, upwards, is generally less steep (20°) and is 110 m high. The profile shows a break in slope indicating the location of a fault. Profile 21 is 310 m high and has a steep slope (31°). The profile displays a narrow debris slope but is still mainly fault-controlled. Profile 22 (Fig. 5.4) is 330 m high and has a moderate gradient (10°) in its upper part but has a steeper mid-slope (27°). The base of the slope has a lower gradient and is composed of colluvial material. The free face and crest of the slope have been eroded and have retreated. The change in the gradient produces a break in the scarp suggesting the location of a fault.

Profile 23 (Fig. 5.4) has the highest fault-scarp in Venta de Bravo area at 500 m. The upper part has a steep gradient (24°), but the slope declines to 13° at the base. This break in slope indicates the position of the fault and the morphology of this profile suggests a fault-controlled escarpment. Profile 24 is 420 m high and exhibits (Fig. 5.4) two escarpments. The frontal scarp is quite steep (30°) in its upper part and at its base. The steepness of this profile suggests fault-control on the scarp. To the

south the profile displays another scarp 170 m high and with a gradient of 21°. There is only a moderate gradient at the base of the slope that probably indicates the initial stage of development of a wash-slope. However, the scarp is still mainly fault-controlled.

To summarize, the morphological characteristics of nine transverse profiles in the Venta de Bravo area suggest fault control over the scarps in the whole area. The fault-scarp analysis has provided evidence of the location of the master fault and parallel faults in this area. Here the youthful morphology of the scarps indicates active tectonism.

iii) Fluvial systems

The longitudinal profiles of nine streams in the Venta de Bravo area have a generally convex form (Fig. 5.3 and 5.5). These profiles exhibit some alternate convex and concave reaches that reflect the location of faults. Steep gradient reaches reflect upstream the presence of faults along the Venta de Bravo mountain front. The effect of abrupt changes in lithology is relatively smooth; while more abrupt changes in the profile gradient expressed as convex segments reflect localised uplift along the mountain front. V_f values along these nine streams range from 0.1 to 2.5 (Table 5.3). The more typical V_f values are between 0.1 to 0.9 and low V_f values are clearly predominant for the studied streams along the Venta de Bravo mountain front. Low V_f values suggest present channel downcutting, presumably in response to active uplift in the area. Cross-valley profiles for most of these streams display mostly V-shaped forms in the Venta de Bravo area (Fig. 5.5). Values of drainage basin shape (B_S) are relatively high compared to those of the areas described above (Table 5.3) with B_S values ranging from 0.9 to 6. These high values reflect the low relative widths of the elongated drainage basins, which are likely to reflect active tectonism (Bull and McFadden, 1977).

5.2.5 Temascalcingo

i) Mountain front.

Mountain front sinuosity was not evaluated for the Temascalcingo area because fault-scarps here are located in the central part of a composite volcano (Fig. 5.2). Despite this fact, facet development, undissected escarpments and dissected mountain fronts were evaluated. The proportion of faceting ranges from 3 to 33 % (Table 5.2). These data show relatively high values of faceting along the southern escarpments of the volcano. Values of undissected escarpments are higher in the northern and central parts of the volcano, being 48.8 %, 40 %, and 50 % for sub-areas I, II and III, respectively. Combining the proportion of faceting and the degree of undissected escarpments, the results show a high value for continuous escarpments for sub-area III.

Values for the degree of dissected mountain front range from 23 to 33 % (Table 5.2). The lowest values of percent of dissected escarpments correspond to sub-area I, a region that also has a high value for undissected escarpment (48.8 %). Sub-areas II and III exhibit triangular facets, whereas sub-area III exhibit an almost continuous escarpment. These morphometric variables indicate active tectonics in the Temascalcingo area, with small variations in the levels of tectonism for the different sub-areas.

ii) Faults scarps

Two profiles were traced from south to north across the volcano of Temascalcingo (Fig. 5.3). A third profile was located to the west of Temascalcingo, across the western projection of the Temascalcingo faults in the central part of the Acambay graben (Fig. 5.3).

Profiles 25 and 26 (Fig. 5.4) show several fault-scarps clearly recorded by breaks in slope. The southern slope of the volcano shows three breaks in slope, but these are related to low scarps less than 20 m high. The central part of the volcano exhibits a series of scarps, one facing to the north and two to the south. The gradient of the 260 m high scarp facing to the north is high (29°) in its upper part but low at its base (10°). The central scarps facing to the south are steep (23°) but lower (110 and 120 m). In this profile the northern slope of the volcano has two fault-scarps facing to the south, with a lower gradient of 27°.

Profile 27, located to the west of Temascalcingo, reveals several scarps facing to the north, with a generally steep gradient of 35° and heights ranging from 50 to 220 m (Fig. 5.4). Most of them do have a basal wash-slope. These morphological characteristics indicate that these scarps are basically fault-controlled. Overall, the central fault-scarps of the volcano of Temascalcingo exhibit geomorphic characteristics that suggest that they are the most actively fault-controlled in this area.

iii) Fluvial systems

The longitudinal profiles of three streams that cross the fault-scarps on Temascalcingo were also studied (Fig. 5.3). Longitudinal profiles exhibit some alternating convex and concave elements. As in the profiles described for other areas in the Acambay graben, these indicate locations where streams cross faults. These convex segments (Wells *et al.*, 1988) along the long profiles also suggest uplift along these faults (Fig. 5.5).

V_f values along these three streams range from 0.4 to 1.8 (Table 5.3). Further downstream, the V_f ratios increase in response to a growth in the amount of lateral stream migration, resulting in valley-floors widening. Valley-cross profiles display a V-shaped form that reflects channel downcutting in response of active uplift (Fig 5.5).

B_S values range from 1.4 to 3.2 (Table 5.3 indicating elongated basins in the Temascalcingo area.

Chapter Six: Field Evidence of Active and Quaternary Tectonics in the Acambay graben

6.1 Introduction

Field recognition was carried out as a step toward the comprehension of the active and Quaternary tectonics of the Acambay graben. Much of the work described in this chapter was undertaken in areas near the Acambay-Tixmadeje, Pastores, Venta de Bravo, Tepuxtepec and Temascalcingo faults, and between the northern and southern flanks of the graben (Fig. 6.1). This work involved a combination of approaches. Structures deforming Quaternary sediments or exhibiting deformation in youthful morphology in the field and on air photographs were mapped at a scale of 1: 50000. Observations on morphology were gathered to constrain offsets of different sizes on faults, and landforms that indicate probable neotectonic deformation were identified. Finally, measurements were made of small-scale features reflecting tectonic strain, such as slickensides and striations.

Major features were clearly visible in the field. Although the Acambay-Tixmadeje and Pastores faults are traceable without major discontinuities for up to about 30 km from east to west, there is a major discontinuity formed by a NNW-SSE lineament and the stratovolcano of Temascalcingo near longitude 100° W, that separates the graben in two parts. To the east it is almost symmetrical, but to the west the graben is asymmetrical and structurally has the form of a half-graben (Fig. 6.1).

Several sites were visited in the field, having been previously selected during the analysis of aerial photographs at different scales (1: 50000, 1: 20000, and 1: 10000). Photointerpretation of morphological features provided identifications of landforms that showed apparent deformation, such as offset rivers, fault scarps and river-terraces. The detailed field evidence is presented in this chapter on the basis of the division of the graben into eastern, western and inner graben areas.

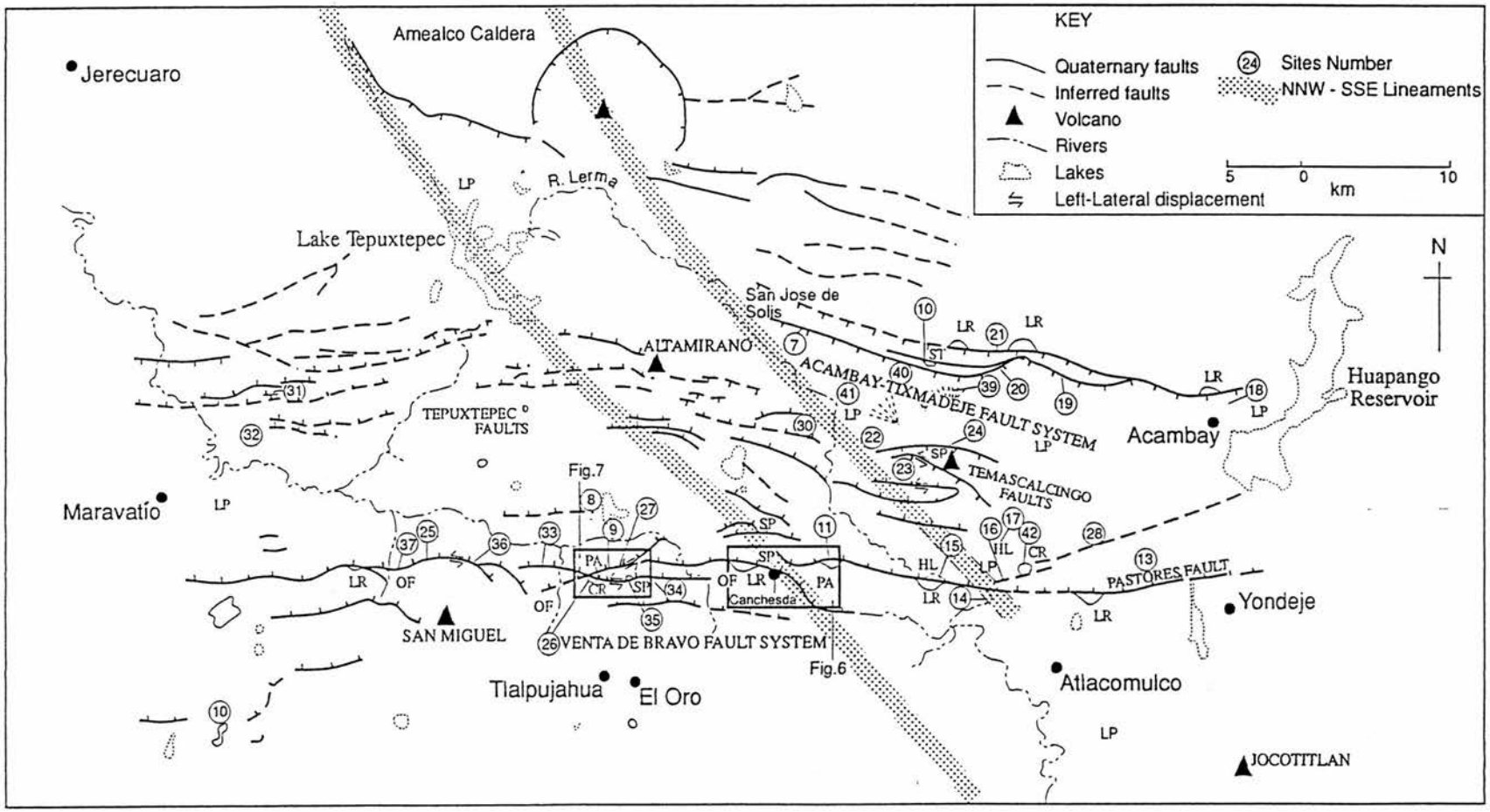

Fig. 6.1 Morphotectonic map of the Acambay graben. Ticks on the fault lines indicate downthrown side. Symbols: LP - lacustrine plain, LR - linear ridge, HL - high level of lake deposits, CR - compression ridges, PA - pull-apart basins, SP - sag ponds, ST - shutter ridges, OF - offset drainage.

6.2 Eastern part of the Acambay graben - Acambay-Tixmadeje and Pastores fault systems.

As mentioned above, the eastern part of the Acambay graben is almost symmetrical. It has one prominent master fault together with a parallel fault (the Acambay-Tixmadeje fault) at the base of a sharp 620 m high mountain front , on its northern flank. The southern flank, by contrast, is mainly formed by one master fault, trending approximately east-west, that displaces Quaternary lavas, lava cones and domes forming the 620 m high mountain front.

The average width of the Quaternary basin (Valle de Los Espejos) in the central part of the graben is about 8.5 km and the difference in elevation between the highest point on the most uplifted footwall (3220 m) and bottom of the valley floor (2500 m) is approximately 700 metres. The large stratovolcano Temascalcingo rises to 3080 m in the centre of this basin closing off the basin to the west.

6.2.1 Acambay-Tixmadeje faults - northern flank of the graben.

Field observations were gathered along the scarp of the Acambay-Tixmadeje fault. Several sites were selected containing present morphological indicators of deformation. The Acambay-Tixmadeje faults are traceable without major discontinuities for a length of 30 km (Fig. 6.1). The associated fault scarp is visible from several points within the Acambay graben. In this study information was gathered from several different sites along the fault system displaying features typical of active-fault scarps.

At the foot of the Acambay-Tixmadeje fault scarp several alluvial fans, visible in air photographs, give rise to a piedmont. The apex of an extensive alluvial fan lies approximately 1.2 km east of highway 55 (Fig. 6.1, Site 18). This fan is located at the

base of the mountain front, on the northern master fault (Acambay-Tixmadeje) of the graben. The fan is deeply dissected by streams giving rise to gullies. It is composed of coarse debris in a tuff matrix. Sediment size is smaller at the front of the fan. The apex of the fan is located 80 m above the level of the nearest basin, Valle de Los Espejos (Fig. 6.2). The fan seems to still be receiving sediments on the fanhead, this be indicative of active tectonics in the area (Bull and McFadden, 1977).

Another alluvial fan was identified at the foot of the northern master fault of the Acambay graben (Fig. 6.1, Site 19). This fan is observed 1 km to the north of the Acambay- Temascalcingo road, 3 km west of Acambay. It is located above the base of the footwall of the mountain front and is formed primarily of coarse sediments. The fan apex is 30 m higher than the adjacent plain at 2520 m. The fan is not entrenched and it still receiving sediment on the fanhead. According to Bull and McFadden, (1977) this morphology is indicative of active tectonics (Fig. 6.3).

Another fault scarp is observed at Tixmadeje Chiquito, on the road to Temascalcingo, approximately 7 km west of Acambay (Fig. 6.1, Site 20). The fault shows a scarp at the footwall and exposes a section of tuff. It is located 50 m above the adjacent plain at approximately 2520 m. Although the scarp is very sharp, there is no micro-morphological evidence, such as striations, of tectonic activity on this wall.

Along the Arroyo Tixmadeje valley, that is parallel to an apparent fault, 2.2 km north from the road to Temascalcingo (Fig. 6.1, Site 21) a fault scarp is exposed to the north and shows the same orientation as the northern master fault. This seems to be a normal fault, with the downthrown block facing to the south.

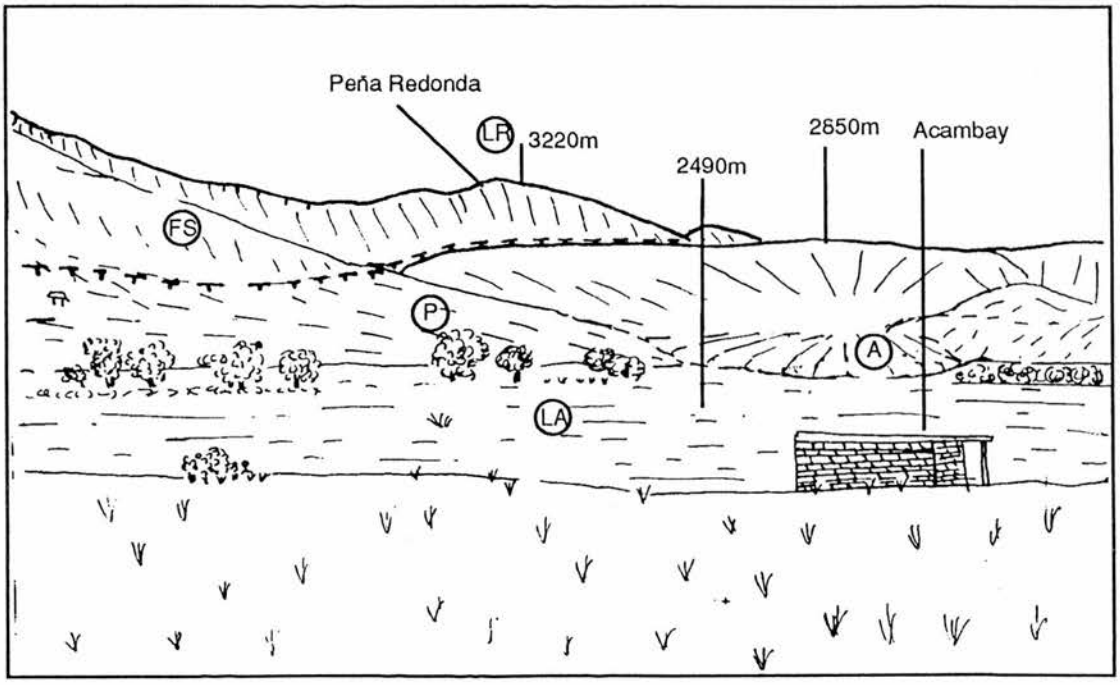

Fig. 6.2 Sketch of the fault scarps of the northern flank of the graben - Acambay -Tixmadeje faults.
A - Alluvial fan FS - Fault Scarp P - Piedmont LA - Lacustrine - Alluvial basin LR - Linear Ridges

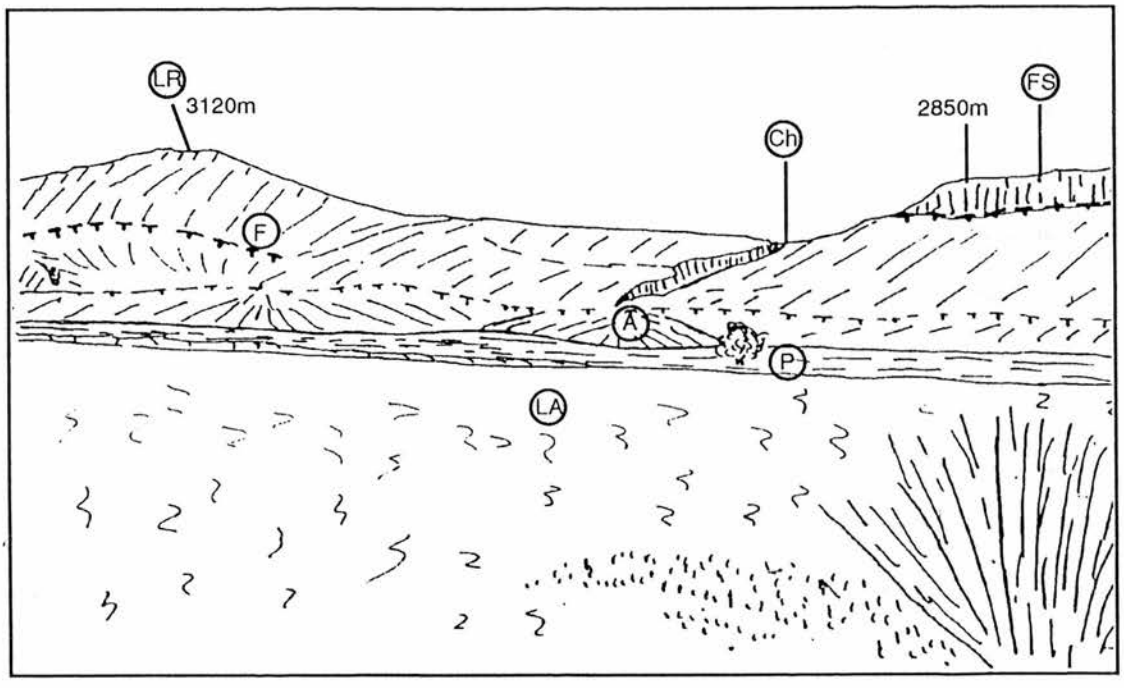

Fig. 6.3 Morphological sketch of a mountain front of the northern flank of the Acambay graben (For location see Fig. 6.1 , site 19)
A - Alluvial fan FS - Fault Scarp P - Piedmont LA - Lacustrine - Alluvial basin LR - Linear Ridges
F- Fault Ch- Channel

On the uplifted footwall, on the northern flank of the Acambay graben (Fig. 6.1, Site 10 and 40) and along the scarp of the Acambay-Tixmadeje fault, a series of well-defined triangular facets, about 150 m high, are separated by ephemeral streams. Here the fault scarp has been strongly dissected by erosion, and on the base of the footwall a wide piedmont has been formed by debris and rock slides, that have produced a low gradient slope of 10^{o} to 14^{o}. Along this fault scarp, and opposite to the volcano of Temascalcingo there is offset drainage, indicating the location of a second fault. On this part of the scarp there are some basaltic cones and elongated ridges that may be interpreted as shutter ridges (Fig. 6.4).

At the western end of the Acambay-Tixmadeje fault (northern master fault of the Acambay graben) (Fig. 6.1, Site 7) La Loma andesite has been brought into contact with pumice fallout deposits, the southern block being down-thrown. The associated scarp marks the westernmost part of the Acambay-Tixmadeje fault. This system of faults does not continue into the alluvium of the Lerma River. The western end of the documented surface rupture of the Acambay-Tixmadeje fault (Urbina and Camacho, 1913) in the 1912 Acambay earthquake, which had a length of 52 km, is also located in this area. Minor faults can be observed in a quarry, within the hanging wall of the Acambay-Tixmadeje fault. They show the same orientation as the master fault (Fig. 6.5) and the fault planes have slickensides and show steps and subvertical striations, also noted by Suter *et al.* (1991).

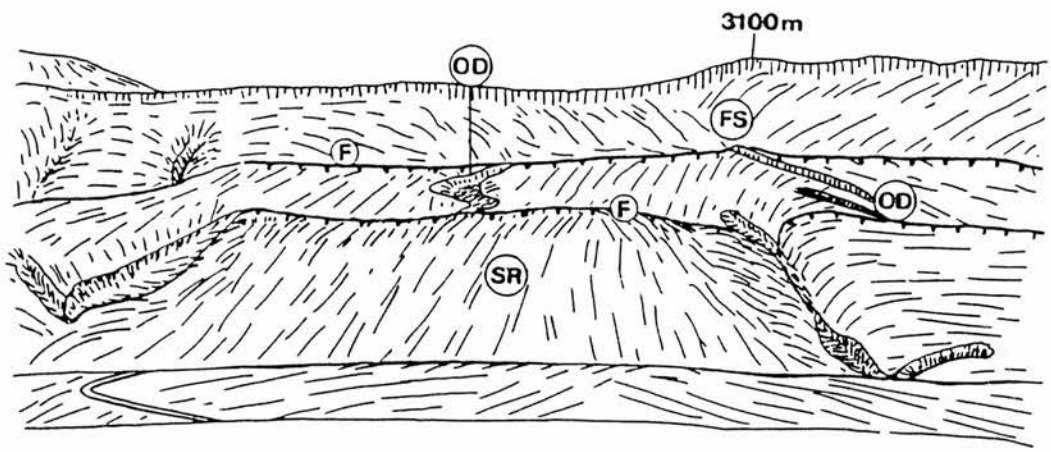

OD Offset drainage
SR Shutter ridge
F Fault
FS Fault scarp

Fig. 6.4. Morphological sketch of the northern flank of the Acambay graben. Linear ridges are exposed on the frontal part of the slope and offset drainage shows the location of displacement by a fault of the Acambay-Tixmadeje system. (For location see Fig. 6.1, site 10).

Fig. 6.9 Folded lake deposits in the Toxi basin. (For location see Fig. 6.1, site 42). Notebook for scale.

Fig. 6.10 Reverse fault displacing lake deposists near the eastern end of the Pastores fault. (For location see site 42, Fig. 6.1). Symbols: a - displaced layer.

6.2.2 Pastores fault - southern flank of the graben.

The major fault forming the southern flank of the eastern part of the graben cuts Quaternary lava flows and displaces cinder and lava cones. Site 13 is located near the eastern end of the southern master fault (Pastores fault) of the Acambay graben, on the unpaved road to San Bartolo Arenal, 250 m form Highway 55 (Fig. 6.1, Site 13). The view to the south and east, from this site, incorporates the scarp of the Pastores fault, a east-west normal fault (southern master fault of the graben). The southern border of the graben is formed by a fault scarp, with an elevation of approximately 250 m. This scarp is continuous and clearly evident on the surface for a distance of 14 km. To the east of the point where the Lerma River cuts the fault , its trace is discontinuous, although it can be detected in some places where cinder and scoria cones have been vertically displaced (Fig. 6.6).

Site 14 is located on the Lerma River, 750 m east from an unpaved road, near the town of Manto del Rio Arriba (Fig. 6.1, Site 14) where it cuts the southern master fault (Pastores fault) of the Acambay graben. Here, two terraces can be seen along the river: the first (I) is approximately 1 m above the river channel and occurs on both sides of the river channel. The second terrace is also observed along both the left and right banks of the river (Fig. 6.7) but is higher than the first terrace (2 m above the river channel), and is broader on the right bank than on the left. These terraces have not been dated, however it is assumed that their probable age is Quaternary. On the way to San Pedro Potla (site 15) one terrace is about 2 m high and can be seen in places along the river, although it is more defined along the left bank.

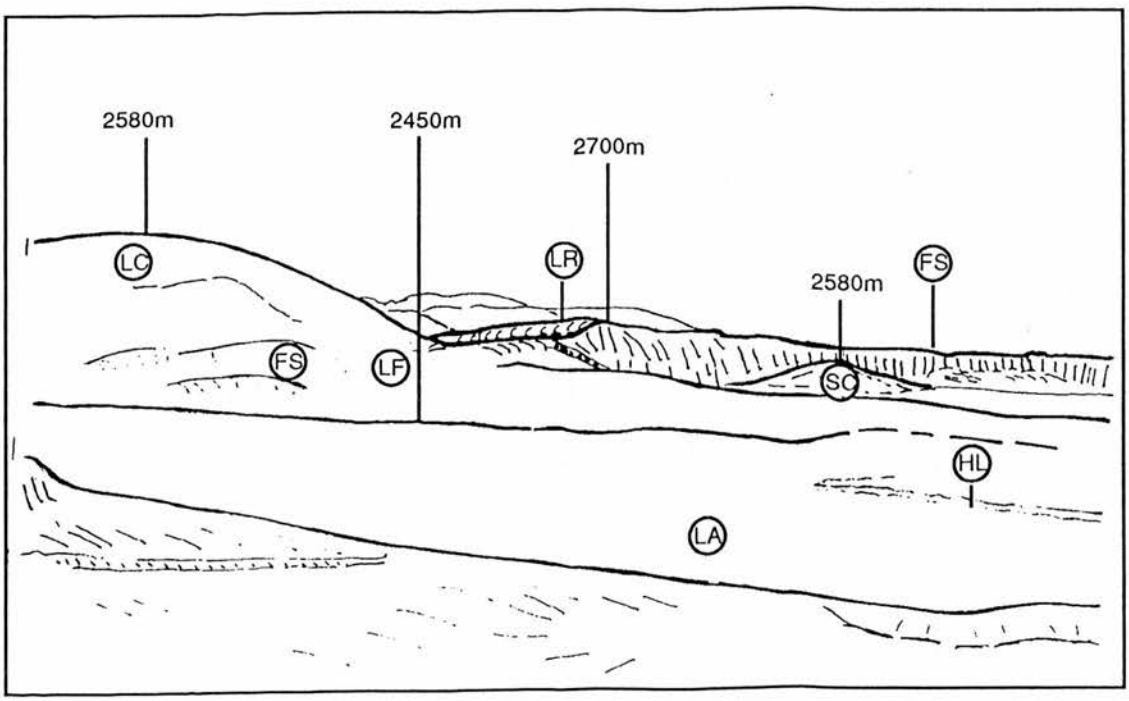

Fig. 6.6 Morphological sketch of a mountain front in the southern flank of the Acambay graben - Pastores fault.
FS - Fault Scarp LC - Lava Cone SC - Scoria Cone LA - Lacustrine - Alluvial basin LR - Linear Ridges
LF - Lava Front HL - High levels of lake deposits

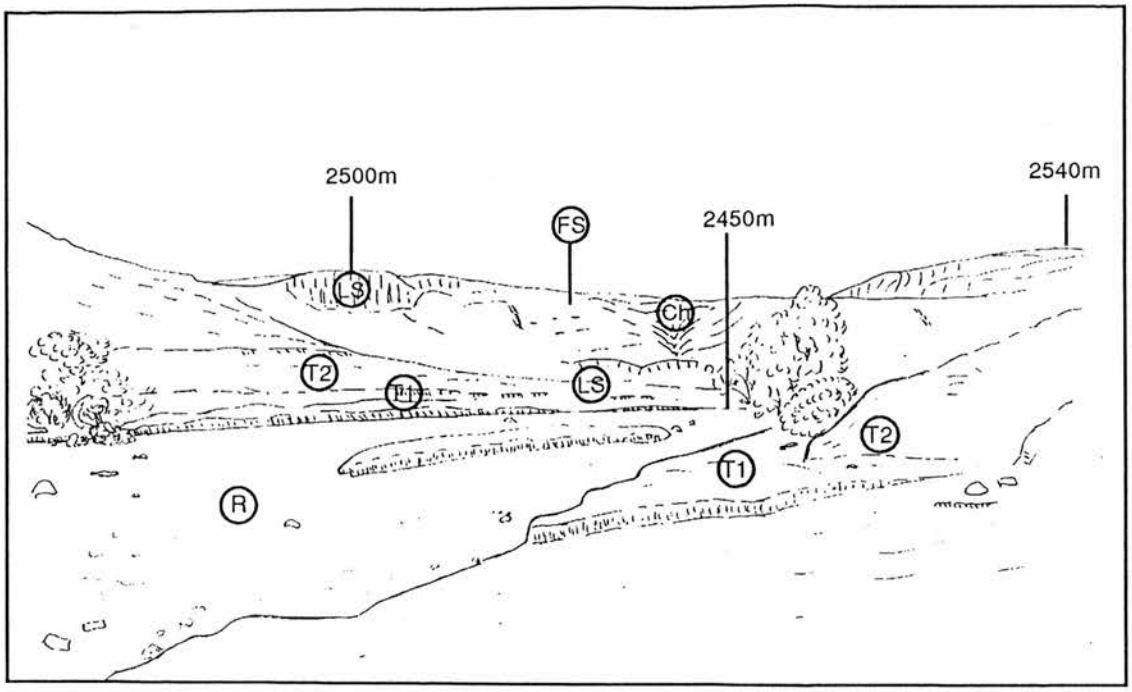

Fig. 6.7 Morphological sketch of the Lerma River and its terraces in the place of intersection with Pastores fault.
FS - Fault Scarp Ch- Channel LS - Lava Scarp T1/T2 - Terraces R - Lerma River

Site 15 is on the Lerma River, south of the volcano of Temascalcingo, on an unpaved road to Pastores (Fig. 6.1). Here, just one terrace can be seen alternately on each side of the river. Near site 15, at San Pedro Potla, continuing activity of the Pastores fault is reflected in high-level lake deposits exposed at the foot of the fault. These deposits are found approximately 20 m above the adjacent plain at 2450 m, and are interbedded with pyroclastic deposits. These deposits appear to tilt slightly to the north.

Site 16 is on the unpaved road from San Juan de Los Jarros to the Lerma River (Fig. 6.1). Urbina and Camacho (1913) reported some scarps and fractures produced in this area during the 1912 earthquake; however the surface evidence of scarps and fractures here may have been obliterated by agricultural activity. Various terraces with small 1m high scarps, can be seen on the plain. However, it is difficult to distinguish them from the terracing produced by agricultural practices. Here, a panoramic view of the Pastores fault shows the overall continuity and linearity of the scarps that follow the trace of the master fault and indicate its recent tectonic origin (Fig. 6.8).

Site 17 is located 8 km northwest of Atlacomulco, near the unpaved road at San Juan de Los Jarros (Fig. 6.1, Site 17). Along this road, at the front of the church, a complete 1 m thick section of lake deposits is exposed 20 m above the present level of the lacustrine plain (2450 m). The lake deposits are overlain by soil and tuff, and underlain by tuff deposits at the base of the section. Tuff deposits and lake deposits are arranged like a series of small terraces tilting sligthly to the north. This arrangment may indicate tectonic displacement of these deposits. To the north of this site, near Cantaxih (La Lagunita), lake deposits are folded into two NW-SE trending antlicline-like hills. These lacustrine deposits are probably Quaternary on the basis of analogous Tierras Blancas lacustrine deposits which have been found to contain a mammoth tusk.

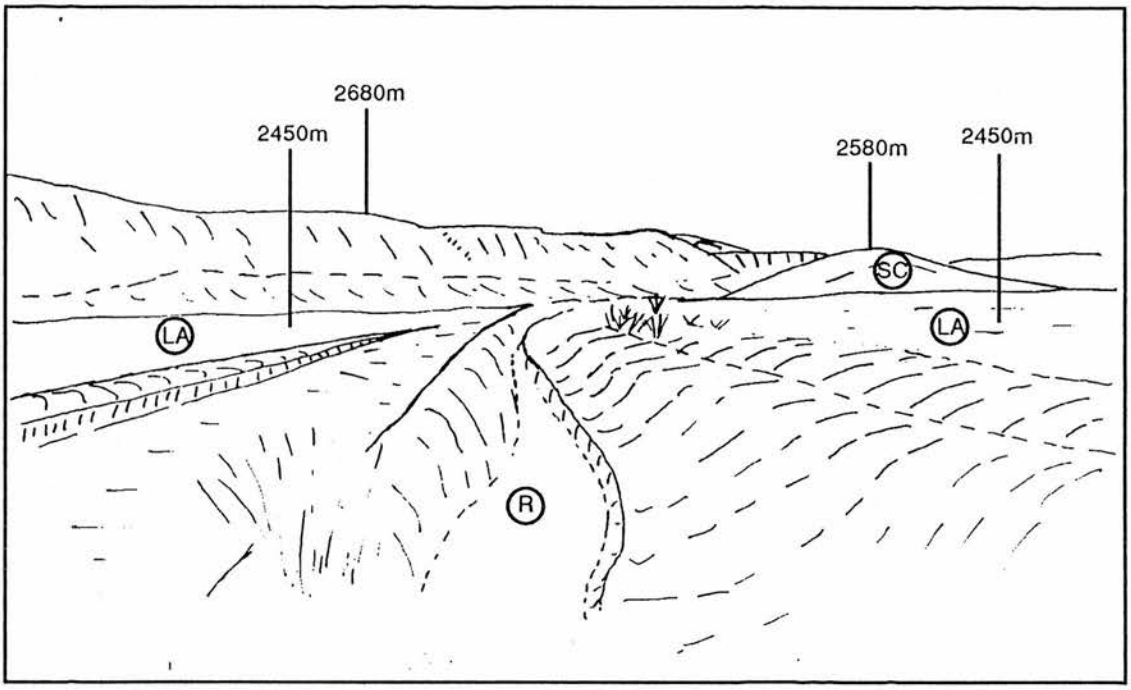

Fig. 6.8 Morphological sketch of the Lerma River along the Pastores fault.
SC - Scoria Cone LA - Lacustrine - Alluvial basin R - Lerma River

Site 42 is located in the east of the Toxi plain, near La Toma irrigation channel, 800 m along the unpaved road from Atlacomulco to San Juan de los Jarros, and north of the Pastores fault (Fig. 6.1). The Toxi plain is a closed depression bounded by lava flows and the scarp of the Pastores fault on its eastern and southern flanks. At this site lake deposits are deformed, having a dip of 86° orientated E-W. Some of the layers of these lake deposits have been overturned to form recumbent folds (Fig. 6.9). At this location there is an apparent fault with N60°E trend. A reverse fault was also detected which may indicate compression stress (Fig. 6.10). These, deformed lake deposits may be part of a compression ridge which is bounded by two arroyos related to faults that cut lake deposits (Fig. 6.11). Furthermore, in the area between the faults, a small depression indicative of subsidence, and a compression ridge reflecting uplift were observed, both features provide evidence of compression.

The western end of the Pastores fault exhibits a striated fault plane (Fig. 6.1, Site 11). The ravine provides excellent outcrops of the hanging wall formed of colluvium and lacustrine deposits. No secondary faults were observed in these outcrops. To the east of this site, in the strike direction of the Pastores fault, the presence of discrete steps on the surface may represent the surface rupture of the 1912 Acambay earthquake (Suter *et al.*, 1992)(Fig. 6.12). Urbina and Camacho (1913) mapped a surface rupture along the Pastores fault in this area. The site is close to the western termination of the Pastores fault, where some of its displacement is transferred to the Venta de Bravo fault. The two faults have a cross-strike separation of 1.0 to 1.3 km and along-strike overlap of 1.8 km. A swampy depression between the two segments at Canchesdá indicates an extensional offset as has been noted by Suter *et al.* (1992) (Fig. 6.13). This constitutes further evidence that the movement along the two fault segments includes a minor left-lateral strike-slip component.

Fig. 6.9 Folded lake deposits in the Toxi basin. (For location see Fig. 6.1, site 42). Notebook for scale.

Fig. 6.10 Reverse fault displacing lake deposists near the eastern end of the Pastores fault. (For location see site 42, Fig. 6.1). Symbols: a - displaced layer.

Fig. 6.11 Pressure ridge compose of lake deposits in the Toxi basin. (For location see site 42, Fig. 6.1).

Fig. 6. 12 Discrete steps on the Pastores fault that may represent the rupture of the 1912 Acambay earthquake (Urbina and Camacho, 1913; Suter *et al.*, 1992). Bar for scale 0.30 m.

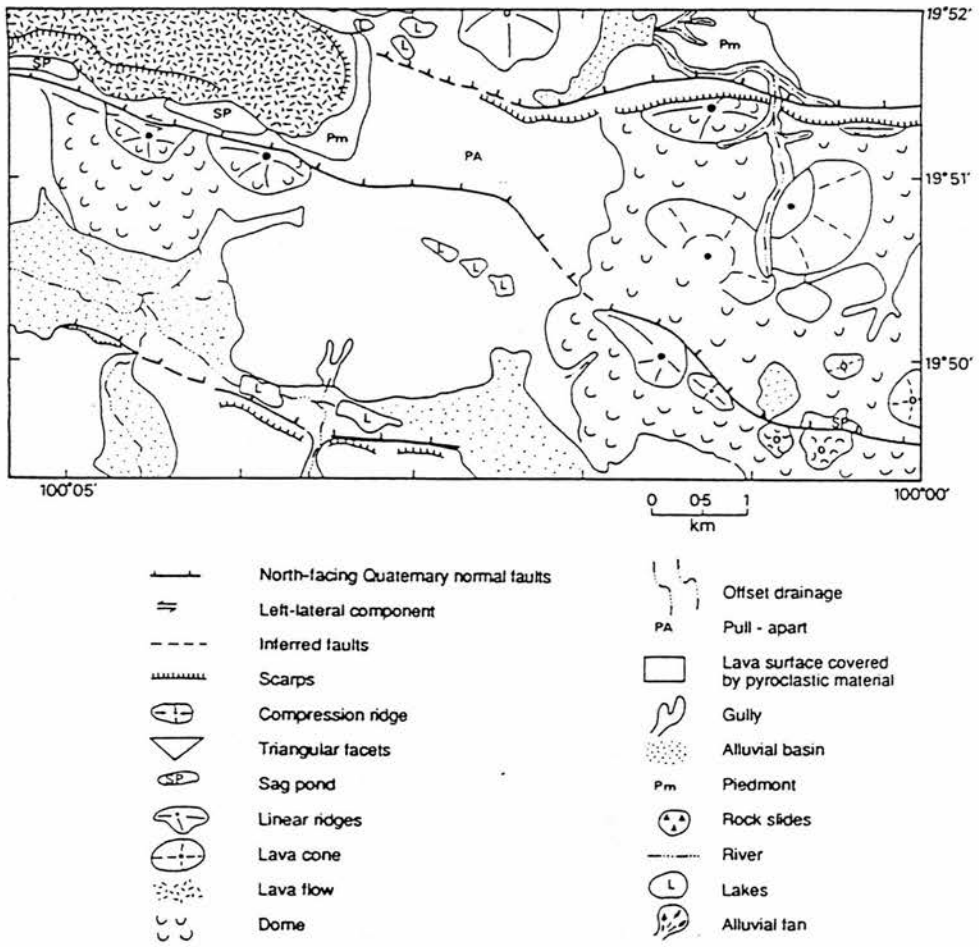

Fig. 6.13 Morphotectonic map of the overlap between the Pastores and the Venta de Bravo faults (See Fig. 6.1, site 11).

6.3 Western part of the Acambay graben

The western part of the Acambay graben is bounded to the east by a NNW-SSE regional lineament that crosses it from north to south. The western part of the graben appears to have a half-graben structure since it is asymmetric with one prominent master fault at the base of a mountain front (3100 m) on the southern side. In contrast, on the northern side, only truncated minor east-west trending normal faults offset volcanic slopes, pyroclastic deposits and lava flows by a few metres. Most of the scarps on the northern flank which has both north- and south-facing faults have an average height of 30 m. Between the northern and southern flanks of the graben there is a broad lava surface covered with pyroclastic material and lake deposits.

6.3.1 Tepuxtepec faults - northern flank

The northern flank of the graben is formed by a system of faults (the Tepuxtepec faults) with an east-west trend. Between San José de Solís, and north of Maravatío, several east-west trending faults, mainly facing to the south, make up the northern flank of the western part of the Acambay graben.

North-facing faults are observed at the western end of the Tepuxtepec fault system (Fig. 6.1, Site 31). The fault scarp gradient is approximately 10^{o} at the site Los Bancos . Here, relief in cross-section shows a series of scarps formed on volcanic rocks (Pliocene andesite) indicating the presence of a system of normal faults. The straigthness of these features may be indicative of their recent formation.

Site 32 on the unpaved road from Maravatío to Los Bancos (Fig. 6.1, Site 32) consists of an exposure of high-level lake deposits along the arroyo Paquisihuato. These lake deposits lie 10 m above the lake plain of Maravatío (2060 m). The deposits are intercalated with lava flows and volcanoclastic material, and they can be found only in this locality.

6.3.2 Venta de Bravo fault - southern flank.

The basin between the Tepuxtepec faults and the Venta de Bravo master fault has an average width of about 7 km. The elevation difference between the highest point on the uplifted footwall (2700 m) and the swampy valley floor (2050 m) is approximately 650 m. Between the villages of Tepuxtepec and Venta de Bravo (Fig. 6.1, Sites 8 and 9), the entire zone is traversed by young normal faults (Fig. 6.14). South of Venta de Bravo, the fault scarp exhibits triangular facets separated by V-shaped valleys (Site 9). Two major creeks breach the scarp. In the westermost creek the footwall rocks show, close to the fault surface, a fracture system which is parallel to the master fault (Suter *et al.*, 1992) (Fig. 6.15). A 5 to 10 cm thick zone of fault gouge exits along some of the fractures, thus indicating that some of the displacement of the fault is distributed along this fracture system by simple shear (Suter *et al.*, 1992). West of the creek, excellent exposures are observed at the base of the scarp where the fault plane is striated (Fig. 6.16). The slip vectors inferred from the striations are subvertical and indicate mostly a left-lateral horizontal displacement component (Suter *et al.*, 1992).

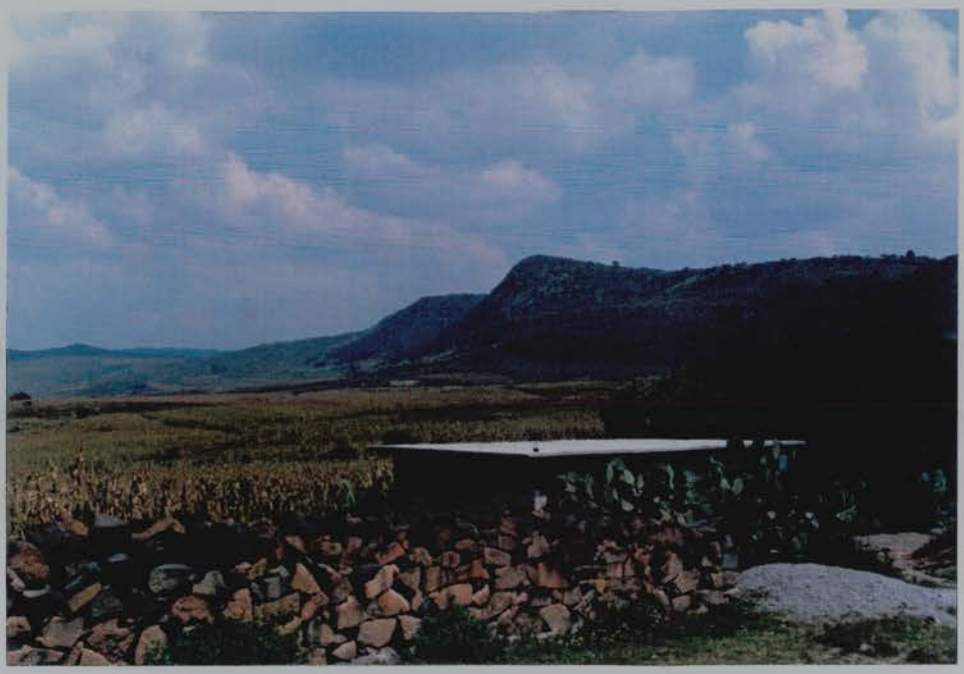

Fig. 6.14 Panoramic view of the fault-bounded mountain front along the Venta de Bravo fault.

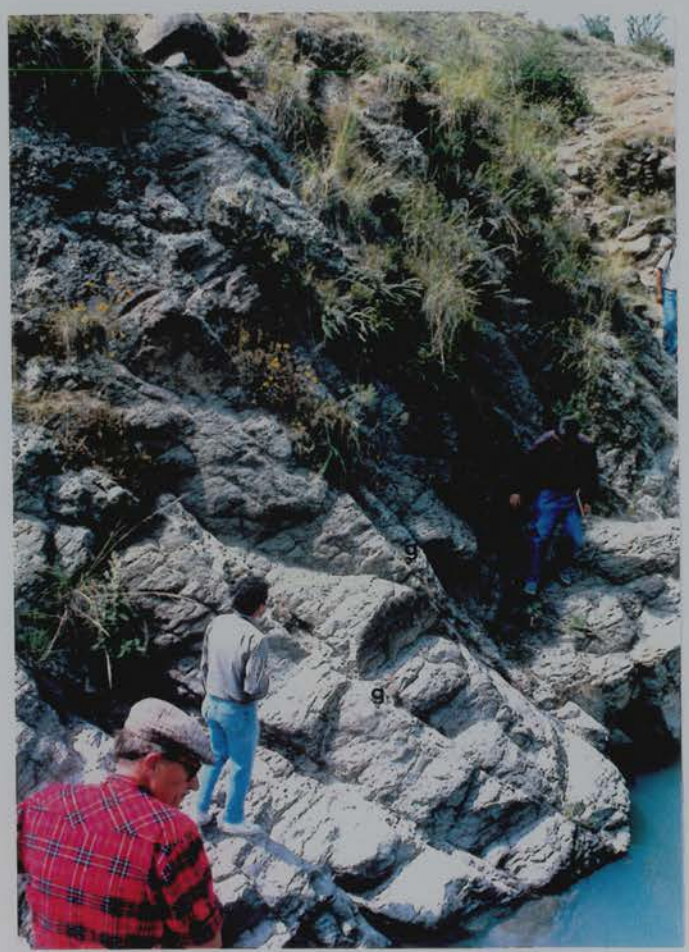

Fig. 6.15 Footwall exposure showing, close to the fault surface, a fracture system which is parallel to the master Venta de Bravo fault. Symbol: g - gouge.

Fig. 6.16 Subvertical striations on a fault plane at the base of the scarp as noted by Suter *et al.* (1992). (See Fig. 6.1, site 9).

Fig. 6.17 Fault plane of the southern Venta de Bravo master fault. (For location see Fig. 6.1, site 25).

At the western end of the Venta de Bravo fault (Fig. 6.1, Site 10), the scarp of the Venta the Bravo fault reaches its maximum relief of approximately 300 m. It is composed entirely of Mesozoic metasedimentary rocks, and behind the faceted scarp is the stratovolcano of t San Miguel. Striations of the Venta de Bravo fault are exposed at site 25 (Fig. 6.1, Site 25). The Arroyo El Cuervo crosses the southern master fault from north to south and exposes a fault plane displaying a series of subvertical striations and a minor parallel fault (Fig. 6.17).

Site 26 is located approximately 800 m east of the road from Tlalpujahua to Venta de Bravo (Fig. 6.1). An apparent compression ridge is developed in the zone of intersection between two faults, both of which have a left-lateral component. There is a pull-apart between the two faults corresponding to a zone of extension. However, a zone of compression occurs at the western extremity of these faults where they are joined. This fault geometry may be the factor in the development of a compression ridge in this area (Fig. 6.18).

Site 27 is located 1.75 km south-east of Venta de Bravo (Fig. 6.1). The channel of the River El Encinal crosses the Venta de Bravo fault where the fault is exposed. The fault plane here is covered by vegetation that masks the exposure of micro-morphological evidence of active tectonics. From this site to the Tlalpujahua road a panoramic view can be obtained of the Venta de Bravo scarp showing its approximately 100 m high triangular facets formed by V-shaped valleys cut in andesitic volcanic rocks. Rock slides, which may be an indicator of recent tectonic activity, can be observed on the scarp.

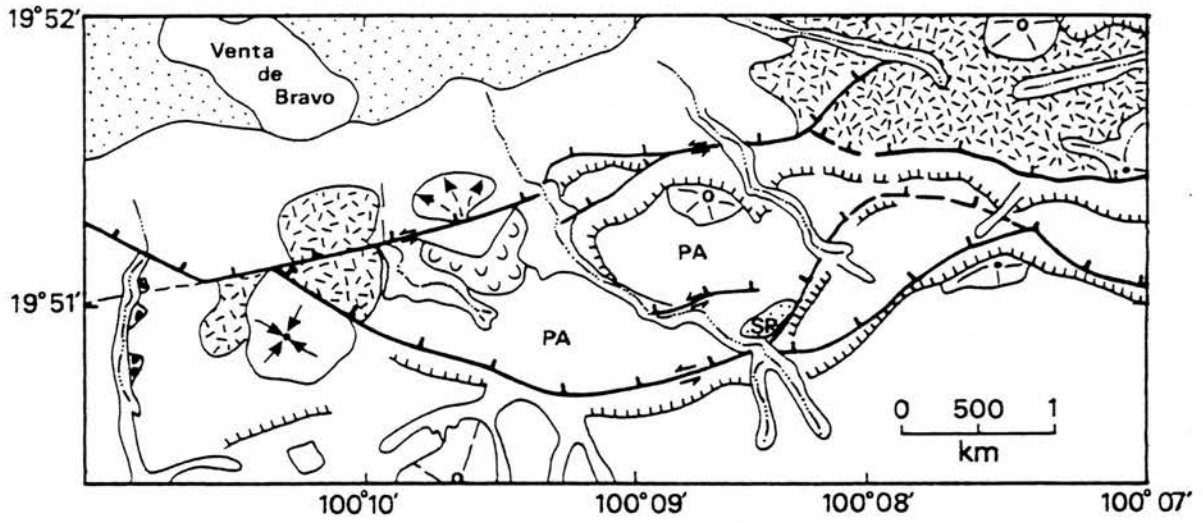

Fig. 6.18 Morphotectonic map showing a pull-apart basin and compression ridge along the Venta de Bravo fault. (For location see Fig. 6.2, site 26). Key as for Fig. 6.13.

Offset drainage occurs between the towns of La Laja and El Moral, and along the Venta de Bravo fault (Fig. 6.1, Site 33). This fault-scarp is approximately 120 m high, and has about a 30^{o} slope. South of the town of Venta de Bravo, along the southern flank of the Acambay graben, lava flows are cut off by the master southern fault (Fig. 6.19). Two parallel faults to the south, have a left-lateral component from the evidence of river offsets. There are also triangular facets along the southern flank of the graben, south-east of Venta de Bravo and near the River El Encinal (Fig. 6.20). These facets are formed on lavas of basaltic composition. There is also a landslide on the scarp of the Venta de Bravo fault near the road from La Laja to El Moral and this provides a further indication of recent tectonic activity. A fault plane was also located on the 30 m high scarp at the town of La Laja, the scarp is 30 m high. The measurement of striations on this fault-plane suggests that the fault is normal with a left lateral component. At site 34 near La Nopalera on the southern flank of the Acambay graben (Fig. 6.1) fault planes were found exposing friction breccia. These faults also seem to be part of the Venta de Bravo fault system.

On the River El Encinal, 250 m from the scarp of the major fault of the Venta de Bravo fault system (Fig. 6.1, Site 35), an apparent tool track (gutter ?) indicative of recent movement was found on a slip plane. This tool track has the same trend as the fault plane (approximately 62^{o} NE), and on its surface there is a thin layer of soapstone (?). It was formed on massive ochre-coloured, coarse-grained tuff. There are some cracks within the tuff filled with mylonite . The track and cracks must be related to the main fault of the Venta de Bravo system.

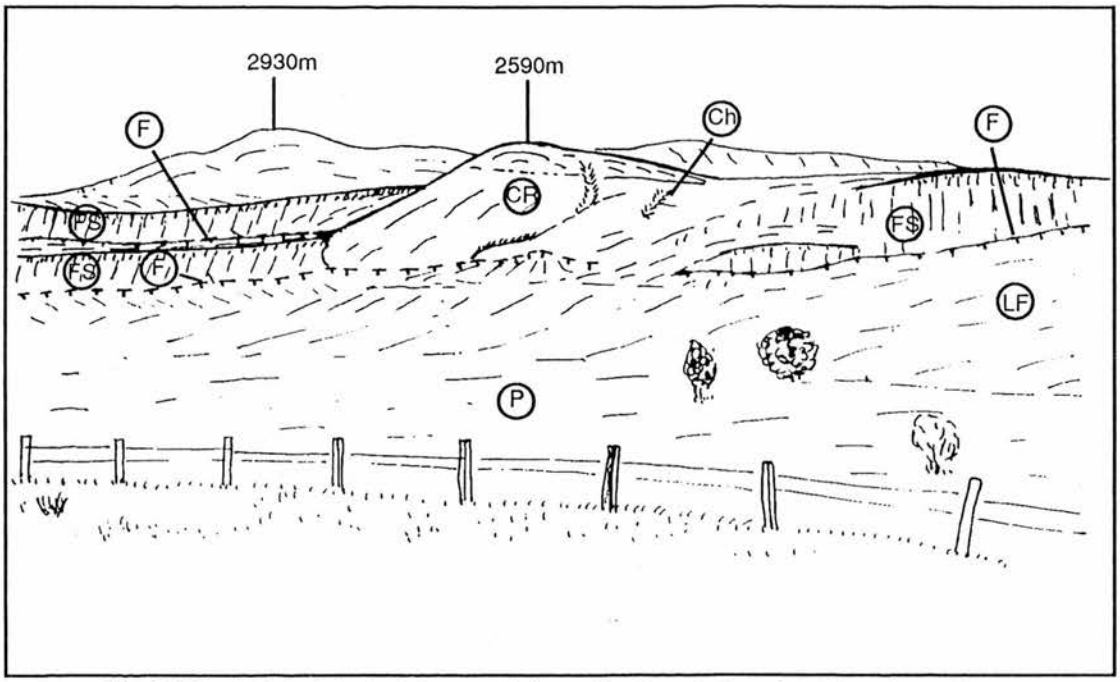

Fig. 6.19 Morphological sketch of the mountain front of the Venta de Bravo fault. Discontinuous lines show the fault. In the central part of the sketch a compression ridge is shown formed at the intersection of two east-west trending faults.

FS - Fault Scarp P - Piedmont LF - Lava Front CR - Compression Ridge F - Fault Ch - Channel

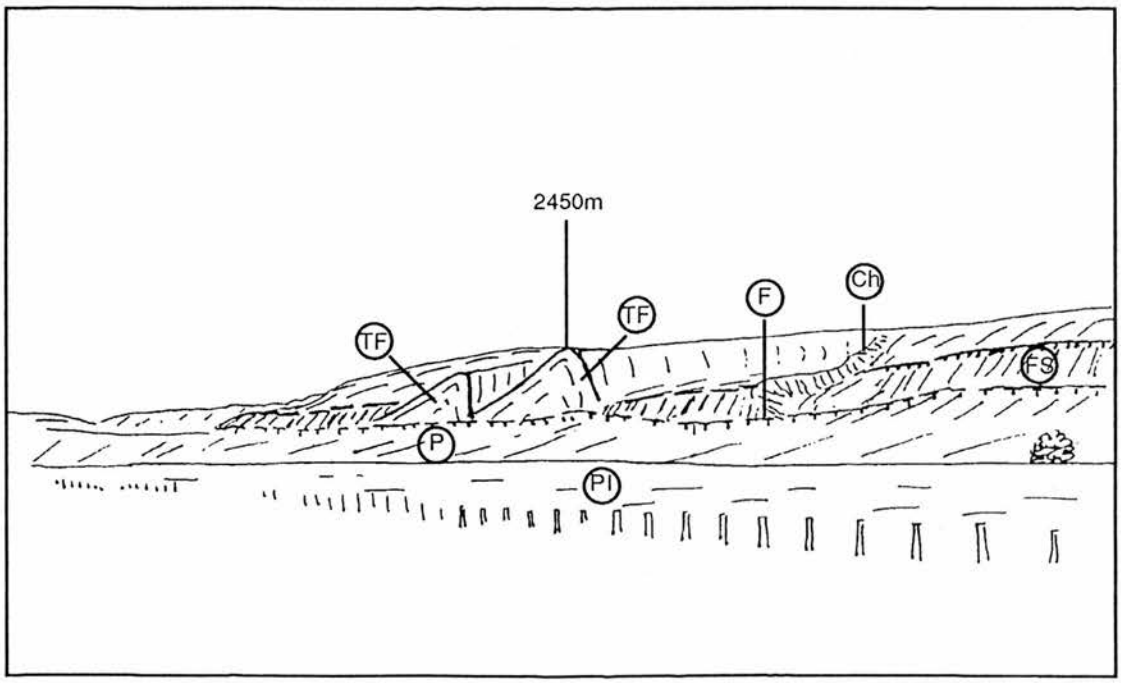

Fig. 6.20 Morphological sketch along the Venta de Bravo fault, near the El Encinal River, showing triangular facets and V-shaped valleys.

FS - Fault Scarp P - Piedmont F - Fault TF - Triangular Facets Pl - Plain

At the base of the section there are lava deposits intercalated with volcanic ash. To the south-east and above the River El Encinal a second scarp related to the main faults of Venta de Bravo system can be seen. These faults which occur in ochre-coloured tuff show different trends NE 54°, NW 61°, NW 64° and one of them seems to be a reverse-fault. The fault planes are associated with friction breccia, mylonite and black soapstone. Other faults were found along the river in basaltic lava. At the base of the main scarp, between two faults, there is a small depression filled with alluvial deposits, that seems to be a sag pond. All this evidence together with stream channel offsets at fault crossings indicate a recent lateral component on these faults.

On the road from Santa Ana to San Miguel el Alto, 3 km north-east San Miguel (Fig. 6.1, Site 36)a fault plane with a north-west trend, was found on metamorphic rocks (shale and slate). To the north there is a scarp that may be evidence of another north-facing fault. These faults are part of the western portion of the southern flank of the Acambay graben.

In the western extremity of the Venta de Bravo fault system, on the road from Presa Quebrada to Las Joyas, two fault planes are exposed (Fig. 6.1, Site 37). One, which cuts a lava flow, near Presa Quebrada has north-east trend and exposes a soft, fine material (gouge?). 750 m to the south the other fault plane, which trends SE 60° has striations and tool tracks (gutters?). These features show that these faults have a left lateral component. Finally, at site 38 south of the town of Venta de Bravo, on the road to Tlalpujahua (Fig. 6.1) there is a fault-scarp with rockslides which may indicate recent seismic activity.

6.4 Inner graben - central faults

Site 22 is located on the road to Temascalcingo, 3.5 km north of Temascalcingo and 1 km north of La Magadalena (Fig. 6.1). There are several alluvial fans on the north-west slope of the volcano of Temascalcingo. The apex of one of the fans is approximately 130 m high above the plain level (Fig. 6.21). This fan exposes a section of lahar deposits (volcanic agglomerate according to Sanchez Rubio, 1984) above the fan apex, and these presumably underlie the fan. At the base of the section a highly compact, ochre-coloured paraconglomerate (matrix>boulders) is exposed. Up-section there is a orthoconglomerate (boulders>matrix) with a tuff matrix, and andesitic cement. The roundness of the conglomerate fragments is 0.5-0.6 according to the Krumbein classification (1951).

Site 23 is located inside the caldera on the northern slope of Temascalcingo on the road from San Pedro el Alto to Pueblo Nuevo and San Mateo el Viejo (Fig. 6.1, Site 23). On this road to site 23 at San Pedro el Alto high-level lacustrine deposits intercalated with volcanic deposits were found. The base of the section consists of pyroclastic deposits with yellow sand. This material was apparently deposited subaqueously. The pyroclastic deposits are overlain by white lacustrine deposits containing some fragments of organic material. The lacustrine deposits are overlain by a 380 mm subaqueously deposited pumice horizon. These pumice deposits are overlain by a 150 mm ivory-coloured horizon of lake sediments. The section is 20 m above the present lake level and appears to indicate lacustrine deposition which may be produced by crustal subsidence (?). However lake desiccation could also occur here. From San Pedro el Alto, 3 km to the north, along the northern fault of Temascalcingo, a small alluvial-filled depression was found, possibly representing a sag pond. Site 24 is approximately 1.5 km east from site 23, on the road to San Mateo el Viejo (Fig. 6.1, Site 24). There, another sag pond can be seen on the northern flank of Temascalcingo along a 50 m high fault scarp.

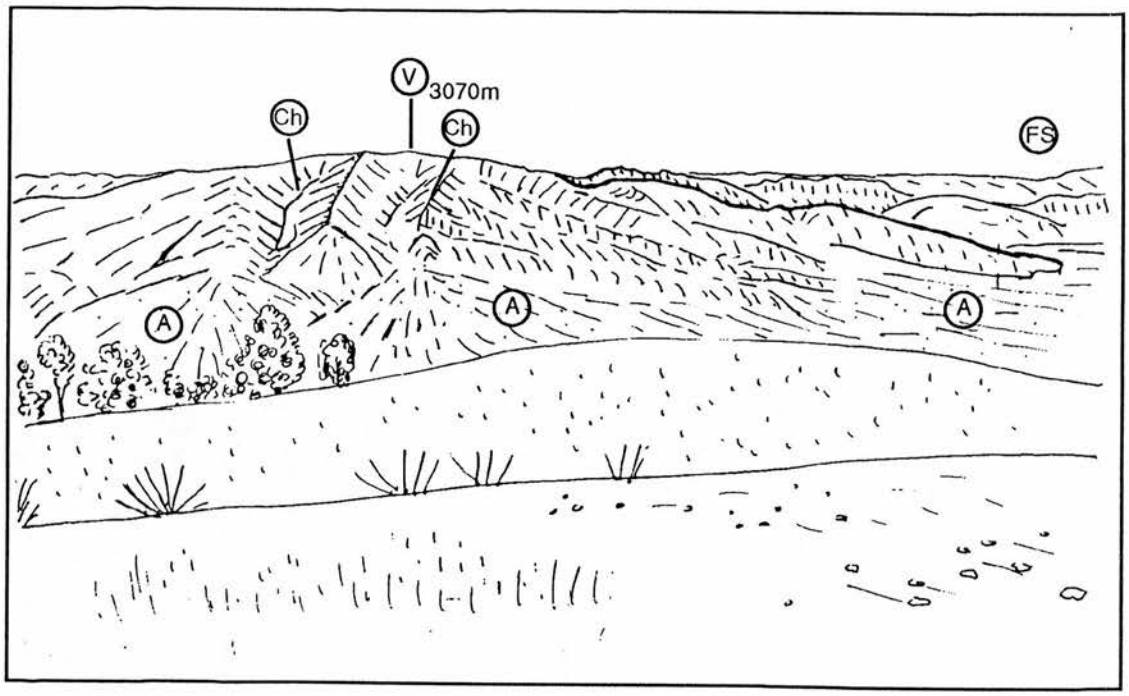

Fig. 6.21 Morphological sketch of the northwestern flank of the volcano of Temascalcingo.

A - Alluvial fan V - Volcano Ch - Channel FS - Fault Scarp

Site 28 is 750 m from the road from Atlacomulco to Acambay (Fig. 6.1, Site 28). This site is located in a small depression that forms a valley, and is bounded by lava flows to the south and east, and by volcanic cones to the north-west and west. Lake deposits containing diatoms and phytoliths were found on an outcrop (2530 m) approximately 60 m above the valley level. They are deformed as a result of impacts by volcanic bombs . The base of this section is formed of fining-up, cross-bedded tuff deposits interlayered with fine volcanic ash and thin lacustrine units. Interpretation of this section suggests that low-energy runoff was followed by aeolian activity which was in turn followed by volcanic ash deposition in a shallow lake. Up-section there are lava flows of basic composition (basalt). Presumably Tierras Blancas was a bound depression filled with lake deposits and volcanic ash that was in turn dissected by streams which produced small valleys flowing to the Toxi plain (SW). Some of these valleys were later filled with lava flows comming from the east. It is assumed that Tierras Blancas has been a lacustrine, fluvial and swampy depression each in turn. The finding of a mammoth tusk suggests a Quaternary age for these deposits (Fig. 6.22).

Site 30 is located to the west of Temascalcingo and southwest of the Lerma River plain (Fig. 6.1, Site 30). It comprises a group of andesitic volcanoes and lava flows (Miocene?-Pliocene), with the entire zone being cut by recently active normal faults. The lava flows were erupted to the north of the volcanoes forming on their frontal northern part, scarps 20 m high. To the south of these lava fronts are a series of north-facing faults arranged en echelon. Some of these faults show small depressions filled with alluvial deposits. These faults are normal and there is no evidence of any lateral component of movement.

Fig. 6.22 Mammoth tusk found in lake deposits near Tierras Blancas, a basin within the Acambay graben.

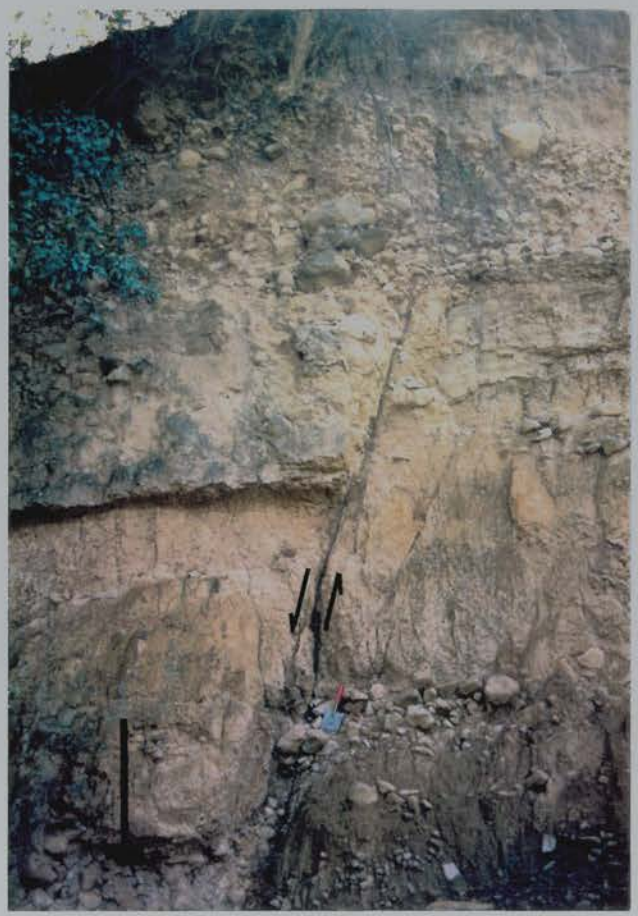

Fig. 6.23 Exposure showing a fault with a 0.87 m vertical displacement of conglomerate on a component of the Temascalcingo fault system. Bar for scale 1 m.

El Tinajal arroyo bounds the alluvial fans on the north-west flank of Temascalcingo (Fig. 6.1, Site 39). Along this arroyo a series of faults were found. An outcrop is exposed. The base of the section consists of conglomerate deposits bedded to the east. This material is overlain by a 3 m brown-coloured horizon of tuff deposits. The tuff deposits are in turn overlain by a 1.50 m east-bedded horizon of conglomerate. This conglomeratic horizon is in turn overlain by a 1 m horizon of soil. The first fault found down-river does not cut the soil layer and the second conglomerate. This fault has east trend (80° azimuth), with a vertical displacement of approximately 870 mm measured using the throw of the lower conglomerate (Fig. 6.23). There is also a horizontal displacement of approximately 1m, so it appears to be a sinistral strike-slip fault. Upstream, there are other faults cutting the tuff and lower conglomerate, one of which has southeast trend (124° azimuth), with a vertical displacement of approximately 600 mm. In this part of the river there is an erosion surface between the tuff and the upper conglomerate.

On the western flank of Temascalcingo there is a lacustrine plain at an altitude of 2360 m, where the Lerma River flows to the north-west (Fig. 6.1, Site 41). To the north of this plain there is a series of lava cones of andesitic composition, and to the south-west the plain is blocked by andesitic lava flows (Pliocene-Miocene?) which are cut by a series of en echelon north-facing faults.

Pressure ridges were found in the Ixtlahuaca lacustrine basin, south of the Pastores fault, and outside the Acambay graben. Here, tuff and volcanic ash layers are folded and elevated 30 m above the Ixtlahuaca basin level forming ESE-WNW trending elongated ridges (Fig. 6.24). These deposits also exhibit reverse faults (Fig. 6.25). Similar ESE-WNW elongated hills are located in the Ixtlahuaca basin and in the inner lacustine basin of

Fig. 6.24 Exposure showing folded layers of tuff and volcanic deposits on a pressure ridge in the Ixtlahuca basin.

Fig. 6.25 Exposure showing a reverse fault in an pressure ridge (See Fig. 6.24).

Toxi. However, the layers of the ridges inside the graben are more deformed suggesting the formation of pressure ridges produced by lateral shear.

6.5 Summary

The Acambay graben is characterised by left-lateral shear producing east-west faults, that are associated with pronounced scarps of Quaternary age. The graben extends roughly east-west from Acambay (Huapango dam) to Maravatío, *sensu stricto,* where the morphological expression of faulting is clearly evident and continuous. Several distinct systems of faults can be identified: (1) the Acambay-Tixmadeje faults, (2) the Tepuxtepec faults, on the northern flank of the graben, (3) the Pastores fault, (4) the Venta de Bravo faults, on the southern flank of the graben, and (5) the Temascalcingo in the central part of the graben.

Morphological evidence associated with tectonic activity, such as changes in river channel patterns, deformation of lake deposits, and the formation of compression ridges can be observed along the faults on the Acambay graben.

The southern master fault (a northern-facing normal fault) of the Acambay graben, is continuous for 14 km. To the east of the intersection with the Lerma River, this fault is broken and this is reflected in the landforms as volcanic cones vertically displaced by the fault. High-level lake deposits were detected in different sites near the Pastores fault, 20 m above the present lake plain. It is suggested that active tectonic uplift produced on the hanging wall of the Pastores fault may have led to the formation of these high-level lake deposits, however, lake desiccation could also produce these elevated lacustrine deposits. Additional morphological evidence of tectonic activity was found in the form of sag ponds along the northern fault of Temascalcingo. Probably one of the most interesting sites was found on the fault-plane of the Venta de Bravo fault, on the

knickpoint of Arroyo El Cuervo that cuts the fault, where a series of striations was found. Using the evidence found along the Venta de Bravo fault it is assumed that this is a normal fault with an apparently significant left lateral component.

Chapter Seven: Geomorphic Evidence for Quaternary Activity Along the Acambay Graben Faults

This chapter provides a synthesis of the geomorphic evidence for Quaternary tectonic activity in the Acambay graben. It summarises the tectonic geomorphology of the central faults of the Acambay graben and the 180 km-long sections of mountain-front escarpments on its northern and southern fault-flanks (Fig. 7.1). The main objectives of the chapter are to identify morphotectonic segmentation along the studied faults and to estimate the relations between the segmentation patterns and relative degrees of late (?) Quaternary fault activity.

7.1 Morphotectonic units in the Acambay graben.

Patterns of surface faulting and degrees of tectonic activity along the faults in the Acambay graben were identified in several stages. The geometry of the surface trace of the fault zone at the base of the two roughly 80 km-long mountain fronts between Acambay and Maravatío and the 20-km-long central fault escarpments (Fig 7.1), was identified primarily on the basis of (1) detailed mapping of fault-scarps and the whole study area from aerial photographs (see chapter 4); (2) the enhancement and interpretation of satellite imagery which provided useful information on regional faults non easily identifiable in aerial photographs (see Fig. 3.10, chapter 3); (3) the collection of field data on scarp morphology from 41 sites distributed along the escarpment selected for detailed study (Fig. 6.1, chapter 6); and (4) morphometric analysis of the mountain fronts to evaluate quantitatively observed variations in landform morphology. The morphology of selected bedrock landforms such as facets, spurs, benches and range-crest summits on the mountain fronts were defined quantitatively by topographic transects and morphometric measurements on topographic maps (See chapter 5). Specific types of morphometric data included fault-scarp profiles, mountain front sinuosity, degree of faceting and dissection of escarpments, longitudinal profiles of the streams transverse to

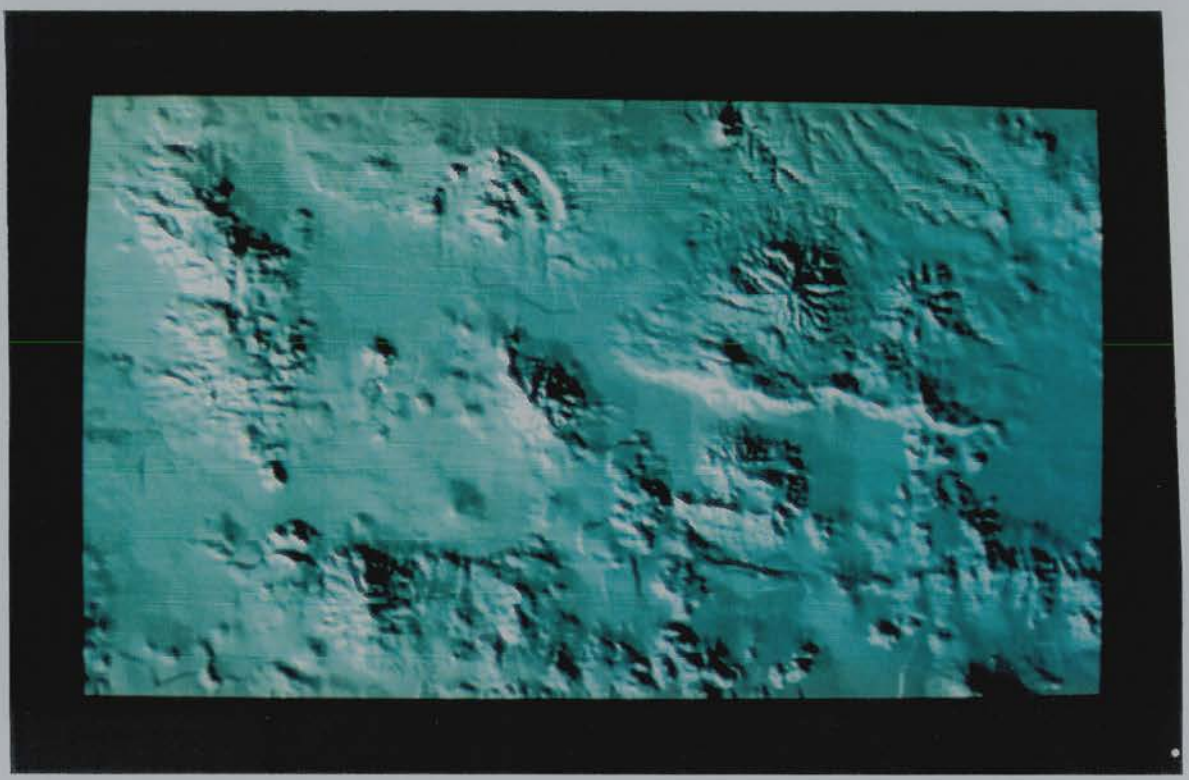

Fig. 7.1 Digital elevation model of the Acambay graben. The digital enhancement of the model shows the location of faults bounding and within the graben.

the escarpments, cross-river sections and cross-valley-relief ratios, drainage basin shape, and river sinuosity.

The analysis of changes in the trend of faults also provided valuable data for the segmentation of faults and the evaluation of the tectonic regime in the area. The contours of 1:50 000 scale topographic maps were digitised in order to produced a digital elevation model (DEM) of the study area using the ARC/INFO 6.1 software. This DEM was used to define regional fault segmentation applying different positions of source of illumination utilising the ILWIS software, and different view-positions of the DEM (Fig. 7.2). The characteristics of the elevations of the whole study area were analysed from an elevation map produced from the digital data (Fig. 7.3).

Profiles along the fault-scarp crests combined with the regional transverse morphological-lithological profiles (profiles including lithological data) were used to observe variations in the morphology with spatial changes along the faults. The combination of field data, morphological observations from remote sensing analysis (including aerial and satellite imagery), and the use of DEMs provided valuable data for the comparison of observed variations in landform morphology with spatial changes in both major tectonic and neotectonic variables. These include morphotectonic (or morphostructural) units, fault segmentation and relative neotectonic activity reflected in seismic activity.

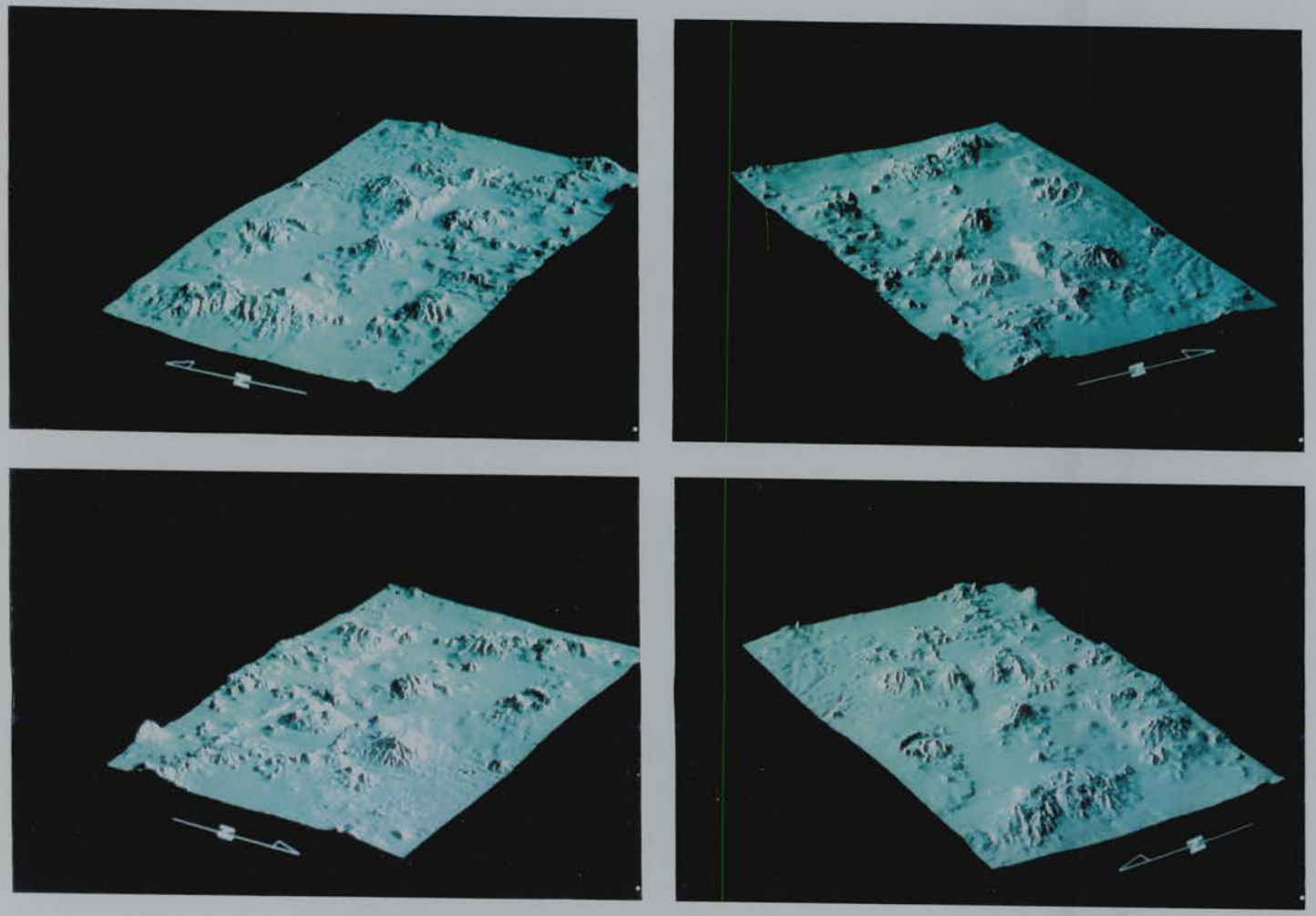

Fig. 7.2 DEMs with different sources of illumination enhancing faults within the graben.

Fig. 7.3 Elevation map.

7.1.1 Criteria of differentiation

Fault segments, that sometimes might be accordant with morphotectonic units or morphostructures (Rantsman, 1979; Menges, 1990), were defined on the basis of at least one of the following criteria:

(1) trend continuity of the faults

(2) breaks in the faults

(3) morphological homogeneity

(4) abrupt changes in lithology

(5) morphometric characteristics (height of scarps, dissection of escarpments, slopes)

(6) historical seismicity

Morphostructural or morphotectonic analysis is based on the concept that tectonic movements have brought about changes in the Earth's surface (Rantsman, 1979; Bathia *et al.*, 1992). The theoretical basis of morphostructural analysis has been widely discussed in the studies by Rantsman (1979); Orlova, (1981); Gvishiani *et al.*, (1986); and others. Three types of morphostructures are identified during morphostructural/morphotectonic analysis: territorial units (blocks); linear zones separating blocks (morphostructural lineaments), and the intersection of various lineaments (morphostructural knots). Blocks, lineaments and knots - in that order, are characterised by an increasing level of tectonic activity (Rantsman, 1979). Morphostructural knots are the focus of analysis in seismic risk studies because all known epicentres of strong earthquakes are found located in the near vicinity of such knots. It is therefore inferred that the epicentres of future earthquakes will also be associated with knots (Rantsman, 1979; Gvishiani *et al.*, 1986; Bathia *et al.*, 1992).

7.1.2 Main geomorphic evidence of segmentation and Quaternary tectonism in the Acambay graben faults.

The regional analysis of the Acambay graben performed in order to define morphostructural (morphotectonic) units included the study of topographic and geologic maps as well as the map derived from satellite imagery. The results of the interpretation of aerial photographs, satellite derived lineaments, morphometric analysis and field work, presented in the previous chapters, were combined with the data obtained from two additional techniques: regional morphological-lithological transverse profiles and longitudinal profiles of the fault escarpments, that is traced along the crest of escarpments.

i) Regional morphological-lithological transverse profiles.

Regional transverse profiles were traced across the Acambay graben from north to south in order to interpret the position of regional faults, to determine the probable subdivision of blocks in the region and access the possible trend of surface tilting in the study area (Fig. 7.4). Profile A-A' shows, from north to south, the regional-block structure of the area. The area seems to be composed of three main blocks: the northern and southern blocks are upthrown and are composed of late Tertiary andesite, and Quaternary andesite and basalt, respectively. The central block, however is downthrown and it is composed mainly of Quaternary alluvial deposits. The northern and southern master faults show associated faults in the inner part that create the borders of minor rank blocks parallel to the main blocks (Fig. 7.5).

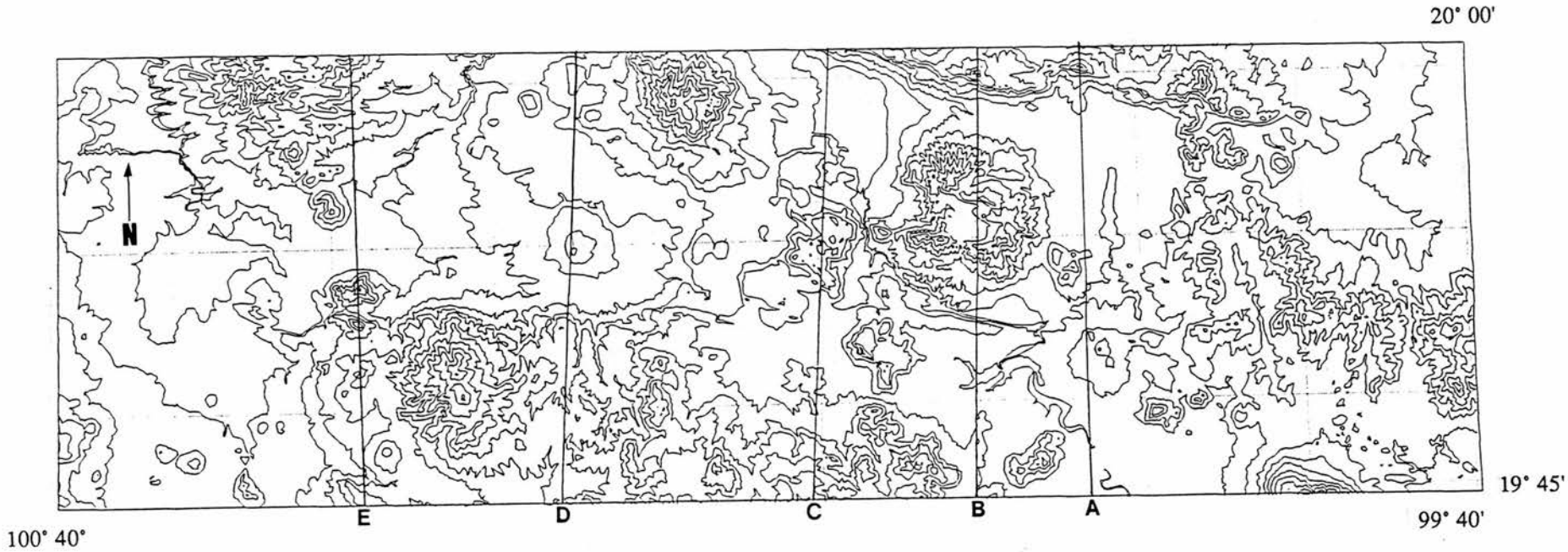

Fig. 7.4 Location of the regional morphological-lithological profiles located transverse to the east-west trending Acambay graben.

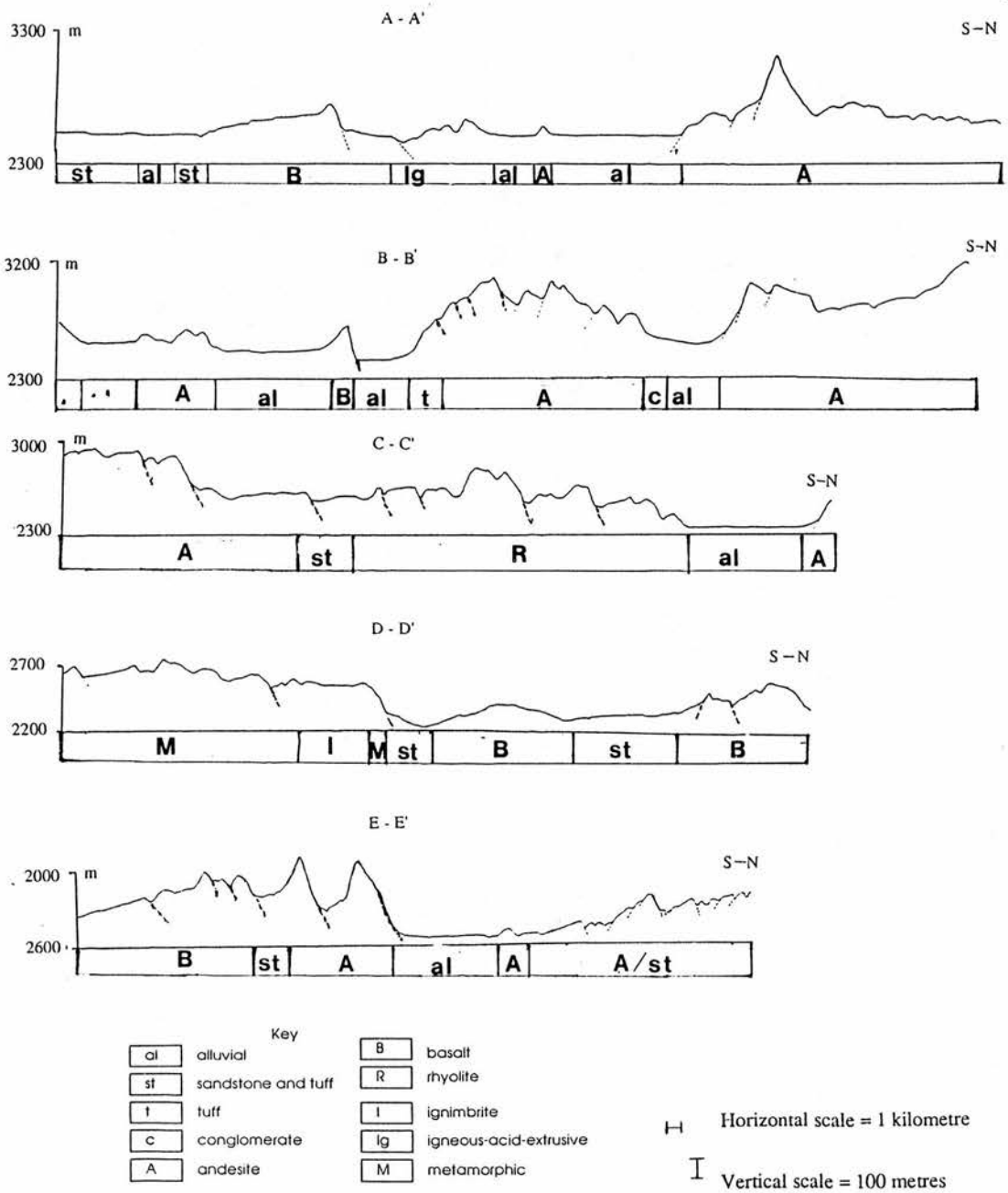

Fig. 7.5 Regional morphological-lithological transverse profiles.

To the west a second regional profile (B-B') shows the apparently north-south block structures of the graben. Here, the profiles show different forms: the northern and southern master faults indicate the position of the upthrown blocks; the central part, however, is now occupied by a volcanic structure that also contains several north and south-facing faults (Fig. 7.5). Faults in the inner part of the volcano show a graben-like structure that corresponds to a downthrown block, while the parallel faults indicate the boundaries of two minor rank blocks in the northern and southern flanks of the volcano. The northern minor blocks are tilted to the north whereas the southern minor blocks are tilted to the south . These observations accord with those from a detailed morphostructural study of the volcano of Temascalcingo by Ortiz and others (1993, in press; personal communication).

Profile C-C' shows the northern and southern flanks of the Acambay graben. To the south the overlap of the Pastores and Venta de Bravo faults is clear from the profile (Fig. 7.5). A significant change in the height and an apparent scarp might indicate the position of a parallel fault that marks the boundaries of another block to the south outside of the graben. The inner part of the graben here consists of a rhyolitic volcanic field that is disrupted by several north facing faults. These faults may indicate second rank boundaries that subdivide the inner part of the graben into minor blocks that seem to be tilting to the north.

A profile trace in the western part of the graben shows the southern master fault that is associated with a marked escarpment, while in the northern part the fault scarp is very subtle and a boundary is produced by small the differences in height (Fig. 7.5, profile D-D'). The inner part of the graben consists of a depression covered by pyroclastic material and disrupted by Quaternary lava cones. The northern-upthrown block shows

several north facing faults disrupting Quaternary lava fields and it seems to be tilting to the south. The southern upthrown block shows a parallel fault to the master fault that indicates the position of an block tilting to the north outside the graben.

The westernmost profile shows a series of three parallel faults indicating the boundaries between three apparent blocks to the south of the master Venta de Bravo fault (Fig. 7.5, profile E-E'). These faults are all facing to the north. The first block from north to south seems to be tilting to the north, while the others do not seem to be tilting. The central part of the graben is an almost flat depression filled with alluvial and pyroclastic material. To the north a series of parallel north facing faults mark the boundaries of three blocks that seem to be tilting to the south.

The profiles traced across the Acambay graben show that the graben is composed of a series of blocks from north to south. The central part of the graben is also disrupted by east-west trending faults that produce parallel minor blocks.

ii) Analysis of longitudinal profiles of the escarpments

Longitudinal profiles were traced along the top of the fault-escarpments of the Acambay graben in order to detect transverse disruptions on the trace of the fault scarp. This analysis enabled the detection of breaks in the faults that in some cases might be coincident with faults transverse to the main east-west trending faults along the graben. It was considered that these disruptions might suggest the location of the boundaries between morphostructural blocks.

The analysis of the longitudinal profile along the tops of the escarpments reveals a segmentation for the faults flanking the Acambay graben. The scarp of the Acambay-Tixmadeje fault is the highest in the whole study area (Fig. 7.6-A). This profile shows breaks reflected as deep V-shaped valleys of the Ganzda and Tepozán rivers. Although

there is not a clear trace of transverse faults, the sudden change in fault orientation and the presence of these transverse rivers marks sharp breaks in the long-scarp profile suggesting segmentation of the Acambay-Tixmadeje fault that might indicate the boundaries between three morphostructural blocks. These apparent blocks have similar elevations and all tilt to the west (Fig. 7.6-A).

The Tepuxtepec system of faults does not constitute a continuous mountain front, but observations from topographic maps and DEMs clearly suggest two apparent morphostructural blocks in this area. The discontinuity along this system of faults is produced by two depressions, that of the Tepuxtepec lake (dam) and the Lerma River basin. The profile of the fault-scarp along the Pastores fault shows two main disruptions that coincide with the valleys of the Lerma and Las Animas rivers, from west to east respectively. The Lerma River valley coincides in this section of its course with a south-east trending fault that controls the channel and probably marks the border of two blocks (Fig. 7.6-C), from west to east, along the Pastores fault-bounding mountain front. The second discontinuity along this front is marked by the Las Animas River that is structurally controlled by an apparently north-south trending fault. This disruption might suggest the position of a boundary between two minor rank blocks. Here the surface seems to tilt slightly to the west, while the eastern part is more even (Fig. 7.6-C).

The escarpment of the Venta de Bravo master fault is the longest in the whole study area, extending for along 46 km. Although this is a system of parallel faults, the trace of the master fault is distinguished by a clear continuous fault scarp. The Venta de Bravo scarp varies from 350 to 60 m and it shows several changes in orientation. These differences in height, sudden changes in fault orientation and several breaks along the edge of the scarp suggest the existence of six segments demarcated by V-shaped valleys, that are in most cases, fault-controlled (Fig. 7.6-B). The western segment (Fig. 7.6-B - I)

is the highest point along this fault at 350 m. The surface here tilts gently to the east. To the east, segments II and III (Fig. 7.6-B) are also high and eastward tilting. Segment IV, located in the central part of the fault, marks a gap in the fault escarpment as it exhibits a variation in the pattern of surface tilting, and it changes from eastward to westward direction. Segments V and VI again show a westward tilt. The altitude of the escarpments also show a decrease from east to west. The segments mentioned above might also suggest the location of morphostructural blocks in an east-west direction, that is transverse to the faults.

The volcano of Temascalcingo shows south- and north-facing escarpments. The southern escarpment (facing to the north) has a maximum height of 350 m. A sharp break in the central part is indicated by a V-shaped valley that follows the trace of a local lineament. This break indicates the border of two apparent segments that do not seem to show any surface tilting in an easterly or westerly direction. The northern escarpment has two breaks marked by the V-shaped valleys of fault-controlled channels. These breaks suggest the presence of three segments along the fault. The height of this scarp at around 200 m does not vary significantly and the three segments do not seem to show any tilting along the whole escarpment.

The longitudinal profiles traced along the crest (top) of the escarpments of the Acambay graben indicate fault segmentation along these faults that also suggest the presence of morphostructural blocks in the region. The Acambay-Tixmadeje master fault has three segments, the Tepuxtepec and the Pastores faults have two segments each, the Venta de Bravo fault has six main segments, and the Temascalcingo northern and southern escarpments have three and two segments respectively. This fault segmentation is used in this study as a basis for further morphostructural zoning.

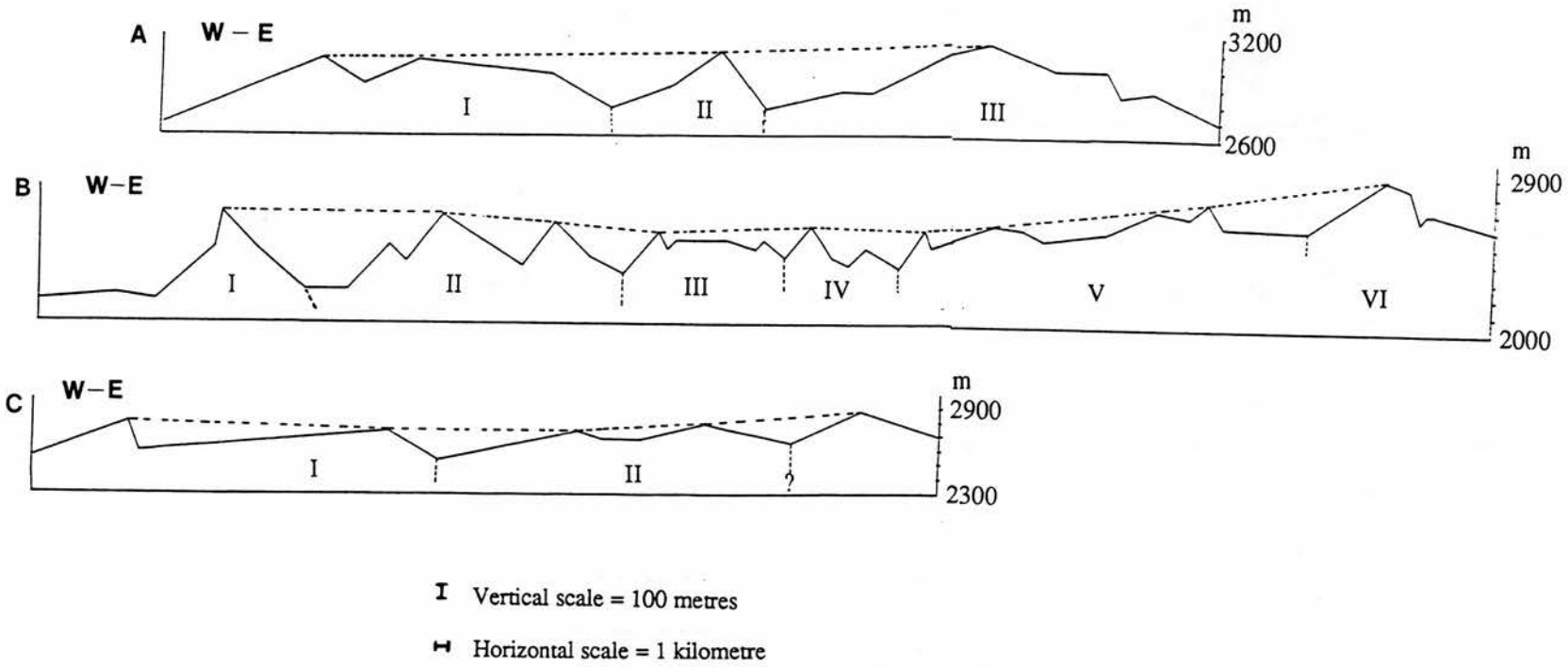

Fig. 7.6 Longitudinal profiles along the escarpments.

7.1.3 Morphotectonic and morphostructural units.

A morphostructural scheme for the Acambay graben was constructed on the basis of a hierarchical ordering of blocks of first (megablocks), second and third rank. The rank of lineaments is also designated as first, second or third depending on their relation to the first, second and third block ranks respectively. Longitudinal lineaments are generally parallel to the predominant strike of large elements of relief. They occur along the boundaries of these elements, separating relatively elevated areas from those of lower altitude. Longitudinal lineaments are also characterised by contrasting types of relief and include the zones of large faults. Transverse lineaments are oriented across, or at an angle to, the predominant strike of large elements of relief. They are normally represented discontinuously on the surface. Morphostructural knots occur in areas that are greater in size than the width of the lineament zones that form the knot (Rantsman, 1979; Bathia *et al.*, 1992).

The morphostructural analysis and geomorphic data presented here confirm the hypothesis that the Acambay graben is a structure which is subdivided in minor morphostructural blocks. Three main megablocks are recognised in the Acambay graben: they generally correspond to different levels of altitude (Fig. 7.7); 1) a northern uplifted megablock bounded to the south by faults of the Acambay-Tixmadeje and the Tepuxtepec fault system; 2) a southern uplifted megablock bounded to the north by the Pastores and Venta de Bravo faults; and 3) the central depression of the graben.

The first rank morphostructural units vary morphologically along the mountain fronts suggesting a second rank subdivision in the following blocks: Acambay-Tixmadeje (I) and Tepuxtepec (II) on the northern flank of the graben; Pastores (III) and Venta de Bravo (IV) on its southern flank; and the Temascalcingo (V) and inner basins (VI) (Fig. 7.7). The second rank blocks can also be further subdivided into third rank units

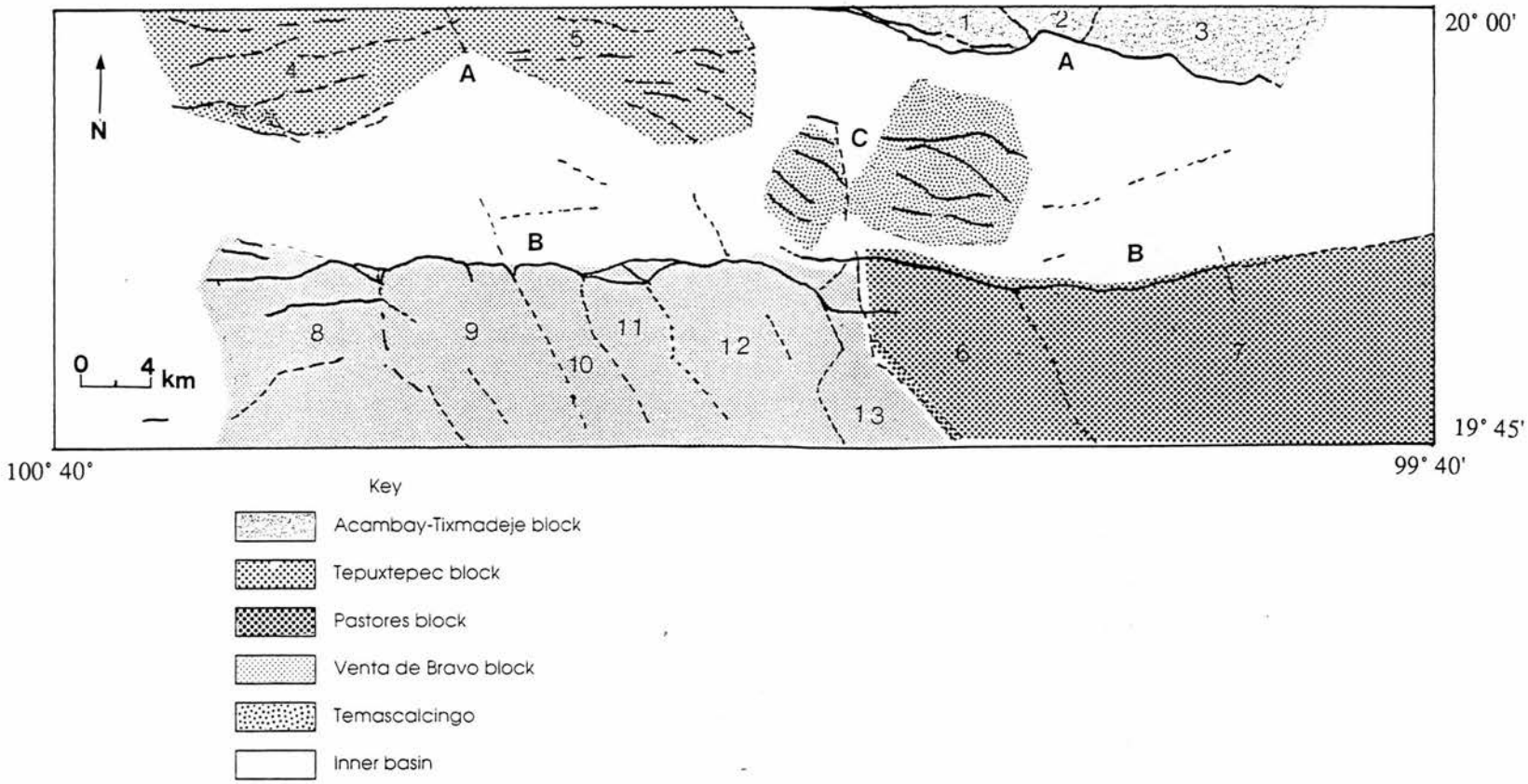

Fig. 7.7 Morphostructural zoning of the Acambay graben. Symbols: capital letters show megablocks: A - northern uplifted Acambay-Tixmadeje and Tepuxtepec block; B - southern uplifted Pastores and Venta de Bravo block; C - central depressions and Mt Temascalcingo. Shading indicate second-rank blocks and numbers - third-rank blocks.

differentiated by their morphological characteristics (Fig. 7.7). This morphological variability reflects the range of tectonic activity in the Acambay graben. The morphological characteristics of these third-rank blocks is discussed below.

(I) Acambay-Tixmadeje

The Acambay-Tixmadeje fault escarpments are mostly formed in bedrock of a mainly andesite composition. The fault trends east-west with the master fault facing to the south, and the southern block being downthrown. The trace of the fault, however, displays some changes of direction, but its sinuosity is still low (see Table 5.2). Morphometric data for this area show different characteristics for the three third rank-blocks (Fig. 7.7: 1, 2 and 3). These data accord with the suggested segmentation of the fault obtained from the long-escarpments' profiles.

Morphometric data such as high values of faceting and low values of dissection, and fault-controlled slopes indicate particularly active faulting along third rank-block 1. The analysis of fluvial systems here revealed convex longitudinal stream profiles, V-shaped valleys and low V_f ratios indicative of downcutting. As discussed in chapter five such downcutting is interpreted as a response to local base level changes imparted by relative local uplift across a mountain front.

The field evidence supports the morphometric trend in the tectonic geomorphic variables and indicates a relative high level of tectonic activity in this area. Minor faults showing the same trend as the master fault were observed in a quarry within the hanging wall of the Acambay-Tixmadeje fault. The western end of the surface rupture of the Acambay-Tixmadeje fault (Urbina and Camacho, 1913) in the 1912 Acambay earthquake (M = 6.9) is located here. The fault-scarp exposes striations and slickensides at the footwall, these micro-morphological features providing evidence of recent tectonic activity. In addition, numerous well-defined triangular facets mark the sharp mountain

front along the fault and testify to Quaternary uplift along the fault. Small elongated ridges that offset streams are interpreted as shutter ridges formed by lateral displacement on the fault that cross the ridge and canyon morphology (Sylvester, 1988).

Morphometric data of third rank-block 2, the smallest in the area, indicate relatively lower rates of tectonic activity than blocks 1 and 3. The scarp is densely dissected and non facets were identified here. However, the fault-scarp here is high with a steep gradient. V-shaped valleys and convex stream long-profiles reflect fault activity. Field evidence confirms this fault activity, with elongated ridges along the fault suggesting lateral displacements. The fault is arcuate in planform giving an abrupt change in direction.

Geomorphic parameters of the third rank-block 3 demonstrate relatively high levels of tectonic activity (Fig. 7.7). The fault-scarp is the highest in the whole area, suggesting a high rate of uplift along this segment of the fault. This is also suggested by the degree of scarp incision. Field evidence such as fault displacement of lava cones, displaced by the fault, elongated ridges and unentrenched alluvial fans also suggests high rates of active faulting. Alluvial fans at the base of the footwall of the mountain front are still receiving sediments at the fanhead and this indicates active tectonics (Bull and McFaddden, 1977) in this area. Instrumental and historic seismic data supports the conclusions from the morphometric and field data. The earthquake in 1912 with a series of aftershocks which had its epicentre in this region had a magnitude of 6.9 (Ms = 7.0) (Urbina and Camacho, 1913). The focal mechanism for this earthquake indicates normal faulting with a left-lateral component (Astiz, 1986).

(II) Tepuxtepec

The north-western side of the Acambay graben is truncated by several east-west trending normal faults, the general height of the scarps here being 30 m. The Tepuxtepec system of faults bounds a non-continuous mountain front. This flank of the Acambay graben is separated from the eastern part by the basin of the Lerma River. To the west the mountain front is again interrupted by the basin of lake Tepuxtepec that appears to be structurally controlled by a north-west trending regional lineament. This might be considered as the boundary of two third-rank blocks despite the fact that most of their morphometric characteristics are rather similar (Fig. 7.7: 4,5). But, differences in lithology of these minor blocks, the eastern part being composed of andesitic rocks of Mount Altamirano while the western part is composed of lava flows of basaltic composition and pyroclastic deposits, indicate the existence of distinct blocks. Morphometric data for both areas suggest a relatively low level of tectonic activity as does the field. The fault-scarps have low relief and low gradients and there is little geomorphic evidence of active faulting along the faults. It is concluded, therefore that the Tepuxtepec faults have an apparently low level of activity.

(III) Pastores

The escarpment of the Pastores fault shows a variety of morphological characteristics that suggested that it can be divided into two segments corresponding to two third-rank block structures. Morphometric characteristics for third-rank block 6 show high values for the undissected escarpment variable, while for third-rank block 7 values for this variable are much more lower. Morphometric data suggest high levels of tectonic activity for the Pastores fault, with higher levels for block 6. These differences amongst the morphometric variables support the existence of two third-rank blocks, and suggest variations in tectonic activity between them.

Field evidence supports active faulting in third-rank block 6. This includes, steep fault-scarps, an almost undissected and continuous escarpment, linear ridges along the escarpments, and river offsets. The Lerma River, that crosses the fault from south to north, marks the boundary between these two third-rank blocks. Here, two river terraces rise and continue downstream, where the river flows on the downthrown block. The origin of these terraces might be the response to the changes in river base level due to the uplift of the southern block. High-level lake deposits, tilted to the north, are exposed at the base of the fault. This geomorphic evidence suggests active faulting in this area. In addition, some scarps and fractures produced in the downthrown block, which is a depression filled with lake deposits, were reported during the 1912 earthquake. Small terraces of probable tectonic origin were also observed on the alluvial plain.

The western termination of the Pastores fault provides micro- and meso-morphological evidence of active faulting. Here, it is possible that some of the displacement of the Pastores fault is being transferred to the Venta de Bravo fault. The swampy depression between the two faults indicates extension in this area, suggesting that movement along the two fault segments includes a minor left-lateral strike-slip component (Suter *et al.*, 1992). Thus, fault activity appears to be high to moderate.

Morphometric variables for third-rank block 7 shows a moderate value of faceting, fault-controlled scarps, elongated drainage basins, and low V_f values that suggest that downcutting is the predominant process in this valleys. This morphometry demonstrates relatively high rates of active faulting in the area. Field evidence in third-rank block 7 reveals variations in escarpment morphology: here the fault exhibits triangular facets developed at the base of the scarp, while the upper part is an almost continuous escarpment. This particular morphology may indicate two different stages of tectonism in this area. Most of the streams here show V-shaped valleys, and the

escarpments exhibit active incision that may be a response of active faulting. Lava flows and scoria cones seem to be vertically displaced, and overall the morphological evidence suggests moderate to high levels of tectonic activity for this segment of the Pastores fault.

(IV) Venta de Bravo

The fault-bounding mountain front of the Venta de Bravo fault is cut by a main master fault facing to the north and several parallel en-echelon master faults located to the south of the front. The escarpment extends in an almost straight line for 46 km. It is mainly composed of extrusive igneous rocks, but in one of the sectors it is formed in metamorphic (metasedimentary) rocks. The overall sinuosity of this mountain front is very low, the lowest in fact in whole Acambay graben, suggesting a high level of active tectonism in this area. Despite the general straightness of the front there are several breaks along the master fault indicating the boundaries between different segments that demarcate third-rank blocks (Fig. 7.7). The existence of different blocks is confirmed by variations in their morphology.

Geomorphic analyses indicate that the fault-bounding mountain front along third-rank block 8 is a straight, laterally continuous and almost undissected escarpment (see table 5.2 chapter 5). These fault-controlled scarps are formed of andesite rocks. Linear ridges and facets observed in the field support the results of morphometric analyses that suggest moderate levels of tectonic activity in the western extremity of this area.

Morphometric data for third-rank block 9 show moderate levels of faceting along the escarpment and a relatively high value for dissection. The morphology of the scarp suggests fault-control and field evidence confirms active faulting in the area. Well-developed triangular facets and V-shaped valleys demonstrate uplift, active incision presumably being produced by active tectonics. Stream offsets indicate lateral displacement of the fault. In addition a fault plane observed in the knickpoint of the El

Cuervo River exposes subvertical striations (La Huerta). Thus, overall the data suggest moderate to high levels of tectonic activity in the area.

The combined morphometric data from third-rank block 10 show moderate faceting of fault-scarps which are predominantly fault-controlled. The drainage basins here are elongated suggesting active tectonics, and the morphology of this sector of the mountain front also displays evidence of active tectonics. The fault scarp exhibits triangular facets and V-shaped valleys. A lava front rises in the piedmont of this escarpment suggesting recent tectonism in this sector. An exposed fault-scarp exhibits micromorphological evidence of active tectonics, that is subvertical striations that also suggest left-lateral displacement of the fault. Offset drainage at the foot of the scarp supports a lateral component of movement of the fault.

Morphometric and field data suggest active faulting in third-rank block 11 (Fig. 7.7). Morphometric data show relatively high values of faceting, steep fault scarps, low V_f values, and convex long-stream profiles, all suggesting relatively high levels of tectonic activity in the area. Field data provide several lines of evidence of active faulting along block 11, including steep fault scarps, triangular facets, river offsets, V-shaped valleys, swampy depressions at the base of the fault scarp (sag ponds), compression ridges, active rockslides, and striations on fault-planes. The scarp exhibits triangular facets divided by V-shaped valleys indicating valley down-cutting. Excellent exposures at the base of the scarp show a striated fault plane. The striations here are subvertical and indicate a minor left-lateral horizontal component (Suter *et al.*, 1992). A compression ridge rises at the zone of intersection of two faults. This ridge is the product of the lateral displacement of these faults producing compression stress in this point and consequent uplift. The area between the faults consists of a depression filled with alluvial deposits indicating extension. The southern fault exhibits sag ponds at the base of the scarp. All

these elements suggest a pull-apart structure. Triangular facets and V-shaped valleys occur on the scarp which is composed of andesitic rocks. Rock slides were observed suggesting recent active tectonics. Fault planes with micromorphological evidence (a tool track and a gutter) of tectonic activity are exposed in the southern parallel fault of the master Venta de Bravo fault. These faults are filled with friction-breccia.

Instrumental seismic data support the results of the geomorphic analyses. One historic earthquake in November 1979 with several aftershocks was documented in this area. The 1979 earthquake epicentre with a magnitude of $m_b = 5.3$ is located in this area. The focal mechanism for the main event suggests a normal fault with a left-lateral component (Astiz, 1980). A high level of tectonic activity is evident in this sector.

Morphometric data for third-rank block 12 indicate high values of laterally continuous undissected escarpment. Fault scarps here are steep in the upper part and exhibit an incipient piedmont at the base of the scarp. The morphology of this area shows linear ridges with asymmetrical slopes. The steep slope on linear ridges indicates the location of a fault. Some triangular facets are developed to the west of this block. Several swampy depressions (sag ponds) are located along the base of the fault scarp. As previously mentioned in block 6, the Venta de Bravo fault here exhibits an along-strike overlap with the Pastores fault. Overall there is high to moderate levels of tectonic activity in this sector of the Venta de Bravo fault.

East of the along-strike overlap between the two faults, the Venta de Bravo fault changes to an almost south-easterly trend for 3 km becoming almost parallel to the Pastores fault as far as its termination. This change in trend and differences in morphological characteristics support the existence of third-rank block 13. Morphometric data show moderate values for laterally continuous undissected escarpment, and scarps have steep slopes suggesting fault-control. The V_f values are very low indicating valley-

downcutting presumably in response of active uplift The morphology of this segment of the fault exhibits steep fault scarps, triangular facets, V-shaped valleys, elongated ridges, and swampy depressions filled with alluvial material at the base of the fault-scarps suggesting moderate to high levels of active tectonics in this area at the termination of the Venta de Bravo fault.

(V) Temascalcingo

Morphometric data on the east-west trending faults crossing the graben indicate that the inner central faults and the northern fault have high undissected escarpment values. The escarpment of the north central fault is almost undissected, and values of faceting are moderate for the southern fault-scarp. The inner scarps are high and steep. These values indicate tectonic activity along these faults, with possibly higher levels of activity along the north-inner fault. Morphological evidence supports the morphometric analysis. This includes fault channel control, triangular facets, high escarpments, and sag ponds located on the base of the northern escarpments, fault planes exposed on the northern flank of the Acambay graben that display vertical and horizontal displacement. Sag ponds and a measured horizontal displacement indicate a lateral component on these faults. The Temascalcingo area show high-to-moderate levels of tectonic activity along these faults.

Some of the faults that cross Mount Temascalcingo continue to the west displacing a group of lava cones and lava flows. Here, lava cones are aligned indicating the location of the faults. There are several faults arranged en-echelon and some of them exhibit escarpments with swampy depressions filled with alluvial material at the base of the faults. Some of these escarpments are dissected by streams with V-shaped valleys that produce triangular facet spurs. Together this morphological evidence suggests a moderate level of fault activity along the western extension of the central faults.

(VI) Inner basins

In the lacustrine basin north-west of Atlacomulco, lake deposits can be found 20 m above the present base level on an WNW-ESE trending elongated ridge. This small ridge is uplifted in the middle of a flat surface and may be interpreted as a pressure ridge. Further evidence of active transcurrent faulting in this area was found to the east of the lake basin, where lacustrine deposits form recumbent folds and give rise to a small ridge indicating compression. A reverse fault displacing lacustrine deposits confirms this interpretation. Two NW-SE trending anticlines in the Tierras Blancas area also suggest compression in this area.

Similar almost E-W trending ridges were observed outside the graben in the Ixtlahuaca basin but these ridges exhibit less folded lacustrine and tuff deposits forming anticlines that could also be interpreted as pressure ridges resulting from lateral displacement.

Elevated lake deposits, lying 60 m above the basin in the central part of the graben (Tierras Blancas), may indicate active tectonics in this area, although they might be produced by the dessication of the lake . A mammoth tusk was found in these deposits, providing evidence for a Quaternary age of the lake deposits in this area. These deposits may be correlated with the deformed lacustrine sediments found in the east of the Toxi basin and north of Tierras Blancas. Thus, deformation of these deposits seems to have occurred during, or more likely after, the Pleistocene.

7.2 Structural and tectonic interpretation

Faults in the Acambay graben have a main east-west trend and a secondary NNW-SSE trend which is oblique to the orientation of the graben. The east-west trending faults give rise to high escarpments clearly expressed in the topography showing a range of geomorphic evidence of tectonic activity, previously discussed in paragraph 7.1.2, while the second rank faults are usually identified by channel- or river-control, but are not apparently reflected in the topography.

The almost straight escarpments and the steep fault scarps of most of the generally east-west trending faults in the Acambay graben suggest the relative youth and high level of activity of these faults. Therefore, the most recent and active faults are those trending east-west that produce the main systems of faults of the graben on its northern and southern flanks, and the inner central faults that cut the volcanic complex of Temascalcingo and the western the lava field. The NNW-SSE trending faults are apparently older reactivated features.

The main master faults, or first order faults, mark the boundaries between the three first order morphotectonic units (macroblocks), mentioned above (see paragraph 7.1). These faults, as discussed in paragraph 7.1, are the longest (about 40 km), with the exception of the Tepuxtepec faults, and show prominent escarpments and a range of geomorphic evidence indicating tectonic activity. These faults are predominantly continuous and seem to be disrupted by the regional NNW-SSE system of faults that mark the boundaries between second order morphotectonic units or blocks.

The master east-west trending faults display in planform a slightly sinuous shape that is produced by several long arcuate segments. This fault configuration may indicate strike-slip faulting. Moreover, the fault segments always show scarps that indicate the position of the downthrown and upthrown blocks, thereby indicating vertical

displacement. In addition, fault segments in most cases indicate the boundaries of morphostructural blocks.

7.2.1 Morphotectonic evidence of strike-slip faults (transcurrent faults).

Geomorphic evidence of active tectonism and different rates of activity have been described above for the faults of the Acambay graben. Geomorphic analysis of the faults, using the characteristics of the master or first rank faults (the trace of the fault, its shape in planform and its surface expression in associated landforms) provides evidence of a strike-slip associated topography.

Several workers have determined deformation models for lateral displacement along faults. These models have led to the identification of several surface features on such faults that indicate the sense of displacement and therefore of stress (Keller and Rockwell, 1984; Sylvester, 1988). The most distinctive characteristics of active, or recently active, strike -slip faults is their extreme structural and topographic linearity over very long distances, together with an array of distinctive morphological features such as elongated basins, ranging from closed depressions (sag ponds), if currently, or previously filled with water (Sylvester, 1988), to rhombochasms, pull-aparts, shutter ridges (Buwalda, 1937), and systematically deflected streams (Wallace, 1968; Burtman, 1980; Sieh, 1984), elongated uplifts, ranging from pressure ridges to long, low hills or small mountain ranges, and linear valleys or troughs, and in some cases scarps (Sylvester, 1988). A similar geomorphic approach is applied in this work in order to interpret patterns of faulting, and the sense of fault displacement and the stress along the Acambay graben.

Analysis of the geomorphic expression of the studied faults point to pull-apart basins, compression blocks, deflected streams, shutter ridges, pressure ridges, sag ponds and changes in the relief of the escarpments according to the convergent or divergent

trace of the fault pattern's configuration. The most important factor governing uplift or subsidence along a strike-slip fault is the bending geometry of the fault surface relative to its slip vector, because this determines whether local convergence or divergence will occur (Crowell, 1974). Where strike-slip movement is inhibited by restraining bends (Crowell, 1974), convergent strike-slip or transpression (Harland, 1971) occurs associated with crowding, crustal shortening, and uplift. Releasing bends (Crowell, 1974) provide for transtension (Harland, 1971) or divergent strike slip accompanied by stretching, crustal extension, subsidence, and the formation of pull-apart basins

The planform view along a strike-slip fault might show "S"-shaped bends or "Z"-shaped bends. For a strike-slip fault with a left-lateral displacement, "S"-shaped sectors of the fault display depressions, forming sites for sediment deposition, produced where strike-slip movement is divergent and crustal blocks sag, subside or tilt (Crowell, 1974; Keller and Rockwell, 1984). For the sectors of the fault that bend with a "Z"-shaped configuration, and have the same left-lateral displacement, convergent strike-slip or transpresion may occur, producing local uplift as a result of compression stress. This mode of deformation would be completely the opposite if the strike-slip was right-lateral (Keller and Rockwell, 1984) (Fig. 7.8). From these relationships it is possible to determine zoning of compressional and extensional stress for a fault, by considering the relief along the escarpments, the arrangement and configuration of the faults.

The topographic elements, (positive (uplifts) and negative (depressions)), located along the Acambay graben faults accord with left-lateral strike-slip faulting. When the trace of the fault bends with a "Z"-shape and the fault displays an abrupt change of direction of 45^{o} or more, there is local uplift and/or an increase in the height of the scarp. By contrast, where the trace of a fault exhibits an "S"- shaped bend, then the landforms are negative with a generally rhomb-like geometry similar to a pull-apart structure (Fig.

7.8). However, it was observed that more abrupt changes of fault direction do not imply that the height of the escarpment (uplift), for "Z"-shape bends, increases in the left-lateral faults of the Acambay graben.

The Acambay-Tixmadeje system of faults shows a braided configuration in planform. "Z"-shaped bends show two relatively high uplifts along the escarpment. The highest uplift is located where convergent strike slip or transpression seems to occur, producing a dome-like landform (Fig. 7.8). The interaction between the Acambay master fault and a parallel fault, with a convergent trend, apparently produces compression in the bend of the bifurcation and the consequent uplift. This structural arrangement might suggests the existence of a structural knot. In addition, this is the location of the epicentre of the Ms = 6.9 earthquake of 1912. A similar structural configuration applies to another uplift in the Acambay-Tixmadeje fault in block 2. However, there are no documented epicentres here.

Pull-apart basins or rhomb grabens are depressional basins. Basins associated with active strike-slip faults can be readily identified because of their morphological expressions as elongated lakes and sag ponds, which often contain young sedimentary deposits and sometimes involve volcanic and geothermal activity (Crowell, 1974; Aydin and Nur, 1982). Pull-apart basins are bounded on their sides by two subparallel, overlapping strike-slip faults, and at their ends by perpendicular or diagonal dip-slip faults, which link the ends of the strike-slip faults (Crowell, 1974). In the place where the Pastores and the Venta de Bravo faults have and an along-strike overlap a pull-apart basin occurs and represents subsidence produced by extensional stress in this area (Fig. 7.8; see Figs 6.1 and 6.13, chapter 6).

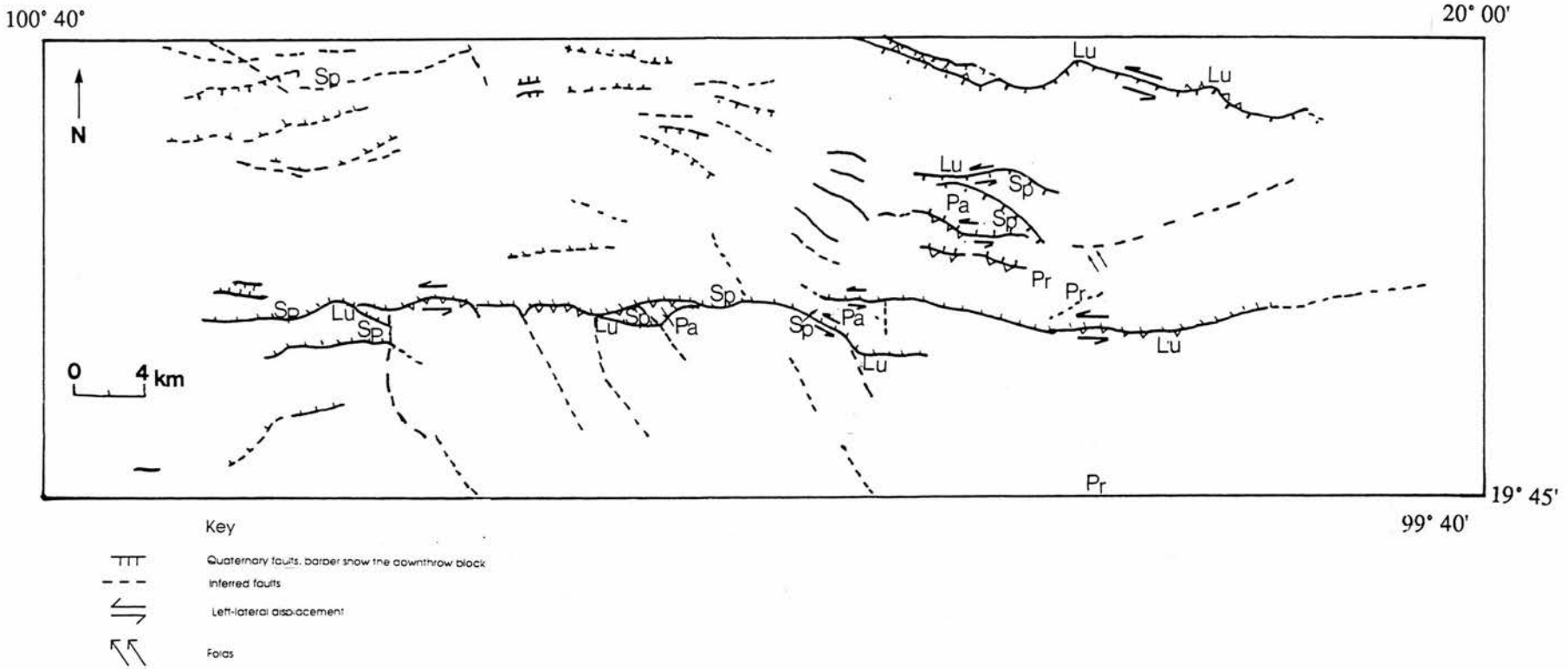

Lu - Local uplift
Sp - Sag pond
Pr - Pressure ridges
Pa - Pull-apart basins

Fig. 7.8 Morphotectonic map showing geomorphological evidence of strike-slip displacement.

The Venta de Bravo fault extends to the east for 6 km displaying an en-echelon arrangement. Strike-slip faults occur in en-echelon patterns with some overlap. This overlap is generally larger as the spacing of the neighbouring faults increases. Fault interaction enhances the growth of en-echelon faults as the inner terminations pass each other and impede their growth after some degree of overlap (Aydin and Shultz, 1990). Moreover, the Venta de Bravo master fault display several "S"-shaped bends in its planform configuration with associated depressional landforms that indicate divergent strike-slip movement or transtension as well as "Z"-shaped bends with associated uplifts indicative of compression stress (Fig. 7.8).

South of the Venta de Bravo an almost parallel associated minor fault, with a downthrown block facing to the north, joins the master fault at its western end creating a rhomboidal depression between the two faults (See Fig. 6.18, chapter 6). The presence of a sediment filled sag pond at the base of the scarp of the associated minor fault to the south, and the left-lateral displacement observed on the El Encinal River where it crosses a segment of the fault, both provide evidence of recent left-lateral movement (Fig. 7.8). This structural configuration is interpreted as an incipient pull-apart structure which indicates extension within the area. In the western wedge, where the two subparallel faults have a convergent trend, compressional stress has produced uplift expressed on the surface as a compressional ridge. It is evident, therefore, that both compressional and extensional stress occurs in this area (Fig. 7.9). This morphostructural configuration is indicative of the existence of a morphostructural knot in the area, and the epicentre of a m_b= 5.3 earthquake was located at depth of 8.2 + 2.9 km near this area. The focal mechanism of the shock, determined by Astiz (1980), indicates a normal fault with a N80^{o}W trend and a dip of 66^o. Since this is similar to the Venta de Bravo faults

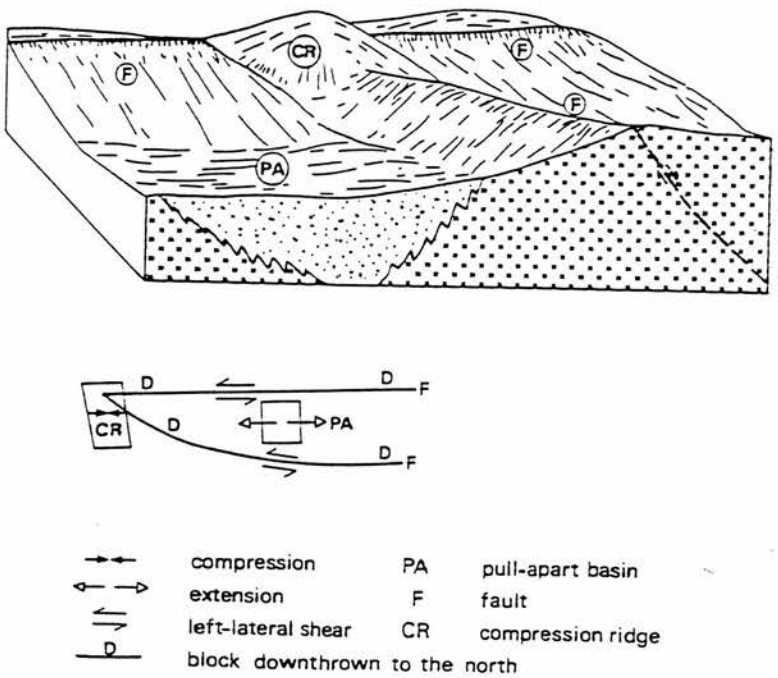

Fig. 7.9 Block-diagram of faulting near a small pull-apart associated with the Venta de Bravo fault system. Inserts show main components of motion.

it suggests that the fault is planar from the surface to the base of the seismogenic upper crust (Astiz, 1986; Suter *et al.*, 1992).

A similar configuration of a pull-apart basin and a compression ridge occurs in the centre of Mount Temascalcingo (Fig. 7.8). Here, in the central part of the volcano, a sediment-filled elongated depression bounded by two parallel faults indicates a pull-apart structure. The central-northern fault converges to the west with a subparallel northern fault. At the intersection of these two faults, local uplift occurs as a result of compressional stress (Fig. 7.8).

Pressure ridges, or rhomb horsts, are uplifted terrains that have been recognised along major strike-slip faults throughout the world. These horst-like ridges usually form conspicuous rectilinear hills along strike-slip faults and are characterised by en-echelon folds (Aydin and Nur, 1982). Elongated hills, with folded materials displaced by reverse faulting, similar to the pressure ridges described above are located in the inner lacustrine basin of the Acambay graben and in the exterior adjacent lacustrine basin of Ixtlahuaca (Fig. 7.8; see Fig. 6.24, chapter 6). Although the trace of a fault is masked in the inner lacustrine basin of Toxi and there is no clear evidence of the fault in the field, the satellite imagery reveals the trace of a fault in this area. The morphology and internal structure of these landforms suggest the existence of pressure ridges in this area and therefore strike-slip faulting.

Folds associated with strike-slip faults are typically arranged in an en-echelon pattern oblique to the principal direction of shear. Typically, en-echelon folds are distributed in a relatively narrow and persistent zone above, or adjacent to, a master strike-slip fault. They may also form a broad zone between two major strike-slip faults (Sylvester, 1988), as they do in the central inner part of the Acambay graben (Fig. 7.8). The crests of en-echelon folds make an angle of almost 45^{o} in plan view with the shear

direction (Fig. 7.8), representing the shortening component of the bulk strain. The direction of the horizontal movement on the strike-slip fault is revealed by the stepping direction of the folds. Left-stepping folds form with left slip (Sylvester, 1988).

7.3 Summary

The main advantage of classifying active faults lies in assessing their liability to future movement, based on the assumption that if a fault has moved frequently in the immediate geological past it is likely to move with a similar frequency in the future. The Acambay graben exhibits major fault discontinuities that divide the graben into two parts from east to west: to the east the graben shows a symmetrical structure, with almost continuous parallel north and south master faults, whereas to the west the graben exhibits an asymmetrical, half-graben structure, the northern flank of the graben being discontinuous and the faults here facing both to north and south. Within the study region differences occur in the morphological expression of fault-bounding mountain fronts (megablocks and blocks) and internal third-rank morphostructural blocks associated with an active tectonic environment. Most of the faults of the Acambay graben exhibit a range of evidence of recent tectonic activity. This evidence varies between blocks pointing to the tectonic characteristics of each block. Most of the east-west trending master faults of the Acambay graben (first rank morphostructural lineaments) have parallel en-echelon associated faults that demarcate the boundaries between first rank blocks; whereas perpendicular or oblique faults to the east-west trending faults indicate the boundaries between second-rank blocks. A range of geomorphic evidence demonstrates left-lateral strike-slip movement along the Acambay graben. Morphostructural and morphotectonic zoning have allowed the identification of fault segments and morphostructural blocks and morphostructural knots, displaying different levels of active tectonics, along the graben

(Fig. 7. 10). So far the most active tectonic and earthquake prone areas derived from the morphotectonic analysis are in decreasing order; the Acambay-Tixmadeje third-rank block 3 (morphostructural knot), the Venta de Bravo third-rank block 11 (morphostructural knot), the Temascalcingo (morphostructural knot), and the Pastores third-rank block 6 (Fig. 7.10).

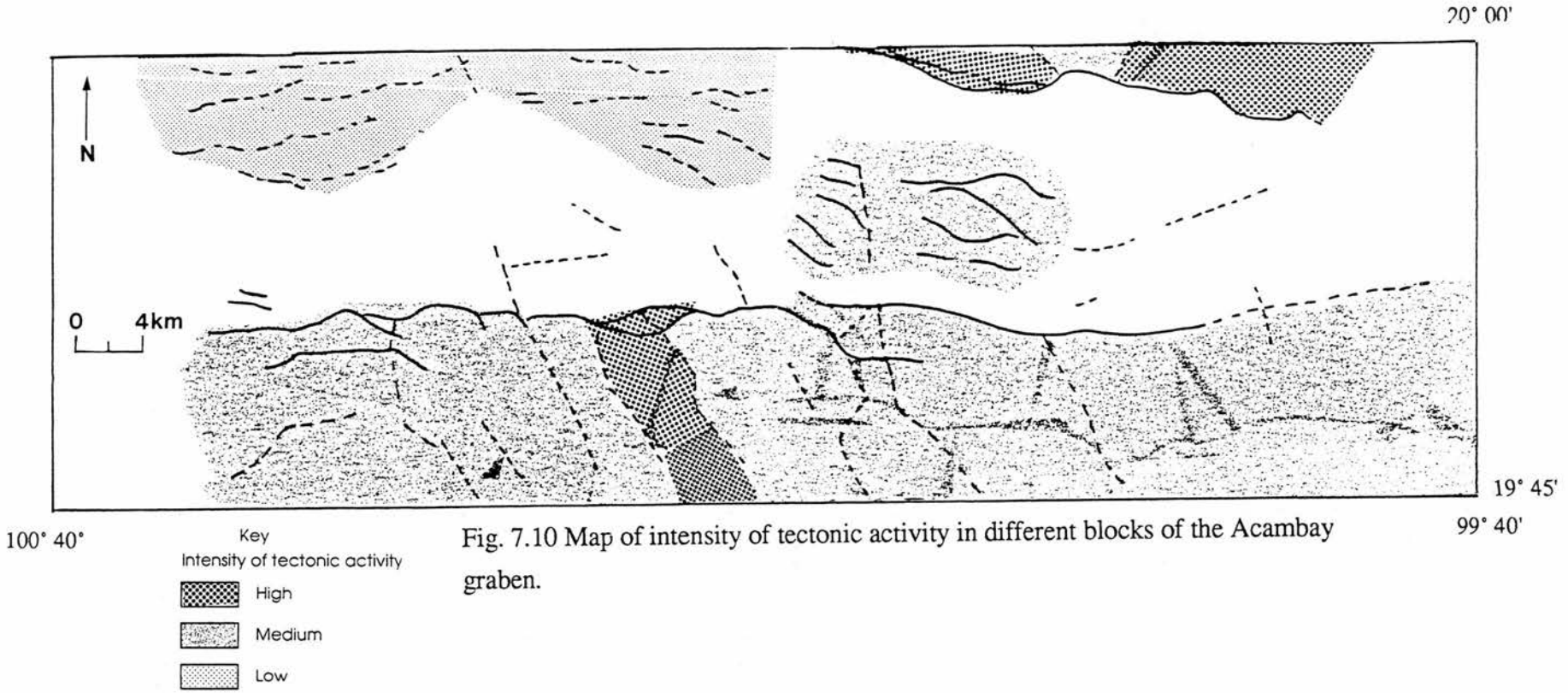

Fig. 7.10 Map of intensity of tectonic activity in different blocks of the Acambay graben.

Chapter Eight: Acambay Graben in the Broader Context and Seismic Hazard

This chapter assesses the wider implications of the neotectonics of the Acambay graben in the regional tectonics of southern Mexico. In this chapter I will assess some of the implications of the observations gathered from the morphotectonic analysis in the Acambay graben and the relationship of this graben to the regional tectonic context of the Mexican Volcanic Belt and consequently with the regional tectonics of southern Mexico. A seismic risk approach is presented.

8.1 Acambay graben in its regional tectonic context

Several workers have suggested that lateral crustal movements along major shear zones in central Mexico and Pliocene-Quaternary vulcanism and tectonism within the Mexican Volcanic Belt may be produced and controlled by large zones of crustal weakness. These zones seem to be reactivated by plate convergence and expressed as a transtensive, left-lateral fault system along the Mexican Volcanic Belt (Mooser, 1972; Cebull and Shubert, 1987; Johnson 1987; Urrutia and Böhnel 1988; Mooser and Ramírez, 1989). Some workers have also proposed normal faulting with a left-lateral strike-slip component as the main neotectonic process in the central part of the Mexican Volcanic Belt (Astiz 1980; Johnson 1987; Suter 1991; Suter *et al.*, 1992). Recent studies suggest that in central Mexico the east-west trending zone of crustal weakness has been reactivated with episodes of right-lateral shear, producing NW-SE faults, and left-lateral shear, producing NE, E and ENE faults. The most recent episode seems to have been controlled by left-lateral shear (Late Pleistocene) and produced ENE faults. This event still dominates the tectonics of central Mexico and is the one that gave rise to the tectonic elements of the Sierra de Chichinautzin (south of Mexico city) and those of the Acambay graben (Mooser *et al.*, 1992). Thus, from this analogy it is possible to infer that the age of the Acambay graben must be similar to that of the Sierra de Chichinautzin, that is

Quaternary (40 ka - assigned from extended relationships between 14C age and cone/flow morphology established by Bloomfield, 1975; Martin del Pozzo, 1982). This study provides a range of morphological evidence for the dominance of left-lateral shear in central Mexico which is further analysed below.

8.1.1 Morphotectonic evidence for large-scale, left-lateral shear in central Mexico.

Inferences drawn from the study of Landsat images are confirmed by observations made in the field and by aerial photographs and morphometric analysis. These provide clear geomorphic evidence for Quaternary throws and left-lateral displacement on east-west trending faults of an apparent Quaternary age.

Despite the fact that most of the Acambay graben faults have high escarpments, (that is, large vertical displacements) the map traces of some of the faults (Venta de Bravo, Acambay-Tixmadeje, Temascalcingo and Tepuxtepec) show parallel faults, discrete fault segments or strands that step aside, and sometimes overlap slightly, to form what is commonly known as en-echelon fault geometry characteristic of strike-slip faults (Aydin and Schultz, 1990). This fault configuration confirms the importance of strike-slip faulting in the tectonic development of this region (Fig. 7.8, see chapter 7). In addition, it is important to mention that the en-echelon geometry of these faults might lead to fault interaction which undoubtedly occurs among nearby faults or fault segments (Aydin and Schultz, 1990). In terms of seismic risk the evaluation of these interaction is extremely important. Nearby faults may transmit or propagate the energy associated with faulting and during an earthquake might increase the area of surface rupture and damage. This probably happened during the 1912 and 1979 earthquakes in the Acambay graben.

Although some workers have described the faults along the graben as normal faults with a "minor" left lateral component (Astiz, 1980, 1986; Martínez-Reyes and

Nieto-Samaniego, 1990; Suter *et al.*, 1991, 1992), the geomorphic characteristics of these faults provide convincing evidence of their lateral displacement in support of models proposing active, large-scale left-lateral shear across central Mexico. Thus, the geomorphic evidence confirms that the main mechanism that produced, and still controls the development and dynamics of the Acambay graben is strike-slip, and this accords with the regional tectonics that produced similar en-echelon grabens in the central part of the Mexican Volcanic Belt. It seems that the role of a lateral component along the Acambay graben faults has previously been underestimated during regional tectonic analysis. I, however, maintain that the question of the importance of a left-lateral displacement in the Acambay graben should be re-examined for the following reasons. First, the map trace of the faults shows a typical en-echelon geometry characteristic of strike-slip faults that has not been noted by previous studies of the area. Secondly, some of the depressions associated with the faults have a rhomboid shape typical of pull-apart basins and thus may be related to strike-slip faulting. Finally, the tectonic geomorphic features occurring throughout the Acambay graben have not hitherto been incorporated into a regional tectonic synthesis.

The assumption of the importance of a lateral component in the formation of the Acambay graben itself is based on the well-known hypothesis that "...vertical uplift of the Earth's crust must involve a compensating horizontal flow of material. Similarly, transcurrent movement on a fault of finite length must involve the accumulation of material in regions toward the ends of the fault, and vertical displacements are to be expected" (Chinnery, 1965). Transcurrent movement may give rise to quite large vertical displacements. Thus, all transcurrent faults are to some extent related to topography (Chinnery, 1965).

As was previously discussed in chapter 7, most of the Acambay graben faults show evidence of transcurrent movement. As has been described, even while crustal blocks move laterally over time, they may alternately rise and sink (Sylvester, 1988). Many of the depressions along the Acambay graben faults have the rhomboid shape characteristic of pull-apart basins and sometimes show S- or Z- shaped basins due to local crustal extension. A considerable body of literature relates this basin geometry to strike-slip faulting (Crowell, 1974b; Aydin and Nur, 1982, Aydin and Schultz, 1990). Pull-apart basins are generally associated with parallel faults or strands of the master faults of the graben that sometimes overlap each other. Elongated ridges or local uplift occur in the sectors of the faults that bend with a "Z"-shaped configuration, and have left-lateral displacement (Fig. 7.8 , chapter 7).

Two good examples of the influence of left-lateral shear in the Acambay graben are apparent in the Venta de Bravo fault and the Temascalcingo faults. The first is located in Mount Temascalcingo and exhibits a "tulip structure" or "negative-flower structure", that is a concave-upward geometry of faults in profile that forms as a result of extension in domains of divergent strike-slip. This structural arrangement indicates that the so called "caldera" in the central part of Temascalcingo is in fact a pull-apart structure (Ortiz, *et al.*, 1993) generated by left-lateral displacement (Fig. 7.8, see chapter 7) . A second example of this type of left-lateral tectonic control in the Acambay graben is an incipient pull-apart basin in the central part of the Venta de Bravo fault which indicates extension within the area (Fig. 7.9, see chapter 7). Convergent strike-slip or transpression provides a component of horizontal shortening across a strike-slip fault which is necessarily accompanied by compensatory uplift of rocks in the fault zone (Sylvester, 1988). This compensatory uplift of rocks is reflected in the fault associated landforms of the Acambay graben as elongated ridges.

Elongated, anticline-like , hills about 30 m high in the inner and outer basins of the graben (Fig. 7.8), show folded deposits and reverse faults characteristic of pressure ridges related to strike-slip faulting (Sylvester, 1988). This structural configuration indicates crustal shortening in the zones of convergent strike-slip.

Several en-echelon folds occur in the inner basin, which is a downdropped fault block of the graben. Thus, the formation of these folds and their arrangement with respect to the trend of the master faults of the Acambay graben suggest their relation to regional strike-slip faulting. The left-stepping folds (NW trending) in the inner basin of the graben indicate left-slip (Fig. 8.1). The left-lateral displacement has produced NW-SE anticlines in lacustrine folded deposits (Pleistocene ?). These deposits are younger than the Temascalcingo volcanic rocks but probably older that some of the small lava cones (less than 40 000 y. - Bloomfield, 1975) surrounding the area, which partially cover the lacustrine folded deposits. Therefore, a stage of tectonic deformation, involving left-lateral shear, might have occurred after the formation of the lake and before the last volcanic activity inside the graben (late Quaternary).

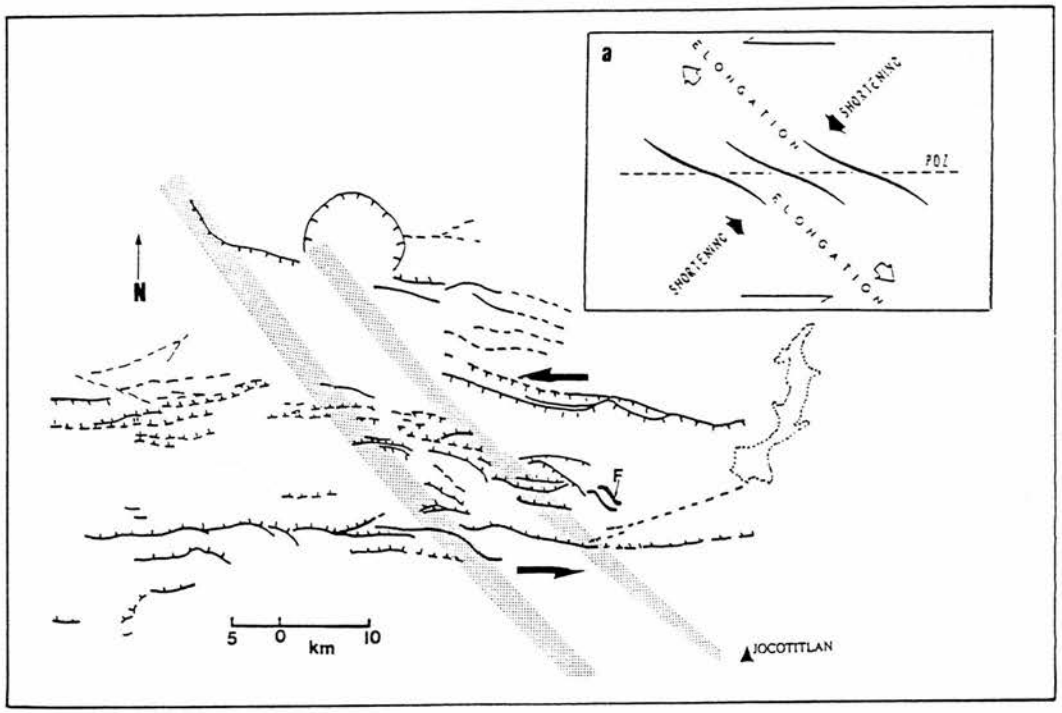

Fig. 8.1 Left-stepping folds (north-west trend) in the inner basin of the graben indicating left slip. Symbols: F inside a circle show NW trending en-echelon folds; a - insert shows geometry of en-echelon folds in left simple shear (Sylvester, 1988); PDZ - principal displacement zone; bulk strain axes are labeled.

This evidence leads to a correlation of local tectonics in the Acambay graben with the regional tectonics of the Mexican Volcanic Belt. Geomorphic evidence along the Acambay graben suggests that: (1) the Acambay graben is the product of a lateral shear along the whole Mexican Volcanic Belt and the consequent fall (collapse) of the inner block due to the resulting extension in the region; (2) the E-W trending faults of the Acambay graben provide evidence of transcurrent movement associated with large-scale regional left-lateral shear along the Mexican Volcanic Belt and across central Mexico.

To summarise, this study has provided geomorphic evidence that supports a model proposing active, large-scale left-lateral shear across central Mexico of probable Pliocene-Pleistocene age.

8.2 Seismic hazard

The term seismic hazard should refer to the types, features, mechanisms, and occurrence of earthquakes, that is, to the energy propagated by them, to the depth at which they occur, to their recurrence intervals, and to the dimensions of the focus area. This type of hazard is also linked to seismotectonic characteristics, or, in other words, the relationship between the focus and faults identified on the surface by geological and geomorphological methods or inferred at depth from seismological studies (Panizza, 1991).

Seismic hazards in a strict sense are connected to the earthquake and seismotectonic characteristics in an area, and should be distinguished from seismic susceptibility, that is a hazard induced by the physical-geographical situations of the area considered (Panizza, 1991). This study has been concerned with morphotectonic and neotectonic investigations conducted to identify active tectonic structures. There is an increasing likelihood of geomorphology being able to make a significant contribution to

the "where" of earthquake prediction, but unfortunately, not to the "when" (Doornkmap and Han, 1985).

8.2.1 History of damage

On November 19, 1912 a large earthquake with $M_S = 6.9$ occurred in Mexico, about 100 km northwest of Mexico City, causing severe damage to structures in towns along the Acambay and El Oro valleys in the states of Mexico and Michoacán. Urbina and Camacho (1913) determined a shallow focus for this event and Figueroa (1970) located it at 19.933 and 99.833. Its epicentre was located within the region of largest intensity (X) near the town of Acambay where 20 people died under collapsed structures. In Mexico City, it was felt with intensity V on the Modified Mercalli scale. The study of historic seismograms (Astiz, 1986) has indicated a normal fault mechanism with a left-lateral strike-slip component. These data are consistent with the field data collected after the earthquake, namely a series of east-west trending cracks from the Huapango dam to the Lerma River, a long east-west trending crack in the northern bank of the Lerma River with average vertical displacement of 60 cm, and 19 km further south a 20 km long "fissure" with less displacement. These features bordered a collapsed block. The analysis of fault plane solutions (Astiz, 1986) indicates that the 1912 Acambay earthquake had a shallow source. This fact could have important implications in seismic risk evaluations in central Mexico, which is one of the most densely populated regions in Mexico.

A detailed study of the damage caused by the November 19, 1912 Acambay earthquake was carried out after the earthquake by Urbina and Camacho (1913). This showed that movement took place along the Acambay-Tixmadeje fault. The most damaged villages were those located along the fault and those located on the steeper slopes. The most remarkable effect of the earthquake was the formation of long east-west

trending fractures (fissures), transverse to the direction of the main intensity, that produced vertical displacement and rupture of the terrain (Fig. 8.2). Several landslides occurred along the Lerma River basin (Fig. 8.3) and some rockslides along the escarpments. The underground waters were affected by the earthquake and they become turbid after the shock. Some of the valleys in the seismic zone recorded water and mud ejection, events that are typical phenomena associated to earthquakes (Urbina and Camacho, 1913).

Most of the villages are located at the foot of the mountain fronts (for instance Acambay, Temascalcingo, San Andres Timilpan, Pueblo Nuevo, La Magdalena) and only a few villages are located in the valleys and basins. Moreover, the villages of Acambay and Temascalcingo lay over alluvial material which increased the amplitude of the earthquakes waves and therefore the amount of damage. The houses were built of adobe, stone, brick and wood (for more detail on the materials and the characteristics of buildings see Urbina and Camacho, 1913). In Acambay there were about 500 houses before the earthquake. Most of the serious damage occurred in this village. Damage was also sustained in several towns in and near the Acambay region. The earthquake was felt throughout central Mexico, across an area of about 100,000 km^2. Evaluation of the damage produced by the 1912 earthquake shows that in the Acambay region more than 500 houses were completely destroyed and several partially damaged (Fig. 8.4). At least 144 were reported killed (preliminary register of deaths, Urbina and Camacho, 1913) over the whole region of Acambay and many injured.

Fig. 8.2 Cracks showing vertical displacement produced during the November 19, 1912 Acambay earthquake (Urbina and Camacho, 1913).

Fig. 8.3 Landslides produced along the right bank of the Lerma River during the November 19, 1912 Acambay earthquake (Urbina and Camacho, 1913).

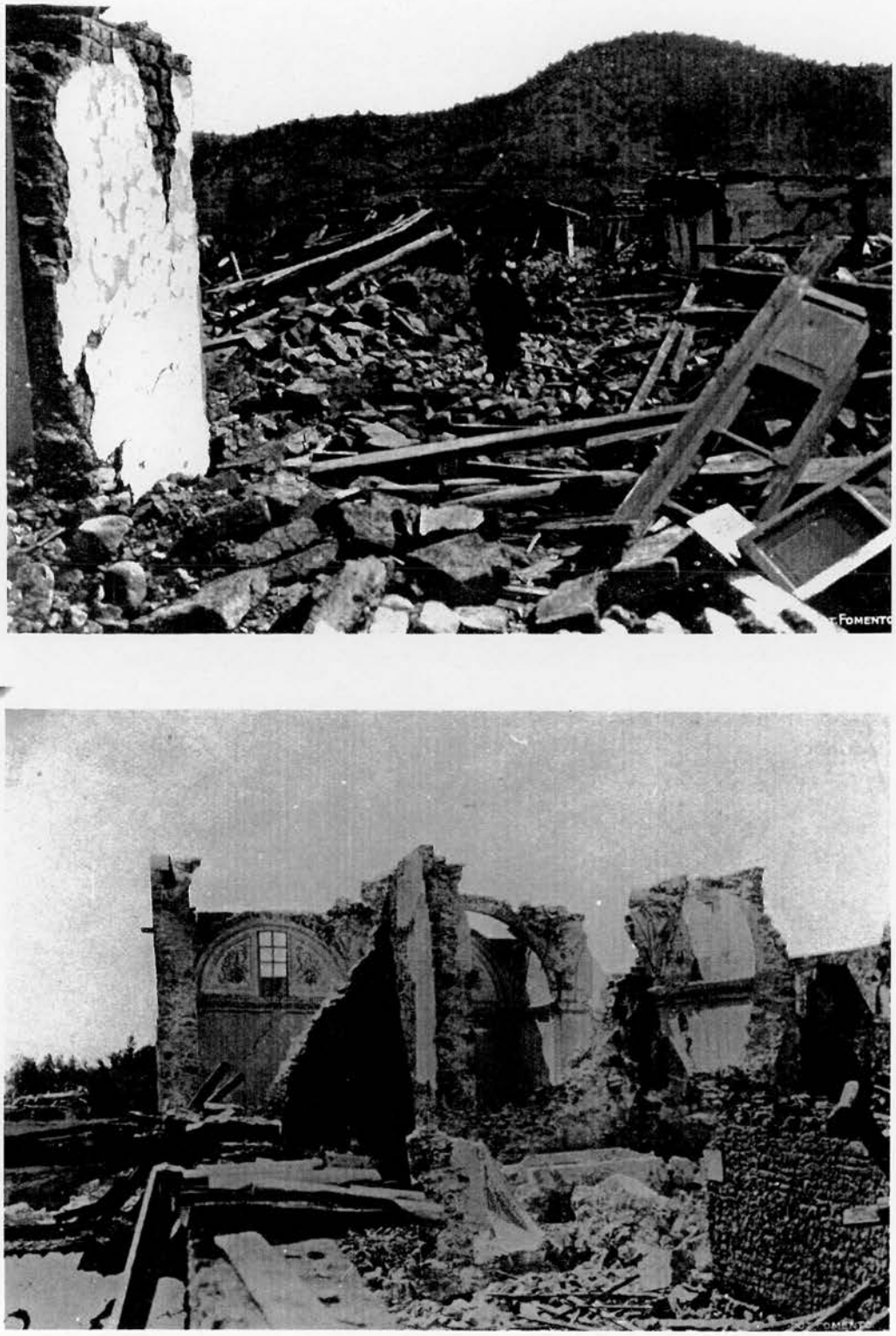

Fig. 8.4 Examples of damage caused by the 1912 earthquake in the village of Acambay (Urbina and Camacho, 1913).

The February 22, 1979 Venta de Bravo earthquake (m_b= 5.3) involved approximately 90 individual events extending over several months from February to June. The focus of the main shock was located 27.8 $\pm$ 4.2 km east of Maravatío at a depth of 8.2 $\pm$ 2.9 km with the epicentre being close to the outcrop of the Venta de Bravo fault. This indicates a shallow earthquake that might have produced some damage in the surrounding area. However, there are no detailed records of the damage caused by this earthquake. The effects of the earthquake were felt in the whole region, but it caused most panic in the town of Maravatío were some damage was reported, such as cracks and fissures in buildings. Landslides and rock slides still taking place in some of the escarpments along the Pastores, Venta de Bravo and Temascalcingo faults, that provide evidence of the active tectonics in this area.

8.2.2 Seismic hazards in the Acambay graben

Focal mechanisms of the Mexican-subduction zone earthquakes reliably located at depths greater than 40 km imply that these shocks occur within the subducted Cocos plate, rather than at the plate interface (Dewey and Suárez, 1991). By contrast only shallow earthquakes my occur along the Mexican Volcanic Belt (Suárez and Ponce, 1986). The shallow earthquakes in the inner North American plate that have occurred in southern Mexico, such as the 1912 earthquake in the Acambay graben, have been extremely destructive (Urbina and Camacho, 1913). Therefore, an evaluation of seismic hazards in this region is of considerable relevance.

In recent years the segmentation of active faults has received wide interest and attention. The probability and size of earthquakes caused by a fault may be entirely different in different segments. Therefore, segmentation of an active fault is a practical and useful means of demarcating earthquake regions or zones, and of searching for and

defining potential earthquake zones (Xie, 1991). A scheme for subdividing the faults of the Acambay graben was outlined in Chapter 7. The segments proposed for each fault coincide with the boundaries of morphostructural blocks along the Acambay graben (Fig. 7.7, chapter 7). In addition, morphostrucutral knots, denoted as the foci of probable earthquake activity, were determined from a scheme of morphostructural zoning (Fig. 7.7, chapter 7). The basic principles of morphostructural zoning were explained in chapter 7 (Rantsman, 1979; Gvishiani *et al.*, 1986, and Bathia *et al.*, 1992). From this analysis and the correlation with seismic activity and earthquake magnitude it is possible to determine areas of high, medium and low seismic hazard (Fig. 8.5).

Correlation of the morphostructural map and the earthquake data (data provided by the US Geological Survey, National Earthquake Information Centre, Servicio Sismológico Nacional, Mexico, and Dr R. Mota-Palomino, Instituto de Geología, Universidad Nacional Autónoma de México) for the Acambay graben indicates that the epicentres of earthquakes with $M \geq 4.0$ known here occurred within or near knots (Fig. 8.5). Attention has been drawn to problems concerning the accuracy of epicentre location, because too great error in the location (coordinates) of epicentres could lead to misleading correlation. The accuracy of earthquake location was improved employing data recorded from seismic monitoring produced with portable seismographs during the periods of March 1989 and August-September, 1990 (Yamamoto and Mota, 1991), and the relocation of events of 1979 to within 5 km (Mota-Palomino, personal communication). The seismic knots were defined, based on studies by Rantsman (1979) Gvishiani *et al.* (1986) and Bathia *et al.* (1992), as those which met two conditions out of the following four: 1) the number of lineaments in the node is larger than two; 2) the highest lineament rank at the knot is first or second; 3) the relief of the knot comprises a combination of mountain slopes and basins; and 4) the magnitude of epicentres associated

to the knot is $M \geq 4.0$.

The correlation of morphotectonic (morphostructural) zoning and the earthquake location along the Acambay graben allowed the identification of a number of morphostructural knots. The Venta de Bravo morphostructural knot (Fig. 7.7:11; Fig. 8.5) shows the intersection of three lineaments (first and second rank) and represents the border between two different terrains (mountain front and a depression). The intersection of these lineaments represents a zone of compression and uplift produced by convergent faults. In addition, a $m_b = 5.3$ earthquake and several smaller events ($m_b = 3.0 - 5.0$) are located in the nearby zone. This structural arrangement suggest a knot that seems to be one of the highest risk in the Acambay region. The Acambay-Tixmadeje morphostructural knot (Fig. 7.7: 3; Fig. 8.5) represents the border between two macroblocks - a mountain front and a basin, demarcated by a first rank lineament. Moreover, a high seismicity ($M = 6.9$ earthquake associated with the Acambay-Tixmadeje master fault) seems to indicate the presence of a morphostructural knot indicating high seismic risk in this area and its surroundings. The Temascalcingo morphostructural knot comprises three lineaments of first and second rank that delimit a basin and mountain terrains. The structural arrangement of this knot is similar to that mentioned above for the Venta de Bravo fault, and suggests the presence of a knot in this area (Ortiz *et al.*, in press). Although there is no associated seismic activity, this area could be a site of potential seismicity (Fig. 8.5). Finally, at the western end of the Pastores fault where the eastern end of the Venta de Bravo fault overlaps, three lineaments divide two different terrains (a basin and mountain front). In this area seismic energy could be transferred between the Venta de Bravo and Pastores faults and this makes it significant for seismic hazard evaluation (Fig. 8.5).

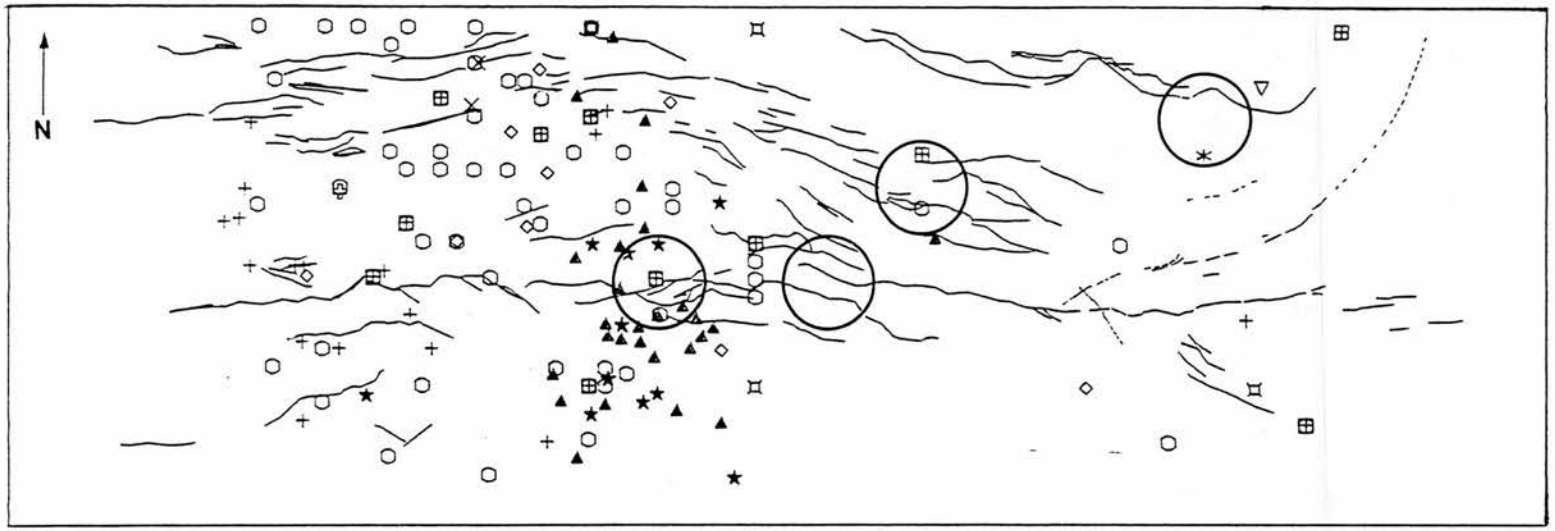

Fig. 8.5 Map of seismic risk and morphostructural knots in the Acambay graben. Circles show sites of morphostructural knots and areas of seismic risk. Lines show faults. Symbols: 1) Magnitudes of the events recorded during 1900 to 1991 (estimated location error 20 km or more): ?- ○ 1- □ 2- △ 3- ▽ 4- ▭ 5- ◇ 6- X 7- ∗ ; 2) Magnitudes of the events recorded during the period March 1989 and relocated events of the 1979 main shock and large aftershocks (estimated location error within 5 km, and for small-magnitude events ± 10 km (Yamamoto and Mota, 1991)): ?- + 1- ● 2- ◆ 3- ▽ 4- ▲ 5- ∗ 6- ■ .

Earthquakes pose a major threat to large parts of the earth, and vulnerability to disaster is increasing as urbanisation and development occupies more areas that are susceptible to the effects of large earthquakes. In order to minimise the loss of life , property damage and social and economic disruption caused by earthquakes, it is essential that reliable estimates of sesimic hazard be available to national decision makers and engineers for land use planning and improved building design and construction. The results provided in this study are an attempt at evaluating the geomorphic characteristics of the Acambay graben region and to propose areas of high seismic risk.

Chapter Nine: Summary and Implications

9.1 Summary

This chapter briefly summarises the objectives and attainments of this thesis. The aim was to investigate geomorphological evidence indicative of neotectonic activity in the Acambay graben in central Mexico and to assess its relationship to regional scale geodynamics. This was accomplished by using morphotectonic and neotectonic analyses. Such an approach provides a means of understanding the recent deformation of the Earth's crust through the study of landforms controlled by tectonic processes. The objectives were:

1) to determine the tectonic regime and evaluate the degrees of active tectonism of the region.

2) to ascertain how far the tectonic landforms of the Acambay graben accord with the current regional tectonic models of southern Mexico.

3) to use tectonic landforms indicative of neotectonic activity in the assessment of the spatial occurrence of seismicity, in other words, to determine areas of seismic risk.

9.2 Large-scale and meso-scale tectonic geomorphology

The use of spatial filtering, principal component analysis, IHS transformations and band ratioing of Landsat TM images enabled the enhancement of major lineaments which reveal the tectonics of the Acambay graben. The results obtained from the application of combined digital remote sensing techniques, geological, topographic and statistical analysis for the lineament trends in the Acambay graben indicate five main directions: E-W, NNW-SSE, ESE-WNW, ENE-WSW, NNE-SSW.

These lineament trends were interpreted as being the product of two major phases of deformation: the subduction of the Cocos plate that is associated with left-lateral shear in central Mexico, and the reactivation of faults produced by a previous (older)

subduction episode - that of the Farallon plate. The E-W trending lineaments were found to be predominant and the most seismically active in the Acambay graben.

The meso-scale geomorphic analysis confirmed the existence of several faults forming the Acambay graben. A range of geomorphic indicators, such as fault escarpments, V-shaped valleys, faceted spurs, elongated ridges, fault-controlled streams and sag ponds, demonstrate active faulting along the Acambay graben. High-gradient scarps, low-levels of denudation of some scarps, active-incision and valley-downcutting in V-shaped valleys prove the relative youth of these faults.

9.3 Morphometric analysis: use of geomorphic indices in the assessment of active tectonics.

The morphometric expression of mountain fronts associated with active tectonic environments show differences within the five study areas. The combined morphometric data, including mountain front sinuosity, facet characteristics, fault-scarp morphology, longitudinal profiles, mean valley morphology and drainage basin shape, provide evidence for relative variations in tectonic activity among the identified areas and sub-areas of the Acambay graben. Low sinuosity, fault-controlled morphology of the scarps, high values of the proportion of faceting and undissected escarpments are representative of the Venta de Bravo mountain front, suggesting a relatively high degree of tectonic activity.

The relatively high degree of dissected mountain fronts in the Venta de Bravo mountain front is a result of the high value of the proportion of dissection of mountain fronts in sub-area II. This high value is produced by differences in lithology of the escarpments. Low values of V_f (mean valley morphology), high values of B_s (drainage basin shape), convex longitudinal profiles and V-shaped cross-river sections provide

additional evidence of the high degree of active tectonics along the Venta de Bravo fault-bounding mountain front.

The combined morphometric data suggest that the Acambay-Tixmadeje mountain front is the second, in decreasing order, in degree of active tectonics, in the Acambay graben followed by the Pastores, Temascalcingo and Tepuxtepec fronts. However, it should be considered that Temascalcingo area does not, strictly speaking, represent a mountain front but the morphology and morphometry of the fault escarpments comprising this area were also evaluated in this analysis.

Variations within areas were identified. For instance, sub-area V in the Venta de Bravo mountain front shows low sinuosity and the highest mean of undissected escarpments. In addition streams in this sub-area show relatively higher values of drainage basin shape, that is, elongated basins, and low V_f values (V-shaped valleys) which are relatively different from the other sub-areas.

The morphometric analysis indicates a general trend of increasing tectonic activity among the fault-bounding mountain fronts of the Venta de Bravo and Acambay-Tixmadeje areas. This high degree of tectonic activity increases in the Venta de Bravo fault and particularly in sub-area V. The degree of tectonic activity appears to decrease in the Tepuxtepec area, which contained the highest sinuosity and lowest values of faceting and laterally continuous escarpments in the Acambay graben.

The morphometric analysis demonstrates different levels of tectonic activity along the Acambay graben faults. Several variables such as the characteristics of the fault scarps, fault-bounded mountain fronts and fluvial systems indicate that a high degree of tectonic activity occurs along the Venta de Bravo fault. The Acambay-Tixmadeje master fault is the second in decreasing order of active tectonics in the Acambay graben, followed by the Pastores, Temascalcingo and Tepuxtepec faults.

9.4 Geomorphic evidence of Quaternary active faulting in the Acambay graben

The general arrangement of the faults composing the Acambay graben shows dominant east-west trend, and a secondary NNW-SSE fault-trend which is oblique to the east-west trending faults of the Acambay graben. The Acambay graben exhibits a major fault discontinuity, which is apparently concordant with the regional NNW-SSE systems of faults, and this highlights the asymmetrical structure of a half-graben in the western part of the graben. Geomorphic features indicate that the most recent and active faults are those of east-west trend and that the NNW-SSE trending faults are apparently older reactivated faults.

Active faults in the Acambay graben are grouped into five major east-west trending systems - the Acambay-Tixmadeje system, the Tepuxtepec faults, the Pastores fault, the Venta de Bravo system, and the Temascalcingo faults. A range of geomorphological evidence indicates recent tectonic activity along the faults bounding the Acambay graben. Such morphological indicators are most evident along the southern flank of the graben, particularly along the Venta de Bravo, Acambay-Tixmadeje and Temascalcingo fault systems. Here prominent fault scarps, triangular-faceted spurs, V-shaped valleys, offset drainage, deformed lake deposits, high-levels of lake deposits, sag ponds, pull-apart basins, shutter ridges, pressure and compression ridges are clearly developed, and high slope gradients demonstrate the freshness of the scarps. In contrast, faults in the Tepuxtepec system exhibit low slope gradients and low fault scarps which may indicate either more prolonged erosion or a lower rate of tectonic activity in this part of the graben. Except for limited historical evidence, there is as yet no absolute dating available for the most recent fault displacements and consequently estimates have to be based on the degree of fault scarp degradation.

The en-echelon arrangement of the faults, the shape of their trace in planform and the surface expression of fault-associated landforms provide evidence of strike-slip associated geomorphology. Distinctive characteristics such as sag ponds, pull-apart basins, shutter ridges, deflected streams, elongate uplifts and pressure ridges, and changes in the relief of the escarpments according to the convergent or divergent trace of the configuration of the fault pattern, producing uplift and subsidence respectively, indicate active or recently active strike-slip faulting in the Acambay graben.

The geomorphological evidence indicative of neotectonic activity described here shows that the Venta de Bravo fault system and the Pastores fault have experienced slip combining normal north-facing faulting and left-lateral displacement; with significant lateral displacements being most clearly expressed in the morphology of the Venta de Bravo fault system. The Acambay-Tixmadeje fault system consists of normal south-facing faults with a component of left-lateral displacement. By contrast, the Tepuxtepec faults are mainly north-facing and where combined with south-facing normal faults give rise to small graben structures. The Temascalcingo faults, in the centre of the graben, are also characterised by a combination of normal south- and north-facing faults with a component of left-lateral displacement, giving rise to a graben structure within the volcano of Temascalcingo. Although the Acambay graben is a complex zone of extension, it also shows some evidence of compression. This is indicated by: 1) two compression ridges, one located on the western end of the pull-apart structure along the central part of the Venta de Bravo fault, and the other situated at the eastern end of the Toxi basin; 2) almost east-west trending elongated uplifts or pressure ridges on the Toxi basin and the basin of Ixtlahuaca, located south from the Acambay graben; and 3) en-echelon northwest trending folds located in the inner basin of the graben. These geomorphic features are associated with active left-lateral displacement.

9.5 The Acambay graben in context

9.5.1 Geomorphic evidence for transcurrent movement and a regional left-lateral shear zone in central Mexico.

Several studies have shown that the central part of the Mexican Volcanic Belt is characterised by generally east-west trending faults of Quaternary age (Mooser, 1969; 1972; Mooser and Ramírez, 1989; Johnson, 1987; Suter *et al.*, 1991). These fault and associated fracture systems appear to exert a structural control over magma routing in the area, leading to an overall tectonic control over volcanism in the central as well as eastern part of the Mexican Volcanic Belt (Johnson, 1987; Urrutia and Böhnel, 1988). The regional scale tectonic framework is related to plate convergence processes which in the Mexican Volcanic Belt have resulted in the activation of a transtensive left-lateral system (Urrutia and Böhnel, 1988).

This study provides geomorphic evidence which supports a model proposing active, large-scale left-lateral shear across central Mexico of probable Pliocene-Pleistocene age. The Acambay graben fault-associated landforms provide evidence of transcurrent movement. The Acambay-Tixmadeje, Venta de Bravo, Pastores and Temascalcingo faults exhibit along their trace several sag ponds, pull-apart basins, elongated ridges, and compression ridges; as well as pressure ridges and en-echelon folds in the inner basin of graben. In addition the shape of the trace in planform and en-echelon arrangement of the faults all indicate lateral shear in this region.

Thus, the geomorphic observations gathered in this study indicate that the Quaternary tectonics in the Acambay graben has been dominated by almost east-west trending normal faults with a left-lateral component which suggests that the origin of the

graben is the result of a regional, active, large-scale left-lateral shear. This left-lateral shear produced along the Mexican Volcanic Belt is the result of the plate convergence in southern Mexico. The subduction of the Cocos plate beneath the North American plate produces an episodically left-lateral shear in the upper brittle section of the crust in central Mexico. The left-lateral shear produces north-south extension and the development of en-echelon graben along the central part of the Mexican Volcanic Belt, among them the Acambay graben.

9.5.2 Seismic hazard in the Acambay graben

Morphostructural zoning and morphotectonic analysis allowed the identification of fault segments, which in most cases are concordant with morphotectonic units, displaying different levels of active tectonics and indicating the place of morphostructural knots along the Acambay graben. The most active tectonic and seismic risk areas derived from this analysis are: the Acambay-Tixmadeje (block 3) and the Venta de Bravo fault (block 11 and morphostructural knot) at similar levels, and in decreasing order the Temascalcingo morphostructural knot and the Pastores fault (block 6). In addition, the correlation of the morphostructural zoning and earthquake location along the Acambay graben indicate that: 1) the structural arrangement of a morphostructural knot and the historic seismic activity (m_b= 5.3) in the central part of the Venta de Bravo fault (block 11) suggest that this is one of the most potential areas for seismic hazard in the Acambay graben; 2) a morphostructural knot with associated historic seismicity (M=6.9 earthquake) indicates high seismic risk in the Acambay-Tixmadeje fault (block 3); 3) the structural arrangement of the Temascalcingo morphostructural knot despite the absence of associated seismic activity should be considered as evidence of a seismic hazard zone;

finally, 4) in the area where the Venta de Bravo and the Pastores faults overlap, seismic energy could be transferred and therefore this suggests a seismic risk area.

9. 6 Conclusions

The following three main conclusions arise from this study:

1. The tectonic landforms of the Acambay graben (prominent fault scarps, triangular-faceted spurs, V-shaped valleys, deformed lake deposits, high-levels of lake deposits) reflect fault activity characterised by normal north- and south-facing faults combined with left-lateral displacement (offset drainage, sag ponds, pull-apart basins, shutter ridges, elongate uplifts and pressure ridges, changes in the relief of the escarpments according to the convergent or divergent trace of the configuration of the fault pattern, producing uplift and subsidence respectively, and compression ridges).

2. Geomorphological data for the Acambay graben are consistent with systems of faults which have experienced transtensive, large-scale, left-lateral shear. Geomorphic evidence in the Acambay graben supports a tectonic model for left-lateral shear, along the Mexican Volcanic Belt, across central Mexico.

3. The clarity of the geomorphological evidence and the historical occurrence of seismicity along the Venta de Bravo system of faults suggest that this is the most tectonically active structure in the Acambay graben. The interaction of two parallel faults, in the Venta de Bravo fault system, with a convergent trace produces uplift and compression that indicate the presence of a morphostructural knot. In addition, associated historical seismicity (m_b= 5.3 earthquake) indicates an area of high seismic risk in the Acambay graben.

Further analysis of neotectonic activity in the region is required in order to document more precisely both spatial and temporal variations in seismicity. This could be

accomplished by establishing a precise chronology of fault displacement and by the geodetic monitoring of fault movement and deformation in the region. I suggest that future research into the Acambay graben should concentrate on dating the morphological chronology proposed here. One possibility is to date sites demonstrating deformation directly due to tectonic activity. For example, deformed lake sediments (with wood and tusk remains), soils, alluvial fill contained in sag ponds, and volcanic ashes containing suitable material in the places of deformation recorded in this research could be dated by the radiocarbon (^{14}C) technique, while displaced lavas and lava cones could be dated by potassium-argon (K-Ar) techniques. Another possibility is to carry out a programme of trenching across the Quaternary fault scarps that could provide data about buried and displaced sediments. Dating of displaced sediments might lead to the ages of surface faulting events. Such investigations have the potential to provide important new insights into fault chronology and seismic recurrence intervals.

References

ANDERSON, T. H. & V. A. SCMIDT (1983): The evolution of the Middle America and the Gulf of Mexico-Caribbean Sea region during the Mezosoic times. - Geol. Soc. Am. Bull., **94**: 941-966.

ALEXANDER, D. & R. FORMICHI (1993): Tectonic causes of landslides. - Earth surface and landforms, **18**: 311-388.

AGUIRRE-DÍAZ, G. J. (1990): The Amealco tuff, a major explosive event in the Mexican Volcanic Belt (abstract). - Geol. Soc. Am., Abstr. Programs, **22**: 350.

ARMIJO, R., P. TAPPONNIER, J. L. MERCIER & TONG-LIN HANG (1986): Quaternary extension in southern Tibet: Field observations and tectonic implications. - J. Geophys. Res., **91**, n° B14: 13803-13872.

ASTIZ, L. M. (1980): Sismicidad en Acambay, Estado de México. El temblor del 22 de febrero de 1979. - B.S. thesis, Univ. Nac. Autón. Méx., México, 130 p.

ASTIZ, L. M. (1986): The 1912 Acambay, Mexico (Ms = 7.0) earthquake: a re-examination (abstract). Bol. Unión Geofis. Mex., epoca II, special issue, 17.

AUBOIN, J., J. AZEMA, J.C. CARFANTAN, A. DEMANT, C. RAGIN, & J. TOURNON (1982): The Middle American Trench in the Geological framework of Central America.- [In:] Init. Rep. DSDP, **67**: 747-755. U.S. Govt. Printing Office, Washington.

AVOUAC, J. P. (1993): Analysis of scarp profiles: Evaluation of errors in morphologic dating. - J. Geophys. Res., **98**, n° B4: 6745-6754.

AVOUAC, J. P., P. TAPPONIER, M. BAI, H. YOU & G. WANG (1993): Active thrusting and folding along the northern Tien Shan and late Cenozoic relation of the Tarim relative to Dzungaria and Kazakhstan. - J. Geophys. Res., **98**, n° B4: 6755-6804.

AYDIN, A. & A. NUR (1982): Evolution of pull-apart basins and their scale independence. - Tectonics, **1**, n°1: 91-105.

AYDIN, A. & R. A. SHULTZ (1990): Effect of mechanical interaction on the developement of strike-slip faults with echelon-patterns. - J. Struc. Geol., **12**, n°1: 123-129.

BERHE, S. M. & D. A. ROTHERY (1986): Interactive processing of satellite images for structural and lihtological mapping in Northeast Africa. - Geological magazine, **123**, n°4, 393-403.

BHATIA, S.C., T. R. K. CHETTY, M. B. FILIMONOV, A. I. GORSHKOV, E. Ya. RANTSMAN & M. N. RAO (1992): Identification of potential areas for the ocurrence of strong earthquakes in Himalayan arc region. - Proc. Indian Acad. Sci. (Earth Planet. Sci.), **101**, n° 4: 369-385.

BISHOP, P & J. C. BOUSQUET (1989): The Quaternary terraces of the Lergue River and activity of the Cevennes fault in the lower Herault valley (Languedoc), southern France. - Z. Geomorph., **33**, n°4: 405-415.

BLOOMFIELD, K. (1975): A late-Quaternary monogenetic volcano field in central Mexico. - Geol. Rundsch., **64**: 476-597.

BRIAS, A., R. ARMIJO, T. WINTER, P. TAPPONNIER & A. HERBECQ (1990): Morphological evidence for Quaternary normal faulting and seismic hazard in the Eastern Pyrenees. - Annales Tectonicæ, **4**, n°1: 19-42.

BRUHN, R. L., P. R. GIBLER & W. T. PARRY (1987): Rupture characteristics of normal faults; An example from the Wasatch fault zone. - [In:] Coward, M. P., J. F. Dewey & P. L. Hancock (ed.) Continental extensional tectonics. Geol. Soc. London Special Publication, **28**: 337-353.

BUCKNAM, R. C. & R. E. ANDERSON (1979): Estimation of fault scarp ages from a scarp-height-slope-angle relationship. - Geology, **7**, n°1: 11-14.

BULL, W. B. (1977): The alluvial fan environment. - Prog. Phys. Geog., **1**: 222-270.

BULL, W. B. (1978): Geomorphic tectonic activity classes of the south front of the San Gabriel Mountains, CA. - Unpubl. Final Rep., U.S. Geol. Surv., Contract No. 14-08-0001-G-349, 59 p.

BULL, W. B. (1984): Tectonic geomorphology. - J. Geol. Educ., **32**: 310-324.

BULL, W. B. & L. D. McFADDEN (1977): Tectonic geomorphology north and south of the Garlock Fault, California. - [In:] Doehring, D.O. (ed.): Geomorphology in Arid Regions: 115-138, Proc. Eighth Annu. Geomorphol. Symp., State Univ. of New York, Binghamton.

BULL, W. B. & P. L. KNUEPFER (1987): Adjustments by the Charwell River, New Zealand, to uplift and climate change. - Geomorphology, **1**: 15-32.

BURTMAN, V. S. (1980): Faults of middle Asia. - Am. J. of Science, 280: 725-744)

BUWALDA, J. P. (1937): Shutter ridges, characteristic physiographic features of active faults. (abstract). - Geol. Soc. Am. Proceedings for 1986: 307.

CAMPOS-ENRIQUEZ, J. O., M.A. AROYO-ESQUIVEL & URRUTIA-FUCUGAUCHI (1990): Basement, Curie izotherme and shallow-crustal structure of the Trans-Mexican Volcanic Belt, from aeromagnetic data. - Tectonophysics, **172**:77-90.

CANON, P. J. (1976): Generation of explicit parameters for a quantitative geomorphic study of the Mill Creek drainage basin. - Oklahoma Geology Notes, **36**, n°1: 3-16.

CEBULL, S. E. & D. H. SHUBERT (1987): Mexican Volcanic Belt: An intraplate transform?. - Geofis. Int. Sp. Vol. on Mexican Volcanic Belt - Part 3A, **26**: 13.

CHINNERY, M. A. (1965): The vertical displacements associated with transcurrent faulting. - J. Geophys. Res., **70**, n°18: 4627-4632.

COSGROVE, J. & M. JONES (1991): Neotectonics and Resources, London, p. 1-6.

CRIPPEN, R. E. (1989): Development of remote sensing techniques for the investigation of neotectonic activity. Eastern transverse ranges and vicinity, southern California. - (abstract) Ph D thesis, Univ. of California, Santa Barbara, 324 p.

CRONE, A. J. & K. M. HALLER (1991): Segmentation and the coseismic behavior of Basin and Range normal faults - Examples from east-central Idaho and southwestern Montana. [In:] Hancock, P. L., R. S. Yeats, & D.J. Sanderson (eds): Characteristics of active faults. - J. Struct. Geol., **13**: 151-164.

CROWELL, J.C. (1974): Origin of late Cenozoic basins in southern California. - [In:] Dickinson, W. R. (ed.): Tectonics and sedimentation. Soc. Econ. Paleontologists and Mineralogists Spec. Pub., **22**: 190-204.

CURRANT, J. P. (1985): Princeples of remote sensing. - Longman, 189-221.

DEMANT, A. (1978): Características del Eje Volcánico Transmexicano y sus problemas de interpretación. - Univ. Nac. Autón. Méx. Rev. Inst. Geol., **2**: 172-187.

DEMANT, A. & C. ROBIN (1975): Las fases de vulcanismo en México: una síntesis en relación con la evolución geodinámica desde el Cretácico. Univ. Nac. Autón. Méx. Rev. Inst. Geol. **75**, n°1: 70-82.

DeMETS, C. & S. STEIN (1990): Present-day kinematics of the Rivera Plate and implications for tectonics in southwestern Mexico. - J. Geophys. Res., **95**, B13: 21931-21948.

dePOLO, C. M., D. G. CLARK, D. B. SLEMMONS & W. H. AYMARD (1989): Historical Basin and Range Province surface faulting and fault segmentation. - [In:] Schwartz, D. P. & R. H. Sibson (eds): Workshop on fault segmentation and controls of rupture initiation and termination: U.S. Geol. Surv. Open-File Report 89-315: 131-162.

DEWEY, J.W. & G. SUAREZ (1991): Seismotectonics of Middle America. [In:] Slemmons, D. B., E. R. Engdahl, M. D. Zoback & D. D., Blackwell (eds): Neotectonics of North America. Boulder, Colorado, Geol. Soc. Am., Decade Map Vol. 1: 309-313.

DOORNKAMP, J. C. (1986): Geomorphological approaches to the study of neotectonics. - J. Geol. Soc. (Lond.), **143**: 335-342.

DOORNKAMP, J.C & M. HAN (1985): Morphotectonic research in China an its application to earthquake prediction. - Prog Phys. Geog., **9**: 353-381.

DRURY, S. A. (1987): Image interpretation in geology. - Allen & Unwin, London, 64-104.

EMBLETON, C. (ed.) (1987): Neotectonics and Morphotectonics. - Z. Geomorph. Suppl., **63**: 1-7.

FERRIZ, H. (1985): Zoneamiento composicional mineralógico en los productos eruptivos del centro volcánico de los Humeros, Puebla, México. - Geofis. Int.Volúmen especial sobre el Cinturon Volcánico Mexicano (Ed. S.P. Verma), **24**, n°1: 97-157.

FLORES, T. (1920): Estudio geológico-minero de los distritos de El Oro y Tlalpujahua. - Bol. Inst. Geol. Méx., **43**: 85 p.

FORD, J. P., R. K. DORKA, R. E. CRIPPEN & R. G. BLOM (1989): JPL Finding Earth faults with TM Processing technique. - [In:] Eosat. Landsat users notes, **4**, n°4: 3-7.

FORD, J. P., R. K. DORKA, R. E. CRIPPEN & R. G. BLOM (1990): Undocumented faults in the Mojave desert, California, newly revealed on Landsat images. - Science, **248**, n°4958: 1000-1003.

FRIES, J., C.S. ROSS & A. OBREGÓN-PÉREZ (1977): Mezcla de vidrios en los derrames cineríticos Las Américas de la región de El Oro-Tlalpujahua, Estados de

México y Michoacán, parte centromeridional de México. - Univ. Nac. Autón. Méx. Bol. Inst. Geol., **70**: 1-84.

GASTIL, R. G. & W. JENSKY (1973): evidence for strike-slip displacement beneath the Trans-Mexican Volcanic Belt. Stanford Univ. Publ. Geol. Sci., **13**: 171-180.

GERASIMOV, I. P. (1946): Experience of the geomorphological interpretation of the geologic-structural scheme of the USSR. - Problems Phys. Geog. 12. (in Russian).

GERASIMOV, I. P. (1954): Application of geomorphological methods in seismotectonic reasearch (in the example of the Issik-Kul lake basin). - Problems of seismic prognosis, Works Geog. Fis. Inst. AS USSR, n° 25 (152), Moscow (in Russian).

GERASIMOV, I. P. & Y. A. MESHERIAKOV (1967): "Morphostructure" and "Morphosculpture" concepts and their use in morphostructural analysis. - [In:] Earth's relief. Nauka, Moscow. (in Russian).

GERASIMOV, I. P. & E. Ya. RANTSMAN (1973): Morphostructure of mountain countries'and their seismicity. - Geomorphologia, n° 1. (in Russian).

GHOSH, T. K. & S. VISWANATHAN (1991): Neotectonic analysis of Mendha river basin, Rajasthan, India. - Int. J. Remote Sens., **12**, n° 12: 2585-2595.

GILLESPIE, A. R. (1980): Digital techniques of image enhancement. - [In:] Siegal, B. S. & A. R. Gillespie (ed.): Remote sensing in Geology: 139-225, New York.

GVISHIANI, A. D. & A. SOLOVIEV (1981): About proximity of strong earthquake epicenters to intersections of morphostructural lineaments in the South America territory. - Computational Seismology, **13**: 45-50. (in Russian).

GVISHIANI, A. D., A. I. GORSHIKOV, V. G. KOSOBOKOV & E. Ya. RANTSMAN (1986): Morphological structures and earthquake sites in the Greater Caucasus. - Izvestiya, Acad. Sci. USSR, Physics of the Solid Earth, **22**, n° 9: 727-735. (in Russian).

GOMBERG, J. S. (1986): The structure of the crust and upper mantle of Mexico as inferred from seismic data. (abstract).- PhD thesis, Univ. Cal., San Diego, 214p.

HACK, J. T. (1973a): Stream-profiles analysis and stream gradient index. - J. Res. U.S. Geol. Surv., **1**: 421-429.

HACK, J. T. (1973b): Drainage adjustment in the Appalachians. - [In:] Morisawa, M. (ed.): Fluvial Geomorphology: 51-69, George Allen and Unwin, London.

HALLER, K. M., M. N. MACHETTE & R. L. DART (1993): Guidelines for U.S. Database and Map. Maps of Major Active Faults, Western Hemisphere International Lithosphere program (ILP) Project II-2. - U.S. Department of Interior, U.S. Geol. Surv., Open-File Reports 93-338: 1-2.

HAN, M. (1985): Tectonic geomorphology and its application to earthquake prediction in China. - [In:] Morisawa, M. & J.T. Hack (eds): Tectonic geomorphology: 367-386, Binghamton Geomorphology Symp., Boston-London.

HANCOCK, P.L. & A. A. BARKA (1987): Kinematic indicators on active normal faults in Western Turkey. - J. Struct. Geol., **9**: 573-584.

HANKS, T. C. & R. E. WALLACE (1985): Morphological analysis of the Lake Lahontan shoreline and Beach front fault scarps, Pershing Country, Nevada. - Bull. Seismol. Soc. Am., **75**: 835-846.

HARLAND, W. B. (1971): Tectonic transpression in Caledonian Spitsbergen. - Geological Magazine, **108**: 27-42.

HOOKE, R. L. (1972): Geomorphic evidence for Late Winsconsin and Holocene tectonic deformation, Death Valley California. - Geol. Soc. Am. Bull., **83**: 2073-2098.

HORST, S. K. (1985): Rates of change and degradation of hill slopes formed in uncosolidated materials: a morphometric approach to date Quaternary fault scarps in Western Utah, USA. - Z. Geomorph. N. F., **29**, n°3: 315-333.

HUMBOLDT, A. De (1808): Essai politique sur le Royaume de la Nouvelle Espagne: Paris. - F. Shoel, (translation into Spanish by V. G. Arano, 1822). - Porruas, México, 905 p.

JOHNSON, C. A. (1987): A study of neotectonics in central Mexico from Landsat thematic mapper imagery. - M.S. thesis. Univ. of Miami, Coral Gabbles, Florida, 112 p.

JOHNSON, C. A. & C. G. A. HARRISON (1989): Tectonics and volcanism in central Mexico: A Landsat Thematic Mapper Perspective. - Remote Sens. Environ., **28**: 273-286.

JOHNSON, C. A. & C. G. A. HARRISON (1990): Neotectonics in Central Mexico. - Phys. Earth Planet. Inter., **64**, n°2-4: 187-210.

KELLER, E. A. (1986): Investigation of active tectonics: use of surficial Earth processes. - [In:] Wallace, R. E. (eds): Active Tectonics. - Studies in Geophys., Nation. Acad. Press: 136-147, Washington, D.C.

KELLER, E. A., M. S. BONKOWSKI, R. J. KORSCH, & R. J. SHLEMON (1982): Tectonic geomorphology of the San Andreas Fault zone in the southern Indio Hills, Coachella Valley, California. - Geol. Soc. Am. Bull., **93**: 46-56.

KELLER, E. A. & T. K. ROCKWELL (1984): Tectonic geomorphology, Quaternary chronology and paleoseismicity. - [In:] Costa, J. E. & P.J. Fleisher (ed.): Development and applications of Geomorphology: 203-239, Springer, Berlin.

KOSTENKO, N.P. (1958): Geomorphological analisis of river valleys in mountain territories. In the example of Kyxistan. - Biul. Comis. AN USSR, n° 22. (in Russian).

KOSTENKO, N. P. (1980): Geomorfologia. - Isd. MGU, Moscow. (in Russian).

KOSTENKO, N. P., V. I. MAKAROV & L. I. (1972): Recent tectonics. - [In:] Geology USSR, 25, Kirgiskaya SSR, 2. Nedra, Moscow. (in Russian).

KRUMBEIN, W. C. (1951): Stratigraphy and sedimentation. - San Francisco, Freeman, 497 p.

LARSON, R. L. (1972): Bathymetry, magnetic anomalies, and plate tectonic history of the mouth of the Gulf of California. Geol. Soc. Am. Bull., **83**: 3345-3360.

LILLESAND, T. M. & R. W. KIEFER (1987): Remote sensing and image interpretation. - 2nd edition, Chichester Willey, New York, 721 p.

LO, C. P. (1986): Applied remote sensing: 164-185, Longman, New York.

LÓPEZ, G.G. (1984): Tectonic structure and development of the Trans-mexican volcanic belt. - PhD thesis, Moscow State University, Moscow. (in Russian).

LOUDERBACK, G. O. (1937): Characteristics of active faults in the Central Coast ranges of California, with application to the safety of dams. - Seismol. Soc. Am. Bull., **27,** n° 1: 1-27.

LOUDERBACK, G. O. (1950): Faults and engineering geology. - [In:] Paige, S. (chmn.): Application of Geology to engineering practice. Geol. Soc. Am., Berkey Volume: 125-150.

LUGO-HUBP, J., ORTIZ-PÉREZ, J.L. PALACIO-PRIETO & G. BOCCO-VERDINELLI (1985): Las zonas más activas en el Cinturón Volcánico Mexicano (Entre Michoacán y Tlaxcala). - Geofis. Int., Volúmen especial sobre el Cinturón Volcánico Mexicano (ed. S.P. Verma), **24**, n°1: 83-96.

LUHR, J.F., S. A. NELSON, J. F. ALLAN & I. S. E. CARMICHAEL (1984): Active rifting in southwestern Mexico: manifestations of an incipient eastward spreading-ridge jump. - Geology, **10**: 37-48.

MACHETTE, M. N., S. F. PERSONIUS, A. R. NELSON (1987): Quaternary geology along the Wasatch fault zone: segmentation, recent investigations and preliminary conclusions. [In:] Gori, P. L. & W. W. Hays (ed.) Assessment of Regional Earthquake Hazards and Risk along the Wasatch Front, Utah. - U.S. Geol. Surv. Open-file Rep. 87-585: A1-A72.

MARTIN del POZZO, A. M. (1982): Monogenetic Vulcanism in Sierra Chichinautzin, Mexico. - Bull. Volcanol., **45**, n°1: 9 - 24.

MARTÍNEZ-REYES, J. & A. F. NIETO-SAMANIEGO (1990): Efectos geológicos de la tectónica reciente en la parte central de México. - Univ. Nac. Autón. Méx., Rev. Inst. Geol., **9**, n°1: 33-50.

MAYER, L. (1984): Dating Quaternary fault scarps formed in alluvium using morphologic parameters. - Quaternary Research, **22**: 300-313.

MAYER, L. (1986): Tectonic geomorphology of escarpments and mountian fronts. - [In:] Active tectonics. Studies in Geophysics: 125-135, Nat. Acad. Press, Washington D. C.

MEDINA, M. F. (1985): On the volcanic activity and large earthquakes in Colima area, Mexico. - Geofis. Int., Special Volume on Mexican Volcanic Belt (ed. S.P. Verma), **24**, n°2: 701-708.

MENGES, C. M. (1987): Temporal and spatial segmentation of Pliocene-Quatenary fault rupture along the western Sangre de Cristo mountain front, northern New Mexico. - [In:] Crone, A. J. & E. M. Omdahl (eds): Proceedings of Conference 39; Directions in Paleosismology: U.S. Geol. Soc. Open-File Reports 87-673: 203-222.

MENGES, C. M. (1990): Late Quaternary fault scarps, mountain-front landforms, and Pliocene-Quaternary segmentation on the range-boounding fault zone, Sangre de Cristo Mountains, New Mexico. - [In:] Krinitzsky, E. L. & D. B. Slemmons: Neotectonics in earthquake evaluation: Boulder, Colorado, Geol. Soc. Am. Reviews in Engineering Geology, **8**: 131-156.

MERRITS, D. & M. ELLIS (eds) (1992): Chapman Conference on Tectonics and Topography. - Am. Geophys. Union, Snowbird, UTAH.

MESHERIAKOV, Y. A. (1965): Structural geomorphology of basin territories. - Nauka, Moscow. (in Russian).
MESHERIAKOV, Y. A. (1972): Relief USSR. (Morphosctructure and morphosculpture). Misl, Moscow. (in Russian).
MINSTER, J. B. & J. H. JORDAN (1978): Present-day plate motions: A summary. - J. Geophys. Res., **83**: 5331-5354.
MOLNAR, P. AND L.R. SYKES (1969): Tectonics of the Caribbean and Middle America regions from focal mechanisms and seismicity. - Geol. Soc. Am. Bull., **80**: 1639-1684.
MOOSER, F. (1969): The Mexican Volcanic belt - structure and development. - Pan-Am. symp. Upper mantle., México, **2**: 15-22.
MOOSER, F. (1972): The Mexican Volcanic Belt: Structure and tectonics. - Geofis. Int., **12**:55-70.
MOOSER, F. & M. MALDONADO (1961): Pene-contemporaneous tectonics along the Mexican Pacific coast. - Geofis. Int., **1**: 1-20.
MOOSER, F. & M. T. RAMÍREZ-HERRERA (1989): Faja Volcánica Transmexicana: Morfoestructura, tectónica y vulcanotectónica. - Bol. Soc. Geol. Mex., T. XLVIII-2: 75-85.
MOOSER, F., A. MONTIEL & A. ZUÑIGA (1992): Nuevo mapa geológico del sur-poniente del Valle de México. - Simposio, experiencias geotécnicas en la zona Poniente del Valle de México, 5-17.
MORISAWA, M. & J. T. HACK (eds) (1985): Teconic Geomorphology. - Binghamton Geomorphology Symp., Boston-London, 390 p.
MÖRNER, N. A., L. A. OWEN, I. STEWART & C. VITA-FINZI (eds) (1992): Neotectonics - recent advances. Abstract volume. Quat. Res. Ass. Cambridge, 80 p.
NASH, D. B (1986): Morphologic dating and modelling degradation of fault scarps. - [In:] Active tectonics. Studies in Geophysics:181-194, Nat. Acad. Press, Washington D. C.
NIXON, G. T. (1982): The relationship between Quaternary volcanism in central Mexico and the seismicity and the structure of subducted ocean lithosphere. - Geol. Soc. Am. Bull., **93**: 514 523.
NIXON, G. T., A. DEMANT, R. L. ARMSTRONG & J. E. HARAKAL (1987): K-Ar nad geologic data bearing on the age and evolution of the Trans-Mexican Volcanic Belt. - Geofis. Int., Special Volume on Mexican Volcanic Belt , **26**, 1: 109-158.
NOBLE, L. F. (1927): San Andreas rift and some other active faults in the desert region of southern California. - Seismol. Soc. Am. Bull., **17**: 25-39.
NOBLE, L. F. (1932): The San Andreas rift in the desert region of southeastern California. - Carneige Inst. Washington Yearbook, **31**: 355-372.
OAKES, G. (1988): A system for the recognition of geological lineaments in remotely sensed imagery. - [In:] Kittler, J. (ed.): International Conference in Pattern recognition 4th, 1988. Cambridge, 646-655.
ORLOVA, A. V. (1975): Block-structures and relief. - Nedra, Moscow. (in Russian).

ORLOVA, A. V. (1980): The moving mosaic of the Planet. - Niedra, Moscow. (in Russian).

ORTIZ-P, M. A. & G. BOCCO-VERDINELLI (1989): Análisis morfotectónico de las depresiones de Ixtlahuaca y Toluca, México. - Geofis. Int., **28**, 3: 507-530.

ORTIZ-PÉREZ, M.A., J. J. ZAMORANO-OROZCO, J. .R. HERNÁNDEZ-SANTANA & J. L. PALACIO-PRIETO (1993): Evidencias geomorfológicas de deformación transcurrente en el complejo volcánico de Temascalcingo, Mexico. - Geofis. Int., (in press).

OTA, Y. (1985): Marine terraces and active faults in Japan with special reference to coseismic events. - [In:] Morisawa, M. & J.T. Hack (eds): Tectonic geomorphology: 345-366, Binghamton Geomorphology Symp., Boston-London.

OUCHI, S. (1985); Response of alluvial rivers to slow active tectonic movement. - Geol. Soc. Am. Bull., **96**, 504-515.

PANIZZA, M. (1991): Geomorphology and seismic risk. - Earth Sci. Rev., **31**: 11-20.

PASQUARÉ, G., L. FERRARI, V. PERAZZOLI, M. TIBERI, & F. TURCHETTI (1987a): Morphological and structural analysis of the central sector of the Transmexican Volcanic Belt. Geofis. - Geofis. Int., Special volume on Mexican Volcanic Belt, **26**, n°2: 177-193.

PASQUARÉ, G., L. VEZZOLI, A. ZANCHI (1987b):Morphological and Structural model of the Mexican Volcanic Belt. -Geofis. Int., Special volume on Mexican Volcanic Belt, **26**, n°2: 159-176.

PASQUARÉ,G., H. GARDUÑO, A. TIBALDI & M. FERRARI (1988): Stress pattern evolution in central sector of the Mexican Volcanic Belt. - Tectonophysics, **146**: 353-364.

RABIE, S. I. & A. A. AMMAR (1990): Pattern of the main tectonic trends from remote geophysics, geological and satellite imagery, Central eastern desert, Egypt. - Int. J. of Remote sensing, **11**, n°4: 669-638.

RAMÍREZ-HERRERA, M. T. (1990): Análisis morfoestructural de la Faja Volcánica Transmexicana (centro-oriente). - M.Sc. thesis. Univ. Nac. Autón. Méx., México D.F., 86 p.

RANTSMAN, E. Ya. (1979): Places of earthquakes and morphostructure of mountain territories. - Nauka, Moscow, 170 p. (in Russian).

ROCKWELL, T.K., E.A. KELLER & D. L. JOHNSON (1985): Tectonic geomorphology of alluvial fans and mountain fronts near Ventura, California. - [In:] Morisawa, M. & J.T. Hack (eds): Tectonic geomorphology: 183-207, Binghamton Geomorphology Symp., Boston-London.

SÁNCHEZ-RUBIO, G. (1984): Cenozoic volcanism in the Toluca - Amealco region, central México. - M.Phil. thesis. Univ. of London, Imp. Coll. of Sci. and Technol., 275 p.

SANDERSON, D. & J. GUTMAINS (eds) (1991): Satellites and neotectonics. - Mtg. at Geol. Dept. Southampton, Abstracts with Program,. Geol. Remote Sens. Group.

SCHULTZ, J. R. & A. B. CLEAVES (1955): Geology in engineering. John Willey & Sons, Inc., New York, N. Y., 592 p.

SCHUMM, S. A. (1986): Alluvial river response to active tectonics. - [In:] Active tectonics. Studies in Geophysics: 80-94, Nat. Acad. Press, Washington D. C.
SCHWARTZ, D. P. & K. J. COPPERSMITH (1984): Fault behavior and characteristic earthquakes; Examples from the Wasatch and San Andreas fault zones. - J. Geophys. Res., **89**, n° B7: 5681-5698.
SCHWARTZ, D. P. & K. J. COPPERSMITH (1986): Seismic hazards; New trends in analysis using geologic data. [In:] Active tectonics. Studies in Geophysics: 215-230, National Academy Press, Washington D. C.
SIEBE, C., J. C. KOMOROWSKI & M. F. SHERIDAN (1988): Conical hills at Jocotitlán volcano, central Mexico: Landmarks of a tectonically controlled debris avalanche deposit. (abstract). - EOS, Trans. AGU, **69**, n°44: 1486.
SIEH, K. E. (1984): Lateral offsets and revised dates of large earthquakes at Pallett Creek. California. - J. Geophys. Res., **89**: 7641-7670.
SIEH, K. E. & R. H. JAHNS (1984): Holocene activity on the San Andreas fault at Wallace Creek, California. - Geol. Soc. Am. Bull., **95**, n° 8 883-896.
SILVA-MORA, L. (1979): Contribution a la connaissance de l'axe volcanique Transmexicain: Etude géologique et pétrologique des laves du Michoacán Oriental. - Thèse de Docteur Ingénieur, part 1, Univ. de Droit, d'Econ. et des Sci. d'Aix-Marseille, France, 145 p.
SIMONOV, Y. G. (1972): Regional geomorphological analysis. Isd-vo MGU, Moscow. (in Russian).
SLEMMONS, D. B. & R. McKINNEY (1977): Definition of "active fault". - U.S. Army Engineer Waterways Experiment Station, Soils and Pavements Laboratory, Miscellaneous Papers-77-8, Vicksburg, Miss, 22 p.
SLEMMONS, D. B., E. R. ENGDAHL, M. D. ZOBACK & D. D. BLACKWELL (eds) (1991): Neotectonics of North America. - Geol. Soc. Am., Decade Map, Vol. I, Boulder, Colorado.
SOLER, A. A. M. (1990): Paleomagnetismo de la región de Acambay, Faja Volcánica Transmexicana. - M.S. thesis. Univ. Nac. Autón. Méx., México, D.F., 110 p.
STEWART, I. & P. L. Hancock (1991): Scales of structural heterogeneity within neotectonic normal fault zones in the Aegean region. - J. Struct. Geol., **13**, n°2: 191-204.
STEWART, I., C. VITA-FINZI, & L.A. OWEN (ed.): Neotectonics and active faulting: papers presented at the International Conference on Neotectonics - Recent Advances, London, June 1992. - Z. Geomorph., 328 p.
SUÁREZ, G. & L. PONCE (1986): Intraplate seismicity and crustal deformation in central Mexico (abstract). Eos: Trans. of the Am. Geophys. Union, **67**: 1114.
SUÁREZ, G. & S. K. SINGH (1986): Tectonic interpretation of the Trans-Mexican volcanic belt. - Discussion. Tectonophysics, **127**: 155-160.
SUMMERFIELD, M. A. (1987): Neotectonics and landform genesis. - Prog. Phys.Geog., **11**: 384-397.
SUMMERFIELD, M. A. (1991): Global Geomorphology. - Longman, Singapore, 537p.

SUTER, M. (1991): State of stress and active deformation in Mexico and western Central America. - [In:] Slemmons, D. B., E.R. Engdahl, M. D. Zoback, D.D. Blackwell (eds): Neotectonics of North America, Boulder, Colo., Geol. Soc. Am., Decade Map Vol. 1: 401-421.

SUTER, M., G. J. AGUIRRE, C. SIEBE, O. QUINTERO & J.C. KOMOROWSKI (1991): Volcanism and active faulting in the central part of the Trans-Mexican volcanic belt. [In:] Walawender, M.J. & Hanan, B.B. (ed.): Geological excursions in Southern California and Mexico. Guideb. An. Mtg. Geol. Soc. Am. San Diego, Calif. Oct. 21-24, 1991: 224-243.

SUTER, M., O. QUINTERO & C.A. JOHNSON (1992): Active faults and State of Stress in the Central Part of the Trans-Mexican Volcanic Belt, Mexico. Part 1: The Venta de Bravo fault. - J. Geophys. Res., **97**, n°B8: 11983-11993.

SYLVESTER, A. G. (1988): Strike-slip faults. - Geol. Soc. Am. Bull., **100**: 1666-1703.

TAPPONNIER, P. (1991): Rates of Holocene slip and recurrence of large earthquakes on active faults: the use of spot panchromatic scenes and quantitative geomorphology. (abstract). - [In:] Sanderson D. & J. Gutmains (ed.): Satellites and neotectonics. - Mtg. at Geol. Dept. Southampton, Abstr. with Program,. Geol. Remote Sens. Group.

THORNBURY, W. D. (1969): Principles of Geomorphology. - 2nd edition, John Wiley and Sons, Inc., 594 p.

TUTKUN, S. Z. & P. L. HANCOCK (1990): Tectonic landforms expressing strain at the Karliova continental triple junction (E Turkey). - Annales Tectonicæ, **4**, n°2: 182-195.

UFIMTSEV, G. F. & XUDIAKOV, G. I. (1976): About geometry, regionalisation, and terminology of geomorphosctructure. Problems of endogenic landform formation. - Nauka, Moscow. (in Russian).

URBINA, F. & H. CAMACHO (1913): La zona megaseismica Acambay-Tixmadeje, Estado de México, conmovida el 19 de noviembre de 1912. - Bol. Inst. Geol. Méx., **32**: 125 p.

URRUTIA-FUCUGAUCHI, J. & H. BÖHNEL (1988): Tectonics along the Trans-Mexican volcanic belt according to paleomagnetic data. - Phys. Earth Planet. Inter., **52**: 320-329.

VENEGAS, S. S., J. J. HERRERA & R. MACIEL (1985): Algunas características de la Faja Volcánica Mexicana y de sus recursos geotérmicos. - Geofis. Int. Volúmen especial sobre el Cinturón Volcánico Mexicano (ed. S.P. Verma), **24**, n°1: 47-81.

VERGELY, P. & H. ZADEH-KABIR (1988): Comparative photointerpretation study of the fracturation of the Largentiereles vans area (Languedoc, France), using aerial photographies, satellite and radar images. - Bull. Soc. Geol. de France: **4**, n°2: 303-314.

VERMA, S. P. (1985): Mexican Volcanic Belt (Preface). - Geofis. Int., Special volume on Mexican Volcanic Belt, **24**, n°1: 7-19.

VERMA, S. P. (1987): Mexican Volcanic belt: Present state of knowledge and unsolved problems. Geofis. Int., Special volume on Mexican Volcanic Belt, **26**, n°3B: 309-340.

VITA-FINZI, C. (1986): Recent earth movements: an introduction to neotectonics. London, 226p.

VITA-FINZI, C. (1991): Satellites and deformation chronologies (abstract). - [In:] Sanderson D. & J. Gutmains (ed.): Satellites and neotectonics. - Mtg. at Geol. Dept. Southampton, Abstracts with Program,. Geol. Remote Sens. Group.

WALLACE, R.E. (1968): Notes on stream channels offset by the San Andreas fault, Southern Coast Ranges, California. - [In:] Dickinson, W. R. and A. Grantz (ed.): Proceedings of the Conference of geologic problems of the San Andreas fault system. Stanford Univ. Pub. in the Geol. Sci., **11**: 374.

WALLACE, R.E. (1976): The Talas-Fergana fault. Kiromiz and Kazakh, USSR. - Earthquake Inform. Bull., **8**: 4-13.

WALLACE, R.E. (1977): Profiles and ages of young fault scarps, North-central Nevada. - Geol. Soc. Am. Bull., **88**: 1267-1281.

WELDON, R. J. & K. E. SIEH (1985): Holocene rate of slip and tentative recurrence interval for large earthquakes on the San Andreas fault, Cajon Pass, southern California. - Geol. Soc. Am. Bull., **96**: 793-812.

WELLS, S.G., T. F. BULLARD, C. M. MENGES, P. G. DRAKE, P. A. KARAS, K. I. KELSON, J. B. RITTER & J. R. WESLING (1988): Regional variations in tectonic geomorphology along a segmented convergent plate boundary, Pacific coast of Costa Rica. - Geomorphology, **1**: 239-265.

WHEELER, R. L. (1987): Boundaries between segments of normal faults: criteria for recognition and interpreation. [In:] Crone, A. J. & E. M. Omdahl (eds): Proceedings of Conference 39; Directions in Paleosismology: U.S. Geol. Soc. Open-File Reports 87-673: 385-398.

WHEELER, R. L. & K. B. KRYSTINIK (1987): Persistent and nonpersistent segmentation of the Wasatch fault zone, Utah. - Geol. Soc. Am. Abstracts with programs, **19**: 342.

WILLIS, B. (1923): A fault map of California. - Seismol. Soc. Am. Bull., **13**: 1-12.

WOOD, H. O. (1916): The earthquake problem in the western United States. Seismol. Soc. Am. Bull., **6**: 181-217.

XIE, G. L. (1991): Analysis of some characteristics of the fault activities in Eastern China by satelllite images. - Acta Geol. Sin., **4**, n°4: 357-369.

YAMAMOTO, J. & R. MOTA (1991): Reporte del monitoreo sísmico realizado en laregión de Maravatío-Acambay durante el periodo marzo de 1989 y agosto-septiembre de 1990. - Geos. Bol. Union Geofis. Mex., **11**, n°4: 18-21.

Appendix 1:

Published papers

Ramírez-Herrera, M.T., M. A. Summerfield & M. A. Ortiz-Pérez (1994): Tectonic geomorphology of the Acambay graben, Mexican Volcanic Belt. - Z. Geomorph. N. F., 38, 2: 151-168.

KEY

Landforms due to endogenic forces

A) Tectonic forms

1) Quaternary normal faults

2) Quaternary faults with left lateral displacement

3) Inferred faults

4) Fault scarps

5) Linear ridges

6) Compression ridges

7) Shutter ridges

8) Offset drainage

9) Triangular facets

10) Sag ponds

B) Volcanic forms

1) Volcano

1.1) Lava dome

1.2) Lava cone

1.3) Scoria cone

1.4) Multiple cones or hummocks

2) Lava flow

3) Lava tongue

4) Lava front

5) Lava surface covered with pyroclastic material

6) Remnants of volcano slopes

7) Volcanic plateau

8) Volcanic mountains

Landforms due to exogenic forces

C) Denudative forms

1) Slopes of fault line scarps

2) Piedmonts

3) Remnants of late mature relief (resistent ridges consisting of crystaline rocks)

4) Coluvial fans

D) Fluvial forms

1) River bed of permanent streams

a) cut in alluvium

b) cut in rock

2) Edges and slopes of river terraces

3) V-shaped valleys

Accumulative fluvial forms

1) Fluvio-lacustrine plains

2) Alluvial terraces plain

3) Alluvial fan

Fluvial denudational forms

1) Gullies

2) Canyons

3) Erosion cirque

Water reservoir

Lake

Village

MARÍA TERESA RAMÍREZ-H 1994

Fig. 4.2 (a) Geomorphological map of the Acambay graben.

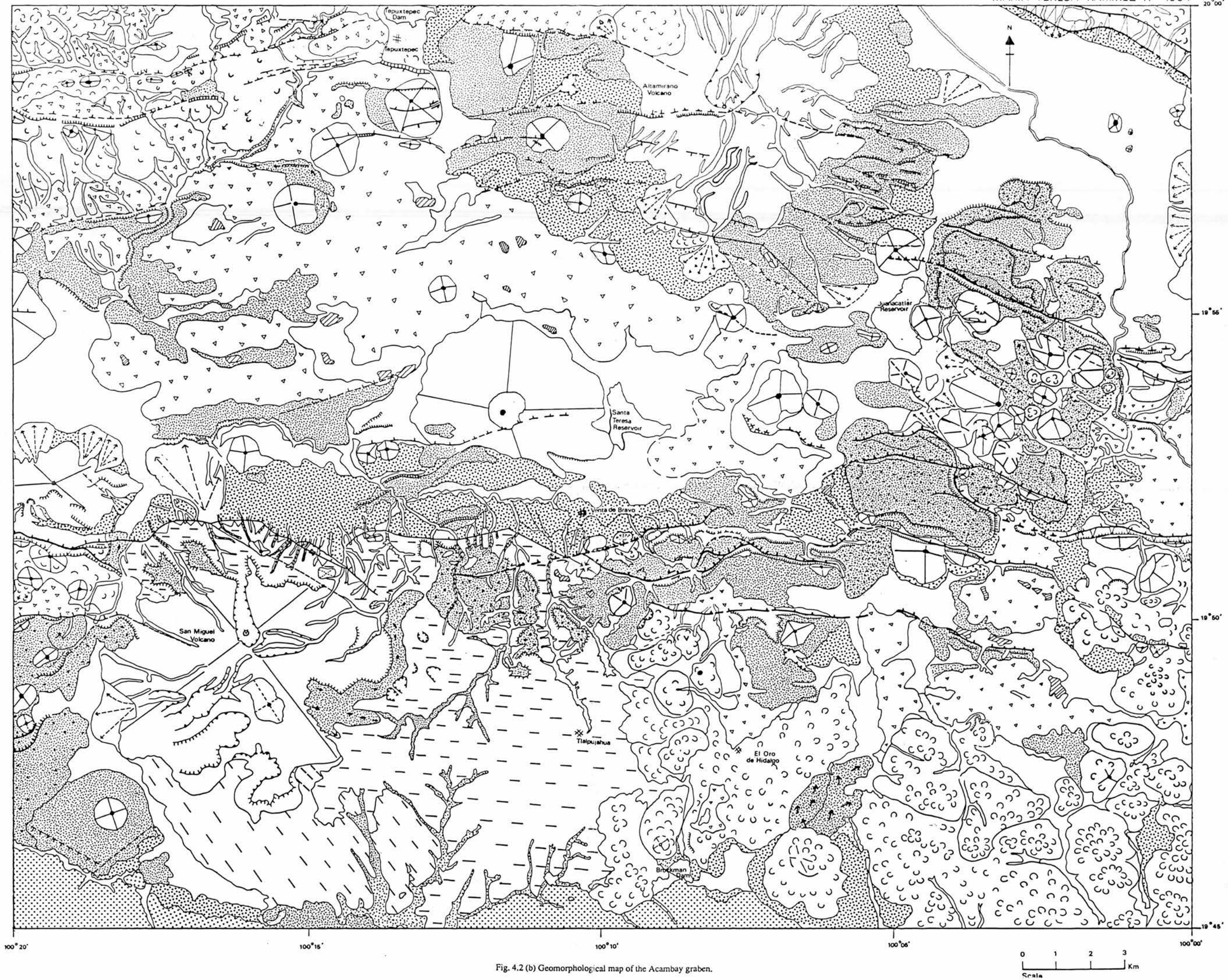

Fig. 4.2 (b) Geomorphological map of the Acambay graben.

MARÍA TERESA RAMÍREZ-H 1994

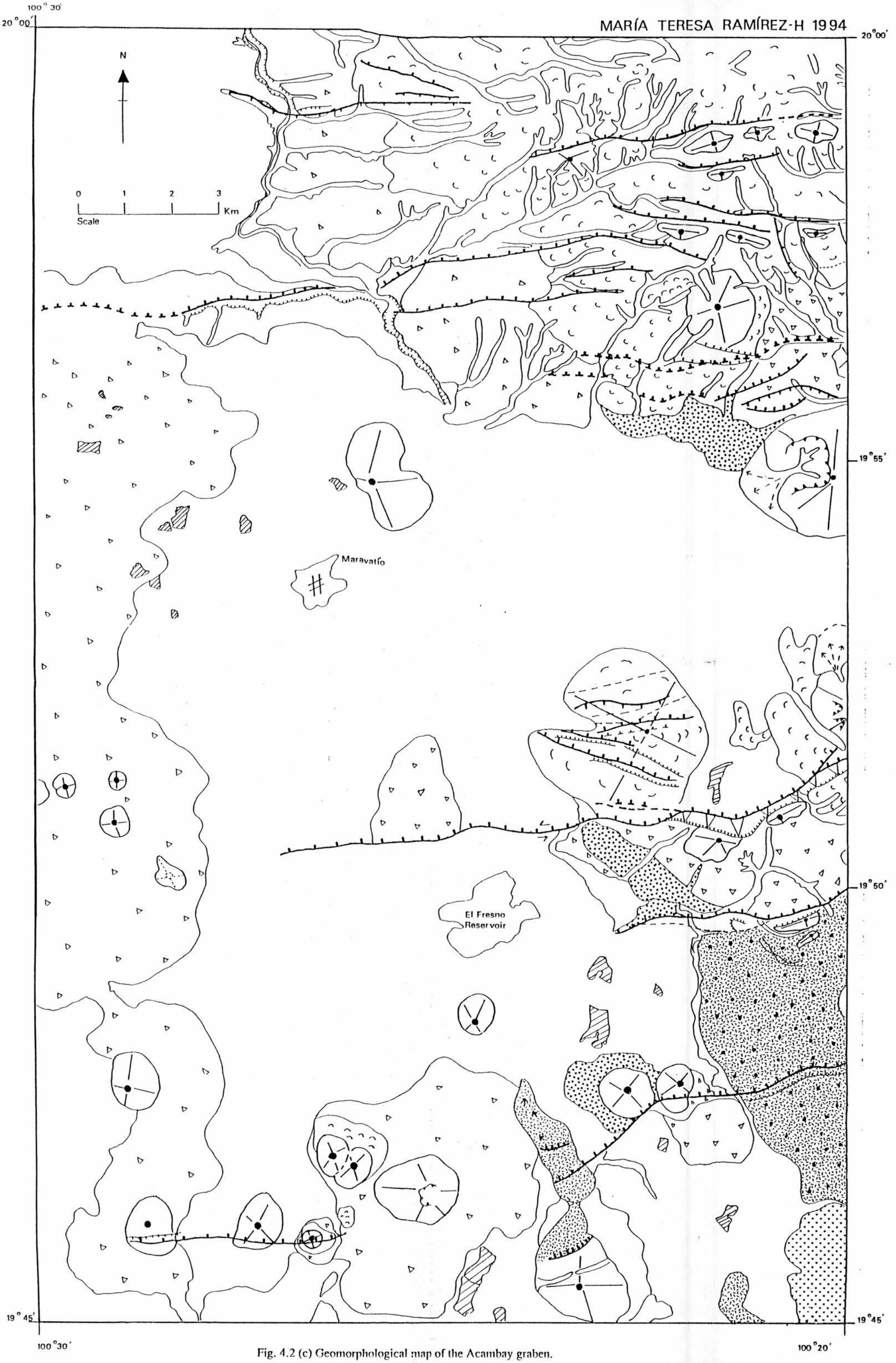

Fig. 4.2 (c) Geomorphological map of the Acambay graben.

Z. Geomorph. N. F.	38	2	151–168	Berlin · Stuttgart	Juni 1994

Tectonic geomorphology of the Acambay graben, Mexican Volcanic Belt

by

M. T. Ramírez-Herrera, Edinburgh, M. A. Summerfield, Edinburgh
and M. A. Ortiz-Pérez, Mexico City
and

with 9 figures

Summary. Tectonics and volcanism in the Mexican Volcanic Belt (MVB) are related to the subduction of the Cocos Plate beneath southern Mexico. Analysis of Landsat imagery employing digital enhancement shows that the Acambay graben located in the central part of the MVB is characterised by Quaternary, generally east-west trending, seismically active normal faults.

Fault system associated with the graben can be categorised on the basis of the morphological features associated with them. Five systems are identified: 1) the Acambay-Tixmadejé faults, 2) the Tepuxtepec faults on the northern flank of the graben, 3) the Pastores fault, 4) the Venta de Bravo faults on the southern flank of the graben, and 5) the Temascalcingo faults located in the centre of the graben. A range of geomorphological evidence indicates neotectonic activity in the Acambay graben. Prominent fault scarps and triangular facets demonstrate normal faulting, while offset drainage, sag ponds and pull-apart basins together with linear and compression ridges confirm an important left-lateral component to fault displacement, a motion which is accordant with regional left-lateral shear along the MVB.

Zusammenfassung. Tektonik und Vulkanismus im vulkanischen Bogen von Mexico (MVB) stehen im Zusammenhang mit der Subduktion der Cocos Platte unter das südliche Mexiko. Gestützt auf digitale Auswertung von Landsat Aufnahmen wird deutlich, daß das Grabensystem von Acambay, welches im zentralen Teil des MVB liegt, von ost-west streichenden quartären Verwerfungen gekennzeichnet ist, welche heute noch seismisch aktiv sind.

Die mit dem Graben verbundenen Verwerfungssysteme können anhand ihrer morphologischen Formen klassifiziert werden. Fünf Systeme können unterschieden werden: 1) die Acambay-Tixmadeje Verwerfungen, 2) die Tepuxtepec Verwerfungen am nördlichen Grabenrand, 3) die Pastores Verwerfung, 4) die Venta de Bravo Verwerfungen am südlichen Rand des Grabens und 5) die Temascalcingo Verwerfungen im Zentrum des Grabens. Eine Reihe morphologischer Belege weist auf eine Neotektonik im Acambay Graben hin. Vorspringende Bruchwände und dreiecksförmige Außenhänge belegen eine normale Verstellung. Versetzte Flußnetze, eingesunkene Seen und verzogene Becken belegen zusammen mit linearen Aufschiebungsketten eine berächtliche Horizontalverschiebung, welche im Einklang mit einer allgemeinen regionalen Horizontalverschiebung entlang des MVB steht.

0372-8854/94/0151 $ 4.50

Résumé. La tectonique et le volcanisme de la Mexican Volcanic Belt (MVB) sont associés à la subduction de la plaque des Cocos sous le Mexique méridional. L'analyse d'images Landsat, accompagnée d'une digitalisation de l'information, montre que le graben d'Acambay situé dans la partie centrale de la MVB est caractérisé par des failles normales d'âge quaternaire, généralement orientées E–W et sismiquement actives.

Les systèmes de failles associés au grabern peuvent être caractérisés par leurs expressions géomorphologiques. Cinq systèmes ont été identifiés: 1) les failles d'Acambay-Tixmadejé, 2) les failles de Tepuxtepec sur le flanc septentrional du graben, 3) la faille de Pastores, 4) les failles de Venta de Bravo sur le flanc méridional du graben, et 5) les failles de Temascalcingo situées au centre du graben.

Une série ded preuves géomorphologiques indique une activité néotectonique dans le graben d'Acambay. De vigoureux escarpements de failles et des facettes triangulaires démontrent le jeu normal de failles, tandis que des décalages de cours d'eau, des bassins en pullapart, et des chaînons de compression confirment une importante composante latérale senestre, déplacement qui est en accord avec un cisaillement régional senestre le long de la MVB.

1 *Introduction*

Tectonic geomorphology (often called morphotectonics) is concerned with the analysis of the relationship between tectonics and landforms irrespective of scale. Tectonic geomorphology is not only concerned with the macro-scale features of the earth's surface and longgeological timespans, but also with the more detailed effects of tectonic processes in recent geological time or even at the present day (Embleton 1987). Recent deformation is often described as neotectonic, although there is no general agreement as to the time scale to which this term refers. In this paper the term neotectonics will be used to refer to tectonic activity during the Neogene and Quaternary.

Modern tectonic geomorphology has applied different approaches to solve the problem of the relationship between neotectonics and landforms at different scales. Examples of the study of neotectonics emplyoing geomorphological evidence at micro- and meso-scales have been summarised by various workers (Morisawa & Hack 1985, Doornkamp 1986, Summerfield 1987, Embleton 1987, Sanderson & Gutmanis 1991, Mörner et al. 1992). The use of satellite and radar imagery has been of great value in assessing the tectonic regime of large areas experiencing neotectonic activity (e.g. Sanderson & Gutmains 1991). Meso-scale morphologic evidence such as lineaments, scarps, triangular facets, straight stream segments and offset drainage are well defined on high-resolution satellite imagery (Armijo et al. 1986, Tapponnier 1991, Brias et al. 1990, Johnson 1987, 1989, Ghosh & Viswanathan 1991). Since tectoniclandform trends provide evidence of the characteristics of the tectonic regime of a region, landforms indicative of neotectonic activity can be used in assessments of the spatial and temporal occurrence of seismicity (Weldon & Sieh 1985, Ota 1985, Doornkamp & Han 1985, Han 1985, Vita-Finzi 1991). However, little of this research has been focused on earthquake risk, most previous work being concerned with the post-seismic effects of earthquakes (Cosgrove & Mervin 1992).

Despite a number of case studies of the large-scale tectonics of central and southern Mexico, morphotectonic approaches have been little used and their full potential has yet to be realised. Although there have been local studies of the morphostructures along the Mexican Volcanic Belt (López 1984, Pasquaré 1987, Ortiz

& Bocco 1989, Ramírez 1990) and meso-scale features, such as lineaments, detected on satellite imagery (Pasquaré et al. 1987, Johnson 1987, Johnson & Harrison 1989, 1990, Martínez & Nieto-Samaniego 1990), an integrated meso- and microscale morphotectonic approach has yet to be applied to an understanding of the neotectonic regime in southern Mexico.

The specific aim of the research reported here is the identification of geomorphological evidence indicative of neotectonic activity in the Acambay graben, a major structure in the central part of the Mexican Volcanic Belt, and an assessment of its relationship to regional scale geodynamics. Relevant geomorphological data were derived from detailed field mapping in conjunction with remote sensing analysis employing large-scale aerial photography and digitally-enhanced Landsat imagery. The Acambay graben, as well as the Mexican Volcanic Belt as a whole, have been the subject of a number of geological and geophysical studies in recent years as a consequence of their potential mineral and geothermal resources and the volcanic and the seismic hazards posed to several major centres of population and industry in the region (Urbina & Camacho 1913, Astiz 1980, 1986, Verma 1985, Lugo-Hubp et al. 1985, Ferriz 1985, Medina 1985, Venegas et al. 1985, Urrutia-Fucugauchi & Böhnel 1988, Martínez & Nieto 1990). There has, however, been little application of geomorphological techniques to the problem of the nature of recent seismic activity, and the relationship between the genesis of micro- to meso-scale tectonic landforms and the regional geodynamic setting.

2 *Tectonic and structural setting*

The Mexican Volcanic Belt is a 20–150 km broad structure extending for around 1000 km in an approximately east-west direction from the Pacific Ocean to the Gulf of Mexico (fig. 1). It is an active, mostly calc-alkaline volcanic chain (Verma 1987), which is genetically associated with subduction of the Cocos plate beneath the North American plate along the Middle American trench. Although the Mexican Volcanic Belt is clearly a component of the Circum-Pacific volcanic chain, its long axis is not parallel to the adjacent subduction zone (Middle American trench) but rather is aligned at an angle of about 15–20° with respect to it (Molnar & Sykes 1969). This difference in orientation may be due in part to the control exerted by fault and fracture systems on the location of volcanism in the central and eastern parts of the Mexican Volcanic Belt (Johnson 1989, Urrutia & Böhnel 1988). Plate convergence, which seems to have been the dominant tectonic factor in southern Mexico since the Late Jurassic, appears to have resulted in the activation of a transtensive, left-lateral fault system along the Mexican Volcanic Belt (Urrutia & Böhnel 1988).

Central part of the Mexican Volcanic Belt. The central part of the Mexican Volcanic Belt is characterised by generally east-west striking faults which form a series of *en echelon* graben along its length. This structural style, which is indicative of an extensional regime, is clearly related to the volcanism and regional scale tectonics of the area. South-east trending lineaments in the Mexican Volcanic Belt's central section are thought to be older reactivated structures related to the subduction of the Farallon Plate (Mooser & Ramírez 1989). It has been proposed by Mooser & Ramírez (1989) that the Acambay graben, along with the other series of *en echelon* graben and

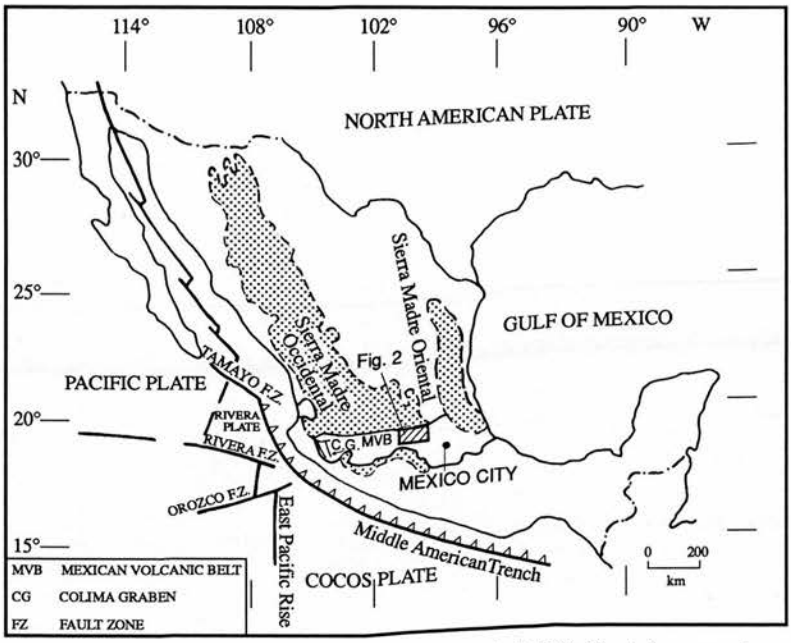

Fig. 1. Tectonic setting of the Mexican Volcanic Belt (MVB). Shaded square shows the location of the Acambay graben.

horsts of the Mexican Volcanic Belt, is the product of episodically active left-lateral shear in the upper brittle section of the crust generated in the Middle American trench and the newly developing Colima graben to the west (Luhr et al. 1985).

Volcanism in the central and eastern part of the Mexican Volcanic Belt appears to be controlled by structures produced by the differential movement of crustal blocks over a magma source in response to large-scale left-lateral shear (fig. 1) (Johnson 1987, Urrutia & Böhnel 1988). On the basis of studies of focal mechanisms, volcanic alignments and the inversion of fault striations Suter (1990) has proposed that the maximum horizontal stress is oblique to the strike of the presently active faults and this accounts for the small component of left-lateral strike-slip observed along them in the central part of the Mexican Volcanic Belt. In this area the maximum horizontal stress is north-south, although there is a gradual transition to an ESE-WNW trend in the eastern part of belt. The upper crust of the central part of the Mexican Volcanic Belt is characterised by a static stress field with $S_V > S_{ENE} > S_{NNW}$ (Suter et al. 1992).

In a detailed study of the stress field of the central part of the Mexican Volcanic Belt Suter et al. (1992) found a minor left-lateral strike-slip component, while on the basis of a fault plane solution for the February 22, 1979 earthquake which occurred on the Venta de Bravo fault Astiz (1980) inferred mainly normal faulting with a left-lateral component. Further evidence bearing on the nature of neotectonic activity

comes from paleomagnetic data which reveal an anti-clockwise rotation in the Acambay graben region (SOLER 1990). This form of displacement is probably associated with block rotations arising from a left-lateral component of crustal movement. SOLER (1990) and several other workers have also proposed normal faulting with a left-lateral strike-slip component as the main neotectonic process in the central part of the Mexican Volcanic Belt (ASTIZ 1980, JOHNSON, 1987, JOHNSON & HARRISON 1990, MOOSER 1969, MOOSER & RAMÍREZ 1989, SUTER 1990, SUTER et al. 1991).

The Acambay graben is located in the central part of the Mexican Volcanic Belt between latitude 19°45′–20°00′ north and longitude 99° 45′–100° 25′ west (fig. 1). Analysis of aerial photographs in conjunction with digitally-enhanced Landsat imagery has revealed east-west trending faults of apparent Quaternary age which give rise to pronounced scarps over a distance of around 70 km. Continuing tectonic activity in the Acambay graben is confirmed by recent well-documented seismic episodes such as the Acambay event of 1912 (URBINA & CAMACHO 1913) and the Venta de Bravo event of 1979 (ASTIZ 1980) the former causing significant vertical displacements along faults flanking the graben.

3 *Seismicity*

Earthquakes have been recorded on several of the faults in the region during historic time. For instance, localised seismic events in the Tlalpujaha-Maravatío region are known from 1734–1735, 1853–1854 and 1979. More than 30 individual shocks were felt in Tlalpujahua between November 1734 and March 1735, while the events of 1853–1854 began in December 1853 and lasted until March 1854 with major earthquakes occurring on the 13 January and 26 February, 1854 (OROZCO & BERRA 1887, based on the newspaper reports in Diario Oficial of January 25, 1854, and siglo XIX of March 10, 1854, cited in SUTER et al. 1992). The Ms = 6.9 Acambay event of 19 November 1912 generated vertical displacements of up to 0.5 m (URBINA & CAMACHO 1913), while the most recent significant seismic activity occurred in 1979. This involved approximately 90 individual events extending over several months from February to June with the main shock (the mb = 5.3 Venta de Bravo event) occurring near the beginning of the sequence on the 22 February (ASTIZ 1980). The location of the 1979 events was based on the instrumental record of 14 stations in central and southern Mexico (ASTIZ 1980). The focus of the main shock was located 27.8 ± 4.2 km east of Maravatío at a depth of 8.2 ± 2.9 km with the epicentre being close to the outcrop of the Venta de Bravo fault. The focal mechanism of the shock, which shows a major left-lateral strike-slip component, has an east-west oriented fault plane with a dip of 60°N. Since this dip is similar to that of the Venta de Bravo fault it suggests that the fault is planar from the surface to the base of the seismogenic upper crust. Focal mechanisms showing normal faulting on nodal planes oriented approximately east-west have also been determined for other shallow earthquakes within the Mexican Volcanic Belt (ASTIZ 1986, SUÁREZ & PONCE 1986).

4 *Geology*

The Mexican Volcanic Belt is formed by calc-alkaline volcanic rocks of Pliocene-Quaternary age and is bordered by Oligocene-Miocene ignimbrites and associated

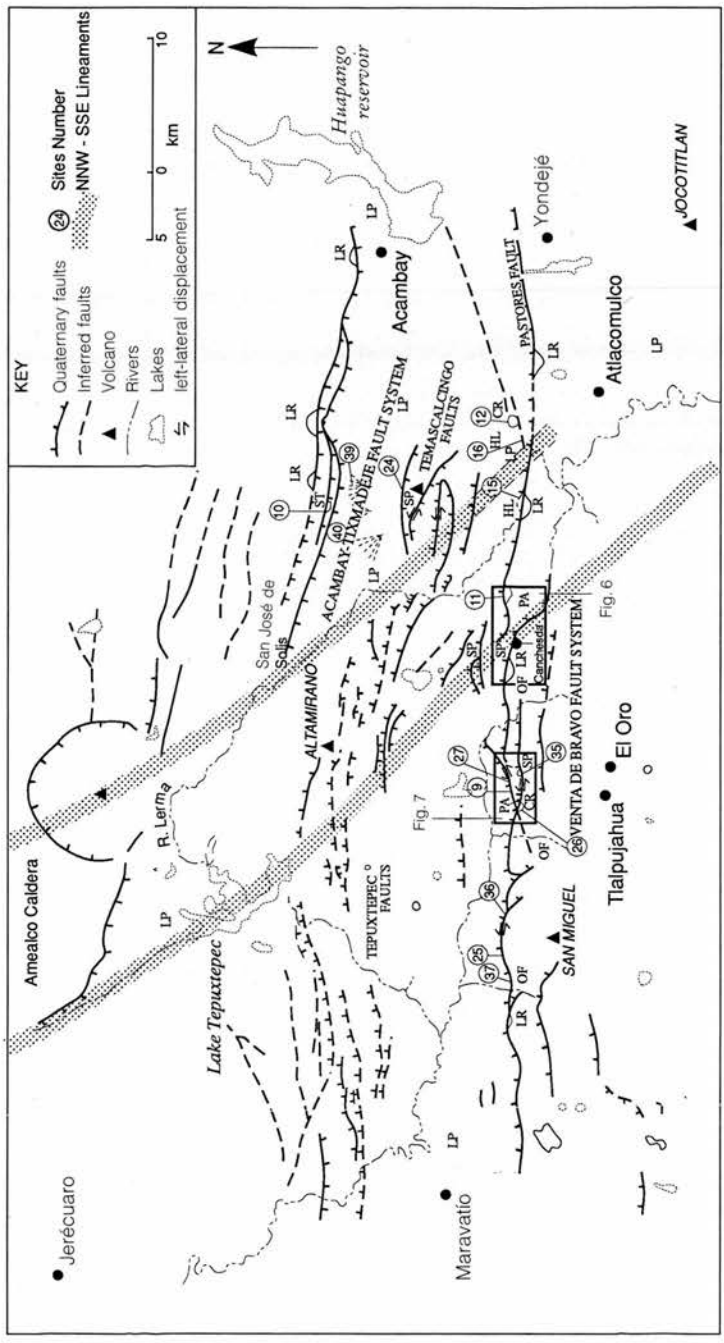

Fig. 2. Morphotectonic map of the Acambay graben. Ticks on fault lines indicate downthrown side. Symbols: LP – lacustrine plain, LR – linear ridge, HL – high level of lake deposits, CR – compression ridges, PA – pull-apart basins, SP – sag ponds, ST – shutter ridges, OF – offset drainage.

rocks of the Sierra Madre Occidental (fig. 1) which form the basement of the region (AUBCUIN et al. 1982). The geology of the Acambay region has been described by FRIES et al. (1977), SÁNCHEZ-RUBIO (1984), and SILVA-MORA (1979). The oldest outcropping rocks truncated by the Venta de Bravo fault system are folded and slightly metamorphosed Mesozoic sediments (FLORES 1920) which in the El Oro region (FRIES et al. 1977) and at Cerro San Miguel (SILVA-MORA 1979) are overlain by andestic-dacitic volcanic rocks (SILVA-MORA 1979). Higher in the sequence lake deposits occur south of Canchesdá, and ignimbrite deposits (Las Americas Formation) cover the mainly flat-surfaced mesas. The ignimbrites, which have a mean thickness of about 50 m, are found north of Tlalpujahua (FRIES et al. 1977, AGUIRRE-DÍAZ 1990). The hanging wall of the Venta de Bravo master fault is composed of the lake deposits of the Ixtapantongo Formation (SANCHEZ-RUBIO 1984), scoria cones with associated basalt flows (SILVA-MORA 1979), and alluvial fan deposits. Although the scoria cones occurring within the study area have not been dated, intercalated paleosoils in cones exhibiting a comparable state of degradation in the nearby Toluca valley have yielded carbon-14 ages of between 8440 ± 70 a and 38950±3210 a (BLOOMFIELD 1975). This suggests that the east-west trending normal faults of the study area have been active in the Late Quaternary (SUTER et al. 1992). Further age constrains on seismic activity are provided by the lake deposits of the Ixtapantongo Formation which have a mimimum thickness of 75 m and C^{14} ages of < 23 ka (SÁNCHEZ-RUBIO 1974). They are displaced by the Pastores fault and are truncated by the Venta de Bravo fault south of Canchesdá (fig. 2). On the basis of an estimated displacement of 50 m and an age of 23 ka for the base of the lake deposits at Canchesdá, SUTER et al. (1992) proposed a mean rate of Late Quaternary displacement of 2 mm a^{-1} along the eastern section of the Venta de Bravo fault.

The eastern end of the Pastores fault, not far from the town of Yondejé, is apparently formed by rocks of the Yondejé andesite formation which consist of massive phorphyritic lavas with a K-Ar age of 13 Ma (SÁNCHEZ-RUBIO 1984). Although the trace of the fault in these rocks is not continuous, there are some lineaments which appear to follow the general east-west trend of the Pastores fault. The Yondejé andesite formation is one of the most extensive formations outcropping in the Acambay graben. It outcrops from the town of Acambay southwards to the south of Yondejé creating a north-south ridge which closes the eastern end of the valley formed by the Acambay graben.

The Atlacomulco Formation (Early Miocene) is also truncated by the Pastores fault. The Pleistocene Atlacomulco andesites form a lava field which appear to partially cover the Pastores fault as well as the lacustrine tuff beds in the area of Atlacomulco.

The scarp of the Pastores fault is formed in basaltic andesites (the Pastores volcanics (Upper Miocene?)). These rock appear to be partly mantled by andesitic conglomerates and pumice-rich tuffs (SÁNCHEZ-RUBIO 1984). At the western end of the Acambay-Tixmadejé fault the La Loma andesite (Pliocene) has been brought into contact with pumice fall-out deposits (K-Ar age < 5 Ma) (SÁNCHEZ-RUBIO 1984) although the fault does not continue into the alluvium of the Lerma River to the west.

The volcano of Temascalcingo is a complex structure formed by massive andesitic lavas as well as by a thick agglomerate of andesitic composition. The northern

flank of Temascalcingo is mainly composed of a thick agglomerate, which appears to lie on massive aphyric adesites underlain by dacitic lavas. By contrast the southern part of the volcano is almost wholly composed of massive andesite. A dome-like body of dacitic composition (K-Ar age 8.5 Ma (Sánchez-Rubio 1984)) occurs inside the graben by the eastern foot of the volcano, where it is partly mantled by tuffs and alluvium.

In the central part of the Acambay graben there are Quaternary rhyolitic lavas truncated by ESE-WNW trending faults and forming lava domes with a K-Ar age of 1.57±0.15 Ma according to Demant & Robin (1975). Several areas in the Acambay region are also covered by the Amealco ignimbrite which has a K-Ar age of < 5 Ma B.P. (Sánchez 1984).

5 *Field observations in the Acambay graben*

In this section we describe the neotectonic structures identified in the Acambay graben from detailed geomorphological mapping. Mapping was carried out at a scale of 1 : 50000 and focused on the eastern part of the graben as far west as Maravatío (longitude 100° 25′ W) (fig. 2), since this is the area in which the geomorphological expression of faults is most evident. Three major areas related to specific neotectonic structures were identified:

1) The Acambay-Tixmadejé fault system and Tepuxtepec faults on the northern flank of the graben;
2) The Pastores fault and Venta de Bravo fault System on the southern margin of the graben; and
3) The Temascalcingo faults in the centre of the graben (fig. 2).

Northern flank

The Acambay-Tixmadejé fault System, which extends from Acambay to San José de Solís and forms the northern boundary of the Acambay graben, is characterised by east-west trending normal faults (fig. 2). Some of the individual faults are up to 30 km long and are associated with fault scarps averaging 400 to 450 m in height. The boundary between the Acambay and Tepuxtepec faults is marked by the valley of the Lerma River and a 180° change in dip azimuth of the normal fault that cuts the southern fringe of the Amealco caldera (Suter et al. 1991). Along the scarps of the Acambay-Tixmadejé system (site 40, fig. 2) there are well defined triangular facets. The scarp, which has a relatively low gradient of approximately 30°, has been deeply eroded and incised and at its foot it is partially covered by colluvium and in some places by alluvial fans (fig. 3). Drainage channels have been blocked by a second fault on the scarp apparently displaying some strike-slip displacement. Basaltic cones and linear ridges appear along this part of the fault (fig. 4). The linear ridges are probably shutter ridges (site 10, fig. 2) and therefore indicate a strike-slip component along the fault (Sylvester 1988).

The Tepuxtepec fault System which extends from Altamirano to a point north of Maravatío is characterised by east-west normal faults (fig. 2). Although the northern flank of the Acambay graben is predominantly characterised by south-facing normal faults, there are some north-facing faults which, where present, give rise to

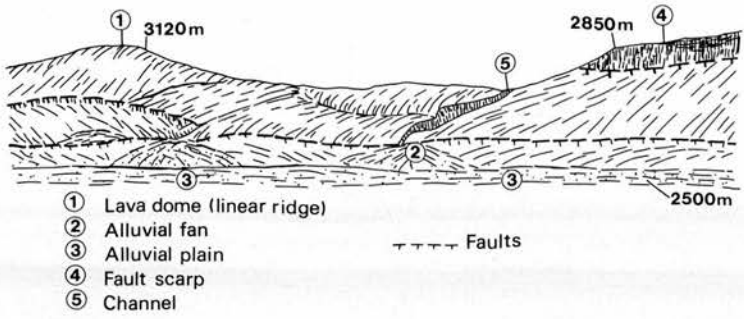

Fig. 3. Morphological sketch of a mountain front of the northern flank of the Acambay graben. (For location see fig. 2, site 39).

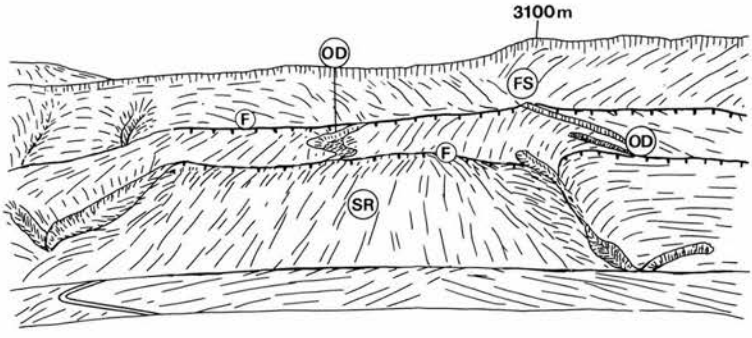

Fig. 4. Morphological sketch of the northern flank of the Acambay graben. Linear ridges are exposed on the frontal part of the slope and offset drainage shows the location of displacement by a fault of the Acambay-Tixmadeje system. (For location see fig. 2, site 10).

small graben and horst structures. Overall the fault system is approximately 40 km long, but individual faults are limited to 8 km in length. The Tepuxtepec system is composed of several truncated faults which have a clear topographic expression and a mean height of around 30 m. In its central part the fault system is partially buried beneath the sediments of Lake Tepuxtepec (fig. 2).

Southern flank

The east-west trending Pastores fault forms the southern boundary of the eastern part of the Acambay graben (fig. 2). The fault is 30 km in length and is associated with a 200 to 250 m high scarp with a gradient of approximately 45° – 70°. The fault

has a clear continuous topographic expression over a distance of 14 km, while at its eastern end its presence is evident through the displacement of cinder and scoria cones. Along the River Lerma, south of the volcanic peak of Temascalcingo, a single river terrace is located alternately on each side of the river valley. Near this site at San Pedro Potla at the foot of the Pastores fault scarp we have identified lake deposits at 20 m above the river plain level (site 15, fig. 2). The proximity of these elevated deposits to the Pastores fault suggests that they may have been displaced by faulting, although they do not show evidence of tilting in this area.

Other terraces with small scarps can be seen on the Toxi Plain north of the Pastores fault (site 16, fig. 2). These may have a tectonic origin although it is difficult to distinguish them from features produced by terracing for agriculture. North of the Pastores fault (site 12, fig. 2), however, there are deformed lake deposits some of which have almost vertical inclination of 86° and east-west trend, while others are deformed into recumbent folds. There is also an apparently 30° WSW trending fault at this location while a reverse fault exposed at this site indicates the presence of compressional stresses (fig. 5). The deformed lake deposits are apparently part of a compression ridge which is bounded by two arroyos associated with two ENE-WSW trending faults which displace lake deposits. It is probable that this area between the two faults has experienced both extension and compression, but further investigations are required to confirm this interpretation.

At the western end of the Pastores fault (site 11, fig. 2) distinct scarplets are evident which may represent the surface rupture of the 1912 Acambay earthquake, and Urbina & Camacho (1913) mapped a surface rupture along the fault in this area (site 11, fig. 2). The site is close to the western termination of the Pastores fault where some of its displacement is transferred to the Venta de Bravo fault (fig. 6). The two faults have a cross-strike separation of 1.0 to 1.3 km and an along-strike overlap of 1.8 km (Suter et al. 1991). A swampy depression between the two fault segments at

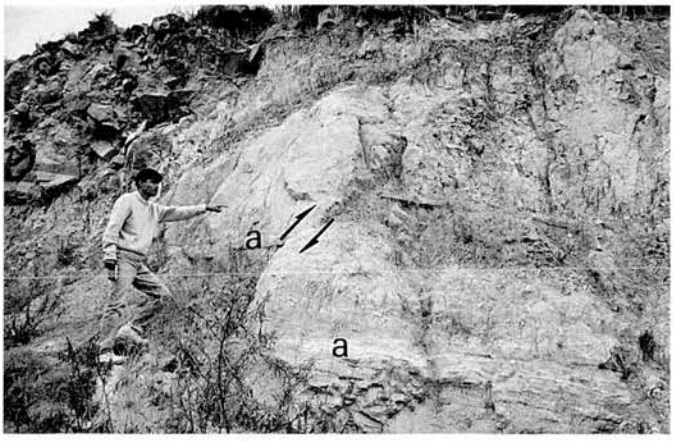

Fig. 5. Reverse fault displacing lake deposits near the eastern end of the Pastores fault (site 42, (see fig. 2)). Symbols: a – displaced layer.

Canchesdá is indicative of a pull-apart basin representing an extensional off-set (SUTER et al. 1991) (fig. 2). This structure provides further evidence that movement along the two fault segments include a minor left-lateral strike-slip component (fig. 6).

The Venta de Bravo fault System, which has been mapped previously by FRIES et al. (1977) and SUTER et al. (1992), consists of a master fault with several shorter east-west striking normal fault segments to the north and south. It is expressed topographically by a continuous, 45 km long north-facing fault scarp which attains a maximum height of 300 m near the strato-volcano of San Miguel (fig. 2). At this location in the central section of the fault, the scarp exhibits triangular facets as-

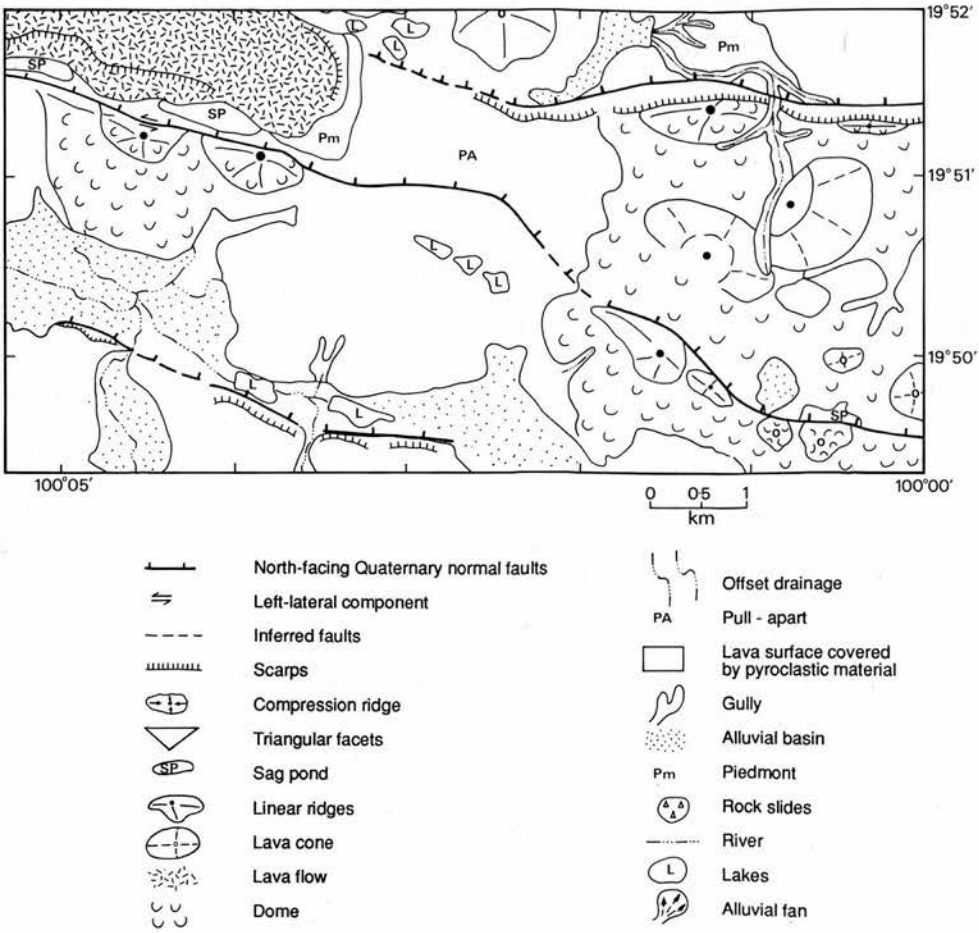

Fig. 6. Morphotectonic map of the overlap between the Pastores and the Venta de Bravo faults (site 11, (see fig. 2)).

sociated with deeply incised V-shaped valleys. This area of maximum relief along the fault system is located approximately 10 km west of the epicentre of the main shock of the 1979 series of seismic events (Suter et al. 1992).

In cross-section the footwall rocks along the Venta de Bravo master fault reveal a fracture system with a spacing between individual fractures of 0.5 to 1 m (site 9, fig. 2). This fracture system is close to the fault surface and is parallel to the master fault.

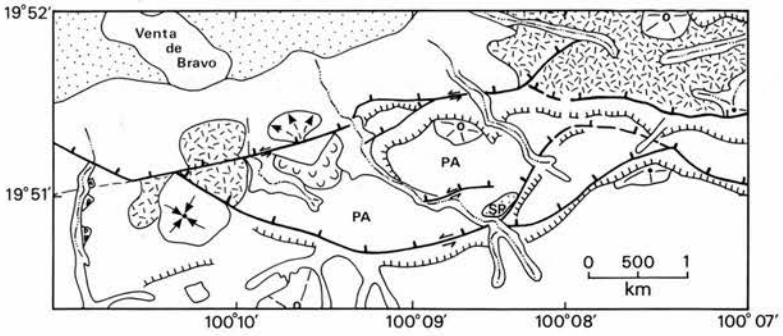

Fig. 7. Morphotectonic map showing a pull-apart basin and compression ridge along the Venta de Bravo fault. (for location see fig. 2). Key as for fig. 6.

South of the Venta de Bravo town an almost parallel associated minor fault, with a downthrown block facing to the north, joins the master fault on its western end creating a rhomboid depression between the two faults (fig. 7, (for location see fig. 2)). The presence of a sediment-filled sag pond at the base of the scarp of the associated minor fault to the south, and the left-lateral displacement observed on the Encinal River where it crosses segments of the fault, both provide evidence of recent left-lateral movement (fig. 7). This structural configuration is interpreted as an incipientpull-apart feature which indicates extension within the area (Suter, et al. 1991, 1992). However, a ridge (site 26, fig. 2) indicative of local compressions is present in the zone of intersection between the two faults (fig. 8).

Along the Venta de Bravo master fault near the El Encinal River (site 27, fig. 2) the presence of triangular facets along the scarp formed by V-shaped valleys cut into andesitic volcanics is indicative of recent fault activity. Other indicators of recent seismicity in this part of the fault scarp include offset drainage and rock slides (fig. 7). The Venta de Bravo fault scarps reveal fault planes at several locations (sites 35, 36 and 37, fig. 2) and at some of these, such as at site 25 (fig. 2) at the western end of the fault, subvertical striations are visible. A fault plane is also exposed at the wall on the right bank of the Encinal River on which we have identified a tool track (Hancock & Barka 1987) trending NE 62°, parallel to the fault plane. Fault planes exposed along the Encinal River are associated with friction breccia, mylonite and black soapstone, which provide evidence of slip along the fault.

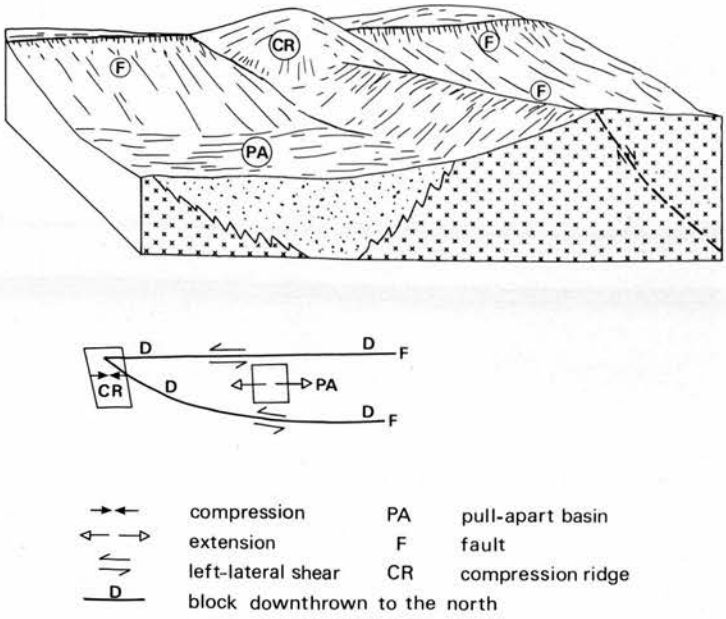

Fig. 8. Block diagram of faulting near a small pull-apart associated with the Venta de Bravo fault system (for location see fig. 2). Insert shows main components of motion.

Central part of the graben

The Temascalcingo faults, which occur in the centre of Acambay graben, form an extensive east-west trending system. The dormant deeply eroded peak of Temascalcingo, which reaches an elevation of 3220 m, is also located in the central part of the Acambay graben. This volcanic structure is truncated in its central part by a series of east-west faults forming a small graben structure within the volcano (fig. 2). The overall fault system extends for 18 km with individual fault segements reaching 11 km in length and having associated fault scarps up to 150 m high. Small sediment-filled depressions (sag ponds), occur along a fault flanking the north of Temascalcingo (site 24, fig. 2). The scarp at this location is approximately 50 m high, but due to the dense vegetation cover striations indicative of recent fault activity have not been observed.

A series of faults is exposed along the arroyo of Tinajal located on an alluvial fan on the north-west flank of Temascalcingo (site 39, fig. 2). Moving upstream at this site the first fault encountered does not truncate the soil layer or the upper part of a conglomeratic horizon exposed on the fan. The fault has a direction of 80°E, and, on the basis of the dislocation of the underlying conglomeratic horizon, it has a vertical throw of 0.87 m and a horizontal displacement of approximately 1 m (fig. 9). It appears to be a strike-slip fault with a left-lateral component. Upstream there are

Fig. 9. Exposure showing a fault with a 0.87 m vertical displacement of a conglomerate on a component of the Temascalcingo fault system. Bar for scale 1.0 m.

several other faults that displace a tuff deposit and the lower conglomeratic horizon; one of these has a vertical displacement of around 0.6 m. On the western flank of Temascalcingo lava flows are cut by a series of ESE-WNW trending, northward dipping faults arranged *en echelon* giving rise to scarps 20 m in height. Some of these faults are associated with small sag ponds, but there is no clear evidence of a lateral component to the faulting in this area.

Discussion and conclusion

Several studies have shown that the central part of the Mexican Volcanic Belt is characterised by generally east-west trending faults of Quaternary age (Mooser 1969, Mooser & Ramírez 1989, Pasquaré et al. 1987, Johnson 1987, Suter et al. 1991). These faults and associated fracture systems appear to exert a structural control over magma routing in the area, leading to an overall tectonic control over volcanism in the central as well as eastern part of the Mexican Volcanic Belt (Johnson 1987, Urrutia & Böhnel 1988). The regional scale tectonic framework is related to plate convergence processes which in the Mexican Volcanic Belt have resulted in the activation of a transtensive left-lateral system (Urrutia & Böhnel 1988).

Active faults in the Acambay graben are grouped into five major east-west trending systems – the Acambay-Tixmadejé system, the Tepuxtepec faults, the Pas-

tores fault, the Venta de Bravo system, and the Temascalcingo faults. A range of geomorphological evidence indicates recent tectonic activity along the faults bounding the Acambay graben. Such morphological indicators are most evident along the southern flank of the graben, particularly along the Venta de Bravo, Acambay-Tixmadejé and Temascalcingo fault systems. Here prominent fault scarps, triangular-faceted spurs, offset drainage, sag ponds and compression ridges are clearly developed, and high slope gradients demonstrate the freshness of the scarps. In contrast, faults in the Tepuxtepec system exhibit shallow gradient slopes and low fault scarps which may indicate either more prolonged erosion or a lower rate of tectonic activity in this part of the graben. Except for limited historical evidence, there is as yet no absolute dating available for the most recent fault displacements and consequently estimates have to be based on the degree of fault scarp degradation.

The geomorphological evidence indicative of neotectonic activity described here shows that the Venta de Bravo fault system and the Pastores fault have experienced slip combining normal north-facing faulting and left-lateral displacement; with significant lateral displacements being most clearly expressed morphologically along the Venta de Bravo fault system. The Acambay-Tixmadejé fault system consists of normal south-facing faults with a component of left-lateral displacement. By contrast, the Tepuxtepec faults are mainly north-facing and where combined with south-facing normal faults give rise to small graben structures. The Temascalcingo faults, in the centre of the graben, are also characterised by a combination of normal south and north facing faults with a component of left-lateral displacement, giving rise to a graben structure within the volcano of Temascalcingo. Although the Acambay graben is a complex zone of extension, it also shows some evidence of compression. This is indicated by two compression ridges, one located on the western end of the pull-apart structure along the central part of the Venta de Bravo fault, and the other situated at the eastern end of the Toxi plain. Since other morphological features indicative of compression have not been detected in the region, these compression ridges are probably secondary structures related to left-lateral motion at fault junctions.

Three main conclusions arise from this study. First, that the tectonic landforms of the Acambay graben reflect fault activity characterised by normal north- and south-facing faults combined with left-lateral displacement. Secondly, geomorphological data for the Acambay graben are consistent with systems of faults which have experienced transtensive, large-scale, left-lateral shear. Thirdly, the clarity of the geomorphological evidence and the historical occurrence of seismicity along the Venta de Bravo system of faults suggest that this is the most tectonically active structure in the Acambay graben. Further analysis of neotectonic activity in the region is required in order to document more precisely both spatial and temporal variations in seismicity. This could be accomplished by establishing a more precise chronology for fault displacement and by the geodetic and geomorphological monitoring of the fault movement and deformation in the region.

Acknowledgements

This research was financially supported by the Universidad Nacional Autónoma de México (UNAM). Travel funds were granted by the Instituto de Geografía, UNAM.

It is a pleasure to acknowledge the help of Prof. C. Vita-Finzi for his thorough review and advice. Special thanks to F. Mooser for many hours of discussion and advice provided during the field work. M. Suter provided many relevant references. J. Zamorano assisted in the field.

References

Aguirre-Díaz, G.J. (1990): The Amealco tuff, a major explosive event in the Mexican Volcanic Belt (abstract). – Geol. Soc. Am., Abstr. Programs, **22**, 350.

Armijo, R., P. Tapponnier, J.L. & Tong-Lin Hang (1986): Quaternary extension in southern Tibet: Field observations and tectonic implications. – J. Geophys. Res. **91**, B14: 13803–13872.

Astiz, L.M. (1980): Sismicidad en Acambay, Estado de México. El temblor del 22 de febrero de 1979. – B.S. thesis, Univ. Nac. Autón. Méx., México, 130 p.

– (1986): The 1912 Acambay, Mexico (MS = 7.0) earthquake: a reexamination (abstract): Bol. Unión Geofís. Mex., epoca II, special issue, 17.

Aubcuin, J., J. Azema, J.C. Carfantan, A. Demant, C. Ragin, & J. Tournon (1982): The Middle American Tranch in the Geological framework of Central America. Init. Rep. DSDP, **67:** 747–755. U.S. Govt. Printing Office, Washington.

Bloomefield, K. (1975): A late-Quaternary monogenetic volcano field in central Mexico. – Geol. Rundsch., **64:** 476–597.

Brias, A., R. Armijo, T. Winter, P. Tapponnier & A. Herbecq (1990): Morphological evidence for Quaternary normal faulting and seismic hazard in the Eastern Pyrenees. – Annales. Tectonicæ, **4,** 1: 19–42.

Cosgrove, J. & J. Mervin (1991): Neotectonics and Resources. – London.

Demant, A. (1978): Características del Eje Volcànico Transmexicano y sus problemas de interpretación. – Univ. Nac. Autón. Méx. Rev. Inst. Geol., **2:** 172–187.

Demant, A. & C. Robin (1975): Las fases de vulcanismo en México: una síntesis en relación con la evolución geodinámica desde el Cretácico. – Univ. Nac. Autòn. Méx. Rev. Inst. Geol., **75,** 1: 70–82.

Doornkamp, J.C. (1986): Geomorphological approaches to the study of neotectonics. – J. Geol. Soc. (Lond.), **143:** 335–342.

Doornkamp, J.C. & M. Han (1985): Morphotectonic research in China an its application to earthquake prediction. – Prog. Phys. Geog. **9:** 353–381.

Embleton, C. (ed.) (1987): Neotectonics and Morphotectonics. – Z. Geomorph. N.F. Suppl., **63:** 1–7.

Ferriz, H. (1985): Zoneamiento composicional mineralólogico en los productos eruptivos del centro volcánico de los Humeros, Puebla, México. – Geofís. Int. Volmen especial sobre el Cinturon Volcánico Mexicano (Ed. S.P. Verma), **24:** 1: 97–157.

Flores, T. (1920): Estudio geológico-minero de los distritos de El Oro y Tlalpujahua. – Bol. Inst. Geol. Méx., **43:** 85 p.

Fries, J., C.S. Ross, A. & Obregón (1977): Mezcla de vidrios en los derrames cineríticos Las Américas de la región de El Oro-Tlalpujahua, Estados de México y Michoacán, parte centromeridional de México. – Univ. Nac. Autón. Méx. Bol. Inst. Geol., **70:** 1–84.

Ghosh, T.K. & S. Viswanathan (1991): Neotectonic anaylsis of Mendha river basin, Rajasthan, India. – Int. J. Remote Sens., **12,** 12: 2585–2595.

Han, M. (1985): Tectonic geomorphology and its application to earthquake prediction in China. – In: Morisawa, M. & J.T. Hack (ed.): Tectonic geomorphology; 367–386. Allen und Unwin, Boston–London.

Hancook, P.L. & A.A. Barka (1987): Kinematic indicators on active normal faults in Western Turkey. – J. Struct. Geol., **9:** 573–584.

Johnson, C.A. (1987): A study of neotectonics in central Mexico from Landsat thematic mapper imagery. – M.S. thesis. Univ. of Miami, Coral Gabbles, Florida, 112 p.

Johnson, C.A. & C.G.A. Harrison (1989): Tectonics and volcanism in central Mexico: A Landsat Thematic Mapper Perspective. – Remote Sens. Environ., **28:** 273–286.

– (1990): Neotectonics in Central Mexico. – Phys. Earth Planet. Inter., **64,** 2–4: 187–210.

López, G.G. (1984): Tectonic structure and development of the Trans-mexican volcanic belt. – PhD thesis, Moscow State University, Moscow. (in Russian).

LUGO-HUBP, J., ORTIZ-PÉREZ, J. L. PALACIO-PRIETO & G. BOCCO-VERDINELLI (1985): Las zonas más activas en el Cinturón Volcánico Mexicano (Entre Michoacán y Tlaxcala). – Geofís. Int., Volúmen especial sobre el Cinturón Volcánico Mexicano (ed. S. P. VERMA), **24,** 1:83–96.

LUHR, J. F., S. A. NELSON, J. F. ALLAN & I. S. E. CARMICHAEL (1985): Active rifting in southwestern Mexico: manifestations of an incipient eastward spreadingridge jump. – Geology, **10:** 37–48.

MARTÍNEZ-REYES, J. & A. F. NIETO-SAMANIEGO (1990): Efectos geológicos de la tectónica reciente en la parte central de México. – Univ. Nac. autón. Méx., Rev. Inst. Geol., **9,** 1:33–50.

MEDINA, M. F. (1985): On the volcanic activity and large earthquakes in Colina area, Mexico. – Geofis. Int., Special Volume on Mexican Volcanic Belt (ed. S. P. VERMA), **24,** 2: 701–708.

MERRITS, D. & M. ELLIS (ed.) (1992): Chapman Conference on Tectonics and Topography. – Am. Geophys. Union, Snowbird, UTAH.

MOLNAR, P. & L. R. SYKES (1969): Tectonics of the Caribbean and Middle America regions from focal mechanisms and seismicity. – Geol. Soc. Am. Bull., **80:** 1639–1684.

MORISAWA, M. & J. T. HACK (ed.) (1985): Teconic Geomorphology. – 390 p., Binghantom Geomorphology Symp., Boston–London.

MÖRNER, N. A., L. A. OWEN, I. STEWART & C. VITA-FINZI (ed.) (1992): Neotectonics - recent advances. – Abstract volume. Quat. Res. Ass. Cambridge.

MOOSER, F. (1969): The Mexican Volcanic belt – structure and development. – Pan-Am. symp. Upper mantle., México, **2:** 15–22.

MOOSER, F. & M. T. RAMÍREZ-HERRERA (1989): Faja Volcánica Transmexicana: Morfoestructura, tectónica y vulcanotectónica. – Bol. Soc. Geol. Mex., T. XLVIII; **2:** 75–85.

ORTIZ-P, M. A. & G. BOCCO-VERDINELLI (1989): Análisis morfotectónico de las depresiones de Ixtlahuaca y Toluca, México. – Geofís. Int., **28,** 3: 507–530.

OTA, Y. (1985): Marine terraces and active faults in Japan with special reference to coseismic events. – In: MORISAWA, M. & J. T. HACK (ed.): Tectonic geomorpholog: 345–366. Allen and Unwin, Boston–London.

PASQUARÉ, G., L. FERRARI, V. PERAZZOLI, M. TIBERI, & F. TURCHETTI (1987): Morphological and structural analysis of the central sector of the Transmexican Volcanic Belt. – Geofís. Int. Special volume on Mexican volcanic belt, *26,* 3B: 177–193.

RAMÍREZ-HERRERA, M. T. (1990): Análisis morfoestructural de la Faja Volcánica Transmexicana (centro-oriente). – M. Sc. thesis. Univ. Nac. Autón. Méx., México D.F., 86 p.

SÁNCHEZ-RUBIO, G. (1984): Cenozoic volcanism in the Toluca – Amealco region, central México. – M. Phil. thesis. Univ. of London, Imp.Coll. of Sci. and Technol., 275 p.

SANDERSON, D. & J. GUTMAINS (ed.) (1991): Satellites and neotectonics. – Abstracts. Geol. Remote Sens. Group Mtg. at Geol. Dept. Southampton.

SILVA-MORA, L. (1979): Contribution a la connaissance de l'axe volcanique Transmexicain: Etude géologique et pétrologique des laves du Michoacán Oriental. – Thèse de Docteur Ingénieur, part 1, 145 p., Univ.de Droit, d'Econ. et des Sci. d'Aix-Marseille, France.

SOLER, A. A. M. (1990): Paleomagnetismo de la región de Acambay, Faja Volcánica Transmexicana. – M.S. thesis. Univ. Nac. Autón. Méx., México, D.F., 110 p.

SUÁREZ, G. & L. PONCE (1986): Intraplate seismicity and crustal deformation in central Mexico (abstract). – Eos: Trans. of the Am. Geophys. Union **67:** 1114.

SUÁREZ, G. & S. K. SINGH (1986): Tectonic interpretation of the Trans-Mexican volcanic belt. – Discussion. Tectonophysics **127:** 155–160.

SUMMERFIELD, M. A. (1987): Neotectonics and landform genesis. – Prog. Phys. Geog. **11:** 384–397.

SUTER, M. (1991): State of stress and active deformation in Mexico and western Central America. – In: SLEMMONS, D. B., ENGDAHL, E. R., ZOBACK, M. D. & BLACKWELL, D. D. (eds.): Neotectonics of North America- – Boulder, Colorado Geol. Soc. of America, Decade Map, 1: 401–421.

SUTER, M., G. J. AGUIRRE, C. SIEBE, O. QUINTERO & J. C. KOMOROWSKI (1991): Volcanism and active faulting in the central part of the Trans-Mexican volcanic belt. – In: WALAWENDER, M. J. & HANAN, B. B. (ed.): Geological excursions in Southern California and Mexico. – Guideb. An. Mtg. Geol. Soc. Am. San Diego, Calif. Oct. 21–24, 1991, pp. 224–243.

SUTER, M., O. QUINTERO & C. A. JOHNSON (1992): Active faults and State of Stress in the Central Part of the Trans-Mexican Volcanic Belt, Mexico. Part 1: The Venta de Bravo fault. – J. Geophys. Res., **97,** B8: 11983–11993.

SYLVESTER, A. G. (1988): Strike-slip faults. – Geol. Soc. Am. Bull., **100:** 1666–1703.

TAPPONNIER, P. (1991): Rates of Holocene slip and recurrence of large earthquakes on active faults: the use of spot panchromatic scenes and quantitative geomorphology. (abstract). – In: SANDERSON D. & J. GUTMAINS (ed.): Satellites and Neotectonics. – Geol. Remote Sens. Mtg. Geol. Dept. Southampton.

Urbina, F. & H. Camacho (1913): La zona megaseismica Acambay–Tixmadeje, Estado de México, conmovida el 19 de noviembre de 1912. – Bol. Inst. Geol. Méx., **32:** 125 p.

Urrutia-Fucugauchi, J. & H. Böhnel (1988): Tectonics along the Trans-Mexican volcanic belt according to paleomagnetic data. – Phys. Earth Planet. Inter., **52:** 320–329.

Venegas, S.S., J.J. Herrera & R. Maciel (1985): Algunas características de la Faja Volcánica Mexicana y de sus recursos geotérmicos. – Geofís. Int. Volúmen especial sobre el Cinturón Volcánico Mexicano (ed. S.P. Verma), **24,** 1: 47–81.

Verma, S.P. (1985): Mexican Volcanic Belt (Preface). – Geofís. Int., Special volume on Mexican volcanic belt, **24,** 1: 7–19.

– (1987): Mexican Volcanic belt: Present state of knowledge and usolved problems. – Geofís. Int., Special volume on Mexican Volcanic Belt, **26,** 3B: 309–340.

Vita-Finzi, C. (1991): Satellites and deformation chronologies (abstract). – In: Sanderson D. & J. Gutmains (ed.): Satellites and Neotectonics. – Geol. Remote Sens. Mtg. Geol. Dept. Southampton.

Weldon, R.J. & K.E. Sieh (1985): Holocene rate of slip and tentative recurrence interval for large earthquakes on the San Andreas fault, Cajon Pass, southern California. – Geol. Soc. Am. Bull., **96:** 793–812.

Addresses of the authors: M.T. Ramírez-Herrera, Instituto de Geografía, Universidad Nacional Autónoma de México, Ciudad Universitaria, México D.F. 01000. Present address: Department of Geography, University of Edinburgh, Drummond Street, Edinburgh EH8 9XP, United Kingdom. – M.A. Summerfield, Department of Geography, University of Edinburgh, Drummond Street, Edinburgh EH8 9XP, United Kingdom. – M.A. Ortiz-Pérez, Instituto de Geografía, Universidad Nacional Autónoma de México, Ciudad Universitaria, México D.F. 01000.